UNIVERSITY OF BIRMINGHAM

INVESTIGATING THE USE OF STABILIZED SUBGRADE SOILS FOR ROAD PAVEMENTS IN KURDISTAN

by

JABAR RASUL

A thesis submitted to
the University of Birmingham
for the degree of
DOCTOR OF PHILOSOPHY

College of Civil Engineering and Physical Science
School of Civil Engineering
The University of Birmingham
June 2016

ABSTRACT

Road pavement design in Kurdistan is based on ASSHTO 1993. However, it seems not to be entirely satisfactory since it is unable to take full account of properties of local soils or those which have been stabilised. To address this, a design procedure applicable to different material and environmental conditions was developed. The associated research consisted of a suite of laboratory experiment allied to the development of a finite element model. The laboratory work was undertaken on three types of subgrade soils found in Kurdistan to determine their permanent deformation behaviour, UCS and resilient modulus for a range of moisture contents. The experimental investigation considered soils stabilised with 2%, 4% cement content and a combination of cement and lime with 2% cement plus 1.5% lime and 4% cement and 1.5% lime. The results were used to develop empirical equations to: (i) predict resilient modulus values of deteriorated modified soils as a function of different stabiliser contents and types; (ii) correlate resilient modulus values of soils with their UCS and stress state; (iii) determine the accumulation of permanent deformation in modified subgrade soils subject to weathering. These relationships, together with the developed finite element model were used to establish the design procedure.

ACKNOWLEDGEMENT

I would like to express my deep gratitude to my supervisors Dr. Michael Burrow and Dr. Gurmel Ghataora for their very kind support, enthusiasm, patient guidance and encouragement. Without their support, the journey of this PhD would be very difficult.

I am particularly very grateful to the Kurdistan Regional Government (KRG) for funding this research project and sponsoring all costs of my PhD study.

I would like also thank the laboratory staff at the University of Birmingham for their assistance; Sebastian, Mike, Mark, Jim and David.

My special thanks to my wife Maleaha Samin and my two kids Nvar and Tnok for their patience with me during the completion of this work.

Many thanks are due to Mrs Janet Hingley for kindly proofreading my thesis.

LIST OF CONTENT

LIST OF FIGURES

LIST OF TABLES

LIST OF SYMBOLS AND ABREVIATIONS

CBR	California Bearing Ratio
MEPDG	Mechanistic-Empirical Pavement Design Guide
EPER	The ratio of accumulated permanent strain to the resilient strain
AASHTO	American Association of State Highway and Transportation Officials
AASHO	American Association of State Highway Officials
PD	Permanent Deformation
Mr	Resilient Modulus
UCS	Unconfined Compressive Strength
UU	Unconsolidated Undrained triaxial test
BS	British Standard
PSI	Present Serviceability Index
P_o	Initial Serviceability Index
P_t	Terminal Serviceability Index
ESAL	Equivalent Single Axle Load
SN	Structural Number
CGF	Cumulative Growth Factor
YDF	Yearly Deterioration Factor
N	Number load repetitions
N_d	Allowable number of load repetitions
M_R	Resilient modulus at a given time and
ME	Modulus of Elasticity
M_{Ropt}	Resilient modulus at a reference condition
σ_{dt}	Deviatoric stress in kPa during a period of time t

M_{rt}	Resilient modulus in MPa for a period of time t
N_t	The number of load repetitions in the period of time t,
T	The design life of the road pavement
M_{rA}	Resilient modulus of stabilised soil before durability test for material *A*
M_{rAWD}	Resilient modulus of stabilised soil after durability test for material *A*
$\mathcal{E}_i$	Initial strain in the mixture
E_i	Initial mixture modulus
σ_d	Deviatoric stress
ε_r	Resilient strain
$\mathcal{E}_{pz}$	Vertical plastic strain in micro strains at depth z
σ_1	Vertical Stress
σ_3	Confining Stress
v	Poisson's ratio
ϵ_z	Vertical Strain
ϵ_r	Radial Strain
ϵ_t	Tangential Strain
σ_z	Vertical Stress
σ_r	Radial Stress
σ_t	Tangential Stress
w_o	Initial Deflection
$\varepsilon_{1,p}$	Accumulated Vertical Permanent Strain
c	Cohesion
ϕ	Angle of Internal Friction
$\mathcal{E}_p$	Accumulated Permanent Strain

σ_s	The soil static stress
σ_{atm}	The reference stress
σ_{oct}	Octahedral Normal Stress
τ_{oct}	Octahedral Shear Stress
θ	Bulk Stress
Sr	The degree of saturation
Ec,s	Stabilised secant modulus of elasticity
σ_p^m	The measured value of the preload stress
σ_a^m	The measured value of the upper stress
RR	the rate of rutting
d	surface deflection in mm
N18	load repetitions/(105) in 80KN ESALs
σ_c	compressive stress on top of base in kPa
PD	permanent deformation
σ_{oct}	octahedral stress
σ_{atm}	atmosphere pressure
τ_{oct}	octahedral shear stress
σ_z	vertical effective stress
σv	vertical stress on top of pavement foundation (kPa)
e	the base of the natural logarithm
s	the slope

CHAPTER ONE

INTRODUCTION

1.1 Background

Romans were the first to build engineered roads; they built thousands of miles of roads from Rome to Britain to Damascus and North Africa (Knapton, 1996; Ninouh and Rouili, 2013). Figure 1.1 shows a Roman way in Jordan. Structurally the roads consisted of a number of layers of various locally sourced materials, to transport carriages.

Figure 1. 1 A Roman road in Jordan

The thickness of early road pavements was constructed purely from experience. From 1920, new pavement design procedures were developed empirically (Huang, 2004). Empirical pavement design methods using soil classification system were developed in 1929 by Hogentogler and Terzaghi (1929). The California Bearing Ratio (CBR) was developed as a

measure of strength used in other empirical pavement design procedures (Huang, 2004). The current methods of pavement design at the present time are divided into two types (e.g. McElvaney and Snaith (2002): empirical and analytical (or mechanistic-empirical). Empirical methods are developed from experimental pavements subjected to traffic loads either from public roads or road test sections; whereas analytical / mechanistic-empirical methods combine structural analysis of the road pavement using mathematical expressions, based on physical laws and material performance measurements determined from laboratory or field experimentation (McElvaney and Snaith, 2002).

Fully developed mechanistic-empirical pavement design methods consist of various processes; first the loads and materials are characterised, then stresses, strains and deflections are determined at critical locations in the model and compared with critical stresses, strains and deflections determined using the models of the material's performance, to formulate the design (Theyse et al., 1996). If a linear elastic theory is assumed for structural analysis, then it is only necessary to determine the material's modulus, Poisson's ratio and the density of each layer. A number of computer programs were developed to perform structural analysis, which assume linear elastic analysis and include JULEA programme (After NCHRP, 2004) and KENLAYER programme (Huang, 1993). However, the performance of road pavement materials is generally non-linear, such as in granular base/subbase and subgrades. These materials respond nonlinearly to the applied load and their resilient modulus is stress dependent. Increases in computational power have however facilitated the development of analytical computer-based methods, which have enabled the non-linearity of materials to be taken into account. These have included techniques developed, among others, using finite element and finite difference methods (Huang, 2004).

Although significant development has taken place regarding the computational analysis of road pavements for determining their response to applied loads, the characterisation of the performance of a road pavement's materials remains a challenge. To formulate the design, the most common critical modes of distress considered in analytical-empirical pavement design procedures are permanent deformation (rutting) and fatigue cracking (McElvaney and Snaith, 2002) .

Many roads are built in environments where the subgrade soils are weak. In such situations, to improve the performance of these soils a variety of stabilisation techniques are often employed; whereby the types and amounts of stabilisers used are determined according to the type of the subgrade soils. Stabilisation of soils by mechanical or chemical means has been shown to improve the properties of these soils considerably (Little, 1987; Bell, 1996; McManis, 2003; Milburn and Parsons, 2004; Rout et al., 2012). Nonetheless, stabilised soils can experience significant deterioration with load repetition and weathering (Wu et al. (2011a). Therefore when stabilised soils are to be used within a road pavement, it is important to properly characterise their performance so that the road pavement can be designed appropriately. Hicks (2002) identified three important considerations for the successful design of a stabilised subgrade layer: the structural design, the material mix's design and the construction of the stabilised layer. Regarding the structural design, the performance criteria to be used depend on the type of stabilisation used. If the stabilised material is considered to be an unbound material, then the thickness is governed by subgrade strain, this type has no significant tensile strength. Where the soil is stabilised with a low ratio of stabiliser, the design criterion is subgrade strain and modification is carried out to increase the strength and to reduce the moisture and frost susceptibility of fine grained soils; and where the stabilised soil can be considered to act as a bound material, the addition of a stabiliser of this type

increases the tensile strength of the layer and the performance criteria are fatigue and erosion (Hicks, 2002). Appropriate stabilisation mix design requires the combination of the soils and the stabilisers in the correct proportions to achieve the required strength and durability (Paige-Green, 2008).

1.2 Problem Statement

The subgrade soils found in Kurdistan's road pavements are mostly classified to be within a range of fine-grained soils. Among these types of soils, the silty sandy soils are susceptible to moisture changes and fail with wetting and drying cycles. In addition, although these types of soils have high resilient modulus values, they may still experience high permanent deformation with repetition of applied loads. Puppala et al. (2009) confirmed that some types of these soils such as silts may have moderate to high resilient modulus values, but they undergo high permanent deformations. It is also important to take into consideration the variability of strength and resilient characteristics of silty sandy subgrade soils (Vorobieff and Murphy (2003). There are a number of means of addressing the above issues of such soils. These include:

- Protecting them from the ingress of the water,
- They can be replaced by soils insusceptible to moisture changes.

However, these two procedures may cause increases in cost and delays in construction.

Li and Selig (1996) suggest two approaches to control the accumulation of permanent deformation on the top of the subgrade layer:

1) The improvement of the subgrade by stabilisation or modification,

2) To reduce the deviator stress by increasing the upper layer thicknesses.

The shortcoming with the second approach may come from the fact that even by controlling the stress level, the subgrade layer could still be exposed to moisture changes and undergo high permanent deformations. Test results in this research show the increase of moisture significantly affects the subgrade soil deformation. Therefore, in these circumstances the improvement of the soil with a stabiliser may be a superior solution for permanent deformation resistance.

For compacted subgrade soils, especially those followed by a drainage layer, cycles of wetting and drying are more likely to occur; therefore these layers should be stabilised.

While considering different pavement design scenarios for reducing the stresses and strains in the subgrade by increasing the overlay resilient modulus values and thicknesses for example, the stabilisation of the subgrade layer may be the most appropriate option. In addition to the increase in resilient modulus value, which will arise due to stabilisation, the resistance of the soil to the changes in moisture content also will be improved considerably (Little, 1995; Li and Selig, 1996; Rout et al., 2012; Abu-Farsakh et al., 2014). However, the application of a stabiliser needs to take into account the soil type and the selection of an appropriate type and amount of stabiliser. In addition, the durability of the selected mix design needs to be checked for structural performance during the design life of the road pavement.

The empirical pavement design procedure followed in Kurdistan is the AASHTO Guide for Design of Pavement Structures 1993, which uses empirical relationships for pavement thickness design. However, these relationships are usually derived from a specified material type, traffic load and environmental condition that are different from the conditions found in Kurdistan (or other parts of the world). Therefore, it is preferable to use an analytical pavement design procedure in which all the mentioned conditions can be considered for different materials, different loading and environmental conditions.

1.3 Aim and Objectives

Aim

The aim of this research project is to assess the requirements for a pavement design procedure, using an analytical methodology, which considers natural and stabilised subgrade soils, taking into account the effect of seasonal variations.

Objectives

In order to achieve the above aim, this research has the following objectives:

1) Explore, via a literature review, the concept of and associated steps, involved in analytical pavement design.
2) To evaluate different factors affecting the behaviour of unstabilised and lightly stabilised (modified) subgrade soils, in terms of the resilient modulus and permanent deformation.
3) To simulate a road pavement response model to analyse different pavement section configurations, material characterisations and loading conditions.
4) Investigate how a procedure can be developed, which utilises the results of resilient modulus and permanent deformation before and after the durability tests, to account for the incremental deterioration of the stabilised subgrade soils in terms of the resilient modulus and permanent deformation.
5) To develop a performance model to predict incremental permanent deformation progression, at different stages of stabilised subgrade soil degradation. From which the suitability of different types of stabilisers can be assessed.
6) Explore the simplification of the analytical pavement design procedure, by developing correlation equations between the resilient modulus and unconfined compressive strength, instead of obtaining the stabilised subgrade soils for resilient modulus from sophisticated and costly available equipment.

1.4 Methodology

This research methodology consists of five tasks: i) a literature review of pavement design procedures with the focus on analytical methods; ii) experimental work which included a wide range of laboratory tests to characterise permanent deformation, resilient modulus, unconfined compressive strength, unconsolidated undrained triaxial test and soil index tests; iii) a performance assessment of stabilised and unstabilised subgrade soils with respect to durability considerations throughout the pavement's design life; iv) numerical modelling of the pavement's responses to the applied load and v) a design procedure, utilising the analytical theory principles and experimentally derived equations to design a typical road pavement structure in Kurdistan, which is capable of resisting traffic and environmental loading for a specified pavement design life.

A thorough literature review was undertaken to understand the types of the pavements and methods of design and analysis. Road pavements are generally classified into two types: flexible and rigid (Yoder and Witczak, 1975). The difference between these two types of pavements is in the way they transmit the applied tyre loads to the subgrade. Yoder and Witczak (1975) also classified methods of solving pavement design problems in two approaches: empirical and mechanistic; however there have been attempts towards moving from purely empirical methods to analytical approaches (Ullidtz, 2002). As the focus of this research is on flexible pavements and the analytical procedures of road design, the literature reviewed focuses on such aspects. The literature review also addresses the analytical-empirical procedure for pavement design. The review considers the means of achieving the components of the analytical design reported in the literature, namely: characterisation of the materials; analysing the pavement section for responses from the applied loads; calculating

the accumulated damage from stresses, strains and environmental conditions; and selecting the most durable and cost effective pavement section for a given design life.

As mentioned in previous section, analytical-empirical pavement design procedures consist of two steps; the first uses a mathematical model to determine stresses, strains and deflections at critical positions and in the second step the allowable stresses and strains are compared with those determined in step one (Ullidtz, 2002). However in more developed procedures the stresses and strains that are determined in step one are used to calculate the rate of deterioration (Ullidtz, 2002). The experimental work carried out herein is used for both of these steps. For the first step the data obtained from the experimental work are used to characterise the subgrade soils for input into the analytical model and for the second, the data from the experimental work are used to develop appropriate models of the material's performance (model of rate of deterioration). In addition to this, experimental work was carried out to assess the behaviour of the stabilised and unstabilised subgrade soils at different stresses and moisture conditions. Accordingly the following experimental tests were carried out on stabilised and unstabilised soil samples respectively:

i) Index and Proctor tests to determine basic soil properties,

ii) Permanent deformation tests (PD),

iii) Resilient modulus tests (M_r),

iv) Unconfined Compressive Strength tests (UCS) and

v) Unconsolidated Undrained triaxial tests (UU).

The details of the tests used are given in Chapter Three.

A variety of performance models for natural materials have been developed and incorporated within road pavement design methodologies. Section 2.5 describes these models in detail. However, little research attention has been given to the characterisation of similar

performance models for stabilised subgrade soils. Therefore, resilient modulus and permanent deformation tests in the experimental work presented in Chapters Four and Five were employed to develop and validate a performance prediction model that can be used for predicting rutting in unstabilised, stabilised and deteriorated subgrade layers. The performance model needs to take into account the material properties and stress within the subgrade layers, in addition to the number of load repetitions.

A thorough literature review was carried out to investigate a suitable numerical model for the purposes of this research. A finite element model of the road pavement in ABAQUS^{TM} was developed using the ABAQUS^{TM} software. The model was used to determine stresses and strains within the different pavement layers. Those stabilised and unstabilised compacted and natural subgrade layers are used in the performance models for rutting calculations. Chapter Six describes the numerical modeling research in detail.

The chosen analytical and performance models, together with the materials' properties, were utilised to develop a procedure to design an appropriate subgrade for Kurdistan to endure the predicted stresses, strains and environmental effects over the design life of the pavement. The design procedure is described in more detail in Chapter Seven of the thesis.

1.5 Novelty and Contribution to Knowledge

The key contribution of the research is associated the development of a rational design of asphalt road pavements with modified subgrade soils. The developed procedure is presented in detail as follows:

- The development of an analytical pavement design procedure which considers: (i) lightly stabilised (modified) soils and (ii) traffic and climate induced deterioration of resilient modulus of the subgrade.

- The formulation of a performance model which is a function of the resilient modulus, deviatoric stress and the number of load repetitions, for predicting the incremental permanent deformation progression.
- The creation of an iterative procedure which takes into account the stress dependency of the unstabilised and lightly stabilised subgrade soils. This ensures the selection of appropriate resilient modulus values in the design for a specified location within the pavement structure.
- The development of a durability equation for predicting the deteriorated resilient modulus, or any other material properties, of stabilised subgrade soils from durability test results obtained for one stabiliser type.
- The development of correlation between unconfined compressive strength (UCS) and resilient modulus for lightly stabilised subgrade soils, taking into account the stress state of the applied (traffic) load.
- The expansion of a novel pavement design procedure which includes characterising the stabilised subgrade layer, taking into account the effect of weathering and aging on the resilient modulus value and calculating the permanent deformation (rutting) of the stabilised subgrade layer.
- The development of a procedure for testing the stabilised subgrade soils to take into consideration weathering (for example wetting and drying).
- The adaptation of a procedure to determine the secant modulus of stabilised subgrade soils using BS EN 12390-13: 2013 method B. The latter is a standard test for determining the secant modulus of hardened concrete.

1.6 Thesis Outline

The structure of this thesis consists of eight chapters. Chapter One presents the background, problem statement, aim and objectives and methodology followed in this research. Chapter Two presents a comprehensive literature review of pavement design types, their procedure steps and requirements, performance models and response models. The moisture change in subgrade soils and methods of stabilisation are also demonstrated in this chapter. Chapter Three describes the materials, equipment, test procedures and selection of the necessary stress levels used in the research. Chapter Four shows the factors affecting the resilient modulus values and how these effects can be addressed in subgrade soil characterisation. The durability study and correlation equations are also derived in this chapter. Chapter Five demonstrates the permanent deformation test results and development of a performance model. The variety of the factors affecting the performance of stabilised and unstabilised soils correspondingly is presented and their effect on rutting of subgrade soils is presented likewise. Chapter Six deals with finite element model development and the nonlinearity behaviour of stabilised and unstabilised subgrade soils with different methods is discussed. Chapter Seven describes how the findings from Chapters Three – Six were used to develop an analytical design procedure for Kurdistan for stabilised and unstabilised subgrade soils. Chapter Eight contains the conclusions and recommendations derived from the research project undertaken herein. References and appendixes are placed at the end of the thesis.

CHAPTER TWO

LITERATURE REVIEW

2.1 Introduction

This chapter of the thesis critically reviews the literature relevant to pavement design types and numerical methods of determining the responses, such as stresses, strains and deflections, from the applied traffic loads and environmental conditions. The distresses occurring as a result of these loads and environmental conditions are discussed subsequently. To obtain road pavement responses to the applied traffic loads the properties of the materials used for different layers of the pavement section are required. As the focus of this research is on the properties of the subgrade layer under varying environmental and loading environments for stabilised and unstabilised soils, the distress types and performance related to the subgrade layers are also reviewed. In analytical pavement design procedures the resilient modulus is used to characterise the subgrade soil and the distress related to the subgrade performance is usually permanent deformation or rutting. Therefore a comprehensive review is carried out on resilient modulus and permanent deformation modelling as well as laboratory work to characterise these subgrade properties. Hence, this chapter consists of three main parts: first, current practices for road pavement design are described and their requirements presented in detail. Then, pavement response models and performance models are reviewed. Finally, the importance of the subgrade soils to provide a foundation for a road pavement is demonstrated and the relevant subgrade problems and possible improvements are discussed.

2.2 Pavement Design

A flexible road pavement is a structural system (Figure 2.1) which is designed to withstand the combined effects of traffic and the environment for a predetermined period of time so that vehicle operating costs, safety and passenger comfort are kept to acceptable levels and the subgrade is adequately protected (McElvaney and Snaith, 2002). The primary objectives of pavement design are therefore to select the appropriate materials and their minimum required thicknesses to achieve an economical design.

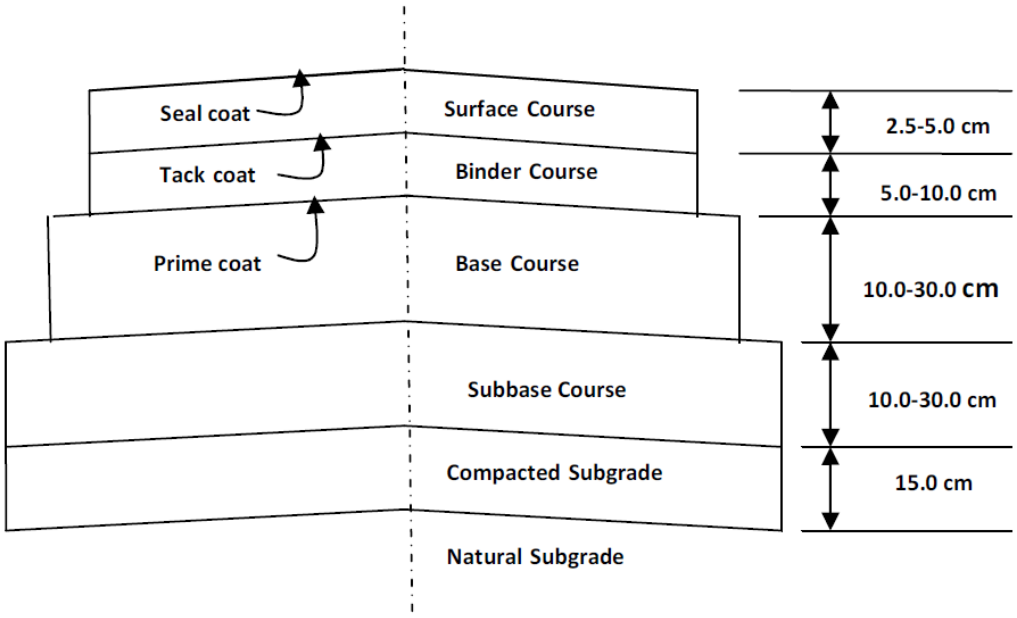

Figure 2. 1 Typical cross section of a conventional flexible pavement. (After Huang, 2004)

Usually road pavements are classified into three major types: flexible pavements, rigid pavements and composite pavements (Huang, 2004). Flexible pavements consist of a bituminous layer or layers over granular treated or untreated materials having natural and/or compacted soil subgrades. Rigid pavements consist of a jointed plain concrete or continuous reinforced concrete layer over the soil sub-grades with or without granular bases. Composite pavements comprise of both of the above mentioned types (Huang, 2004).

Methods of pavement design fall into two broad categories: empirical and analytical. Empirical methods are typically developed from experimental pavement sections exposed to normal traffic or test tracks. On the other hand, analytical methods consist of both a theoretical model and also models of material performance, developed in the laboratory (or via field trials) which may be regarded therefore as empirical. The two are combined to formulate the design. The following sections describe the requirements and processes associated with empirical and analytical pavement design methodologies.

2.2.1 Empirical Pavement Design

Empirical pavement design methods make use of experimental pavement sections subjected to controlled or normal traffic loads and the performance of the pavement is monitored, from which empirical relations of performance are derived (O'Flaherty, 2002). Early attempts at empirical pavement design relied on soil classification without a strength test, in which the subgrade soils were classified under different index groups (Huang, 2004). In 1929 the California Highway Department used a strength test to relate the thickness of the pavement to the strength of the subgrade determined from a measure of material strength known as the California Bearing Ratio (CBR) (Huang, 2004). The CBR was later researched by the 'U.S. Corps of Engineers during World War II and became a very popular method after the war' (Huang, 2004). Using the CBR as a pavement design property is criticised by Brown (1997); he corroborated his views by research carried out on the CBR. Brown (1997) stated that the CBR is a shear strength index by quoting from Thurnbull (1950); while according to Croney (1977), the shear strength is not of direct interest to road engineers. Brown (1997) emphasised that mechanical properties and tests should be used instead of CBR values and tests. One significant disadvantage of empirical methods in general, which is also emphasised by a number of researchers, is that the empirical relations derived are valid only for the material

type and the environmental and loading conditions of the site where the experiments were carried out. From the many empirical procedures developed from the early 1920s to date, in the following sections two empirical design procedures, AASHTO and Overseas Road Note 31 (ORN31) respectively are briefly described and the necessary inputs are discussed.

2.2.1.1 AASHTO Guide for Design of Pavement Structures 1993

This guide is the extension and revision of the AASHTO guides 1972 and 1986, which were initially derived from the AASHO road tests in Illinois, USA from 1958 to 1960 (Highway and Officials, AASHTO, 1993). The design procedure and input variables of the method are summarised below:

Performance criteria: the AASHTO guide makes use of the present serviceability index (PSI) which is an empirical measure of the pavement condition, see Table 2.1. An initial serviceability indexes (P_o) of 4.2 to 4.5 were observed at AASHO road test after construction before opening the road to traffic. A terminal serviceability index (P_t) of 2.5 or higher is suggested for major highways. However, the serviceability index cannot reflect different mechanisms that affect the performance of the pavement (Daleiden et al., 1994), because it focuses on ride quality and the individual distresses that occur in a road pavement are not considered.

Table 2. 1 Present Serviceability Index ranges

PSI range	Poor	very good
	0.0	5.0
Initial serviceability index (P_o)	4.2 to 4.5	
Terminal serviceability index (P_o)	2.5	

Traffic: the damage caused by the accumulated traffic loads over the design period of a road pavement is a fundamental input into any pavement design procedure (both empirical and analytical). To this end, the concepts of a standard axle and an equivalent number of standard axles (ESALs) were first developed during the AASHO road tests. The standard axle was defined as a single load of 80 kN (18 kips) and an equivalent number of standard axles was the number of actual axle loads, which would cause the same damage to the road pavement as one application of a standard load. For the purposes of design, the number of applied axle loads of all load configurations is converted to a number of equivalent ESALs for the design period. For example, the damage caused by the passage of one 98 kN (22 kips) axle load is the same as that of 2.17 passages of 80 kN (18 kips) (ESALs). This equivalent single axle factor was determined using the Asphalt Institutes' method, in which the equivalent single axle factor is determined from a simple equation (Equation 2.1); while AASHTO uses a complicated regression equation which was derived from the results of road tests.

$$ESAF= (W_{tx} /W_{t18})^4 \quad (2.1)$$

Where ESAF= equivalent single axle factor, W_{tx} = the load for which the Equivalent Single Axle Factor (ESAF) is required and W_{t18} = load of 18,000 lb

Material properties for structural design: the required material properties are the resilient modulus and the Poisson's ratio. The Poisson's ratio in this design guide (AASHTO, 1993) is estimated. The two most important environmental factors affecting the performance of the pavement are the temperature and moisture changes. These can also result in frost heave and swelling, affecting the serviceability of the pavement through aging. The change of the moisture content influences the resilient modulus of the road foundation. To account for this, the guide presents two different procedures for determining the seasonal variations of the

resilient modulus. The first procedure makes use of resilient modulus values obtained from laboratory experiments at different moisture contents. The second specifies that the resilient modulus can be obtained through back calculations of deflectometer strength measurement equipment undertaken during different seasons. The seasonal data are then translated to an effective road-base resilient modulus using charts given in the procedure, in which the year is divided into 12 months or 24 half months. The resilient modulus of each month or half month is determined from a chart and the relative damage is computed from a scale or by using the following equation of relative damage:

$U_f = 1.18*10^8*M_r^{-2.32}$ (AASHTO, 1993) (2.2)

Where Uf is relative damage factor and M_r is resilient modulus in Ksi.

The effective resilient modulus is obtained by using another chart, which relates the average damage to the effective resilient modulus. This procedure for determining the effective resilient modulus is only applied to pavement designs that use the serviceability criteria.

Reliability: due to uncertainties in predicting design traffic loads, represented by the accumulated number of ESALs and the prediction of pavement performance during the design life, reliability factors (R) are used to help to ensure that the pavement lasts for the period of time for which it was designed. The reliability factors have different values for different pavements according to their functional classification, i.e. whether they are urban or rural, motorways or local roads. Reliability factors are specified in the range from 99.9% to 50%. These factors depend on the functional classification of the road and whether the road is urban or rural, for example for motorways this reliability factor ranges from 85% to 99.9%, while for local roads it could be within a range of 50% to 80%.

Layer coefficients: the structural number (SN) is used within the AASHTO design guide to represent the required structural strength of road pavement layers and it is determined using the following empirical equation:

$$SN=\sum a_i D_i \quad (2.3)$$

Where a_i is the structural layer coefficient of layer i and D_i is the thickness of layer i.

The structural layer coefficient of an asphalt concrete course, a_1 is estimated from a chart relating the coefficient to the resilient modulus at 68°F (20 ^{0}C). The structural coefficient of base layers, a_2 can be determined by various means depending on the material. For granular material it is estimated from the CBR, R-value or the resilient modulus. For cement treated bases it can be determined from an unconfined compressive strength or resilient modulus test. In the case of bituminous treated bases it can be obtained from a Marshall Stability or resilient modulus test. Structural coefficients of the granular sub-base layer, a_3 may be estimated from the CBR, R-value or resilient modulus tests.

2.2.1.2 TRL Overseas Road Note 31(ORN 31) (ROLT, 1995)

ORN 31 is an empirical method for the structural design of flexible pavements in tropical and sub-tropical countries carrying up to 30 million equivalent single axle loads (ESAL). The design, in terms of thickness and number of layers, is determined from a series of catalogues as a function of the traffic, subgrade strength, properties of available materials and prevailing moisture conditions. The subgrade strength of the road is assessed via a CBR test and the moisture conditions are classified according to the depth of the water table and the amount of rainfall. Crushed stone and naturally occurring granular materials are specified to be used as road-base materials. Sub-base and road-base materials are characterised by grading, particle size distribution and mechanical properties which are tabulated in the guide.

Bitumen-bound materials consist of coarse aggregate, fine aggregate, filler and bitumen. They are the most important layer in a pavement structure. The guide mentions common types of the bituminous layer, they are: asphaltic concrete, bituminous macadam, rolled asphalt, flexible bituminous surfacing and design to refusal density. Some of these types have mix design procedures and some are made to recipe specifications without design procedures.

Structural catalogues have been presented in the guide, which are applicable to a range of traffic classes (T) of equivalent single axle loads (ESAL) starting from T1 of 0.3 million to T8 of 17-30 million (T_i is Traffic class) and a range of subgrade strength classes of CBR% from S1 of 2% CBR to S6 +30% CBR (S_i is subgrade strength class). The ORN 31 states that the structural catalogues have been determined from "the results of full-scale experiments where all factors affecting performance have been accurately measured and their variability quantified" and "studies of the performance of as-built existing road networks".

2.2.2 Analytical Pavement Design

In contrast to the empirical pavement design methods, analytical or mechanistic methods consider the mechanical behaviour of the pavement materials in an iterative method to determine the thicknesses fulfilling the requirements of the design (Huang, 2004; O'Flaherty, 2002). In an analytical pavement design the influence of stresses, strains and deflections due to the accumulated traffic loads and environmental conditions on the deterioration of the pavement structure is also considered. Most of the analytical pavement design methods use linear elastic theory (see section 2.3) to determine stresses, strains and deflections (Tutumluer, 1995) such as Chevron (Warrenand Dieckman, 1963) and BISAR (De Jong *et al*., 1973). The theory assumes materials of the pavement structure behave linear elastically; are homogeneous and isotropic; and require only the modulus of elasticity and Poisson's ratio for characterisation. In addition to the response determination, analytical pavement design

requires a prediction of the performance of the pavement structure; in this regard, most performance models relate the type of deterioration such as rutting and fatigue cracking to the number of load repetitions to failure (O'Flaherty, 2002). Though the use of linear elastic theory simplifies the analysis of the pavement structure, the materials used to construct road pavements do not behave linearly, in particular unbound granular base and subgrade layers. Design procedures such as Mechanistic Empirical Pavement Design Guide (MEPDG) (2004) use a multilayer elastic theory where the pavement materials are treated as linear elastic and a finite element code is used where the nonlinearity of unbound layers is considered.

2.2.2.1 Design Variables

Design criteria: among the many modes of distresses (see section 2.4) that a pavement structure experiences, wheel path rutting and bituminous layer cracking are the primary modes of deterioration resulting from traffic loading. The 1963 Shell analytical pavement design (Read and Whiteoak, 2003) used the horizontal tensile strain at the bottom of the bituminous layer and vertical compressive strain at the top of the subgrade as the major design criteria (Read and Whiteoak, 2003). As explained in sections 2.2.3.2 and 2.2.3.3 respectively other critical locations are used in other analytical procedures. For example, the vertical compressive stresses and strains within the hot mix asphalt and base/subbase layers are used for predicting the rutting and horizontal tensile strain at the bottom of the cemented layers is used for predicting the fatigue cracking are included in the MEPDG (2004) design guide and Austroads (2008), respectively.

Design loading: in empirical design procedures as mentioned in previous sections (see section 2.2.1), the loading traffic is expressed in terms of the Equivalent Standard Axel Loads (ESAL). Analytical pavement designs also tend to use the same procedure for traffic determination. Some procedures however, use the complete spectra of traffic loads expected

to occur over the life of a pavement to determine the stress, strain and deflection. Usually, for numerical modelling purposes, the critical responses are determined using a standard 40 kN dual-wheel that acts normally over two circular loaded areas and the contact stresses are assumed to be uniform and equal to the tyre pressure (Yoder and Witczak, 1975).

Pavement material properties for the purpose of analysis: for a conventional flexible pavement construction, bituminous materials are used for surfacing, unbound granular materials for base/subbase and soil for subgrades, each of which may be modified or stabilised to improve specific properties. As mentioned above, these materials behave non-linearly under load and accurate pavement design therefore requires the non-linearity to be accounted for during the modelling process.

Bituminous mixtures are viscoelastic materials; their properties depend on the time under which they are loaded and their temperature. Modulus of elasticity and fatigue resistance are two material properties that are required for analytical pavement design. These are usually determined in the laboratory using flexural, direct axial and indirect tensile tests (O'Flaherty, 2002). Typically the tests are conducted in two modes; the first mode is under controlled-stress in which the amplitude of stress is kept constant during the test and at a specified strain for failure, or the number of repetitions of the stress is recorded as the fatigue life of the bituminous sample. The second mode is a controlled-strain in which the strain amplitude is kept constant throughout the test and the stress is reduced as the test progresses due to a decrease in the modulus of elasticity of the bituminous sample under repetitions of strains. At a specified stress or percentage of the initial stress the number of strain repetitions is recorded as the fatigue life. Equation 2.4 is a general form of a controlled-stress model for fatigue life, from which the number of constant stress amplitudes that cause failure can be found (O'Flaherty, 2002).

$$N = K(\mathcal{E}_i)^{-m}(E_i)^{-c} \quad (2.4)$$

Where N= number of constant stress repetitions

$\mathcal{E}_i$= initial strain in the mixture (=σ/E_i)

E_i= initial mixture modulus

K and m are material constants

c is a constant indicative of the influence of the modulus.

Unbound granular materials are used for base/subbase and subgrade layers with or without treatment agents; the properties of these materials that are of interest are modulus of elasticity and the shear strength (McElvaney and Snaith, 2002). The material typically shows two types of deformation responses to the applied load in each load application; the greater part of this deformation is recoverable, which is elastic and the smaller portion is plastic and unrecoverable. Sections 2.6 and 2.7 describe further the elastic and plastic (permanent deformation) properties of granular materials and related equations and models for their characterisation are discussed. For the purpose of improving some properties of the materials used for base and subgrade layers, a portion of stabiliser agent will be added (Little and Nair, 2009; Rout et al., 2012). The improvements in properties which can accrue from such methods of stabilisation include changes to index properties such as plasticity index, modulus, strength and other engineering properties. Section 2.7 will present the stabilisation methods and types and the impact of stabilisation on modulus of elasticity and permanent resistance of granular materials.

Damage computation: for the purposes of determining the proportion of damage resulting from the spectrum of traffic loads to which a road pavement is subject, Miner's Law (Equation 2.5) is often used (Miner, 1945)**.**

$$\sum_{i=1}^{r} \frac{n_i}{N_i} = 1 \qquad (2.5)$$

Where:

n_i = number of repetitions of strain, stress, or load i

N_i = number of strains, stresses, or loads i that cause failure

r = number of different strain, stress or load amplitudes in the load spectrum.

The procedure for this computation can be summarised as follows (Huang, 2004):

1) Divide the year into intervals of constant layer modulus such as seasons or each month.

2) For each interval assign a modulus and calculate the maximum stresses, strains and deflections using the response models.

3) Use the performance model for the specified distress to determine fatigue or permanent deformation life.

4) The number of loads is calculated for each interval, from which the ratio of the damage is determined.

5) The ratios obtained in the previous step are summed up to determine the accumulated permanent deformation or fatigue cracking. This value is assumed to be constant for the whole year throughout the design period years.

Huang (2004) proposed a modified version of Equation 2.5 to account for seasonal variation as follows:

$$D_r = \sum_{i=1}^{p} \sum_{j=1}^{m} \frac{n_{i,j}}{N_{i,j}} \qquad (2.6)$$

Where:

D_r = the ratio at the end of a year

$n_{i,j}$ = the predicted number of load repetitions for load j in period i

$N_{i,j}$ = the allowable number of load repetitions from fatigue or rutting equations

P = the number of periods in each year (e.g. P=12 to represent monthly changes)

m = the number of load groups.

2.2.2.2 AASHTO Mechanistic-Empirical Pavement Design Guide, MEPDG (2004)

In contrast to the empirical methods in which the thicknesses of the layers of a pavement section are determined from design charts, MEPDG is an iterative process. The traffic load and the material properties at different environmental conditions are used as inputs to the analysis procedure and then the responses from theoretical relationships are determined. Thereafter, if the performance criteria are satisfied according to the material performance models used, the designed section is evaluated for economic considerations; Figure 2.2 shows this process schematically (MEPDG, 2004).

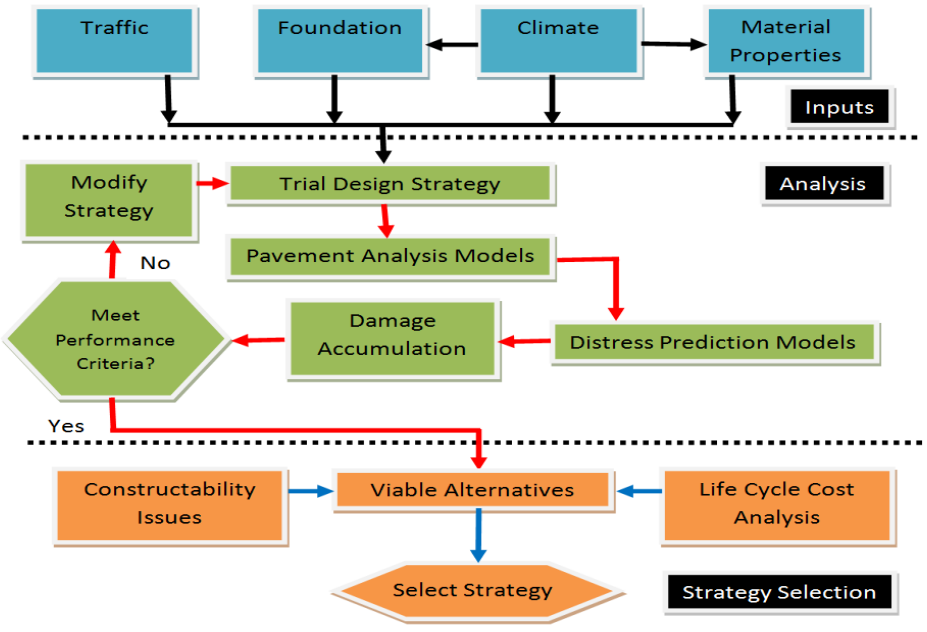

Figure 2. 2 Overall design process for flexible pavements (After MEPDG, 2004)

The design of flexible pavement in a mechanistic-empirical method is an iterative process in which a design trial is arranged to be examined for different steps of analysis; the procedure can be summarised in the following steps (MEPDG, 2004):

1) Deciding on a performance criteria for distresses and a reliability level.

2) Computing the pavement responses: stress, strain and displacement of the trial design assembly by inputting climate, traffic data and material properties.

3) Predicting the distresses: rutting, fatigue cracking (top down and bottom up), thermal cracking and roughness.

4) Comparing the predicted distress with performance criteria; if convergence is not achieved the trial section is modified (typically by modifying one or more layer thicknesses) until all the requirements of the design are satisfied.

Design inputs: three levels of input data are allowed in this design guide. Level 1: material properties and traffic data are obtained directly from the laboratory testing and field measurements. Level 2: correlation equations are used to obtain the required inputs. Level 3: default values from the existing database are applied. Different levels of inputs can be used in one trial design if the required data are not available. These inputs are then processed to obtain incremental or seasonal values of traffic, climate and material inputs.

Pavement response determination: where the layer materials are treated as linear the multi-layer elastic theory is used and for non-linearity considerations a finite element code is used. The purpose of the pavement response models is to determine the stresses, strains and displacements from the traffic loads, environmental conditions and material properties at critical locations in the road pavement. The responses of the pavement layers at critical

locations are then inputted into distress prediction models. The critical locations that are considered in the MEPDG (2004) are presented below:

- *Tensile horizontal strain at the bottom/top of the HMA layer (for HMA fatigue cracking).*
- *Compressive vertical stresses/strains within the HMA layer (for HMA rutting).*
- *Compressive vertical stresses/strains within the base/subbase layers (for rutting of unbound layers).*
- *Compressive vertical stresses/strains at the top of the subgrade (for subgrade rutting).*

Distress prediction: the distresses considered in the MEPG (2004) are: fatigue cracking, longitudinal and alligator cracking, permanent deformation, fatigue cracking of chemically stabilised layers and thermal cracking. These distresses are also used together to determine the roughness of the road pavement surface in terms of the International Roughness Index (IRI). The IRI model uses the initial IRI and subgrade climatic factors in addition to the effect of the mentioned distresses to predict roughness.

Design reliability: many uncertainties arise from future traffic loading predictions and environmental conditions. Each predicted distress in the MEPDG (2004) guide is a random variable for reliability design, because each distress is quantified separately and has an individual performance criterion. Therefore different reliability levels can be set for different distresses, for example the reliability level of rutting can be 90% and it can be 95% for fatigue cracking.

2.2.2.3 Austroads (Mechanistic Procedure)

The Austroads guide to pavement technology part two (2008) describes structural design methods for flexible and rigid pavements. Section eight of this part deals with the mechanistic

procedure to flexible pavement design. The following paragraphs describe the necessary steps for a mechanistic pavement design in this guide (Jameson, 2008).

The pavement design with this guide requires propose a trial pavement section; the next step is to evaluate the input parameters. These are:

1) Environment conditions - the effect of temperature on asphalt and moisture on the subgrade and unbound granular layers.

2) Material and performance criteria - the properties of the materials that are input to the analysis procedure are the modulus of elasticity and Poisson's ratio. The non-linearity of the unbound material is treated by dividing the layer into five sublayers and determining the modulus of elasticity and Poisson's ratio for each of these sublayers separately.

3) Design traffic load - the cumulative of heavy vehicle axle groups is calculated (N_{DT}) from traffic data and a cumulative growth factor for 20 years.

4) Reliability - from the desired reliability which ranges from 80% to 97.5%, the reliability factor (RF) is found and used in performance models of fatigue cracking of asphalt and cemented layers.

A trial pavement section, utilising the above inputs is analysed using a computer program known as Circular loads Layered system (CIRCLY) which is based on linear elastic theory to determine the responses of the pavement section. The tensile strain beneath the asphalt and cemented layers and compressive strain at the top of the subgrade are used to determine the allowable traffic loads. This allowable traffic is then compared with the design traffic, from this comparison the trial section is either accepted or modified (and the above procedure is repeated).

The performance prediction models for predicting the allowable traffic are given by Equations 2.7, 2.8 and 2.9 respectively.

For asphalt fatigue cracking:

$$N = RF[\frac{6918(0.856V_b+1.08)}{S_{mix}^{0.36}\mu\varepsilon}]^5 \quad \text{(Austroads, 2008)} \qquad (2.7)$$

Where *N*= allowable number of repetitions of the load; $\mu\varepsilon$= tensile strain produced by the load (micro-strain); V_b= percentage by volume of bitumen in the asphalt (%); S_{mix}= asphalt modulus (MPa); *RF*= reliability factor for asphalt fatigue (ranged from 2.5 to 0.67 for reliabilities from 80% to 97.5%).

For fatigue cracking of cemented layers:

$$N = RF[\frac{(113000/E^{0.804}+191)}{\mu\varepsilon}]^{12} \quad \text{(Austroads, 2008)} \qquad (2.8)$$

Where *E* is cement material modulus (MPa); *RF* is the reliability factor for cemented material fatigue (ranged from 4.7 to 0.5 for reliabilities from 80% to 97.5%).

For permanent deformation of subgrade layer:

$$N = [\frac{9300}{\mu\varepsilon}]^7 \quad \text{(Austroads, 2008)} \qquad (2.9)$$

Where *N* is the allowable number of repetitions of a standard axle at this strain before an unacceptable level of permanent deformation develops; $\mu\varepsilon$ is the vertical strain, in units of micro-strain, at the top of the subgrade.

It is of note that the permanent deformation of the granular base layer is not considered. Therefore the design of thin asphalt surface pavements is not recommended by this method as granular materials are a greater constituent of these types of pavements.

2.2.3 Resilient Modulus

Elastic parameters, such as modulus of elasticity and Poisson's ratio of each layer, are necessary elements to characterise the numerical models used in analytical pavement design methods (Ullidtz, 1987; O'Flaherty, 2002). The resilient modulus can be defined as the recoverable strain under repeated load applications (Equation 2.10) (Huang, 2004). Most pavement materials are not elastic and have two types of strains: a recoverable strain and permanent or plastic strain. Figure 2.3 shows the resilient and permanent strains of a soil (known as A-4) in this research.

$$Mr = \frac{\sigma_d}{\varepsilon_r} \qquad (2.10)$$

Where *Mr* is the resilient modulus; σ_d is deviatoric stress and ε_r is resilient strain.

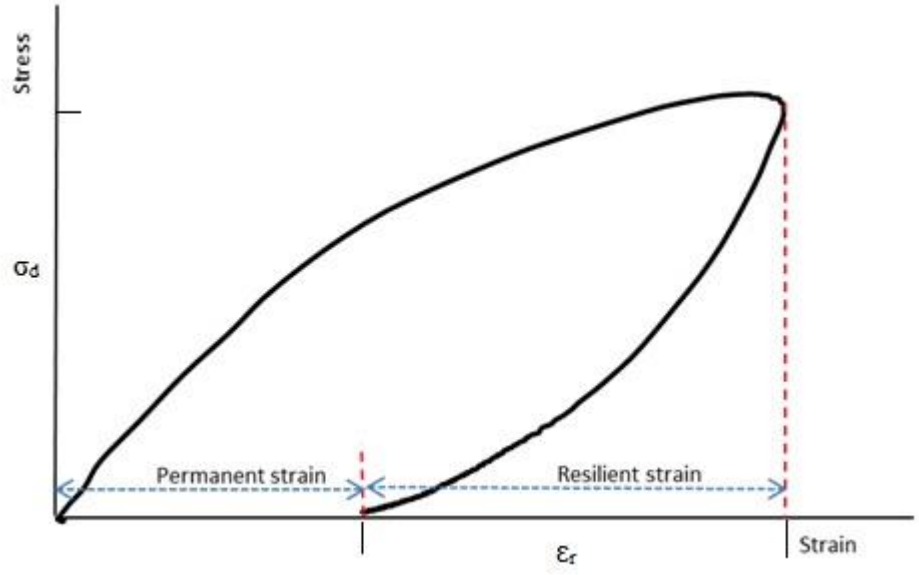

Figure 2. 3 Resilient and permanent strains of the fourth cycle of soil A-4

Another characteristic of the resilient behavior response of granular materials and subgrade soils is their non-linearity of the resilient modulus. Lekarp et al. (2000b) concluded from the literature that non-linearity is affected by many factors including stress, density, particle size distribution, moisture content, soil type, stress history, the number of load repetitions,

duration, frequency and sequence. The effects of these factors on resilient modulus behaviour are presented and discussed in detail in Chapter Four. Among these effects the influence of the stress on resilient behaviour is more significant and included in constitutive models for resilient modulus prediction and determination. Fine-grained soils have different responses to the increase in stress levels than coarse granular soils, as their resilient modulus decreases with an increase in the stress level or stress softening; while for coarse granular materials, the resilient modulus increases with an increase in the stress level or stress hardening (Huang, 2004).

Huang (2004) used a K-θ model (Equation 2.11) for granular materials and a bilinear model (Equation 2.12) for fine-grained soils. Kim (2004) used a bilinear soil model within the ABAQUS™ finite element program in his study of non-linearity of subgrade soils.

$$M_r = K_1(\theta)^{K_2} \quad (2.11)$$

Where M_r is the resilient modulus; θ is bulk stress ($\theta = \sigma_1+\sigma_2+\sigma_3$) or ($\sigma_1+2\sigma_3$) and K_1 and K_2 are regression constants from laboratory data.

$$M_r = K_1 + K_3 * (K_2 - \sigma_d) \text{ for } K_2 \leq \sigma_d \quad (2.12a)$$

$$M_r = K_1 + K_4 * (K_2 - \sigma_d) \text{ for } K_2 \geq \sigma_d \quad (2.12b)$$

Where K_1, K_2, K_3 and K_4 are constants from RLT test and σ_d is deviatoric stress ($\sigma_d = \sigma_1 - \sigma_3$).

The standard test for determining the resilient modulus of subgrade soils is included in different versions of the AASHTO standard test starting from T274-82 to the most recent version T307. Details of the test procedure and requirements for preparing samples and equipment are presented in Chapter Three.

Resilient and permanent deformation properties of the subgrade soils depend on stress levels and environmental conditions; however research by Puppala et al. (2009) showed that soils

with higher values of resilient modulus do not necessarily have higher resistance to permanent deformation. Therefore these two properties of the soils should be studied for a better understanding and improved subgrade pavement design. Section 2.5 reviews the permanent deformation of granular materials and subgrade soils; details on permanent deformation development in different soil types and stabilised subgrade soils are presented in Chapter Five.

The resilient modulus of subgrade materials is problematic to determine in the laboratory, since it involves using specialist laboratory equipment that may be complex to operate and expensive (See Chapters Three and Four). Therefore a number of researchers have attempted to correlate the resilient modulus with other properties of the material. In some of these correlation models, the resilient modulus of soils is determined from strength properties such as the CBR, the R-value and unconfined compressive strength (UCS); and in others from classification soil properties such particle size distribution, plasticity index and moisture content. Puppala (2008) presents a useful summary of the literature of correlations between resilient modulus and other properties of subgrade and unbound granular material, see Equations 2.13 and 2.14 for example, see Puppala (2008) for further details.

$$\mathrm{M_r} = 1200 * \mathrm{CBR} \qquad (2.13)$$

Where *CBR* is California Bearing Ratio

$$\mathrm{M_r} = a * \mathrm{S}_u\ 1.0\% \qquad (2.14)$$

Where a is regression constant and $S_u\ 1.0\%$ is the axial stress at 1.0% axial strain in unconfined compressive strength tests.

Summary

Road pavement design types were presented in this section. At present time two types of pavement designs are used worldwide, which their requirements were described and discussed. Empirical procedures use the experimental pavement sections' data to derive empirical relations of performance; while the analytical pavement design consist of two parts, in first part mathematical equations are used to determine pavement responses to the applied load and environmental conditions and in the second part performance models are used to predict the pavement's life. Analytical pavement design procedures facilitate the use of different material types and traffic load configuration in various environmental conditions. Therefore in this research analytical design procedures were investigated for the inclusion of the design of the stabilised and unstabilised subgrade soils to replace AASHTO design guide 1993, which is used at the present time in Kurdistan.

2.3 Pavement Response Models

The purpose of the pavement response models is to determine the stresses, strains and deflections from traffic loads and environmental conditions. The critical values of these responses are used as input in the distress models or transfer functions to predict the life of the pavement; this facilitates design, management and setting maintenance strategies for the road pavements.

2.3.1 Multi-Layer Elastic System

Boussinesq's theory was the only solution for determining stresses, strains and deflections before the development of the layered theory by Burmister (Huang, 2004). Boussinesq assumed a concentrated load, applied on one homogeneous, half-space, isotropic and linearly elastic layer with modulus elasticity of (E) and Poisson's ratio (v). By integrating the

responses from a concentrated load, stresses, strains and deflections of a circular loaded area can be determined at any point within the half-space (Huang, 2004), see Figure 2.4. Flexible pavements with thin surface asphalt and base layers, and a modulus ratio between the pavement and subgrade close to unity, can be analysed with this theory (Huang, 2004).

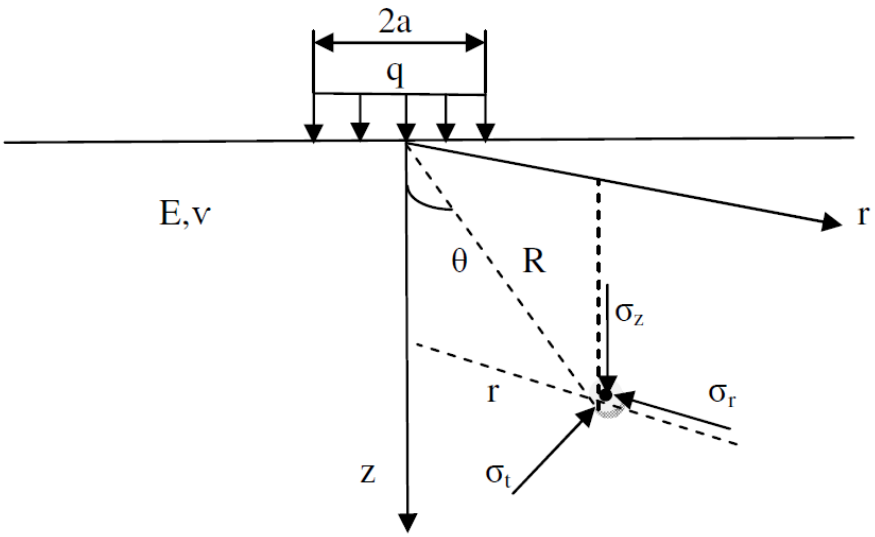

Figure 2. 4 Stresses in Boussinesq's theory (After Huang, 2004)

Vertical stress (σ_z), radial stress (σ_r), tangential stress (σ_t), shear stress (τ_{rz}) and vertical deflection (w) can be determined from charts presented by Foster and Ahlvin (1954). Strains then can be obtained using the following equations:

$$\epsilon_z = \frac{1}{E}[\sigma_z - v(\sigma_r + \sigma_t] \quad (2.15)$$

$$\epsilon_r = \frac{1}{E}[\sigma_r - v(\sigma_t + \sigma_z] \quad (2.16)$$

$$\epsilon_t = \frac{1}{E}[\sigma_t - v(\sigma_z + \sigma_r] \quad (2.17)$$

Where ϵ_z, ϵ_r and ϵ_t are vertical, radial and tangential strains, E is modulus of elasticity and v is Poisson's ratio

2.3.2 Two Layer System

Burmister (1943) developed the theory of a two layer system. He assumed the pavement system to be homogeneous, linearly elastic, isotropic layers with infinite horizontal dimensions and weightless layers resting on a semi-infinite subgrade layer.

The theory assumes a constant Poisson's ratio (v) of 0.5 for all layers and the stresses depend on the modulus ratio E_1/E_2 and the thickness ratio h_1/a (Figure 2.5). The deflection factor (F_2) is obtained from charts and used in Equation 2.18 to determine the surface deflection (w_o), which is the pavement design criterion.

$$w_o = \left(\frac{1.5qa}{E_2}\right) * F_2 \qquad (2.18)$$

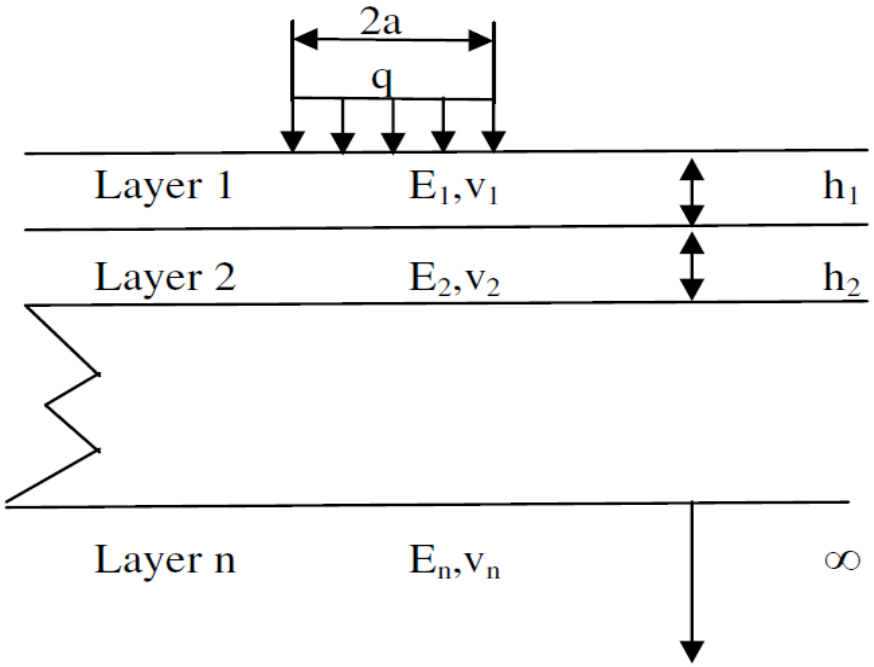

Figure 2. 5 An n layer system subjected to a circular load. (After Huang, 2004)

Vertical interface deflection can also be used as a criterion of pavement design instead of tensile and compressive strains. The expression is the same; the difference is in changing the deflection factor that can be obtained from another graph. In this theory the critical tensile strain at the bottom of the asphalt layer has been used to characterise the fatigue cracking properties of the asphalt layer. Huang (1973a) has developed charts to determine the strain factor for single, dual and dual-tandem wheels that can be used in Equation 2.19 to obtain strains (Huang, 2004).

$$e = \left(\frac{q}{E_1}\right) * F_e \qquad (2.19)$$

One example for two layer pavements is a full-depth pavement which consists of one thick asphalt layer over a subgrade layer. For more than two layers using the two layer theory, the asphalt layer and base layer, or base layer and subgrade layer, can be combined for example for determining the stresses and strains in a three layer pavement consisting of asphalt, base and subgrade layers (Huang, 2004).

2.3.3 Three Layer System

Burmister (1945) broadened his theory of layered systems to a three layer system and solved the problems of determining the responses at different positions in the three layer system, as shown in Figure 2.6. These responses are: vertical stress at the first interface (σ_{z1}); the radial stress at the bottom of layer 1 and the top of layer 2 (σ_{r1} and σ'_{r1}); vertical stress at the second interface (σ_{z2}); and the radial stress at the bottom of layer 2 and the top of layer 3 (σ_{r2} and σ'_{r2}).

On the axis of symmetry the radial and tangential stresses are identical and the shear stress is equal to zero; taking a Poisson's ratio of 0.5 for the three layers the strains are obtained as in Equations 2.20 and 2.21:

$$\epsilon_z = \frac{1}{E}(\sigma_z - \sigma_r) \quad (2.20)$$

$$\epsilon_r = \frac{1}{E}(\sigma_r - \sigma_z) \quad (2.21)$$

Stresses in a three layer system depend on the modular ratios K_1, K_2, respectively, A and the ratio of the thicknesses of the layers, H, (Huang, 2004).

$K_1=E_1/E_2$, $K_2=E_2/E_3$, $A=a/h_2$, $H=h_1/h_2$

Jones (1962) presented tables for determining stresses; and Peattie (1962) represented Jones' tables in graphical forms that can be used for determining strain factors and can be replaced in Equation 2.22 to obtain radial strain at the bottom of layer 1 (Huang, 2004).

$$\epsilon_r = \frac{q}{E} * (RR1 - ZZ1)/2 \quad (2.22)$$

Where RR1 and ZZ1 are factors obtained from the graphs.

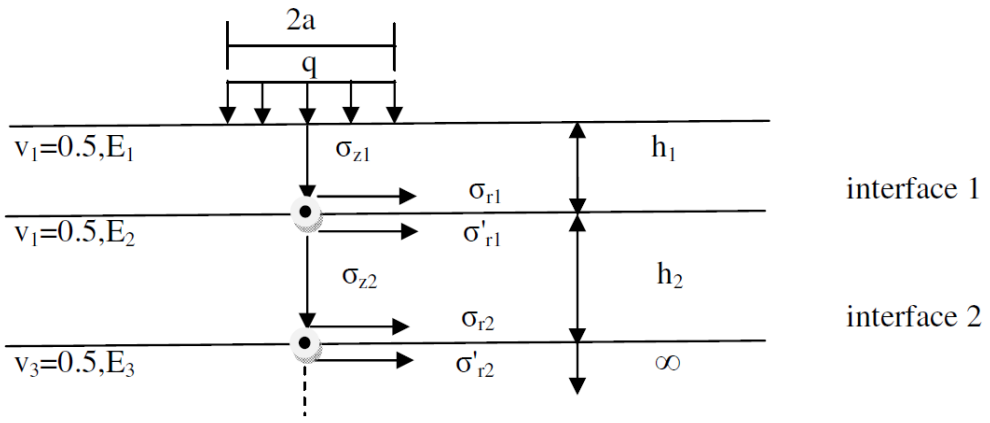

Figure 2. 6 Stresses at interfaces of a three layered system (After Huang, 2004)

In the 1970s development in computer technology made theoretical analysis easier. KENLAYER programme (Huang, 1993) is one of the programmes that can be used for determining stresses, strains and displacements in a multi-layer pavement system. It utilises an elastic multi-layer system under a circular loaded area. It can be applied to any pavement system whether they are linear or non-linear elastic or viscoelastic under single, dual, dual-tandem and dual-tridem wheels. JULEA (After MEPDG, 2004) is another program that has been used in the MEPDG (2004) for determining the pavement responses. Other programs have been developed to obtain pavement responses using multi-layer elastic theory and finite element methods; these include BISAR, CHEVRON and WESLEA (Huang, 2004).

2.3.4 Finite Element Analysis

Finite element methods are one of the techniques available for determining road pavement responses to applied traffic loads and environmental conditions (MEPDG, 2004). According to (Huang, 2004) the first researcher who applied finite element methods in pavement analysis

was Duncan et al. (1968). Later models of road pavement for analytical design such as ILLI-PAVE (Raad and Figueroa, 1980) and MICHI-PAVE (Harichandran et al., 1989) were developed using finite element methods.

The main features of a finite element model are: the model geometry, the properties of the constituent materials, modelling the load, boundary conditions setting, meshing the model and convergence of the finite element model. Many researchers (Zaghloul and White, 1993; Hjelmstad and Taciroglu, 2000; Hornych et al., 2002; Schwartz, 2002; Tutumluer and Kim, 2007) used three layer pavement sections consisting of an asphalt layer, granular base and subgrade layers for analysis in finite element modelling. However, others (Chen et al., 2004; Mulungye et al., 2007; Chandra et al., 2008; Soares et al., 2008) used finite elements with more layers, including the subbase layer.

In axisymmetric two-dimensional finite element modelling, a circular contact area is used for modelling the applied load (Chen et al., 1995, Helwany et al., 1998, Kim, 2007, Sadrnejad et al., 2011). However, in three-dimensional finite element analysis the contact area of the load is modelled as an equivalent rectangle of two semi-circles and a rectangle (Bodhinayake, 2008, Mulungye et al., 2007, Saad et al., 2005); while Zaghloul and White (1993) modelled the contact loading area as two semi-circles and a rectangle. The boundary condition was set to be a roller in the horizontal direction and fixed in the vertical direction (Zaghloul and White, 1993; Saad et al., 2005; Kim, 2007; Mulungye et al., 2007).

Finer mesh sizes provide more detailed and accurate results than the coarse mesh; however the memory capacity and time required for analysis of finer meshes necessitates a compromise between accuracy and speed. Therefore, researchers (Zaghloul and White, 1993;

Chen et al., 1995) used a finer mesh size close to the load and coarser mesh sizes for other elements far from the load.

An important part of a finite element model is the material characterisation. Of these properties the non-linear behaviour of unbound base/subbase and subgrade materials is of major interest. Zaghloul and White (1993) modelled asphalt material as a viscoelastic material using instantaneous and long-term shear moduli; granular material was modelled through using the Drucker-Prager model (Drucker and Prager, 1952); and the Cam-clay model (Roscoe, 1968) was used for fine grained materials. Sukumaran et al. (2004) and Saad et al. (2005) also used the Drucker-Prager model for granular materials and the Cam-clay model for fine grained materials. The Drucker-Prager model for base aggregate materials was also used by Arnold (2004) and Chazallon et al. (2009). These models and a few other material models are available in ABAQUS™; however, other researchers including (Han et al., 2011, Tutumluer and Kim, 2007) used the user material subroutine in ABAQUS (UMAT) to write codes for material characterisation with constitutive models, such as the universal model for prediction of resilient modulus non-linearity.

Summary

In this section pavement response models were presented that are used to determine stresses, strains and deflections. Boussinesq's theory was the basic for the development of multilayer elastic theory for the solution of the one layer, two layer and three layer pavement analysis. Pavement design programmes and procedures were developed throughout the last century using multi-layer elastic theory that assumes a concentrated load, applied on one homogeneous, half-space, isotropic and linearly elastic layer with modulus elasticity of (E) and Poisson's ratio (v). However, pavement materials are not linearly elastic, therefore to include the nonlinearity of these material (especially the granular base and subgrade

materials) finite element models were developed. In this research to obtain an accurate results and considering the nonlinearity of unstabilised and modified subgrade soils a finite element model developed in ABAQUS™ was used for the determination of pavement responses. In addition the KELAYER™ programme used for comparison purposes.

2.4 Pavement Performance and Distresses

Pavement performance is the pavement structural or functional condition as a function of the elapsed time or age (O'Flaherty, 2002). FWA (2006) defines the performance as the change of pavement condition with time or traffic. The repetition of applied traffic loads with time deteriorates the pavement; its serviceability decreases until it reaches an unacceptable condition, when it should be rehabilitated or reconstructed. Therefore predicting the end of the pavement's life is of great importance. According to (Lytton, 1987) the current procedures for predicting the pavement's performance are: empirical, empirical-mechanistic, probabilistic and mechanistic-empirical and there is no pure mechanistic or theoretical method to predict pavement performance.

2.4.1 Factors Affecting the Performance of the Pavement

Among the many factors affecting the performance of flexible pavement, traffic, environment, material type and construction methods are presented below (FWA, 2006):

Traffic: the characteristics of the traffic that affect the pavement performance include the magnitude of the traffic load, the tyre pressure, the speed of a vehicle and the number of load repetitions. The predominant distresses resulting from the road pavement include fatigue cracking (manifesting itself primarily in the wheel path) and wheel track rutting.

Environment: the change of subgrade moisture content in the unbound layers can affect the performance of the pavement structure. An increase in moisture content more than the

equilibrium moisture content reduces the strength of the subgrade materials. Higher temperatures have a direct influence on pavement performance; as the temperature rises the pavement surface can soften, resulting in rutting under traffic loads.

Soil and pavement materials: good and high quality subgrade soils and pavement materials can resist the diverse effects of the traffic load and environmental conditions. The superiority of these materials can be checked from their mechanical properties such as: resilient modulus, temperature and moisture susceptibility, durability, elasticity and plasticity. These properties determine the response capabilities of the soil and pavement materials to applied traffic loads and changes in environmental conditions.

Construction and maintenance practice: the method of construction affects the pavement performance. For example excessive compaction of asphalt concrete layers can reduce the number of voids in the asphalt and cause bleeding or rutting. Poor compaction on the other hand can result in an excessive void that can cause cracking. Poor compaction of the subgrade soils results in further permanent deformation during the service life of the pavement.

2.4.2 Pavement Performance Prediction

Lytton (1987) classifies performance models into primary response models, structural performance models, functional performance models and damage models. Response models predict the stresses, strains and deflections from applied traffic loads, environmental conditions and material properties. Structural performance models predict different forms of distresses and functional performance models predict the surface condition of the pavement such as roughness. Damage models are derived from structural or functional models from which load factors are determined.

Section 2.3 presented the response models and concepts, which are used to determine the stresses, strains and deflections. The determination of these responses is considered as the mechanistic part of mechanistic-empirical pavement design procedures in which theoretical mathematic equations are used. Regarding the structural performance models section 2.4.3 describes the distresses that can be determined from these models to evaluate the life of the pavement from a design criteria set at the beginning of the design. These models are considered as the empirical part of the mechanistic-empirical design procedure and derived from laboratory and/or field data.

Functional performance models are predicting the pavement condition, which is the main component of pavement management system (PMS); this helps the decision makers in managing the maintenance and rehabilitation times for road pavements (Luo, 2005). MEPDG (2004) uses International Roughness Index (IRI) to evaluate the pavement condition; the IRI is predicted from pavement distresses such as fatigue cracking, rutting and thermal cracking and other factors such as subgrade swelling and frost heave.

2.4.3 Pavement Distresses

As mentioned in section 2.4, traffic load applications, environmental conditions and quality of materials affect the performance of the pavement structure and cause deterioration of the pavement with time. Many types of deterioration or distresses can occur in a pavement during its life. Miller and Bellinger (2003) classified these distresses for flexible pavements as presented in Table 2.2:

Table 2.2 Types of distresses and their measuring unit

Distress Type		Unit of Measurement
1. Cracking		
	1.1. Fatigue cracking	Square Meters
	1.2. Block cracking	Square Meters
	1.3. Edge cracking	Meters
	1.4. Longitudinal cracking	Meters
	1.5. Reflection cracking	Not measured
	1.6. Transverse cracking	Numbers, Meters
2. Patching and Potholes		
	2.1. Patch deterioration	Number, Square Meters
	2.2. Potholes	Number, Square Meters
3. Surface Deformation		
	3.1. Rutting	Millimeters
	3.2. Shoving	Number, Square Meters
4. Surface Defects		
	4.1. Bleeding	Square Meters
	4.2. Polished Aggregate	Square Meters
	4.3. Raveling	Square Meters
5. Miscellaneous Distresses		
	5.1. Lane to Shoulder drop off	Not Measured
	5.2. Water Bleeding and Pumping	Number, Meters

Most analytical pavement design procedures consider fatigue cracking and rutting as the critical measures of pavement performance. However, the MEPDG (2004) also takes into account thermal cracking. While fatigue cracking is related to the tensile strains exerted underneath asphalt concrete and cemented layers only, permanent deformation is formed from the deformation contribution of all layers of the pavement section. Uzan (2004) determined the permanent deformation of asphalt concrete, granular and subgrade layers from equations relating the ratio of accumulated permanent strain to the resilient strain (EPER).

2.4.3.1 Fatigue Cracking

Due to repeated applications of traffic load, bound and stabilised layers undergo tensile strains and stresses, which lead to the initiation of cracks. There are two mechanisms of crack propagation (Arnold, 2004). The common mechanism is bottom up crack initiation and propagation, which can be explained by the action of the repeated load causing bending at the bottom of the layer, resulting in the occurrence of the cracking. The other mechanism which is not clearly defined yet in a mechanistic viewpoint is top down cracking. However, as cited by (Arnold, 2004), in a research study on the top-down cracking of pavements by Thom et al. (2002), most cracks on the major highways in the UK are top-down cracking. It is believed that the tensile stresses or shear stresses at the surface due to heavy tyre pressures are the source of this type of cracking (MEPDG, 2004). Figure 2.7 shows fatigue cracking of a flexible pavement.

Figure 2. 7 Fatigue cracking (PavementInteractive, 7 April 2009)

2.4.3.2 Rutting (Permanent Deformation)

Permanent deformation or rutting is the depression of the pavement surface under the wheel path. In some mechanistic-empirical design methods the total permanent deformation is related to controlling the permanent deformation on the top of the subgrade; for example,

Austroads (2008) flexible pavement designs. However, more logically, as the total rut is the sum of the rutting of all layers of the pavement, other design procedures such as the MEPDG (2004) sum up the strain occurring in all layers (MEPDG, 2004). Figure 2.8 shows rutting of a flexible pavement. According to Uzan (2004) there are two approaches to compute the rut in an analytical model. The first approach was proposed by Barksdale (1972), where the permanent strain of all layers under the wheel load in the same vertical line is calculated and summed up; the second approach consists of computing the rate of permanent deformation caused by each load application and integrating it over the design life of the pavement. Although permanent deformation is obtained by the summation of permanent deformation of all layers, a number of authors including Brown et al. (1985) and Theyse et al. (1996) have suggested that controlling the permanent deformation can be controlled by setting a compressive strain limit on the top of the subgrade layer. However, in this research the permanent deformation of the subgrade soil and lightly stabilised subgrade soils is taken into account as a portion of the total permanent deformation occurring on the surface of the pavement. This may be more logical as each layer of the pavement has permanent deformation under the traffic load and environmental conditions.

Figure 2. 8 Rutting (PavementInteractive, 6 May 2008)

Summary

Section 2.4 presented the definition of the pavement performance which is the pavement's structural or functional condition as a function of elapsed time. Also the factors affecting the pavement performance were explained. The performance of the pavement is predicted from models relating the life of the road pavement to the progression of different types of distresses. Section 2.4.3 presented different types of distresses and their measuring units, among these distresses fatigue cracking and rutting (permanent deformation) are used in most of the analytical pavement design procedures. The focus of this research is on the rutting distress in subgrade layer, therefore performance models predicting the permanent deformations are reviewed in detail.

2.5 Modelling of Permanent Deformation

Several researchers have modelled permanent deformation. A number of these have related the permanent deformation to the number of load repetitions (Barksdale, 1972, Khedr, 1985, PAUTE, 1988, Sweere, 1990, Wolff et al., 1994), others linked it to the applied stresses (Duncan and Chang, 1970, Lashine, 1971, Lentz and Baladi, 1981, Pappin, 1979); and others (Lekarp et al., 2000a, Li and Selig, 1996, Puppala et al., 1999, Puppala et al., 2009) modified

these models through introducing different conditions and parameters, such as moisture change and strength properties. A large amount of interest has been paid to the stress level and the number of load repetitions in the modelling of permanent deformation. However, there are many other effects that have influence on progressing permanent deformation in unbound granular materials and subgrade soils, such as the soil type, particle size distribution, fines content and moisture changes. Table 2.3 summarises the permanent deformation models.

Table 2. 3 Permanent deformation models

Model	Reference	Equation	Parameters
Models that Relate Permanent Deformation to the Number of Load Repetitions			
$\varepsilon_{1,p} = a + b.log(N)$	*Barksdale (1972)*	*2.23*	$\varepsilon_{1,p}$=accumulated permanent strain N = number of load repetitions *a*, *b*, *m*, *A* and *B*= materials' constants
$\varepsilon_{1,p} = a\,N^{b}$	*Sweere (1990)*	*2.24*	
$\varepsilon_{1,p} = (m.N + a).(1 - e^{-bN})$	*Wolff & Visser (1994)*	*2.25*	
$\frac{\varepsilon_{1,p}}{N} = A.N^{-m}$	*Khedr (1985)*	*2.26*	
$\varepsilon_{1,p} = A.[1 - (\frac{N}{100})^{-B}]$	*Paute et al. (1996)*	*2.27*	
Models that Relate Permanent Deformation to the Stress state			
$\varepsilon_{1,p} = \frac{\frac{q}{K.\sigma_3^n}}{1-[\frac{(R_f.q)/2(C.cos\phi+\sigma_3.sin\phi)}{(1-sin\phi)}]}$	*Barksdale (1972)*	*2.28*	$\varepsilon_{s,p}$ = accumulated permanent shear strain; fnN = shape factor; L = stress path length; $q°$ = modified deviator stress $=\sqrt{\frac{2}{3}}\,q$; $p°$= modified mean normal stress $\sqrt{3}.p$ $\varepsilon_{1,p}(N_{ref})$=accumulated permanent axial strain at a given number of cycles N_{ref}; N_{ref} >100; L = length of stress path q= deviatoric stress p= mean normal stress $(q/p)_{max}$= maximum stress ratio P_o= reference stress
$\varepsilon_{s,p} = (fnN).L.(\frac{q^\circ}{p^\circ})^{2.8}_{max}$	*Pappin (1979)*	*2.29*	
$\frac{\varepsilon_{1,p}(N_{ref})}{(\frac{L}{p_0})} = a.(\frac{q}{p})^{b}_{max}$	*Lekarp and Dawson (1998)*	*2.30*	

Continued			
Models that Relate the Resilient Strain to Plastic Strain			
$\varepsilon_{1,p} = a.\varepsilon_r.N^b$	*Veverka (1979)*	*2.31*	ε_r = resilient strain δ_a = permanent deformation for the layer/sublayer (in) N = number of traffic repetitions $\varepsilon_\circ$, β and ρ = material properties ε_r = resilient strain imposed in laboratory test to obtain the above listed material properties, $\varepsilon_\circ$, β and ρ (in/in) ε_v = average vertical resilient strain in the layer/sublayer as obtained from the primary response model (in/in) h = thickness of the layer/sublayer (in)
$\delta_a(N) = \beta_{SG}\left(\frac{\varepsilon_\circ}{\varepsilon_r}\right)e^{-\left(\frac{\rho}{N}\right)^\beta}\varepsilon_v h$	*Tseng and Lytton (1989)*	*2.32*	
$log\frac{\varepsilon_p}{\varepsilon_r} = a_o + b_o * logN$	*Uzan (2004)*	*2.33*	
Models include the number of loads and stress state			
$\varepsilon_p = AN^\alpha[\frac{\sigma_z}{\sigma}]^\beta$	*Ullidtz (1993)*	*2.34*	ε_p = permanent deformation *PD*=permanent deformation (mm) σ_d = deviator stress σ_s = static strength $\sigma_{oct} = \frac{\sigma_1+\sigma_2+\sigma_3}{3}$ σ_{atm} = atmosphere pressure σ_{oct}=(σ_1+2σ_3)/3, $\tau_{oct} = \left(\frac{\sqrt{2}}{3}\right)(\sigma_1 - \sigma_3)$; σ_z is vertical effective stress σ_v is vertical stress on top of pavement foundation (kPa); e is the base of the natural logarithm s = the slope; c= the intersect of the straight line relationship between A and N on a log-log scale $\alpha_1, \alpha_2, \alpha_3, \alpha_4$, a, b, m, A, α *and* β are regression parameters
$\varepsilon_{1,p} = a.(\frac{\sigma_d}{\sigma_s})^m N^b$	*Li and Selig (1996)*	*2.35*	
$\varepsilon_p = AN[\frac{\sigma_{oct}}{\sigma_{atm}}]^\beta$	*Puppala (1999)*	*2.36*	
$\varepsilon_p = \alpha_1 N^{\alpha_2}(\frac{\sigma_{oct}}{\sigma_{atm}})^{\alpha_3}(\frac{\tau_{oct}}{\sigma_{atm}})^{\alpha_4}$	*Puppala (2009)*	*2.37*	
$PD = A\,(e^{B\sigma_v} - 1)$ $lnA = s.ln(N) + c\ or A = e^c N^s$ $PD = e^c\,N^s\,(e^{B\sigma_v} - 1)$	*Theyse (1997)*	*2.38a* *2.38b* *2.38c*	
Using Deflection as a Parameter in a Permanent Deformation Model			
Log (RR) = -7.424 + 1.151 Log (d) + 0.486 Log (N18) + *1.26 Log (σc)*	*Chen and Lin (1999)*	*2.39*	*RR*= the rate of rutting *d*= surface deflection in mm *N18*= load repetitions/(105) in 80KN ESALs *σc*= compressive stress on top of base in kPa. *PD*= permanent deformation *N*=the number of load repetitions *a*, *b* and *m* are regression coefficients

The number of load repetitions given by Equations 2.23 to 2.27 determines the permanent deformation without direct consideration of the stress level. Monismith (1988) concluded that the parameter (b) in power model ($\varepsilon_{1,p} = a\,N^{b}$) depends only on soil type and parameter (a) plays the main role in the development of permanent deformation. A number of researchers have found the power model acceptable for practice especially for fine-grained soils (Elliott et al., 1998). They concluded that the confining pressure is not a significant factor for permanent deformation development.

To account for the influence of the stress level on the permanent deformation, a number of authors have proposed relationships between the permanent deformation, the deviatoric stress and confining pressure (e.g. Lekarp and Dawson, 1998). Two such models proposed by Barksdale (1972) and Pappin (1979), which do not take into account the number of load cycles. These two models neglect the effect of the number of load repetitions.

As mentioned previously (section 2.2.3) an important property of the unbound granular materials in pavement design is the resilient modulus. Resilient properties of the subgrade materials and their resistance to the permanent deformation are necessary for an appropriate pavement design. Veverka (1979), Equation 2.31, correlated resilient and plastic properties. According to Lekarp et al. (2000a), Sweere (1990) could not confirm this equation for base course materials and sands. However, MEPDG (2004) used Tseng and Lytton's equation (Tseng and Lytton, 1989), Equation 2.32, for determining the rutting of the subgrade layer in a pavement system. Also Uzan (2004) proposed a model for clayey subgrades to predict the ratio of permanent deformation to resilient strain from the number of load repetitions as presented by Equation 2.33; these two models include resilient strain in the model. In Chapter Five an equation has been modified to consider deviatoric stress and resilient modulus for subgrade soils investigated in this research.

Lekarp and Dawson (1998) conducted a series of repeated load triaxial tests on five different aggregates and compared the data with the models (Equations 2.23 to 2.31). Their work showed that the Paute et al. (1996) model has the least error in most cases. Then a model developed by Lekarp et al. (1998), Equation (2.30), that includes the maximum shear stress ratio $(q/p)_{max}$ and the length of the stress path (L). The increase of the maximum shear stress ratio results in an increase in accumulation of permanent strain.

Li and Selig (1996) modified the power model which relates the rate of cumulative plastic strain to the number of repeated load applications. They believed that introducing some properties of the soil such as moisture content and density directly into the model is neither common nor convenient. Therefore they incorporated the static strength of the soil to represent moisture content and density in the general power model, see Equation 2.35. Li and Selig (1996) constructed a railroad track to check the validity of the modified model and found a good correlation between the subgrade plastic deformations predicted from the model and the experimental test results.

Puppala et al. (1999) modified the model developed by (Ullidtz, 1993), Equation 2.33, which included the vertical stress effects. They introduced the octahedral stress (σ_{oct}) into the model described by Equation 2.36 to account for confining pressure which they believed it had influence on permanent deformation of soils. Puppala (1999) carried out repeated load triaxial tests on three soil types to find the parameters of the model and he found a coefficient of determination ranging from 0.79 to 0.93. Field evaluations also verified the predicted plastic deformation.

Puppala et al. (2009) reported the drawback of models that combine the effect of deviatoric stress and confining pressure on plastic strains. To account for this they developed a four-

parameter permanent strain model which separated the influence of deviatoric stress and confining pressure, see Equation 2.37.

Theyse (1997) used the data collected from a Heavy Vehicle Simulator (HVS) test to develop a model of permanent deformation that related the permanent deformation to the number of repeated loads and the vertical stress on the top of the pavement foundation. The data obtained from a Multi-Depth Deflectometer (MDD) was used to develop the model further. 'The MDD system is basically a stack of linear variable displacement transducers (LVDTs) referred to as MDD modules, installed at predetermined depths in the pavement structure with a reference point at the anchor, normally at 3 m depth' (De beer et al., 1989). In the model developed by Theyse (1997), the permanent deformation, PD, is determined as presented in Equation 2.38a. From the relationship of the number of load repetitions and coefficient (A) Equation 2.38b is obtained. Substituting A in Equation 2.38a yields Equation 2.38c.

Chen and Lin (1999) used data from the Texas Mobile Load Simulator (MLS) to develop a model predicting permanent deformation. The model relates the rutting to surface deflection, load repetitions and compressive stress at the top of the base, see Equation 2.40.

$$R = -5.841 + 25.419\, d + 0.29\, N_{18} - 0.015\, \sigma_c \qquad (2.40)$$

Where R is rutting in mm; d is surface deflection in mm; $N18$ is load repetitions/(10^5) in 80KN ESALs; σ_c is compressive stress on top of base in kPa.

Then a ten-based logarithm was applied to Equation 2.38 to obtain Equation 2.41:

$$\text{Log}(R) = -3.17 + 0.141\, \text{Log}(d) + 0.564\, \text{Log}(N_{18}) + 1.505\, \text{Log}(\sigma_c) \qquad (2.41)$$

Then Equation 2.39 has been transformed to model the rate of rutting (i.e. the future condition) as presented by Equation 2.39 in Table 2.3.

As demonstrated in this section the progress of the permanent deformation were modelled using different parameters such as stress state, resilient strain, surface deflection, material

properties and the number of load repetitions. In this research a performance model for predicting the permanent deformation was attempted for unstabilised and modified subgrade soils in which the deviatoric stress, resilient modulus and the number of load repetitions is considered.

Summary

In this section a detailed literature was reviewed on permanent deformation modelling. The development of permanent deformation in these models is related to the number of load repetitions, stress state, resilient strain, deflections and material properties. However, some researchers developed their model taking into consideration one or two of these parameters. The performance model comprises a major part of analytical pavement design therefore a performance model was developed in this research to take into consideration a higher number of parameters, especially when the deterioration of the modified subgrade soils is included in the design procedure. Chapter Five in addition to presenting the development of the performance model for prediction of the permanent deformation demonstrates in detail the factors affecting the development and progress of permanent deformation for stabilised and unstabilised subgrade soils.

2.6 Subgrade

Subgrade layers are an important component of a road pavement; their properties affect the selection of the upper layers' materials and properties (Austroads, 2008). Subgrade layers with high quality materials minimise the chance of subgrade failure, otherwise however good the quality of the upper layers, the pavement section may still be susceptible to failure (Mokwa and Akin, 2009).

2.6.1 Subgrade Soil Characterisation

As demonstrated in sections 2.2.1 and 2.2.2, both methods of pavement design, whether they are empirical or analytical, take into account the characterisation of the subgrade soil. In early pavement designs, the characterisation of the subgrade simply consisted of the classification of the soils; later on strength tests were introduced to characterise the subgrade soil.

Laboratory tests for subgrade soil strength and stiffness characterisation include the California Bearing Ratio (CBR), Resistance value (R-value) and the resilient modulus test. In-situ methodologies also exist and these include: the falling weight deflectometer method, plate load and the dynamic cone penetrometer (Mokwa and Akin, 2009). Subgrade CBR values of more than 10 are necessary for pavement sections which are required to carry anything other than low traffic volumes (Mokwa and Akin, 2009). There is general agreement that subgrade soils with CBR values of less than 10% can deflect excessively under traffic loads, causing the subbase to deflect similarly (Schaefer et al., 2008). More lately analytical pavement design methodologies have moved away from using the CBR to characterise subgrades and specify the use of the resilient modulus instead; this is because the CBR value represents shear strength of the soils, rather than the mechanical properties (Brown et al., 1996). An example is the AASHTO design guide 1986 and its later versions.

2.6.2 Criteria

Most mechanistic methods use vertical strain on the top of the subgrade as a design criterion for limiting permanent deformation (Read and Whiteoak, 2003); MEPDG, 2004; Austroads, 2008). The limiting permanent deformation can be the compressive strain on the top of the subgrade or the rut depth at the surface of the pavement. However, research by Theyse et al. (2006) suggests that total deflection on the top of the subgrade to be a better indicator of

permanent deformation. Section 7.6 of Chapter Seven presents a detailed discussion of the different performance criteria applied in analytical pavement design procedures.

2.6.3 Moisture in Subgrade

The resilient response of subgrade materials is affected by many factors including, moisture change. Any increase in moisture content tends to result in a decrease in resilient modulus value and a corresponding increase of permanent strain. Further, research by (Frost et al., 2004; Uthus et al., 2006; Soliman et al., 2009) showed that seasonal variation of the moisture in the subgrade affects the resilient modulus value. Increases of moisture resulted in a decrease in the resilient modulus of different types of soils by different percentages; these results are necessary in pavement design procedure. Soils with more than 15% fine fraction are most complex fill as their behaviour significantly is affected by water content before and after construction (Nowak and Gilbert, 2015). According to Nowak and Gilbert (2015) a good management of surface water and ground water is essential for earth fill as the water affects significantly the strength of the soils; especially some types of soils such as silts, which are susceptible to water. Section 4.2.1 of Chapter Four discusses the effect of moisture on the resilient modulus value in detail. The rate of this seasonal moisture change is controlled by the type of the subgrade soil; for example sandy soils reach a wet condition faster than clay soils (Austroads, 2008). Permanent deformation parameters are also affected by variation of moisture content; such that, for the same stress level at a range of moisture contents, the permanent deformation development changes (Lekarp et al., 2000a). Werkmeister et al. (2003) found this difference for Huurman-model (Huurman, 1996) parameters at two moisture contents for one unbound granular base course material.

The MEPDG (2004) uses a sophisticated model: the Enhanced Integrated Climatic Model (EICM), for the impact of climatic condition on pavement and subgrade materials in

mechanistic-empirical pavement design. Regardless of what level of data input (level 1, 2 and 3) are applied, the MEPDG (2004) incorporates the effect of moisture and temperature in the design procedure. An adjustment factor for adjusting the resilient modulus value is determined from the EICM model, which considers the moisture, suction and temperature factors; see Equation 2.45.

$$M_R = F_{env}\, M_{Ropt} \tag{2.45}$$

Where M_R is the adjusted resilient modulus value considering environmental conditions; F_{env} is the adjustment factor; and M_{Ropt} is the resilient modulus value at optimum moisture content.

Then the adjustment factor is determined from Equation 2.46.

$$log(F_{env}) = log\frac{M_R}{M_{Ropt}} = a + \frac{b-a}{1+EXP\left(ln\frac{-b}{a}+K_m\,(S-S_{opt})\right)} \tag{2.46}$$

Where a is the minimum of $\frac{M_R}{M_{Ropt}}$; b is maximum of $log\frac{M_R}{M_{Ropt}}$; K_m is the regression parameter; and (S-S_{opt}) is the variation in degree of saturation in decimal.

Gupta et al. (2007) suggested two models to include the effect of soil suction on resilient modulus implicitly and explicitly (Equations 2.47 and 2.48). The models are given by the following:

$$(M_r)_{us} = K_1 P_a \left(\frac{\sigma_b}{P_a}\right)^{k_2} \left(\frac{\tau_{oct}}{P_a}+1\right)^{k_3} + k_{us} P_a \Theta^k (u_a - u_w) \tag{2.47}$$

$$(M_r)_{us} = \left[K_1 P_a \left(\frac{\sigma_b - 3k_6}{P_a}\right)^{k_2} \left(\frac{\tau_{oct}}{P_a}+k_7\right)^{k_3}\right] + \alpha_1 (u_a - u_w)^{\beta_1} \tag{2.48}$$

Where:

$(M_r)_{us}$ = resilient modulus of unsaturated soil

P_a = atmospheric air pressure

σ_b = bulk stress = $\sigma_1 + \sigma_2 + \sigma_3$

τ_{oct} = octahedral shear stress = $\frac{\sqrt{2}}{3}(\sigma_1 - \sigma_3)$ for $\sigma_2 = \sigma_3$

k_{us} = constant, linear fitting coefficient

$\Theta = \frac{\theta}{\theta_s}$ = normalized water content; θ is the volumetric water content; θ_s is saturated volumetric water content

k = fitting parameter

$u_a - u_w$ = soil suction

α_1 and β_1 are intercept and slope of the $(M_r)_{us}$ at a given σ_b and τ_{oct} versus suction relationship

K_1, K2, K3, K6, K7 are regression parameters.

The sources of moisture in a subgrade and pavement system can be one of or a combination of: the seepage from high ground, pavement edge, surface discontinuities and capillary action or vapour movement from high water table (Christopher et al., 2006).

To control or minimise the effect of moisture in a pavement system one of the following approaches may become necessary (Christopher et al., 2006):

- *Prevent moisture from entering the pavement system; this might be achieved by sufficient cross and longitudinal slopes to speed up the surface runoff of water and sealing surface cracks to prevent infiltration of water.*
- *Use materials that are insensitive to the effects of moisture; cement and asphalt stabilised soils for example.*
- *Quickly remove the moisture that enters the pavement system; there are drainage features that are used to remove moisture from a pavement system such as under drains and ditches.*

Using stabilisers such as cement can help to ensure the stability of foundation layers in case of the ingress of water into the subgrade from different sources. This research focuses on the second approach in which a variety of agents or additives can be mixed with the soil to increase its resistance to permanent deformation.

Summary

In this section the importance of the subgrade soils was demonstrated. The compressive strain on the top of the subgrade is used extensively in analytical pavement design procedures therefore the characterisation of the subgrade soils is fundamental in pavement design. Afterwards the effect of the moisture on the behaviour of the subgrade soils was explained and discussed and models that determine the resilient modulus values at different moisture contents were presented. The degree of saturation as discussed in Chapter Four has an effect on the resilient modulus value, this has been verified from experimental work in this research and an equation from the literature was selected for the purpose of the design.

2.7 Subgrade Soil Stabilisation

As mentioned in section 2.6.3, subgrade soils are exposed to moisture changes from different sources. The existence of moisture, as will be demonstrated in detail in Chapters Four and Five, reduces the strength and mechanical properties of the subgrade soils, in terms of resilient modulus and resistance to permanent deformation. Li and Selig (1998) suggested two methods by which the accumulation of the permanent strain can be controlled. The first method is to improve the subgrade layers using a stabiliser agent which increases their resistance to the applied loads; and the second is to reduce the induced stresses. To reduce the effect of the applied stresses, overlay layers must be of good quality and their thicknesses need to be increased. However, the shortcoming with the second approach may come from the fact that even by controlling the stress level, the subgrade layer could still be exposed to moisture change and undergo high permanent deformations. Therefore, in these circumstances the improvement of the soil with a stabiliser may be a superior solution for permanent deformation resistance (Rasul et al., 2015).

2.7.1 Stabilisation Methods and Types

The earliest record of using soil-cement roads is believed to be of roads constructed in the USA, near Johnsonville in 1935 (Bowers et al., 2013). Since then a wide range of soil stabilisation types and methods have been reported in the literature and are practiced in road pavement construction. In the following paragraphs the types of stabilisations, different classifications, characterisation tests and the design criteria for stabilised subgrade layers are discussed.

The stabilisation of the subgrade soils can be classified into mechanical, cementitious and asphalt stabilisation (Jones et al., 2010). Mechanical stabilisation can be carried out by compaction, blending or using geosynthetics. Cementitious stabilisation includes cement, lime, fly ash, cement kiln dust, lime kiln dust and blast furnace slag stabiliser agents. Types of asphalt stabilisation are: asphalt emulsion, foamed asphalt, cutback or liquid asphalt stabilisation and tar (Jones et al., 2010). However, chemical stabilisation is widely used for subgrade and granular layers. Figure 2.9 shows a methodology for determining the additive from the index properties of subgrade soils. It has been developed by the Texas Department of Transportation based on modifying charts developed by Currin et al., 1976, Smith and Epps, 1975 and Little et al., 1995.

In order to understand the applications of lime, cement and combination of both lime and cement for stabilisation of soils for general fill and capping, the Design Manual of Roads and Bridges (DMRB), volume 4, section 1, part 6 presents a table (Table 2.4) in which the application of lime and cement to different soil classes and various purposes has been presented.

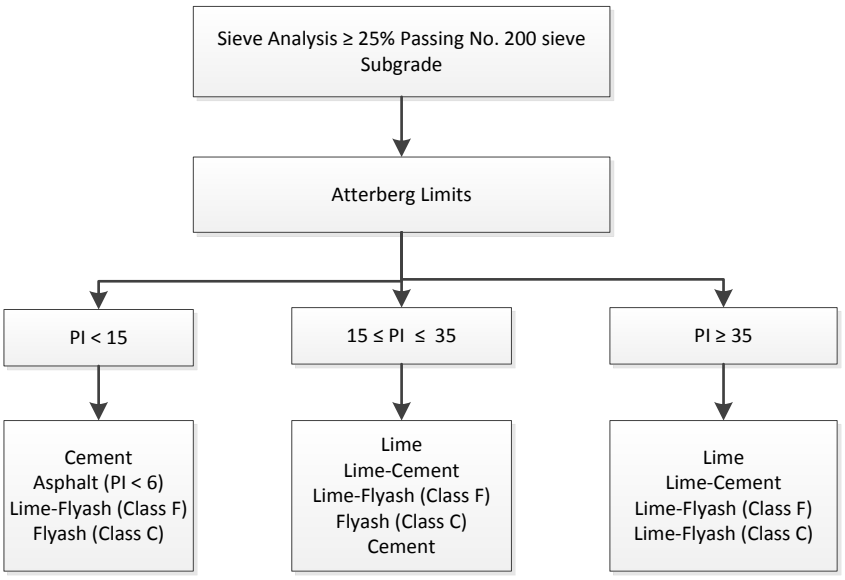

Figure 2. 9 Additive selection for subgrade soils using soil classification (After TxDOT (2005))

Table 2. 4 Applications of Lime and Cement Treatment for General Fill and Capping

Constituent	Process	Application	Initial Class	Primary purposes of constituent	Resultant Class
Lime	Improvement	General granular fill	Class U1A	Reduction in mc (or increase in MCV)	Class 1A, Class 1B, Class 1C
Lime	Improvement	General cohesive fill	Class U1A	Increase in MCV (or reduction in mc); reduction in PI	Class 2A, Class 2B, Class 2C, Class 2D, Class 2E
Lime	Improvement	General chalk fill	Class U1A	Reduction in mc	Class 3
Lime	Stabilisation	Selected cohesive fill capping	Class 7E	Increase in MCV (or reduction in mc); increase in bearing ratio; reduction in PI	Class 9D
Cement	Stabilisation	Selected granular fill capping	Class 6E	Increase in bearing ratio	Class 9A
Cement	Stabilisation	Selected cohesive fill capping	Class 7F, Class 7G	Increase in bearing ratio	Class 9B, Class 9C
Lime and cement	Stabilisation	Selected cohesive material capping	Class 7I	Increase in MCV (or reduction in mc); increase in bearing ratio; reduction in PI	Class 9E
Lime and cement	Stabilisation	Selected granular fill capping	Class 6R	Reduction in mc (or increase in MCV); increase in bearing ratio	Class 9F

Note: 1. Improvement – rendering unacceptable material acceptable 2. Stabilisation – change in use of acceptable material 3. mc = moisture content 5. PI = Plasticity Index 4. MCV = Moisture Condition Value 6. Bearing ratio = California Bearing Ratio

In general, chemical stabilisers are classified into three main groups: (i) traditional stabilisers which depend on pozzolanic reaction, such as lime, Portland cement and fly ash; (ii) by products such as lime kiln dust (LKD) and cement kiln dust (CKD); and (iii) non-traditional stabilisers such as sulfonated oils, ammonium chloride, enzymes, polymers and potassium components (Little and Nair, 2009). According to ARMY (1994) the factors that are considered in selecting the stabiliser type are: the soil type, the required strength and durability and the environmental conditions. The combination of two or more of these stabilisers compensates for the deficiency of each of the stabilisers in improving the soil. For instance, the stabilisation of plastic clays with cement or bitumen alone may not provide a satisfactory stabilisation result. However, if lime is added, the plasticity reduces and the cement or bitumen is mixed adequately with the soil.

Typically, the classification of the stabilisation was dependent on the type of the stabiliser, for example lime stabilisation or cement stabilisation. However, with the new mechanistic pavement design procedures the stabilisation types are classified according to their performance (Hicks, 2002). These types are in three categories in terms of their performance criteria: (i) unbound material; for which the thickness is governed by subgrade strain, this type has no significant tensile strength; (ii) modified material; the design criteria is subgrade strain and modification is carried out to increase the strength and to reduce the moisture and frost susceptibility of fine grained soils; (iii) bound material; the addition of a stabiliser of this type increases the tensile strength of the layer and the performance criteria are fatigue and erosion (Hicks, 2002). The research herein applied the second criterion in order to conform it to the method of analysis used in the proposed stabilised subgrade design procedure, in which the subgrade soil is lightly stabilised.

Whilst the most widely used and recognised analytical road pavement design procedures, allow for the use of stabilised subgrade layers, they do not take into account the deterioration of the mechanical properties of these layers. Such design procedures include using: USA (ASHTO MEPDG, Texas DOT, Florida DOT and Illinois DOT); ii) UK design method; French design method and Australian design methods (Queensland DOT, Victoria design method and Roads and maritime services design methods). A useful summary of these design methods to the consideration of stabilised subgrade layers is given by Jameson (2013).

2.7.2 Characterisation of Stabilised Subgrade Soils

As explained in section 2.2, the first step of any pavement design method is to characterise the pavement materials. Of these materials, the subgrade soil first must be characterised to decide on the upper layers' materials and thicknesses.

For subgrade soils or any other stabilised layers, the material mix design, structural design and construction of the layer are three important considerations for a successful design (Hicks, 2002). Two general methods are carried out for stabilised layer construction: (i) in-situ stabilisation; and (ii) pug-mill type stabilisation. Regarding the structural design, the stabilised subgrade layer is considered to be an unbound material without a performance criterion for design purposes; however if the stabilisation is for making a working platform and increasing the strength properties, it is treated as a subbase layer (Hicks, 2002). The purpose of the stabilisation mix design is to optimize the combination of soils and stabilisers to achieve the requirements of strength and durability; the quantity not in excess of optimum stabiliser content, causing other problems to the pavement, neither less than of optimum to deteriorate early (Paige-Green, 2008).

Different properties and characteristics of the stabilised subgrade soils are used for performance assessment. According to (Hicks, 2002) the most important of these

characteristics are: strength, durability, shrinkage, setting and curing, moisture susceptibility, erodability, stiffness, fatigue performance and variability. The most common strength test for stabilised soils is unconfined compressive strength (UCS) (Chittoori et al., 2012, Little, 1987, Solanki et al., 2009, Vorobieff and Murphy, 2003, White et al., 2005, Wu et al., 2011b). However, as a requirement input of analytical pavement design methods, research on the behaviour of the resilient modulus of stabilised subgrade soils has increased (Chauhan et al., 2008, Puppala et al., 2011, Rout et al., 2012, Solanki et al., 2010). A brief summary of the literature is presented below.

Rout et al. (2012) utilised AASHTO T307 to study the behaviour of the resilient modulus of lime-cement treated subgrade soils. For all the three soils they considered, untreated subgrade soils showed a decrease in the resilient modulus with an increase of deviatoric stress; in contrast the treated subgrade soils showed increased resilient modulus with deviatoric stress. They used a constitutive model proposed by Witczak and Uzan (1988) to characterise the resilient modulus determined from laboratory tests. Witczak and Uzan's (1988) model relates resilient modulus to bulk stress (θ) and octahedral shear stress (τ_{oct}). In addition to resilient modulus, Rout et al. (2011) tested the soils for unconfined compressive strength (UCS) in order to develop a correlation equation for resilient modulus.

Chittoori et al. (2012) studied the premature failure of eight treated high plastic clays with different clay mineralogy. Samples were subjected to 21 cycles of 5 hours wetting in water followed by 42 hours of drying in an oven a temperature of 60˚C. Stiffness values which were used in the numerical modelling were calculated from the stress-strain relation obtained from an unconfined compressive strength test and compressive strains on top of the subgrade were determined. The values of strains on the top of the subgrade are used later in performance models for pavement design and analysis.

Solanki et al. (2010) determined the resilient modulus of four types of stabilised subgrade soils; three of these soils were tested for modelling and the other used for validation. In order to calculate the resilient modulus they used four different constitutive models to determine coefficient *k*-values. An increase in resilient modulus was seen for all types of stabilisers, nevertheless the cement kiln dust stabilised samples showed the greatest increase in resilient modulus values. The models were evaluated using statistics (ratio of standard deviation of errors to the standard deviation of samples and the square of coefficient of correlation R^2) and via visual assessment to compare the predicted and measured values. From the test results, Solkani et al. (2010) developed correlations between the resilient modulus coefficients (k_1, k_2 and k_3) and compacted specimen properties, including the UCS, soil properties such as the plasticity index and additive properties such as silica content.

The Mechanistic Empirical Pavement Design Guide (MEPDG), 2004 assumes no permanent deformation in stabilised layers. However, laboratory and field research available in the literature show that the stabilised subgrade layers undergo permanent deformation with an increase in applied traffic loads.

For example, Chauhan et al. (2008) carried out laboratory permanent deformation tests on a silty sand subgrade soil stabilised with fly ash and two types of fibres with different stabilisation combinations. Stabilisation of the soil with fly ash and optimum synthetic fibre content reduced the permanent deformation from 3.5% to 2.4%; while stabilisation with fly ash and optimum coir fibre content reduced the permanent deformation to 2.15%.

Wu et al. (2011b) studied chemically stabilised clayey subgrade soils. They found that stabilisation with cement resulted in higher modulus values and a better performance in wet conditions, than lime stabilisation, for silty clays. They utilised durability and wetting-drying

tests to determine the strengths of treated and untreated subgrade soils. Thereafter they constructed two pavement sections, each of which had the same pavement layer properties and thicknesses, except for the subgrade layer which was built using lime and cement stabilised soils respectively. Both sections exhibited ruts which exceeded 12.5 mm (0.5 inches) in depth. However, the cement stabilised subgrade layer performed better than the lime stabilised layer. For the former, 786,000 ESALs loads were required to achieve 12.5 mm of rut depth; while for the latter the same rut depth was achieved after only 121,000 ESALs. It was found that for the cement stabilised system, approximately 85% of permanent deformation was due to the crushed stone base layer and only a small portion was due to the cement stabilised subgrade layer. For the lime stabilised subgrade layer, the permanent deformation contributed up to 20% of the total permanent deformation.

Abu-Farsakh et al. (2014) studied the resilient modulus and permanent deformation behaviour of very weak subgrade soils treated/stabilised with cement. The samples were prepared at three different moisture contents, at the wet of optimum moisture content for three types of soils, simulating the wet conditions of the subgrade soils during construction. The resilient modulus and permanent deformation were found to be a function of the water to cement ratio. An increase in the water to cement ratio was found to increase the permanent deformation and decrease the resilient modulus. The permanent deformation decreased from 4% to 0.08% with an increase in cement content from 1% to 8%.

Summary

This section presented the types and methods of the subgrade stabilisation. It was demonstrated that stabilisation can be classified as mechanical, cementitious and asphaltic. The selection of stabiliser type and ratio depends on the soil index properties, application and purpose of improvement. Also in this research a number of researches were summarised that

assessed the use of stabilisation techniques for improvement of subgrade soil properties such resilient modulus and resistance to permanent deformation and including these properties within pavement design. However, different classification method considering the performance criteria of stabilised subgrade layer is demonstrated. In this classification method there are three categories in terms of their performance criteria as presented in section 2.7.1. In this research the soils were modified to improve the susceptibility of soils to moisture, in this case the performance criterion is subgrade strain and was used within the pavement design.

2.8 Summary

This chapter presented different structural pavement design procedures and their associated input requirements. Analytical pavement design procedures were reviewed in detail and the main steps in the design procedure were described. These steps were associated with determining materials' properties; developing and utilising appropriate response performance models; and establishing design life and associated criteria. As the focus of this research is on subgrade soils, their characterisation and sensitivity to moisture changes were demonstrated. The resilient modulus value which is a key design element was discussed and the permanent deformation property and its prediction models were demonstrated in detail. Finally, stabilisation of the subgrade soils was reviewed. It was found that the laboratory and field tests associated with this stabilisation, described in the literature, were carried out without considering the durability of the subgrade soils. However, as the stabilisation includes a very wide range of stabiliser types and stabiliser ratios, the durability studies are of vital importance for a long term assessment of stabilised subgrade soil behaviour for resilient modulus and permanent deformation. To address this, the suite of tests on stabilised soils described in Chapters Four and Five of this research show how the resilient modulus and permanent deformation behaviour of stabilised subgrade soils can be influenced when durability is taken into account.

CHAPTER THREE

EXPERIMENTAL PROGRAMME AND MATERIALS USED

3.1 Introduction

In order to complete this study, it was necessary to undertake a laboratory investigation on both unstabilised and stabilised subgrade soils to determine their properties; which then could be input into pavement analysis/design. One of the significant variables in operation is the change in the moisture content and this study examined the effect of this change on the properties of soil and its impact on the performance of road pavement.

3.2 Materials

3.2.1 Subgrade Soils Used and Index Properties

This study was designed to simulate conditions in Kurdistan, including typical soil types. In order to achieve the former all the tests were conducted in terms of a range of standards described later in this chapter and in Chapters Four and Five. In order to simulate the latter, three types of subgrade soils: A-4, A-6 and A-7-5 as per the AASHTO soil classifications, were manufactured and investigated. These soils were typical of subgrade soils found in Kurdistan in the area of Erbil, see Figure 3.1.

In general, subgrade soils in Kurdistan are classified under the A-4, A-6, A-7-5 and A-7-6 categories. For the area around Erbil in Kurdistan, there are typically16 types of soils; their properties are summarized in Table 3.1. Only the first three categories were examined as they occur more frequently in the area of interest. The aim was to simulate three different soil classifications that fall within the property ranges specified in Table 3.1. After many trials the combination of 10% kaolin plus 90% quarry fines, 25% kaolin plus 75% quarry fines and 25% quarry fines plus 75% kaolin were obtained for soils A-4, A-6 and A-7-5, respectively as

per the AASHTO soil classification system. The properties of these three soils are presented in Table 3.2.

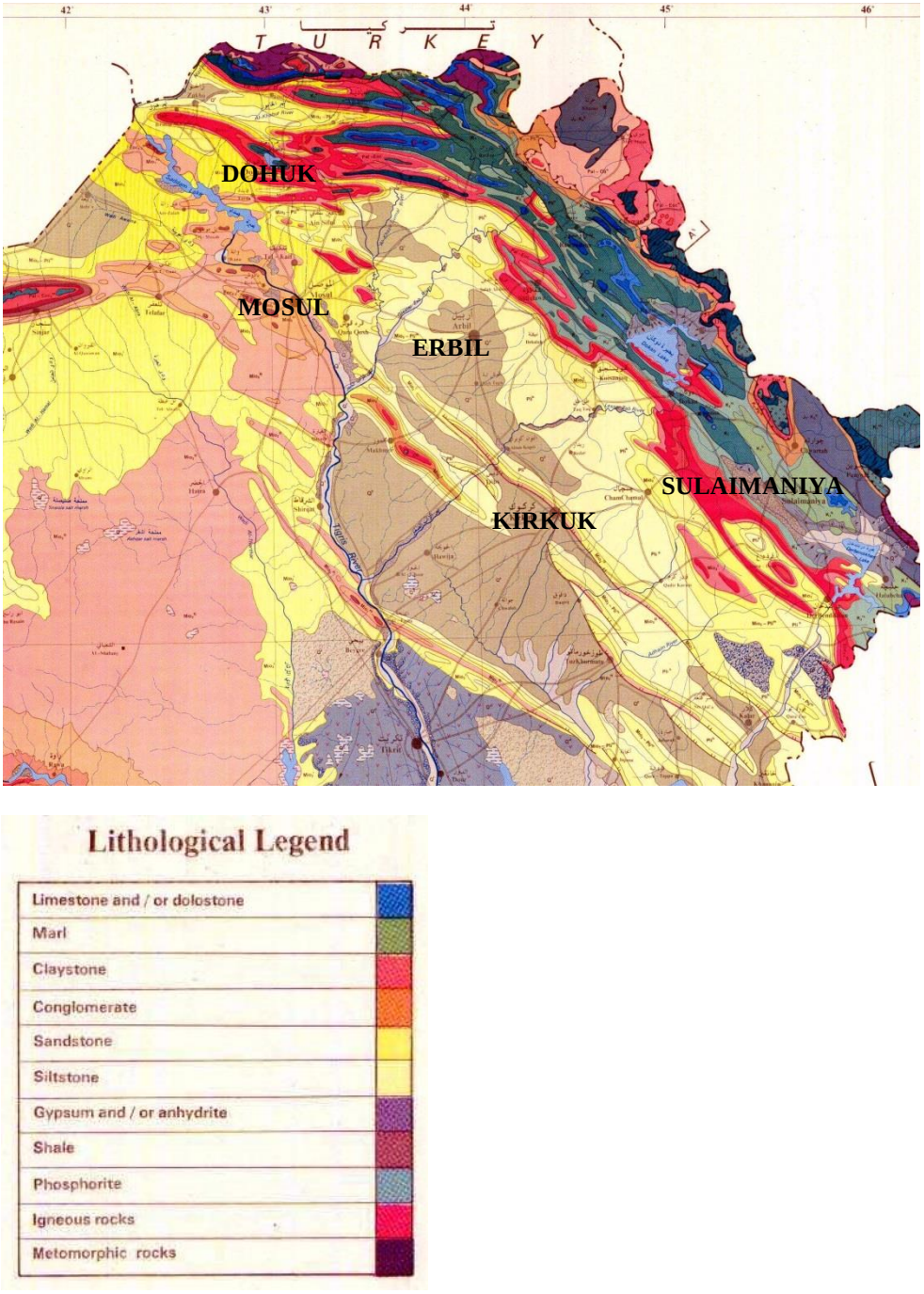

Figure 3. 1 Geology map of Kurdistan (after Sissakian, 1997)

Table 3. 1 Properties of subgrade soil found in Kurdistan near Erbil

Property or test type	Range	Requirement (Iraqi specification) SORB*
% passing sieve 75μm	63--98	–
Maximum dry density (gm/cm³)	1.75--2.04	1.7 Min.
Optimum moisture content (%)	9.6--17.0	–
CBR value at 95% compaction (%)	3.78--10.1	4 Min.
Liquid limit (%)	35--48	55 Max.
Plasticity index	10--20	30 Max.
Organic material (%)	0.02--0.39	12 Max.
Total soluble salts (dilution 1:50)	0.17--0.31	10 Max.
Specific gravity	2.65--2.74	–
Clay content (%)	50--64	–
Silt content (%)	33--47	–
Sand content (%)	2--6	–
Gravel content (%)	0--1	–
AASHTO soil classification	A-4, A-6, A-7-5, A-7-6	

* The Standard Specification for Roads & Bridges (SORB)

After deciding on these proportions for each soil, the wet particle size distribution and sedimentation tests were carried out. The results are shown in Figure 3.1. From the particle size distribution, the quarry fines were separated into three different groups according to particle size: from 4.47 mm to 1.18 mm; from 1.18 mm to 0.30 mm; and finer than 0.30 mm. The required proportion of kaolin was then added to a pre-determined proportion of quarry fines from the three differently sized groups. The separated size fractions were remixed later according to the particle size distribution for each soil type. This procedure guaranteed the homogeneity of the samples.

Table 3. 2 Properties of simulated soils, A-4, A-6 and A-7-5

Property and test type		A-4	A-6	A-7-5
% Passing	Sieve 5.00 mm	100.00	100.00	100.00
	Sieve 3.35 mm	100.00	91.41	98.97
	Sieve 2.00 mm	100.00	82.00	98.00
	Sieve 1.18 mm	99.95	76.45	97.49
	Sieve 0.600 mm	89.66	71.56	96.97
	Sieve 0.425 mm	85.45	69.81	96.74
	Sieve 0.300 mm	81.59	68.20	96.53
	Sieve 0.212 mm	79.30	67.23	96.35
	Sieve 0.150 mm	77.07	66.18	96.01
	Sieve 0.075 mm	69.27	61.64	93.79
Maximum dry density (gm/cm^3)		1.913	1.889	1.485
Optimum moisture content (%)		10.3	11.0	21.5
Liquid limit (%)		21.0	35.0	51.0
Plasticity index		6.0	14.0	20.0
Specific gravity		2.72	2.71	2.64
Clay content (%)		16	26	52
Silt content (%)		50	34	41
Sand content (%)		34	22	5
Fine gravel content (%)		0	18	2

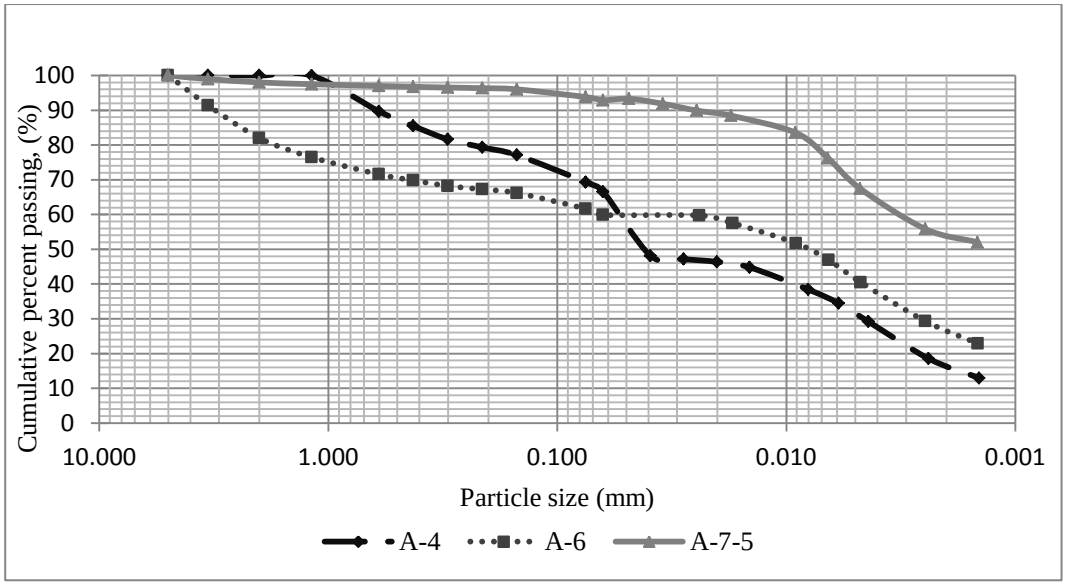

Figure 3. 2 Particle size distribution of the three soil types

Discussion

Two soils were available at the laboratory of the University of Birmingham to simulate the soils used in this research, which presented in section 3.2.1. These two soils were Kaolin and limestone quarry fines. Many trials were attempted to prepare soils close in properties to those found in Erbil area, these properties are tabulated in Table 3.1. These properties are recommended for subgrade soils in the Standard Specification for Roads & Bridges (SORB) of Iraqi specification. The simulation attempts resulted in obtaining soils that reflect the soil types found in Kurdistan/Erbil; they were A-4, A-6 and A-7-5 according to AASHTO soil classification system. However, not all the properties of the simulated soils concur with those of the Erbil area, for example the plasticity index of soil A-4 is less than the range available for these three soils, see Tables 3.1 and 3.2. Nevertheless, these soils can be accepted to represent soils found in the area of Erbil, because the AASHTO classification system includes a wide range of materials' properties and index values.

3.2.2 Stabilisers

In order to improve deformation resistance and durability of subgrade soils, they are stabilised with lime or cement or a combination of both lime and cement, depending on the soil type and application. Section 2.7.1 describes the conditions of stabiliser selection for the stabilisation of soils. However, in this research normal portland cement and quick lime were used for stabilisation of subgrade soils to assess the suitability of using a stabiliser type and its content for different soil types; since during road construction different types of soils may occur and it is more practicable to have one stabiliser type for the whole road subgrade stabilisation. The proportion of lime was determined from the Initial Consumption of Lime test (ICL), BS 1924-2:1990, section 5.4. The pH value of 12.4 at 25°C is required to preserve the reaction between the lime and the stabilised material. The test consists of preparing five soil samples of 20 gm

each, and then a range of lime proportions of 2%, 3%, 4%, 5% and 6% is added to these soil samples. If the pH value of 12.3 is reached at 2% lime content, the test is repeated with lower proportions of lime content (BS 1924-2:1990, section 5.4.7.4). Also if the pH value of 12.4 is achieved at 3% lime content the test is repeated using additional lime contents of 0.5%, 1.0%, 1.5% and 2.5%. However if the pH value of 12.4 is achieved at 5% lime content, the test is repeated with higher proportions of lime content. The initial consumption of lime content of 1.3%, 1.13% and 1.5% lime content is determined at 12.4 pH value for soils A-4, A-6 and A-7-5, respectively. Therefore, whenever lime and cement are used in combination for the stabilisation of these three soils an amount of 1.5% lime content is used.

The notation of the different stabilisation proportions are as below and are used throughout this thesis:

- 2% cement content, 2%CC.
- 4% cement content, 4%CC.
- 2% cement content plus 1.5% lime content, 2%CC+1.5%LC.
- 4% cement content plus 1.5% lime content, 4%CC+1.5%LC.

These soils were lightly stabilised to improve the subgrade soil properties and protect them against moisture changes. At the same time as the subgrade layers have a subbase and/or granular base overlays, the modular ratio aspect of the layered system should be secured and in no cases should the resilient modulus of the subgrade be greater than the upper layers; this is explained in the pavement design examples in Appendix F. All these samples were cured in a moist cabinet at a temperature of 21±1.7°C and a humidity of 100%. Furthermore, the samples were enclosed in plastic bags to protect them from dropping water drops and to maintain a constant condition for all the samples.

3.3 Repeated Load Triaxial Tests (RLTT)

The repeated load triaxial test was conducted for two purposes; first to determine the resilient modulus value and secondly to investigate the permanent deformation of subgrade soils. The repeated load triaxial apparatus was supplied by Cooper Technology Ltd; it was the NU 14 for testing in accordance with AASHTO T307 (see Figure 3.3). It was used for ascertaining both resilient modulus and permanent deformation. A data sheet for collecting the data information is shown in Appendix A, which was modified from research by (Abushoglin and Khogali, 2006).

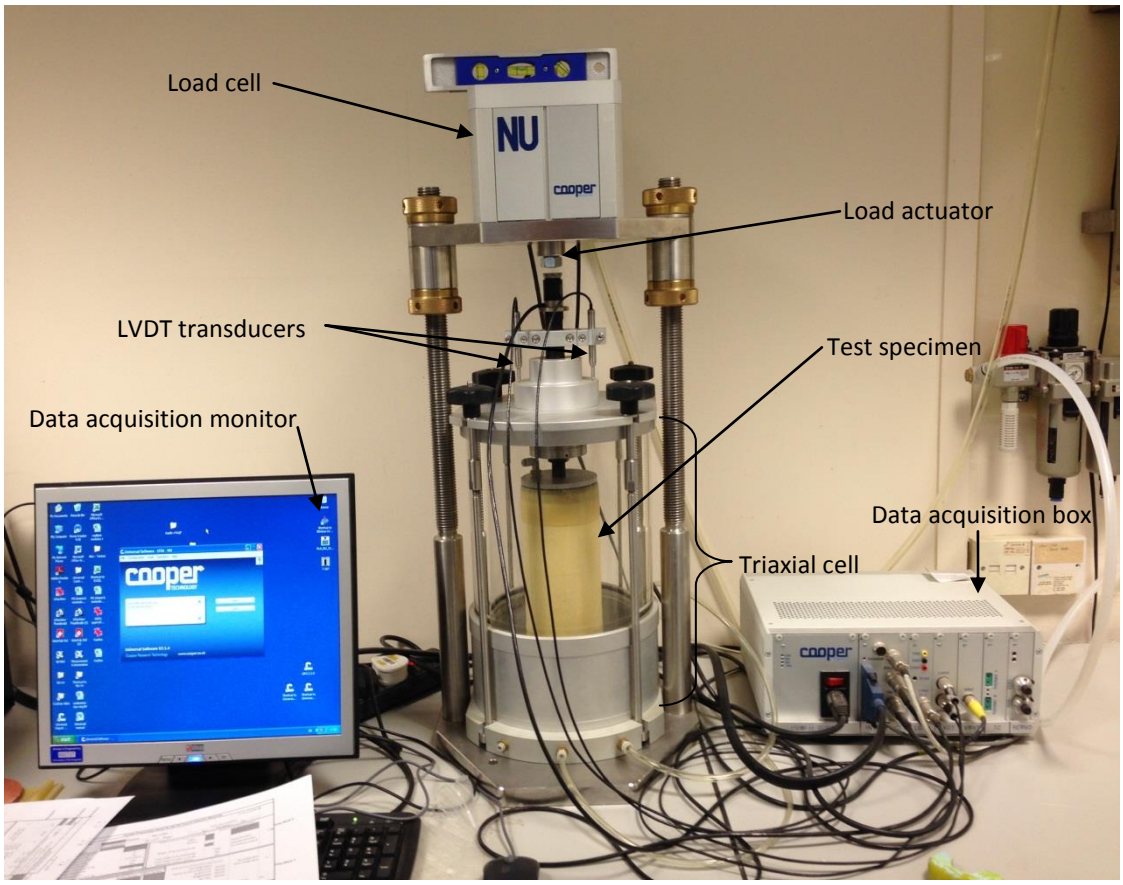

Figure 3. 3 Repeated load triaxial apparatus set up

3.3.1 Resilient Modulus (M_r) Test

Five different resilient modulus values for stabilised and unstabilised subgrade soils were obtained using the AASHTO T307 test apparatus with modified procedures (as shown below):

- From AASHTO T307 - determining the resilient modulus of soils and aggregate materials, in which 500-1000 cycles was applied for sample conditioning and 15 stress combinations were applied for resilient modulus values at different stress levels. These stress combinations consisted of five deviatoric stresses of 12.4, 24.8, 37.3, 49.7 and 62.0 kPa and three confining pressures of 13.8, 27.6 and 41.4 kPa.
- From the single-stage permanent deformation test after 50000 cycles - by taking the average of the last five cycles for deviatoric stresses of 62.0 and 120.0 kPa.
- From multi-stage permanent deformation tests at five stress levels and 10000 cycles each stage - the last four cycles were averaged for resilient modulus determination.
- From permanent deformation tests for a range of stabiliser ratios at the end of 50000 load cycles - after 25 cycles of wetting and drying for deviatoric stress of 120.0 kPa.
- From the AASHTO T307 test - after the permanent deformation test after 25 cycles of wetting and drying.

3.3.2 Permanent Deformation (PD) test

As described in Chapter Two, various researchers have used different methods for the study of permanent deformation of granular and subgrade soils. The BS EN 13286-7 describes the procedure for determining both resilient modulus and permanent deformation of granular unbound mixtures at high and low stress levels. Permanent deformation of stabilised and unstabilised soils was determined in this research as follows:

- Single-stage permanent deformation test for 50000 cycles at 62.0 kPa deviatoric stress and 27.6 kPa confining stress, respectively, for one stabiliser content.
- Multi-stage permanent deformation test for 50000 cycles at 12.4, 24.8, 37.3, 49.7 and 62.0 kPa deviatoric stresses and 27.6 kPa confining stress for five stages of 10000 cycles each.
- Single-stage permanent deformation test for 50000 cycles at 120.0 kPa deviatoric stress and 12.4 kPa confining stress for a range of stabiliser ratios and types.
- Single-stage permanent deformation test for 50000 cycles at 120.0 kPa deviatoric stress and 12.4 kPa confining stress after 25 cycles of wetting and drying, for a range of stabiliser ratios and types.
- The permanent deformation tests were carried out for the three unstabilised soils using schemes presented in bullet points one, two and three.

The scheme of these permanent deformation tests are presented in Tables 3.3-3.5 and the following chapters describe the adaptation of these schemes for different purposes.

Discussion:

In the data acquisition scheme of Tables 3.3 and 3.4 the successive cycle of data was obtained; from which the behaviour of the soil sample at different stages of the loading can be studied. For example, to discover how permanent deformation develops for 6 successive cycles, this necessitates processing data to obtain a smooth curve; while the scheme in Table 3.5 gives a smoother curve without processing, Figures 3.5 and 3.6 compare these two ways of data acquisition. In Table 3.6, the successive data acquisition gives a clear understanding of the permanent deformation progression of the soil. Cycles 1 to 10 show how the rate of permanent deformation for stabilised soil decreases compared to unstabilised soil; also for cycles from 1000 to 1004 and 49995 to 49999 the permanent deformation of the cycles is not consistent for stabilised and unstabilised soil. However, the accumulative permanent deformation gives a clear understanding of permanent deformation development with an increase in the number of load cycles. The other reason for using cumulative permanent deformation was the pattern of the load cell actuator that reached the target applied deviatoric stress after a few cycles of cyclic loading. Figure 3.4 shows the required load cycles to reach the target deviatoric stress of 62.0 kPa. Li and Selig (1996) used the first cycle to compare the influence of the deviatoric stress on coefficient A in a power model of permanent deformation; the data were obtained from line-intercept values for this purpose. Wu et al. (2011a) used the first cycle data for developing an elasto-plastic model for permanent deformation of a stabilised base/sub-base and subgrade soils. Therefore, the first cycle of a permanent deformation test was usually analysed separately by many of the researchers. However, in this research, the main purpose was to assess the effect of moisture on resilient modulus and the final permanent deformation after 50000 cycles and then evaluate the degree of improvement

the stabilisation made to subgrade soils, in terms of permanent deformation. Furthermore, the durability study carried out for stabilised subgrade soils is assessed in terms of cumulative permanent deformation. The latter is used to develop a durability model and correlation equations, correlating resilient modulus with unconfined compressive strength. Permanent deformation models for both stabilised and unstabilised soils were developed from the cyclic load test data.

Table 3. 3 Data acquiring scheme single-stage, 6 data points in each sequence

Sequence	Cycles	Number of cycles	Cycles of logging data	Confining pressure (kPa)	Deviatoric Stress (kPa)	Constant stress kPa
1	1_60	60	60	27.6	62.0	6.9
2	100_105	45	6	27.6	62.0	6.9
3	500_505	400	6	27.6	62.0	6.9
4	1000_1005	500	6	27.6	62.0	6.9
5	2000_2005	1000	6	27.6	62.0	6.9
6	5000_5005	3000	6	27.6	62.0	6.9
7	7500_7505	2500	6	27.6	62.0	6.9
8	9995_10000	2495	6	27.6	62.0	6.9
9	11000_11005	1005	6	27.6	62.0	6.9
10	13000-13005	2000	6	27.6	62.0	6.9
11	16000_16005	3000	6	27.6	62.0	6.9
12	19995_20000	3995	6	27.6	62.0	6.9
13	22000-21005	2005	6	27.6	62.0	6.9
14	25000-25005	3000	6	27.6	62.0	6.9
15	28000-28005	3000	6	27.6	62.0	6.9
16	29995-30000	1995	6	27.6	62.0	6.9
17	32000-32005	2005	6	27.6	62.0	6.9
18	35000-35005	3000	6	27.6	62.0	6.9
19	38000-38005	3000	6	27.6	62.0	6.9
20	39995-40000	1995	6	27.6	62.0	6.9
21	42000-42005	2005	6	27.6	62.0	6.9
22	45000-45005	3000	6	27.6	62.0	6.9
23	48000-48005	3000	6	27.6	62.0	6.9
24	49995-50000	1995	6	27.6	62.0	6.9
Summation		50000	198			

Table 3. 4 Data acquiring scheme multi-stage, 4 data points in each sequence and 20 data points at the beginning of each stage

Sequence	Cycles	Cycles of logging data	Confining pressure (kPa)	Deviatoric Stress (kPa)	Constant stress (kPa)
1	1_45	45	27.6	12.4	1.4
2	100_103	4	27.6	12.4	1.4
3	500_503	4	27.6	12.4	1.4
4	1000_1003	4	27.6	12.4	1.4
5	2000_2003	4	27.6	12.4	1.4
6	5000_5003	4	27.6	12.4	1.4
7	7500_7503	4	27.6	12.4	1.4
8	9997_10000	4	27.6	12.4	1.4
9	10001_10020	20	27.6	24.8	2.8
10	10100_10103	4	27.6	24.8	2.8
11	11000-11003	4	27.6	24.8	2.8
12	15000_15003	4	27.6	24.8	2.8
13	19997_20000	4	27.6	24.8	2.8
14	20001-20020	20	27.6	37.3	4.1
15	20100-20103	4	27.6	37.3	4.1
16	21000-21003	4	27.6	37.3	4.1
17	25000-25003	4	27.6	37.3	4.1
18	29997-30000	4	27.6	37.3	4.1
19	30001-30020	20	27.6	49.7	5.5
20	30100-30103	4	27.6	49.7	5.5
21	31000-31003	4	27.6	49.7	5.5
22	35000-35003	4	27.6	49.7	5.5
23	39997-40000	4	27.6	49.7	5.5
24	40001-40020	20	27.6	62.0	6.9
25	40100-40103	4	27.6	62.0	6.9
26	41000-41003	4	27.6	62.0	6.9
27	45000-45003	4	27.6	62.0	6.9
28	49997-50000	4	27.6	62.0	6.9
Summation		217			

Table 3. 5 Data acquiring scheme for single-stage permanent deformation at 120.0 kPa deviatoric stress for a range of stabiliser contents and unstabilised soils

Sequence	Cycles	Number of cycles	Cycles of logging data	Acquired cycles	confining pressure (kPa)	Deviatoric Stress (kPa)	Constant stress (kPa)
1	1_100	100	Every cycle	100	12.4	120.0	12.0
2	100-1000	900	Every 100 cycle	9	12.4	120.0	12.0
3	1000-50000	49000	Every 500 cycle	98	12.4	120.0	12.0
Sum.		50000		207			

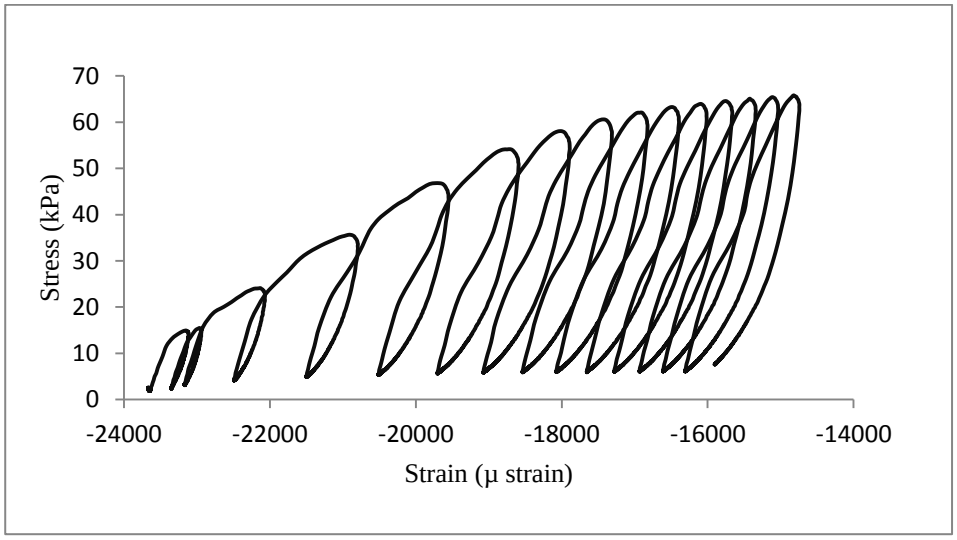

Figure 3. 4 Fifteen successive load cycles showing the required load to reach the target deviatoric load of 62.0 kPa for soil A-4

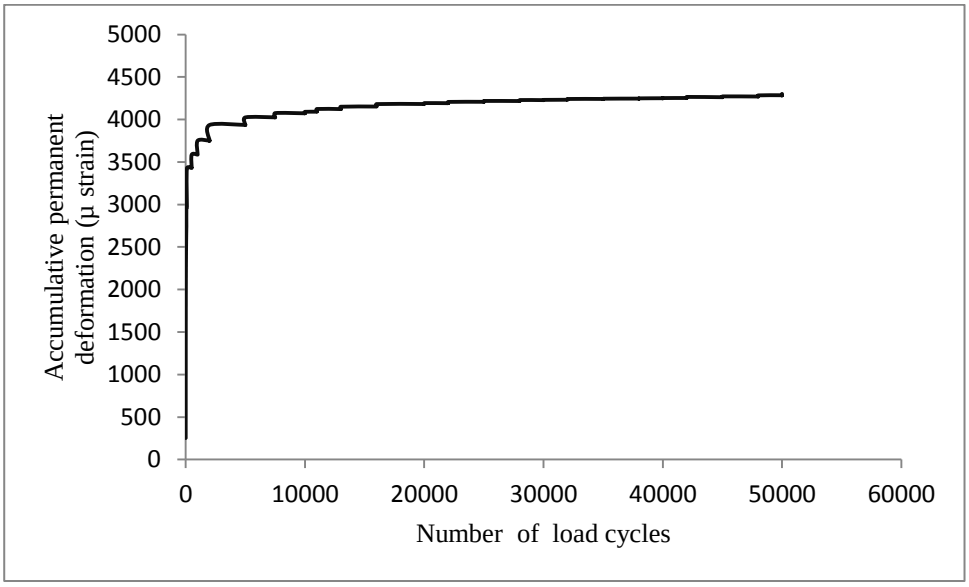

Figure 3. 5 Acquiring data for successive cycles; soil A-6 at 62.0 kPa deviatoric stress

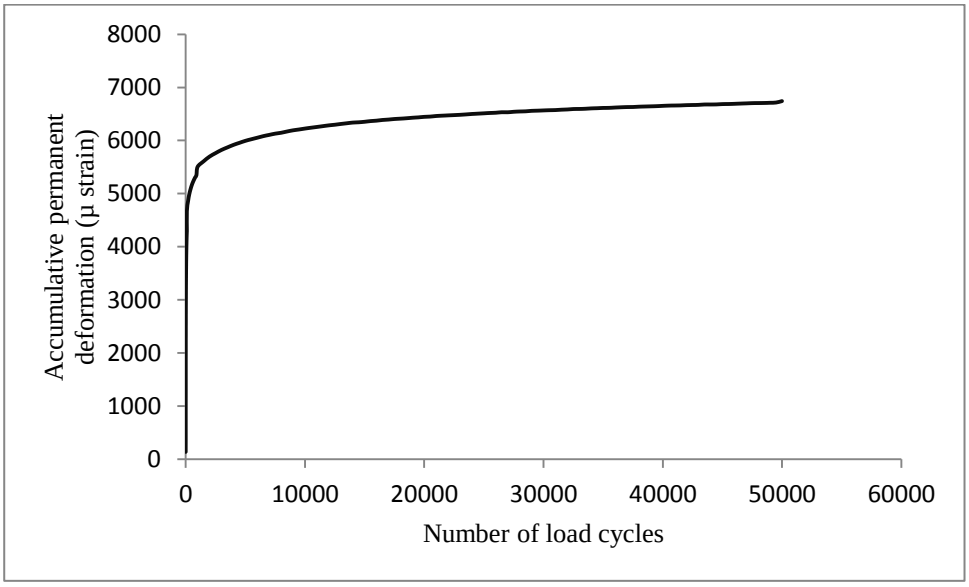

Figure 3. 6 Acquiring one data point at hundreds of cycles, soil A-6 at 120.0 kPa deviatoric stress

Table 3. 6 Behaviour of sample at successive load cycles for stabilised and unstabilised soil A-6

Unstabilised			Stabilised		
Cycle	Permanent deformation (µ strain)	Accumulative permanent deformation (µ strain)	Cycle	Permanent deformation (µ strain)	Accumulative permanent deformation (µ strain)
1	252.959	252.959	1	119.153	119.153
2	153.620	406.579	2	88.727	207.880
3	242.192	648.771	3	97.596	305.476
4	268.142	916.914	4	76.439	381.915
5	216.268	1133.182	5	44.795	426.711
6	185.541	1318.723	6	22.044	448.754
7	134.901	1453.623	7	14.017	462.772
8	112.553	1566.177	8	9.629	472.400
9	93.397	1659.574	9	7.592	479.992
10	81.854	1741.428	10	6.031	486.022
1000	0.022	3586.284	1000	0.751	543.953
1001	-0.011	3586.273	1001	0.020	543.973
1002	0.416	3586.690	1002	0.385	544.358
1003	0.778	3587.467	1003	-1.176	543.182
1004	0.810	3588.278	1004	-0.811	542.371
49995	1.600	4285.383	49995	1.572	602.255
49996	-2.806	4282.577	49996	-1.592	600.663
49997	1.621	4284.198	49997	0.010	600.673
49998	0.395	4284.593	49998	1.196	601.870
49999	-1.611	4282.982	49999	-0.801	601.069

Resilient modulus and permanent deformation test configuration: The configuration of the tests for the determination of the resilient modulus and permanent deformation for stabilised and unstabilised soils is shown in Table 3.7. It should be noticed that the AASHTO T307 procedure requires a contact stress of 0.1 of the maximum axial stress to be applied for all permanent deformation tests. However, a contact stress of 0.2 of the maximum axial stress was examined to assess its suitability for stabilised subgrade soils, especially for soils with higher strength that possess small resilient strains, as higher contact stress maintains the sample tighter and hold it without excess oscillations. The result shown in Figure 3.7 indicates that the accumulated permanent deformation is nearly twice that of 0.1 contact stress. Furthermore, the resilient modulus value at the end of 50000 cycles was 190 MPa and 272 MPa for 0.1 and 0.2 of the maximum axial stresses, respectively. However, the contact stress of 0.1 of the maximum axial stress (MAS) is used in this research because the soils were lightly stabilised.

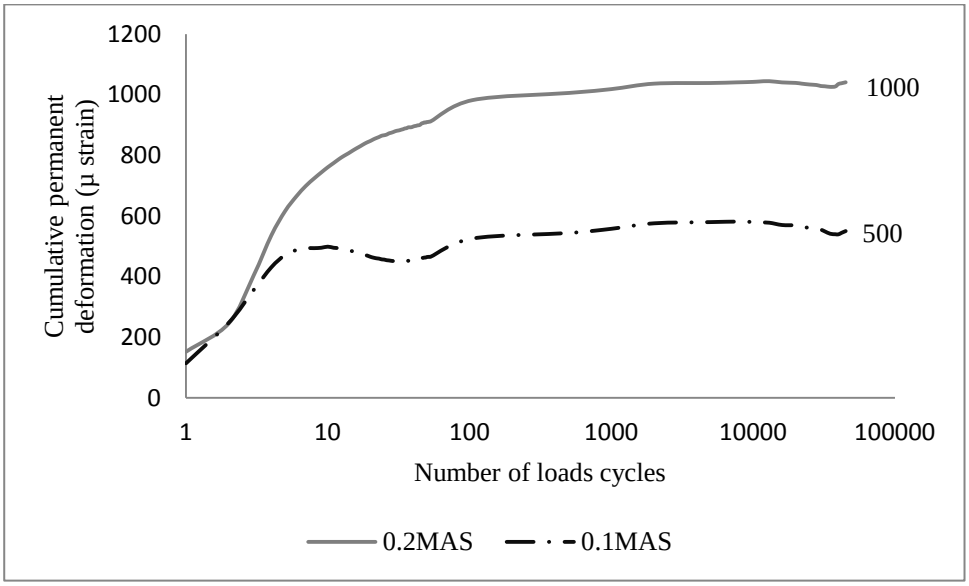

Figure 3. 7 Comparison of permanent deformation for 0.1 and 0.2 of the maximum axial stress as contact stress for stabilised soil A-4 at 100% OMC

Table 3. 7 Repeated load triaxial test configuration for determination of resilient modulus and permanent deformation

Specimen size	Compaction method	Confining pressure (kPa)	Deviatoric stress (kPa)	Load duration (sec)	Rest period (sec)	No. of Loads for permanent deformation	Moisture content (%)
100 mm dia. by 200 mm height	Static compaction	27.6 and 13.8	12.4, 24.8, 37.3, 49.7, 62.0 ,120.0	0.1	0.9	50000 for single stage and multi-stage	Dry of OMC, OMC and wet of OMC

3.4 Compaction Tests (Moisture-Density Relationships)

Compaction tests were carried out to determine the optimum moisture content (OMC) and maximum dry density (MDD) of both unstabilised and stabilised subgrade soils. These results were determined in accordance with the procedure described in British Standard BS 1377-4: 1990-3.3, the method uses a 2.5 kg rammer for soils with particles up to medium-gravel size and British Standard BS 1924-2: 1990-2.1.3, this method uses a 2.5 kg rammer for unstabilised and stabilised soils, respectively. The results of these tests were used as guides for preparing permanent deformation (PD), resilient modulus (Mr), unconfined compressive strength (UCS), modulus of elasticity (ME) and unconsolidated undrained (UU) triaxial tests. These specimens were prepared at OMC and ± 20% of OMC. These moisture contents were expected to occur in subgrade soils in Kurdistan; however, the variability of moisture change other than equilibrium moisture content is dependent on a specified geographical area. Dry density- moisture content relationships for both unstabilised and stabilised soils with (2% cement content) are shown in Figures 3.8 and 3.9; the graphs for stabilised soils with different stabiliser contents can be found in Appendix A. The maximum dry density and optimum moisture content for unstabilised and stabilised soils tabulated in Table 3.8 show that adding 2% cement does not have a significant impact on MDD; however, there is a small increase in OMC with the addition of cement.

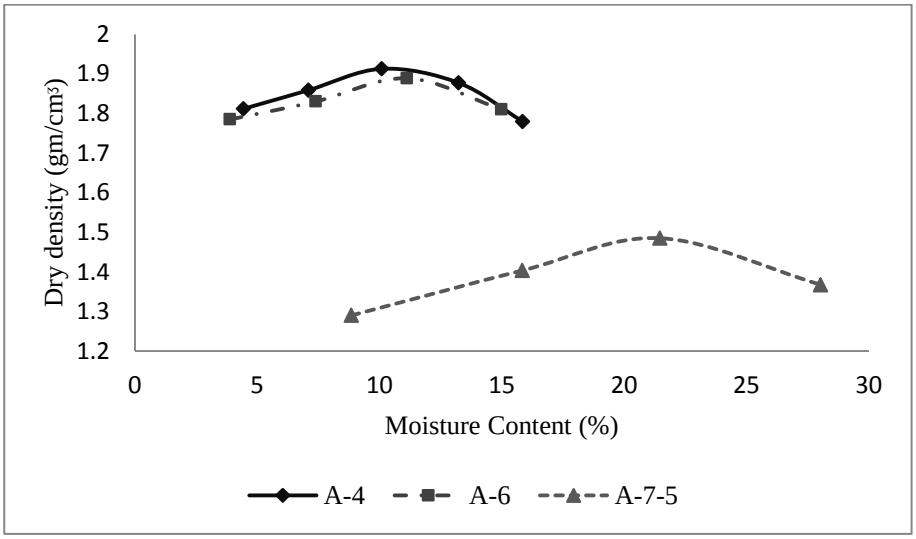

Figure 3. 8 Moisture to density relation for unstabilised subgrade soils

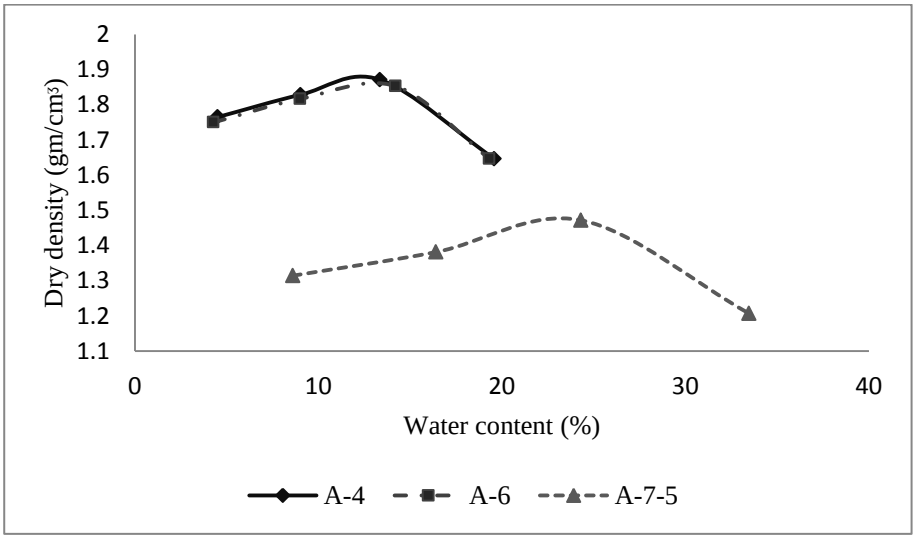

Figure 3. 9 Moisture to density relation for subgrade soils stabilised with 2% cement content

Table 3. 8 Maximum dry density and optimum moisture contents for stabilised and unstabilised soils

Soil type	MDD (gm/cm^3)	OMC (%)	Relevant standard
Untreated			
A-4	1.913	10.3	BS1377-4:1990 section 3
A-6	1.889	11.0	
A-7-5	1.485	21.5	
Treated 2%CC			
A-4	1.853	12.3	BS1924-2:1990 section 2
A-6	1.862	13.0	
A-7-5	1.48	23.0	
Treated 4%CC			
A-4	1.847	13.2	
A-6	1.845	13.5	
A-7-5	1.465	23.5	
Treated 2%CC+1.5%LC			
A-4	1.845	13.0	
A-6	1.847	13.4	
A-7-5	1.472	24.0	
Treated 4%CC+1.5%LC			
A-4	1.838	14.0	
A-6	1.842	14.0	
A-7-5	1.463	24.5	

3.5 Sample Preparation

3.5.1 Samples of 100X200 mm

Static compaction procedure given by AASHTO T307, ANNEX C was followed for compacting samples for resilient modulus and permanent deformation tests. The procedure consists of compacting soil in five equal layers with a predetermined weight and volume of the soil to achieve the required density. The first layer is positioned in the middle of the mould by placing first long spacer in the mould and pouring in the first fifth of the sample, followed by the insertion of the second longest spacer and applying the load in a steady rate until the plunger of the compacting machine reaches the edge of the mould. This load is held for not less than one minute. For the second layer, one spacer is removed and the surface of

the soil is scarified using a screwdriver; and then the second fifth portion of the sample is added and the first medium spacer is inserted. The load is applied and this procedure is continued for the other layers. The variations from the AASHTO T307, ANNEX C procedure were the dimensions of the mould. The mould dimensions in AASHTO T307, ANNEX C, were 71 mm diameter and a 142 mm height; while for this research a mould and the spacer plug sets were fabricated to produce samples with 100 mm diameter and 200 mm height. Figure 3.10 shows the mould and spacer plugs. The height of the mould was 320 mm with an inner diameter of 101 mm, the longer spacers' height was 140 mm, the medium spacers were 100 mm in height and the shorter spacers were 60 mm. This method of sample preparation ensures the homogeneity of the sample and even surfaces; these are important, especially for the permanent deformation tests as any irregularity of the sample's surface affects the results. Figure 3.11 shows the surface of the compacted sample in which the porous stone rested on the surface evenly.

3.5.2 Samples of 50X100 mm

These samples were prepared also with a static compaction method, but using three layers instead of five layers. Samples of this size were used for unconfined compressive strength, unconsolidated undrained triaxial and modulus of elasticity tests. The repeatability of the test results can be observed from the results presented in the following sections. The unstabilised samples were tested directly after the compaction; however the stabilised samples were cured for seven days in a moist cabinet of 100% relative humidity at 21ºC before testing.

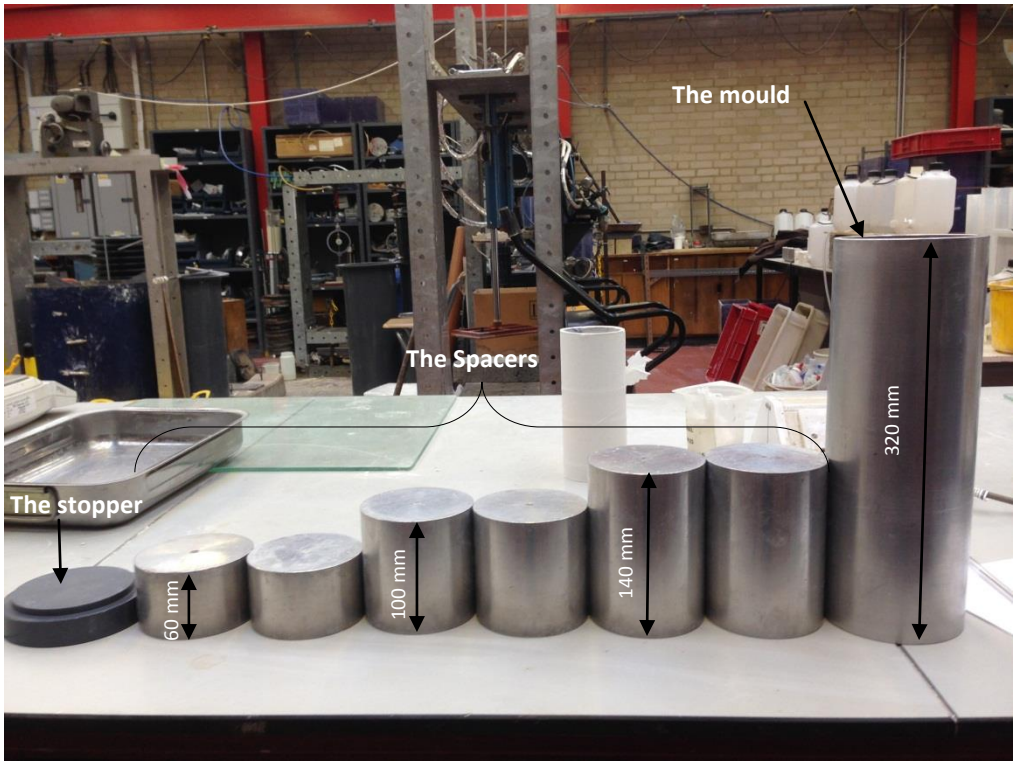

Figure 3. 10 Mould and spacers used for preparing sample sizes of (100X200) mm

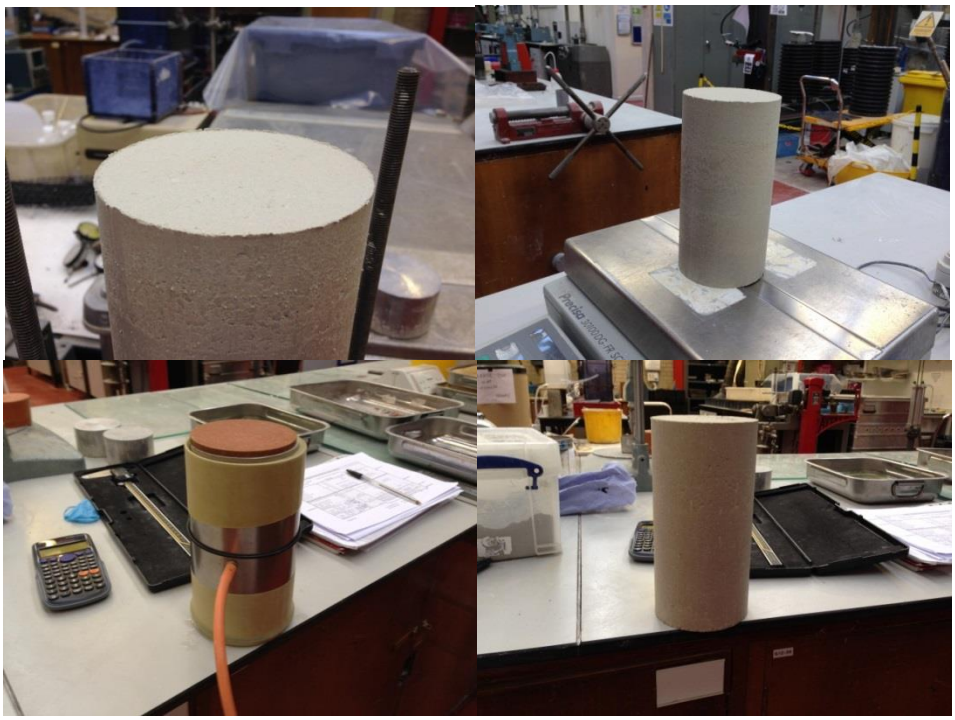

Figure 3. 11 The even surface of the sample and the porous stone resting on the surface of the sample evenly

3.6 Unconfined Compressive Strength (UCS)

The reasons for using the unconfined compressive strength test in this research are described below:

- To gauge the strength of soils of shallow depth in accordance with (ASTM; D2166, 2004).
- The test is used extensively for comparison of different soil types stabilised with various stabilisers.
- It is used as a durability measurement of the stabilised soils with freeze-thaw and wetting-drying durability tests.
- The test is also used to develop correlations with other properties of the stabilised and unstabilised soils for design purposes. The UCS test is a much simpler compared to the test used for measuring resilient modulus, which requires complicated equipment.
- The test was carried out on the stabilised and unstabilised subgrade soils to assess the sensitivity of different soil types to moisture changes.
- In addition to the above, it may be useful to examine the repeatability of soil samples before starting a comprehensive test programme on other properties of the soil, which would take up more time, need complicated equipment and be expensive. See Tables A-1 and B-1 in Appendices A and B, respectively.

Stress to strain relationships of unstabilised soil with three different moisture contents are shown in Figures 3.11, 3.12 and 3.13 for soils A-4, A-6 and A-7-5, respectively. These figures show the sensitivity of soils with high proportions of sand and silt to moisture changes. Soil A-7-5, while it is weaker than the other two soils with the optimum dry and optimum moisture contents, shows a higher compressive strength at the optimum wet condition. This is shown not only for strength but also for a higher resistance to axial deformation, where it

undergoes 2.5% axial strain. Whereas soils A-4 and A-6, deform by 3% and 5% strains at failure respectively, as depicted in Figures 3.12-3.14. This trend is demonstrated in Chapter Five more clearly through the permanent deformation test results; this shows the importance of unconfined compressive strength in the assessment of strength and permanent deformation resistance capabilities of soils, where a complete testing program is not available. Samples of stabilised soils with different stabiliser contents were prepared and tested for the derivation of correlation equations; samples with 4%CC+1.5%LC were prepared with three different compacting water contents for the three soils. Whereas samples with 2%CC, 4%CC, 2%CC+1.5%LC and 4%CC+1.5%LC were prepared for regression analysis and validation of the correlation models.

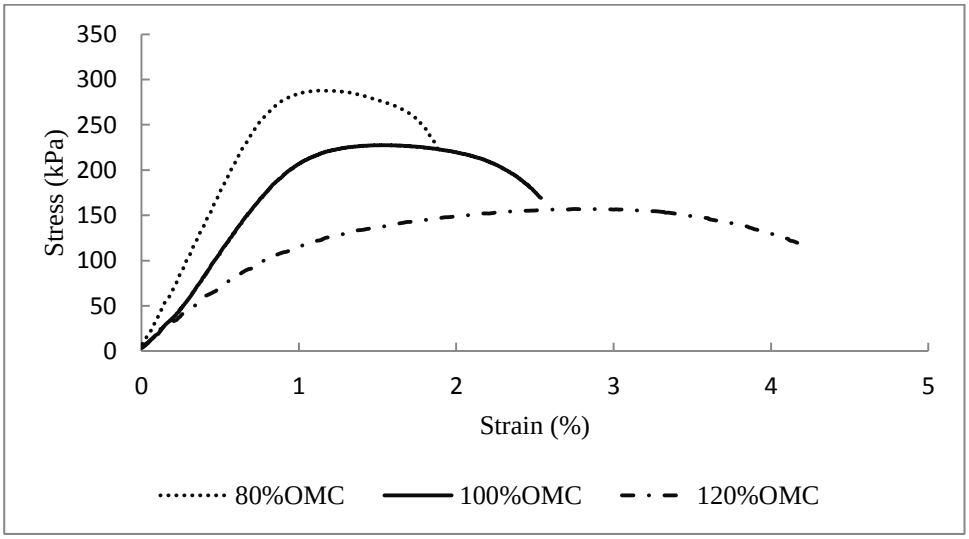

Figure 3. 12 Stress to strain relationship of unstabilised soil A-4 with three different moisture contents

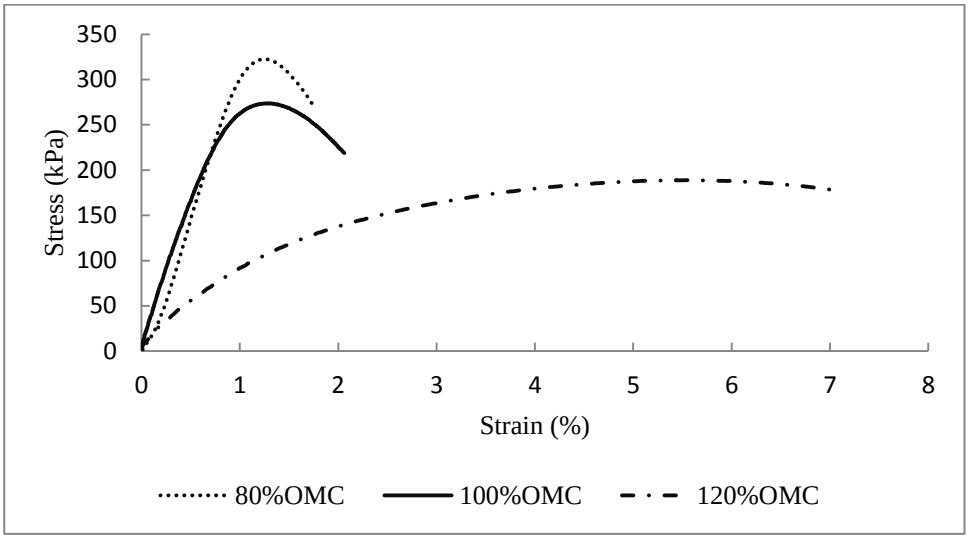

Figure 3. 13 Stress to strain relationship of unstabilised soil A-6 with three different moisture contents

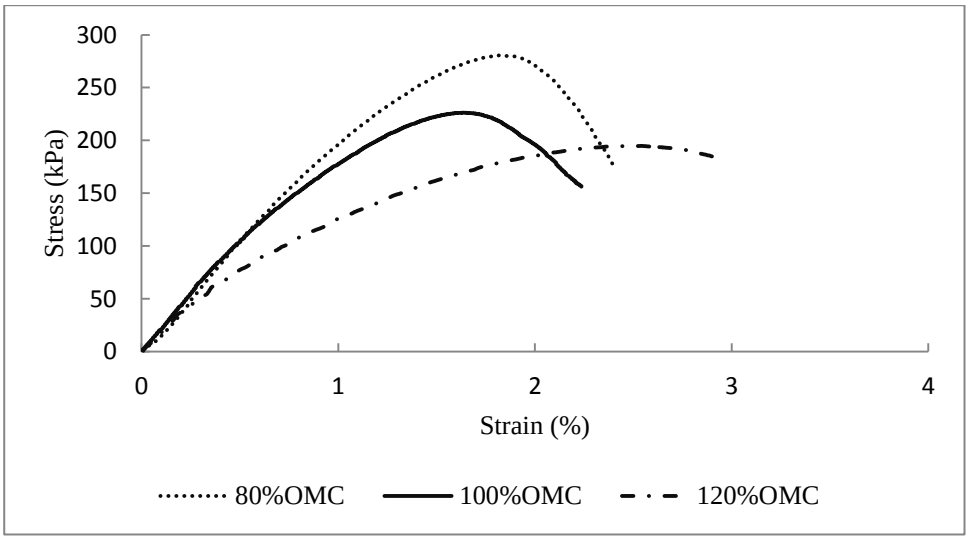

Figure 3. 14 Stress to strain relationship of unstabilised soil A-7-5 with three different moisture contents

3.7 Unconsolidated Undrained Triaxial (UU) Test

The threshold stress is defined as the deviatoric stress above which the repetition of loads causes the accumulation of permanent deformation in soils and consequently the failure (Putri et al., 2012). Brown (1996) concluded from test results that the plastic strains and pore pressure below the threshold stress are negligible. According to Frost et al. (2004) for design

purposes in analytical pavement design procedure a threshold stress of 50% of deviatoric stress at failure can be used. To set the deviatoric stress and confining pressures for the resilient modulus and permanent deformation tests in this research, first the stress levels in AASHTO T307 were used. These are recommended for the resilient modulus determination of subgrade soils. The second set of stress levels would be decided based on the UU test. Puppala et al. (2009) used a percentage of deviatoric stress (0.2, 0.4 and 0.6) at failure from the UU test for the deviatoric stress that had transmitted to subgrade soil. Arnold (2004) set stress limits for repeated load triaxial tests from monotonic shear failure tests. Table 3.9 shows the results from an unconsolidated undrained triaxial test for these three soils at 80%OMC, 100%OMC and 120%OMC. From these results a deviatoric stress of 120.0 kPa is chosen that is 0.67 τf, 0.71τf and 0.72 τf of the failure shear stress from the Mohr-Coulomb failure envelope line for soils A-4, A-6 and A-7-5 respectively at 100%OMC. This deviatoric stress has been used for stabilised and unstabilised samples to compare these soils with unstabilised and different stabiliser contents at 100%OMC. However, for moisture assessment and equation derivations, five deviatoric stress levels of 12.4, 24.8, 37.3, 49.7 and 62.0 kPa were used for multi-stage and 62.0 kPa for single-stage permanent deformation tests. Figures 3.15-3.17 show the relationship between shear stress and normal stress for three confining pressures of 27, 50 and 80 kPa; from which the data for the friction angle (ϕ) and cohesion (c) values were obtained at 100%OMC. Figure 3.18 shows the failure of the A-7-5 soil samples at 100%OMC; they suggest there is bulk at the central part, which is expected. The stress-strain relationship of these samples is presented in Figure 3.19; Appendix A gives these curves for soils A-4 and A-6.

Table 3. 9 Results from unconsolidated untrained triaxial tests for soils

Soil type and MC%	Friction angle (φ)	Cohesion, *c* (kPa)	σs at 27kPa Confining pressure	Shear failure *τf*
A-480%OMC	31	45	300	225
A-4100%OMC	31	32	236	180
A-4120%OMC	17	44	181	99
A-680%OMC	29	40	257	182
A-6100%OMC	31	30	229	168
A-6120%OMC	–	–	–	–
A-7-580%OMC	24	74	310	212
A-7-5100%OMC	23	60	253	167
A-7-5120%OMC	20	54	198	126

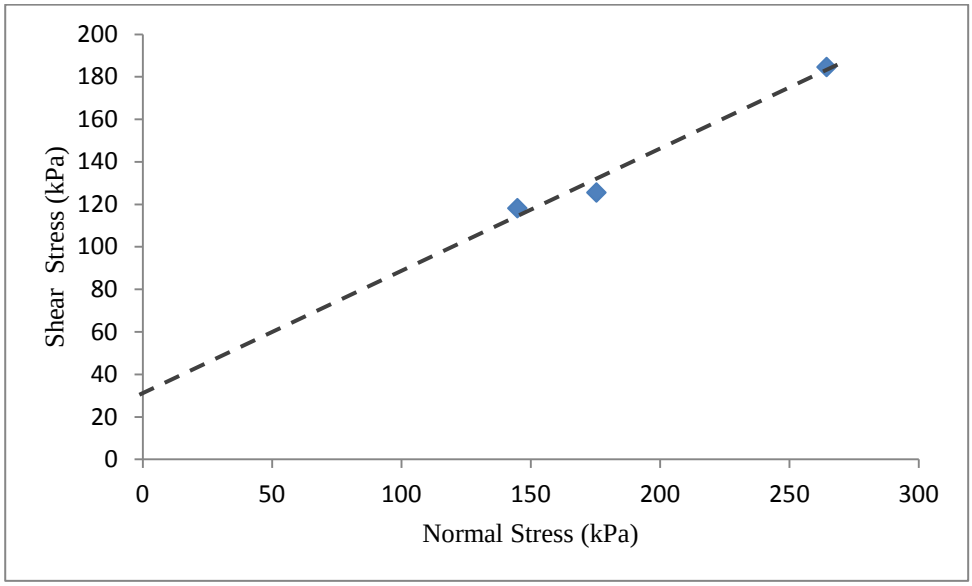

Figure 3. 15 Normal stress to shear stress relation for determination of cohesion and friction angle for soil A-4 at 100%OMC

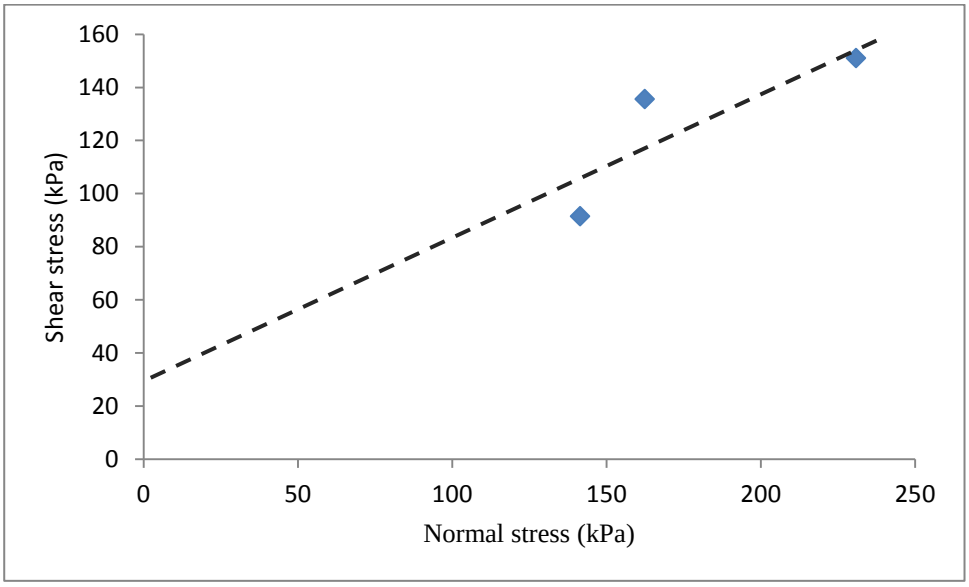

Figure 3. 16 Normal stress to shear stress relation for determination of cohesion and friction angle for soil A-6 at 100% OMC

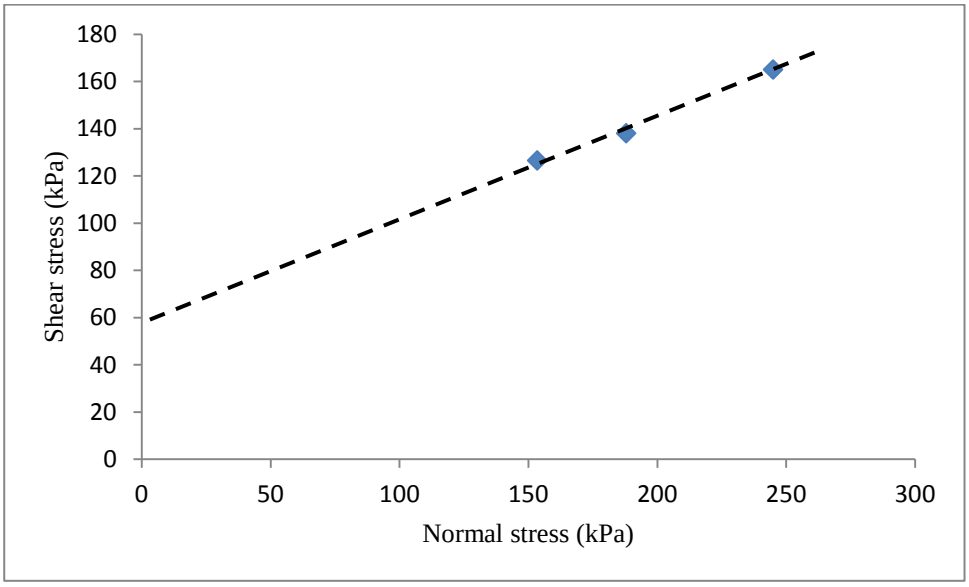

Figure 3. 17 Normal stress to shear stress relation for determination of cohesion and friction angle for soil A-7-5 at 100%OMC

Figure 3. 18 Failure of unconsolidated untrained triaxial test for soil A-7-5 at 27, 50 and 80 kPa confining pressures at 100%OMC

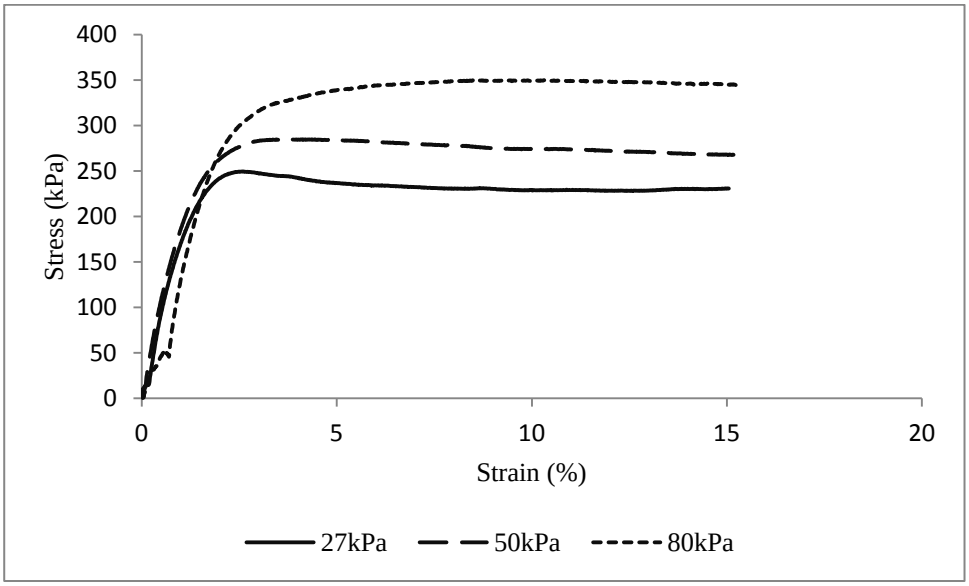

Figure 3. 19 Stress-strain relationship for soil A-7-5 at 27, 50 and 80 kPa in unconsolidated untrained triaxial test

3.8 Wetting and Drying Durability Test (W-D)

Durability tests were carried out on stabilised soils to assess the effect of weathering and aging. The American Society for Testing and Materials' (ASTM, D559) standard test method for wetting and drying compacted soil-cement mixtures were followed for this study. The variation in the test was that the number of cycles of wetting and drying was 25 instead of 12, to represent 25 years. The comparison between the properties of the samples before and after the wetting and drying cycles was made by resilient modulus and permanent deformation tests, instead of examining soil-cement losses and water content and volume changes. The test involved submerging the stabilised samples in water for 5 hours at room temperature, the samples had been prepared and cured for seven days; this was followed by placing the samples in an oven with a temperature of 71º±3ºC for 42 hours. This procedure was repeated for 25 cycles where each cycle took 48 hours, including the time for moving the samples between the wetting and drying cabinets. Chittoori (2008) allowed the samples to swell and shrink laterally and vertically, as the volumetric change in this way would be close to field conditions without restricting the soil samples in the vertical and horizontal directions, according to research by (Punthutaecha et al., 2006). Therefore, the samples were submerged in water for the wetting cycles without restrictions vertically and horizontally.

The first set of samples, cured for seven days, was tested for resilient modulus after 20 cycles of wetting and drying. These samples were prepared with 4% cement plus 1.5% lime and three different compacting water contents of 80%, 100% and 120% of the optimum moisture contents. The second set of the samples was prepared with 2% cement, 4% cement, 2% cement plus 1.5% lime and 4% cement plus 1.5% lime at 100% OMC for the three soil types. The later samples were tested after curing for seven days for permanent deformation with 50000 cycles at 120 kPa and at the end they were tested for resilient modulus using the

AASHTO T307 procedure. Immediately after the resilient modulus test the samples were submerged in water for 5 hours followed by 42 hours of drying; these cycles of wetting and drying continued for 25 cycles. At the end of this stage, these specimens were tested for permanent deformation of 50000 cycles. This was followed by resilient modulus determination in accordance with AASHTO T 307.

As presented in Table 3.10, different samples produce dissimilar behaviour with the wetting and drying cycles. Samples of soil A-7-5 failed at the first few cycles, except the samples with 4%CC+1.5LC; the A-6 samples survived the 25 wetting and drying cycles except at 2% cement content, which deteriorated and so it was not possible to test it. However, all samples of soil A-4 endured 25 cycles of wetting and drying with inconsiderable change, as in Figures 3.20 and 3.21. Soils A-4 and A-6 contained a higher proportion of silt and sand, these soil particles gained strength after seven days of curing when stabilised with cement; while soil A-7-5 which contained a high proportion of clay did not show this gain in strength. Clayey soils interact with lime especially if they cured for a longer time, therefore these soils failed at the beginning of the wetting and drying cycles.

Table 3. 10 Number of cycles for three types of soils stabilised with different stabiliser types and ratios

Soil type	Unstabilised	2%CC	4%CC	2%CC+1.5%LC	4%CC+1.5%LC
A-4	0	25	25	25	25
A-6	0	20	25	25	25
A-7-5	0	1	1	4	25

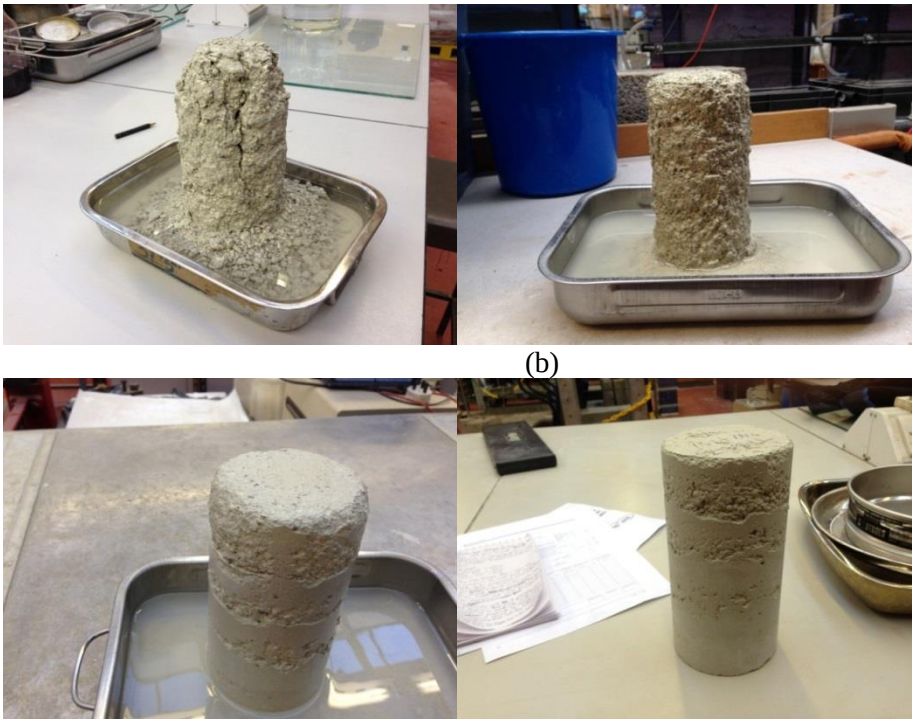

(a) (b)

(c) (d)

Figure 3. 20 Stabilised soil A-7-5; (a) 2%CC after 1 cycle, (b) 4%CC after 1 cycle, (c) 2%CC+1.5%LC after 4 cycles and (d) 4%CC+1.5%LC after 25 cycles of wetting and drying

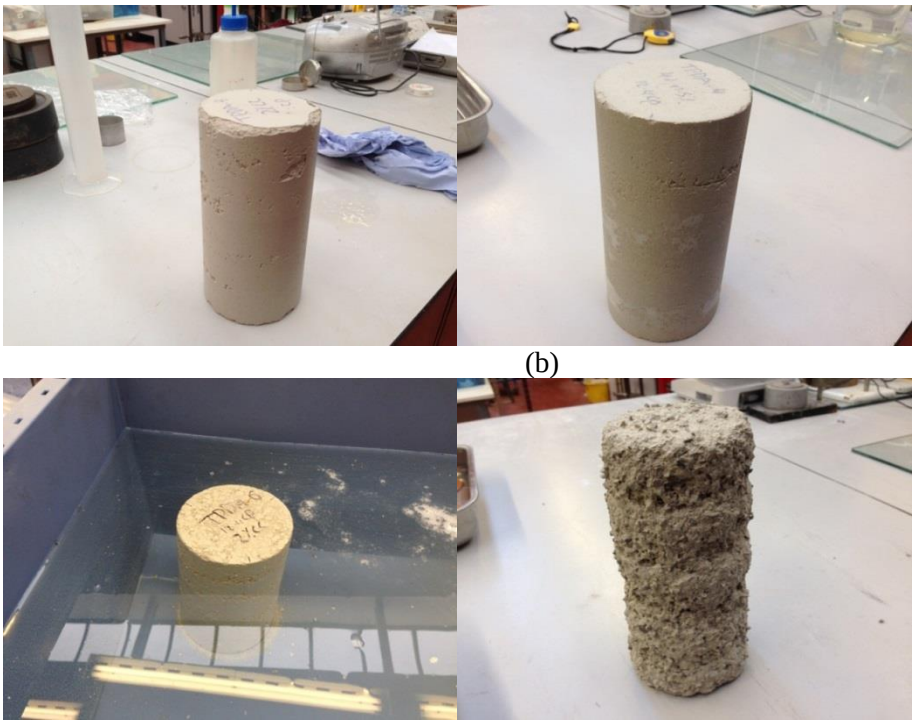

(a) (b)

(c) (d)

Figure 3. 21 Stabilised soils A-4 and A-6; (a) A-4_2%CC after 25 cycles, (b) A-4_4%CC+1.5%LC after 25 cycles, (c) A-6_2%CC after first cycle and (d) A-6_2%CC after 20 cycles of wetting and drying

3.9 Modulus of Elasticity Test (ME)

The focus of this research concerned the resilient modulus value and permanent deformation of stabilised and unstabilised subgrade soils. However, the analytical design of a road pavement considers fatigue cracking as one of the important criteria. The modulus of elasticity is therefore one input necessary for a performance model. To obtain the modulus of elasticity of the stabilised subgrade soils, BS EN 12390-13: 2013 method B, testing hardened concrete, determination of secant modulus of elasticity in compression, was utilised. The procedure used was easy to implement and can be considered as a good presumptive value. The test consists of applying three cycles of loading and unloading according to predetermined stresses; these stresses are defined according to the equation below:

$$E_{c,s} = \frac{\Delta\sigma}{\Delta\varepsilon_s} = \frac{\sigma_a^m - \sigma_p^m}{\varepsilon_{a,3} - \varepsilon_{p,3}} \quad (3.1)$$

Where: Ec,s is stabilised secant modulus of elasticity; σ_p^m is the measured value of the preload stress; σ_a^m is the measured value of the upper stress; $\varepsilon_{a,3}$ is the average strain at upper stress on loading cycle 3; and $\varepsilon_{p,3}$ is the average strain at preload stress on loading cycle 3.

The notation in Figure 3.22 is as follows: σa is the nominal upper stress= fc/3; σb is the nominal lower stress = arbitrary value between 0.1 and 0.15 of fc; σp is the nominal preload stress = arbitrary value between 0.5 Mpa and σb ; and fc is the compressive strength. For stabilised soils, compressive strength was determined from the first sample from which the parameters were calculated and used for the procedure of the secant modulus of elasticity determination. The first and second cycles were used to stabilise the material and check the changes to strain, which must not vary by more than 20% from the value of the previous stain; and then the third cycle was applied to obtain the secant line, which from its slope the modulus of elasticity was determined. Figure 3.23 shows the three cycles applied to sample

A-6 at 4%CC+1.5%LC, from which the secant modulus was obtained. The same sample is loaded to failure to obtain unconfined compressive strength (UCS); graphical representation of this is shown in Figure 3.24. From the test results the parameters of Equation 3.1 for soil A-6_4%CC+1.5%LC were found to be: measured upper stress = 291.3 kPa, measured preload stress = 59.8 kPa, average strain at upper stress = 0.00427 and average strain at preload stress = 0.00286.

From Equation 3.1 the secant modulus of soil A-6 at 4%CC+1.5%LC was determined as follows. The results of other soil types and stabiliser contents are shown in Table 3.11.

$$E_{c,s} = \frac{291.3-59.8}{0.00427-0.00286} = 164184 \text{ kPa} = 164 \text{ MP}$$

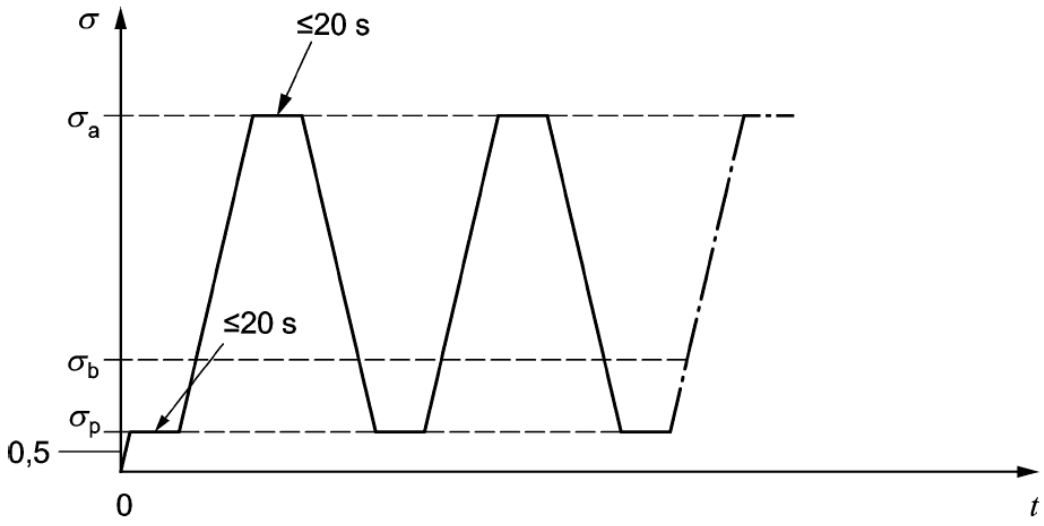

Figure 3. 22 Cycle for the determination of stabilised secant modulus of elasticity, method B, (BS NE 12390-13: 2013)

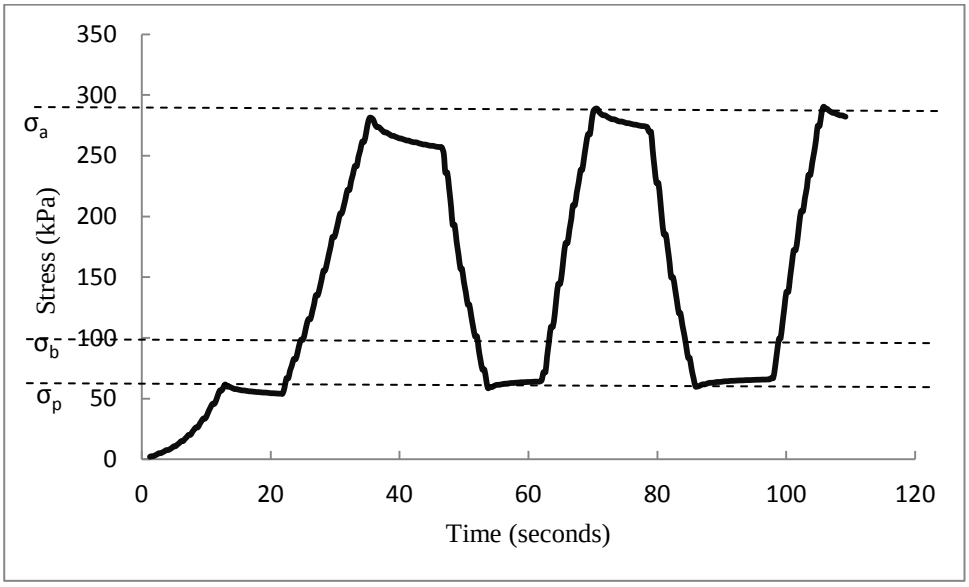

Figure 3. 23 Three cycles for the determination of stabilised secant modulus of elasticity for A-6 stabilised with 4%CC+1.5%LC

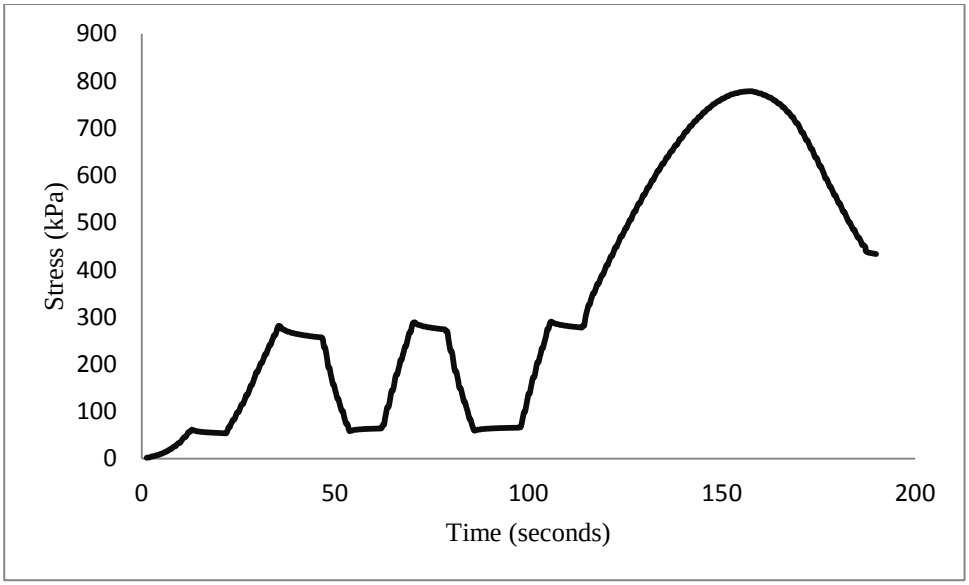

Figure 3. 24 Continuation of loading to failure to obtain UCS after three cycles of loading and unloading for soil A-6 at 4%CC=1.5%LC

Table 3. 11 Results of modulus of elasticity from the method in BS EN 12390-13: 2013 method B and the UCS from the same samples

Soil type and stabiliser	UCS(kPa)	ME (MPa)
A-4_Untreated	197	81
A-4_2%CC	580	144
A-4_4%CC	969	187
A-4_2%CC+1.5%LC	618	141
A-4_4%CC+1.5%LC	955	172
A-6_Untreated	189	77
A-6_2%CC	559	144
A-6_4%CC	845	173
A-6_2%CC+1.5%LC	574	155
A-6_4%CC+1.5%LC	774	166
A-7-5_Untreated	171	41
A-7-5_2%CC	275	83
A-7-5_4%CC	357	98
A-7-5_2%CC+1.5%LC	427	124
A-7-5_4%CC+1.5%LC	501	137

The aforementioned method is a quick way to obtain the modulus of elasticity as the whole test takes about three to four minutes. One unconfined compressive strength test must be carried out from which the nominal upper and lower stresses are determined and used for the modulus of elasticity test. In a simpler method, researchers (Solanki et al., 2009) applied two loading and unloading cycles and the modulus of elasticity was determined from the average of the two slopes drawn from the unloading to loading points. This method is also applied to the three soils stabilised with different stabiliser ratios and combinations. Figure 3.25 shows the stress-strain relationship for soil A-7-5 at 4%CC for two stages of the load/unload test for determining the modulus of elasticity. Such relationships for the other soils used in this study are shown in Appendix A. The modulus of elasticity from any of these two methods can be used in performance models for fatigue cracking distress calculation. However, the modulus

of elasticity is examined for permanent deformation model in this research as presented in Appendix B.

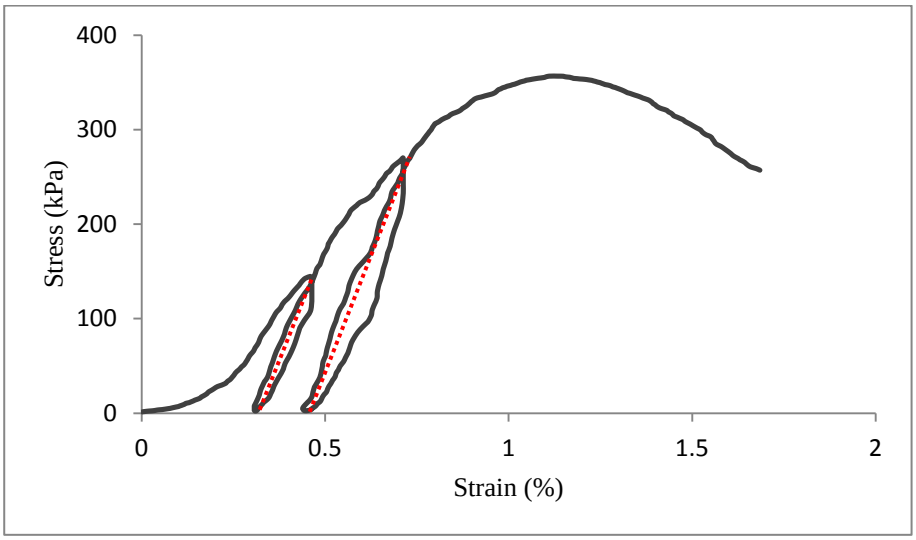

Figure 3. 25 Modulus of elasticity from the slope of two cycles in an unconfined compressive strength test for soil A-7-5 at 4% cement content

3.9 Summary

This chapter presented the materials used in this research. The required procedures for different tests carried out were described in detail. Since the focus of this research was on resilient modulus and permanent deformation test procedures, the schemes of these tests suggested herein were designated. For resilient modulus and permanent deformation tests it is important to set a detailed test configuration that should include specimen size, load duration, rest period of the load, the confining pressure and deviatoric stress. Regarding the deviatoric stress the concept of threshold stress is available from which it is possible to predict the progression of permanent deformation. Unconsolidated Undrained triaxial test was carried out to set a deviatoric stress level for resilient modulus and permanent deformation tests that were used for derivation of equations developed in this research. However, different set of deviatoric stress levels were used for different test sets that were less than 50% of deviatoric stress at failure. These set of deviatoric stresses were used for tests presented in Chapters Four and Five.

CHAPTER FOUR

RESILIENT MODULUS

4.1 Introduction

Resilient modulus is used to characterise the subgrade soils in analytical pavement design procedures. According to Austroads guide to pavement technology (2008), the suitable value of resilient modulus for design purposes is obtained from a laboratory resilient modulus test of the material at its in-situ density and natural moisture content. In this chapter the results of resilient modulus determinations of stabilised and unstabilised subgrade soils are discussed. Resilient modulus were determined for soils for different conditions: (i) range of moisture contents for unstabilised soil and compaction water contents for stabilised subgrade soils, (ii) resilient modulus values after permanent deformation tests, (iii) resilient modulus after cycles of wetting and drying from an AASHTO T307 test and from a permanent deformation test after wetting and drying. The results from these tests are later used in a finite element model to assess the effect of these factors on road pavement performance.

4.2 Resilient Modulus Characterisation

The use of the resilient modulus as a key input into the analytical pavement design procedures make it necessary to characterise and understand its behaviour under various conditions. Lekarp et al. (2000c) reviewed the research carried out to model the resilient modulus and the factors affecting the resilient response of unbound granular materials. According to their research these factors are: stress level, density, grading, soil type, moisture content, stress history and number of load cycles and load duration, frequency and load sequence. The same effects are assessed and applied to the fine grained subgrade soils. Stabilisation of subgrade soils changes the behaviour of these soils, and accordingly their resilience response. With

aging, weathering and application of loads, these responses are affected and lead to progressive deterioration of these layers. Therefore, durability tests are essential to predict the performance of stabilised and unstabilised subgrade soils at different stages of road pavement design life.

4.2.1 Effect of Moisture Content

It is preferred to compact subgrade soils at their optimum moisture content. However, for practical purposes they are usually operated to be compacted at about 95% of their maximum dry density and within a narrow range of its optimum moisture content, typically of 2%. This is to simulate the subgrade condition after the road construction has been completed. In other words the effect of moisture on the resilient modulus of subgrade soil for post-compaction is assessed.

As shown in Figure 4.1, the increase in moisture content results in decrease in resilient modulus value for all soil types used in this study. The effect of moisture content on the mechanical behaviour of unsaturated soils has been interpreted in different ways. Any increase in pore water pressure is followed by a decrease in effective stress and a decrease in strength, which is well known to geotechnical engineers from Terzaghi's principle. Lekarp et al. (2000c) referred to the research by (Mitry, 1964; Seed et al., 1967 and Hicks, 1970) which stated that the resilient modulus decreases with increase of moisture content only if the total stress is used in the analysis, and accordingly the resilient modulus remains unchanged if the effective stress is used in the analysis. However, other researchers (Khoury et al., 2003, Liang et al., 2008, Zaman and Khoury, 2007) relate the decrease in resilient modulus value to changes to suction caused by changes in moisture content. To more clearly demonstrate the effect of suction Yang et al. (2008) developed a suction-controlled set up to measure the

resilient modulus value of subgrade soils, and his tests showed clearly an increase in matric suction results in an increase in resilient modulus value. However, (Gallipoli et al., 2003) believe that both the suction function and the degree of saturation should be accounted for in analysing the mechanical behaviour of unsaturated soils. He introduced a variable ξ (equation 4.1) into an elasto-plastic model for unsaturated soils for this purpose.

$$\xi = f(s)(1 - Sr) \qquad (4.1)$$

Where: $f(s)$ is the suction function and *Sr* is the degree of saturation

In a study by Sharma and Mohamed (2006) the relation between the suction matric and the degree of saturation of unsaturated soils is assessed in static equilibrium and during dynamic flow of water. In which an increase in degree of saturation resulted in a decrease in matric suction head, and consequently a decrease in mechanical properties of the soil.

From above, one can conclude that the degree of saturation adversely influences the mechanical behaviour of soils such as its resilient modulus. Table 4.1 shows the degree of saturation of the soils used in this research. The results are the average of two replicate samples, and from the Figure 4.1and Table 4.1 it can be seen that the increase in degree of saturation resulted in a decrease in resilient modulus value for all soil types, although at different rates. It is also worth mentioning that void ratio and porosity values shown in the last two columns of Table 4.1 which are constant for different moisture contents. In the light of this discussion a model was selected for resilient modulus adjustment for different seasons of the year (Equation 7.4). This model is presented in Chapter Seven and it is used in the pavement design example.

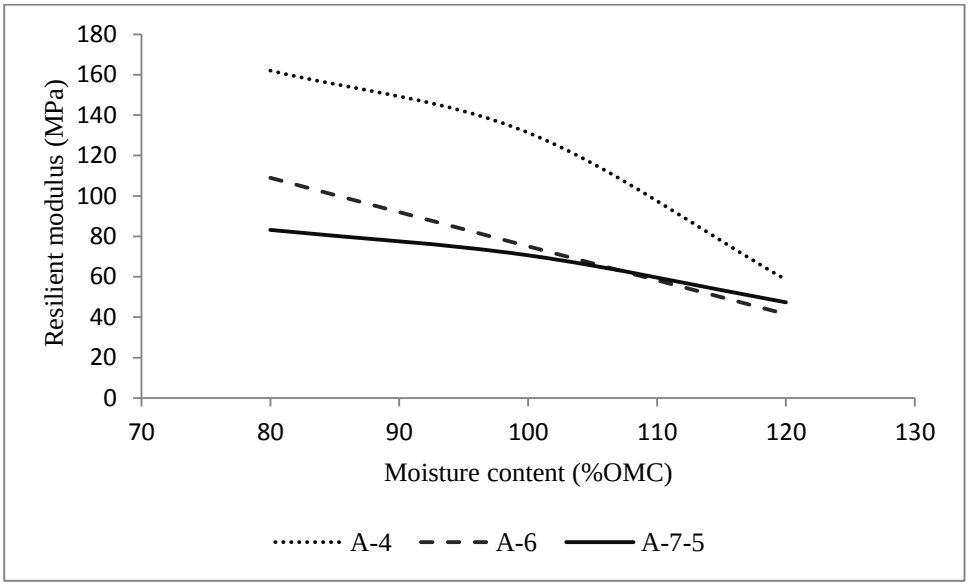

Figure 4. 1 Effect of moisture change on resilient modulus from single stage permanent deformation test for unstabilised soils

Figure 4.2 shows the effect of compaction moisture content on the resilient modulus for stabilised soils. As can be seen, the increase of compacting moisture content results in a decrease in resilient modulus value. The figure plotted from data for 80% OMC and 120% OMC to show the effect of compacting moisture content on resilient modulus more clearly. Austroads guide of pavement technology (2008) states that in general there is a slight increase in resilient modulus value accompanied by an increase in compaction moisture up to optimum moisture content after which the resilient modulus decreases with any further increase of compaction moisture content. The increase in the resilient modulus at optimum moisture content is due to the increase in maximum dry density. In this research which intends to compare the effect of compaction moisture content on the resilient modulus value the dry density is taken to be constant with a range of compacting water contents.

Table 4. 1 Degree of saturation at three different moisture contents for subgrade soils

Soil type & %OMC	Weight (g)	Volume (cc)	ρb (g/cc)	*w* (%)	Gs (%)	ρw at 20 °C (g/cc)	Sr (%)	Void ratio (e)	Porosity (n)
A-4_80%OMC	3141.2	1619.07	1.940	8.79	2.72	1	45.5	0.525	0.344
	3142.3	1619.26	1.941	8.50	2.72	1	44.4	0.521	0.342
Average	3141.75	1619.17	1.940	8.64	2.72	1	44.9	0.523	0.343
A-4_100%OMC	3209.6	1607.62	1.996	10.68	2.72	1	57.2	0.508	0.337
	3203.7	1607.68	1.993	10.67	2.72	1	56.8	0.511	0.338
Average	3206.65	1607.65	1.995	10.68	2.72	1	57.0	0.509	0.337
A-4_120%OMC	3272.2	1600.47	2.045	12.38	2.72	1	68.0	0.495	0.331
	3268.7	1604.42	2.037	12.74	2.72	1	68.6	0.505	0.336
Average.	3270.45	1602.44	2.041	12.56	2.72	1	68.3	0.500	0.333
A-6_80%OMC	3145.8	1621.67	1.940	9.26	2.71	1	47.7	0.526	0.345
	3146.1	1618.12	1.944	9.53	2.71	1	49.0	0.527	0.345
Average	3145.95	1619.90	1.942	9.39	2.71	1	48.4	0.526	0.345
A-6_100%OMC	3215.8	1611.96	1.995	11.77	2.71	1	61.6	0.518	0.341
	3216	1612.57	1.994	11.52	2.71	1	60.6	0.515	0.340
Average.	3215.9	1612.26	1.995	11.65	2.71	1	61.1	0.517	0.341
A-6_120%OMC	3285.4	1607.59	2.044	14.64	2.71	1	76.3	0.520	0.342
	3287.9	1612.29	2.039	14.01	2.71	1	73.7	0.515	0.340
Average	3286.65	1609.94	2.041	14.32	2.71	1	75.0	0.518	0.341
A-7-5_80%OMC	2557.8	1626.51	1.573	15.95	2.64	1	44.5	0.946	0.486
	2557.7	1631.15	1.568	15.85	2.64	1	44.0	0.950	0.487
Average	2557.75	1628.83	1.570	15.90	2.64	1	44.3	0.948	0.487
A-7-5_100%OMC	2645.5	1626.91	1.626	20.18	2.64	1	56.0	0.951	0.487
	2643.8	1630.88	1.621	19.86	2.64	1	55.1	0.952	0.488
Average	2644.65	1628.90	1.624	20.02	2.64	1	55.5	0.952	0.488
A-7-5_120%OMC	2737.3	1631.79	1.677	23.61	2.64	1	65.9	0.945	0.486
	2740.6	1630.00	1.681	24.07	2.64	1	67.0	0.948	0.487
Average	2738.95	1630.89	1.679	23.84	2.64	1	66.5	0.947	0.486

Both water and water to cement ratios for the three different soils are shown in Table 4.2. In this way the difference between the dry of optimum moisture content to wet side can be compared. The results suggest that during construction extra compacting water content, more than the optimum, results in a decrease in the resilient modulus value and strength properties. In other words for the same dry density of 95% the increase of compacting water content adversely affects the strength properties of a compacted stabilised layer, see Figure 4.2.

However, in multi-stage permanent deformation tests a consistent trend couldn't be found regarding compacting moisture content. This may be because of the changes that higher numbers of load repetitions make to the samples.

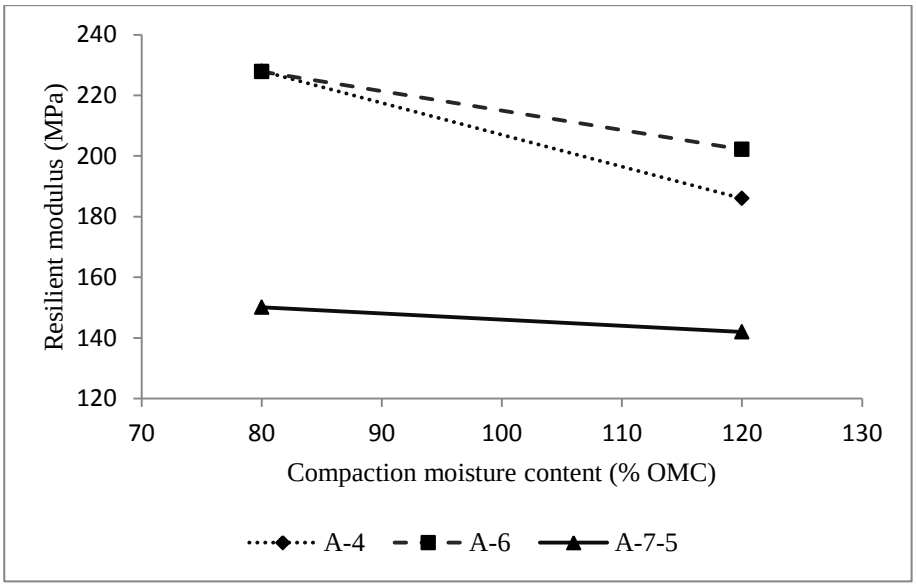

Figure 4. 2 Effect of compaction moisture content on resilient modulus for stabilised soils

Table 4. 2 Cement and water quantity for each soil at three compaction moisture contents

Soil type	cement content (gm)	Water content (gm)			water to cement ratios		
		80%OMC	100%OMC	120%OMC	80%OMC	100%OMC	120%OMC
A-4	124.46	311.15	388.94	466.72	2.50	3.13	3.75
A-6	123.16	307.82	384.78	461.73	2.50	3.12	3.75
A-7-5	94.18	452.04	565.06	678.06	4.80	6.00	7.20

4.2.2 Effect of Stress Level

The response of soils is nonlinear to the applied load. The resilient modulus of coarse grained soils increases with any increase in stress level, whereas the one of fine grained soils decreases with any increase of stress level (Huang, 2003). Although the three soils in this research are fine-grained soils the response to the applied stress do not following this general trend for one of the soils. Soil A-4 which is a sandy silt (contains 84% silt and sand) showing

an increase in resilient modulus with an increase in deviatoric stress at different moisture contents. However, soils A-6 and A-7-5 exhibit a decrease in resilient modulus value with an increase in deviatoric stress for optimum moisture content and wet side of optimum (see Figures 4.3-4.5). This implies an inter-relationship between stress level and moisture content in their effect on resilient modulus behaviour. However, for soil A-4 at 120% OMC in multi-stage permanent deformation test there is a decrease in resilient modulus value with an increase in deviatoric stress. This may be interpreted as; the increase in number of load repetitions changes the behaviour of these soils. The combined effect of moisture and the stress level on resilient modulus from multistage permanent deformation tests can be expressed as follows.

- The soil samples' dry densities are constant at three moisture contents of dry, OMC and wet.
- At dry side all the three soils show increases in resilient modulus with increases in deviatoric stress.
- At OMC the resilient modulus of soil A-4 increases with an increase in deviatoric stress and the other two soils A-6 and A-7-5 show a contrasting trend.
- At wet of OMC the resilient modulus of the three soils show different trends.

For stabilised subgrade soils the increase in deviatoric stress is accompanied by an increase in resilient modulus value for all soils and compaction moisture contents. This shows the effect of cementitious material in bonding the soil particles to create agglomerate that gaining higher strength properties; see Figures 4.6-4.8.

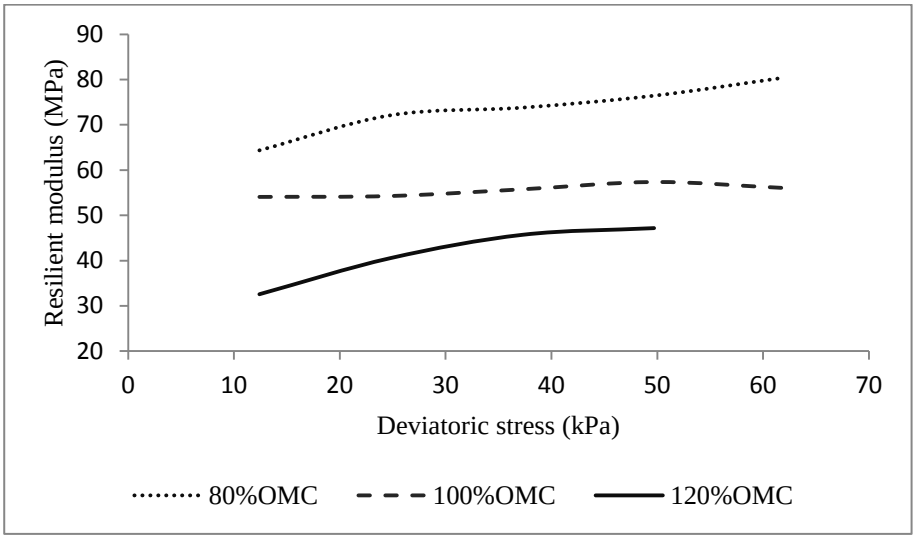

Figure 4. 3 Effect of deviatoric stress at different moisture conditions for unstabilised soil A-4

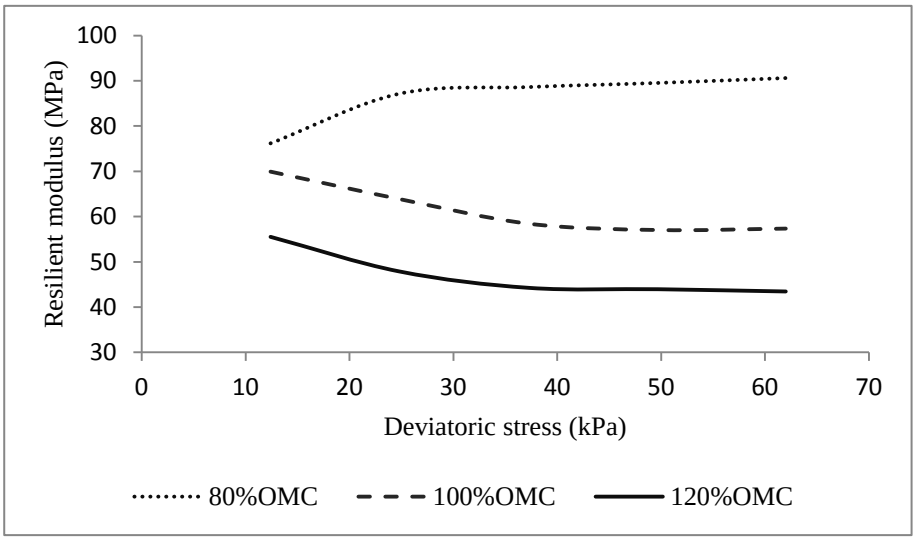

Figure 4. 4 Effect of deviatoric stress at different moisture conditions for unstabilised soil A-6

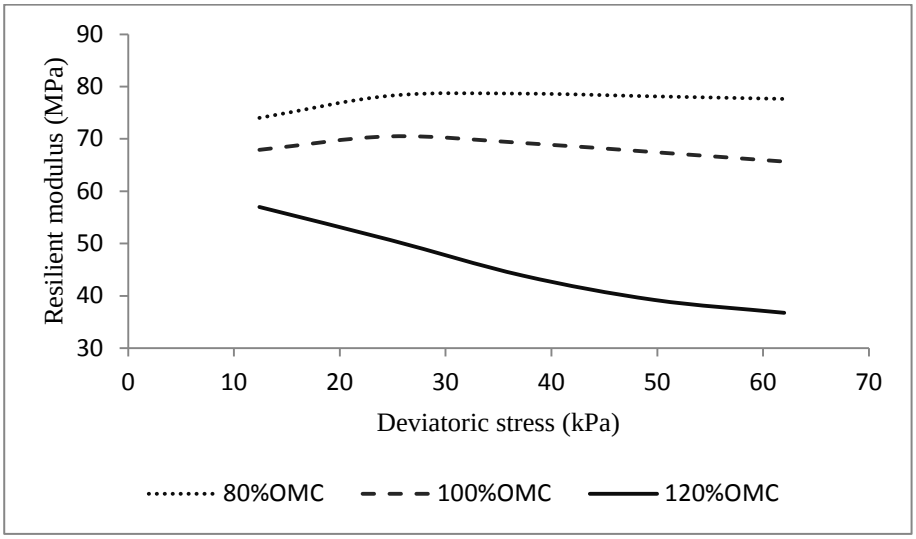

Figure 4. 5 Effect of deviatoric stress at different moisture conditions for unstabilised soil A-7-5

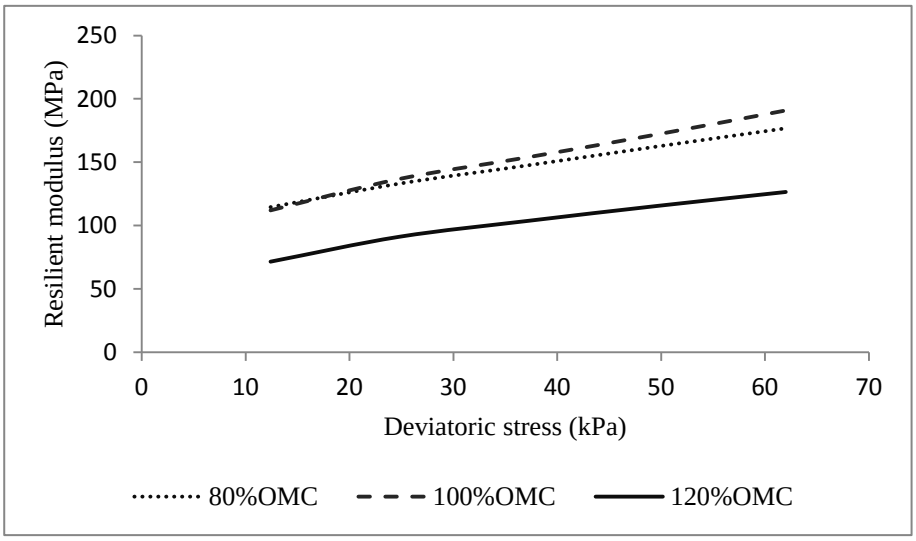

Figure 4. 6 Effect of deviatoric stress at different moisture conditions for stabilised soil A-4

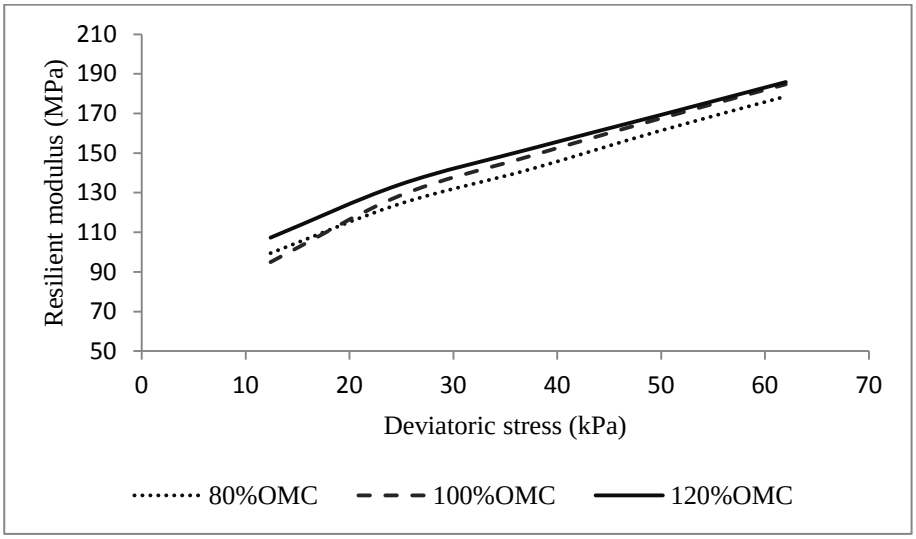

Figure 4. 7 Effect of deviatoric stress at different moisture conditions for stabilised soil A-6

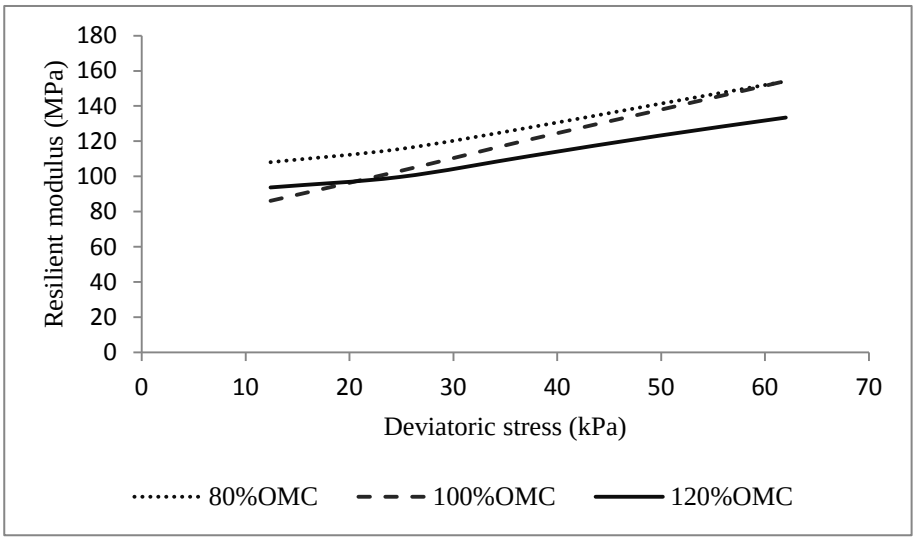

Figure 4. 8 Effect of deviatoric stress at different moisture conditions for stabilised soil A-7-5

4.2.3 Effect of Soil Type

While the effect of stress level and moisture content were presented in sections 4.2.1 and 4.2.2, soil type also has great influence on the resilient modulus value. Here the results are separated into different moisture contents for the three soil types: Figures 4.9-4.14 show this comparison for both stabilised (with 4%CC+1.5%LC) and unstabilised soils. These Figures

show the results of multistage permanent deformation tests from which the resilient modulus values are calculated. Soil A-4 shows a higher resilient modulus value than the other two soils at dry and optimum moisture contents, while at higher moisture content (Figure 4.11), soils A-4 and A-6 are affected to a higher degree by increases in moisture content. This indicates the sensitivity of both sandy and silty soils to moisture changes and the necessity of improving these types of soils. Figures 4.12-4.14 show that soils A-4 and A-6 exhibit increases in resilient modulus values at different compaction moisture contents. At optimum moisture content soils A-6 and A-7-5 show decreases in resilient modulus with increases in deviatoric stress, see Figure 4.10, while soil A-4 demonstrates the reverse. This may be due the proportion of clay content which is 16% in soil A-4 and 42% and 65% for soils A-6 and A-7-5 respectively. Therefore, it can be said that the clay content affects the resilient modulus value depending on the degree of saturation, such that soils with a low ratio of clay content tend to decrease their resilient modulus value with increases in their degree of saturation earlier than soils with a high ratio of clay content. For example soil A-4 and A-7-5 have nearly the same degree of saturation, 68.3% and 66.5% respectively (from Table 4.1), however the resilient modulus of soil A-4 decreases very rapidly compared to soil A-7-5, which has a lower resilient modulus value at optimum moisture content and dry condition (see Figures 4.9 and 4.10).

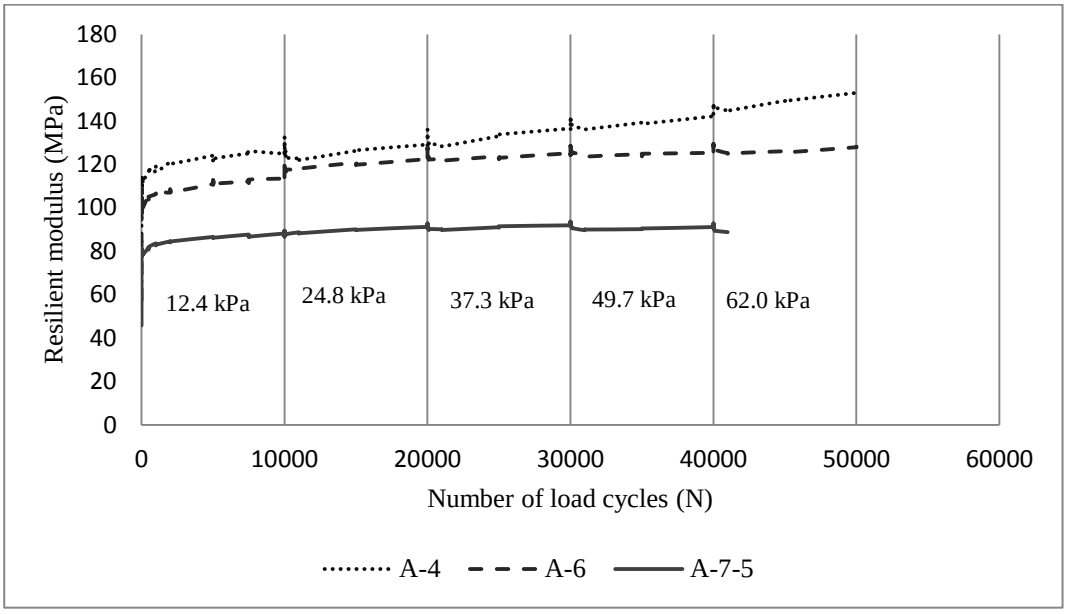

Figure 4. 9 Comparison of the soils at 80%OMC and different deviatoric stresses for unstabilised soils

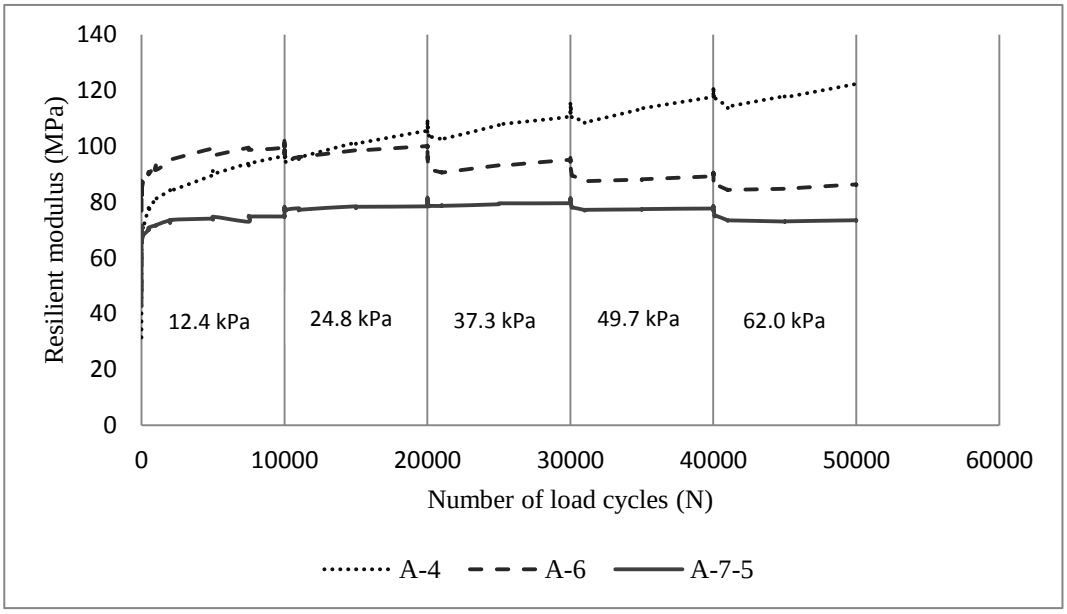

Figure 4. 10 Comparison of the soils at 100%OMC and different deviatoric stresses for unstabilised soils

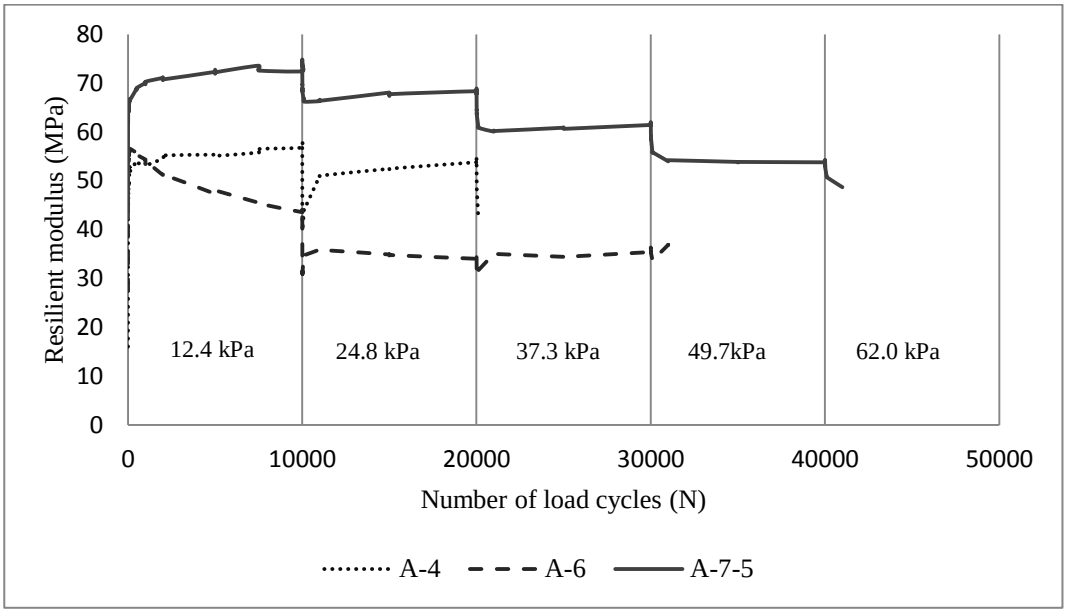

Figure 4. 11 Comparison of the soils at 120%OMC and different deviatoric stresses unstabilised soils

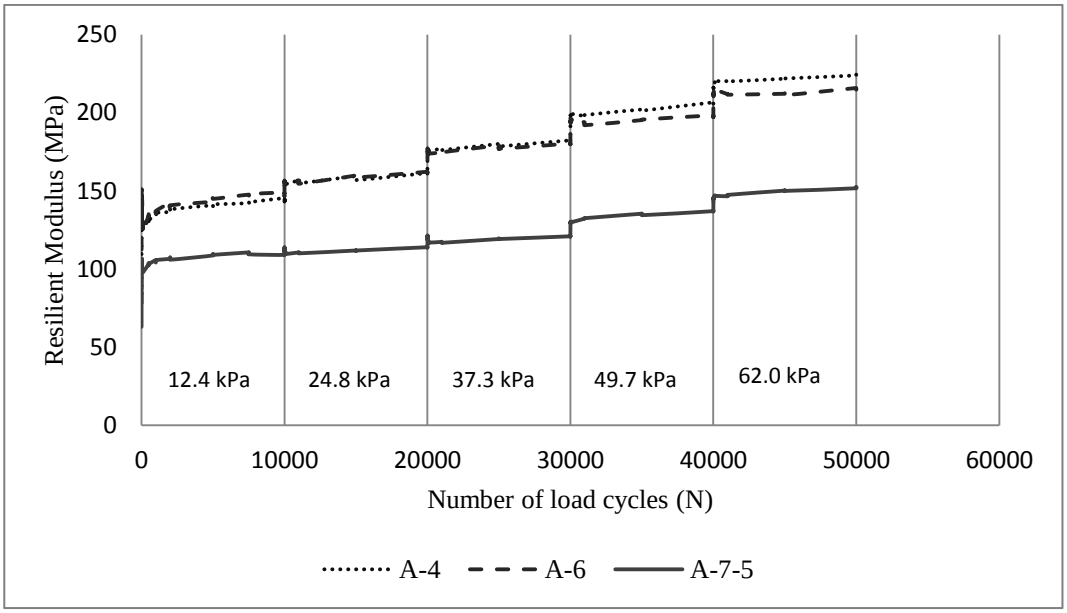

Figure 4. 12 Comparison of the soils at 80%OMC and different deviatoric stresses for stabilised soils with 4%CC+1.5%LC

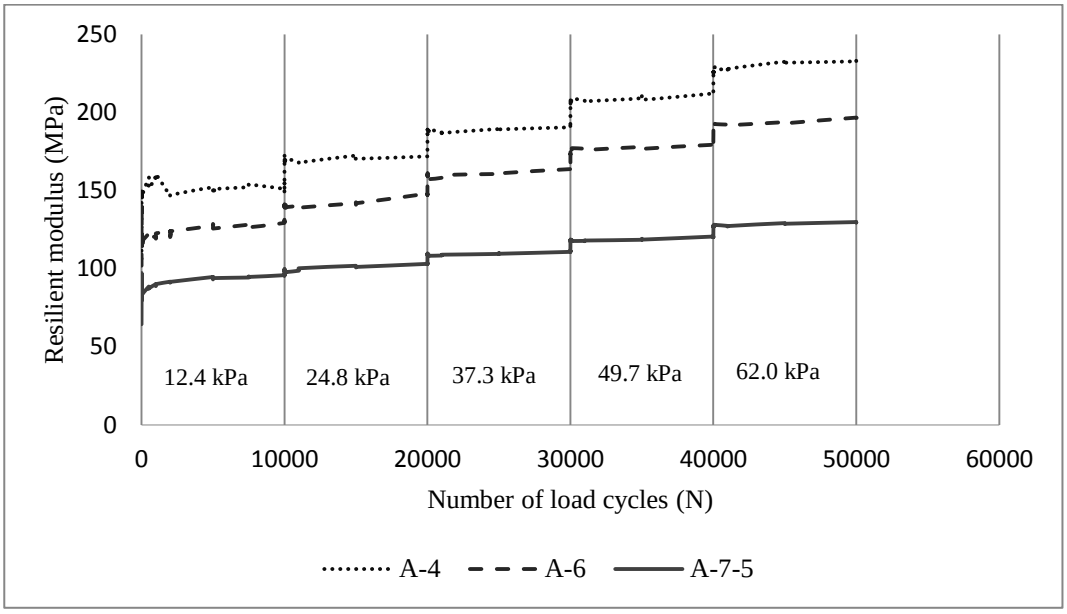

Figure 4. 13 Comparison of the soils at 100%OMC and different deviatoric stresses for stabilised soils with 4%CC+1.5%LC

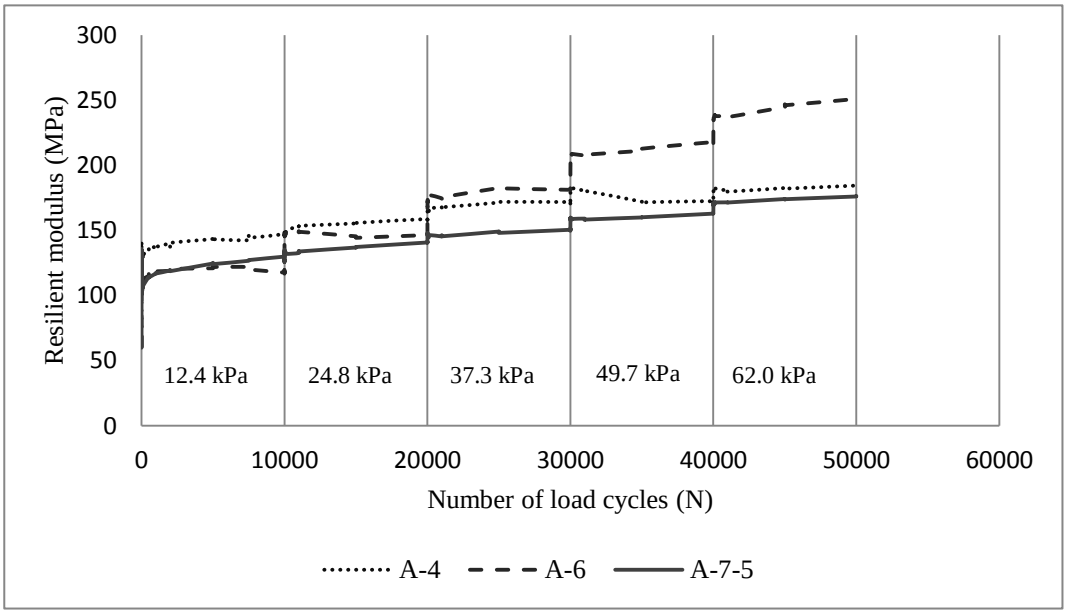

Figure 4. 14 Comparison of the soils at 120%OMC and different deviatoric stresses for stabilised soils with 4%CC+1.5%LC

4.2.4 Effect of Number of Loads

Effect of stress history and the number of load repetitions is assessed through single stage permanent deformation tests in which the resilient strain in each cycle is determined and used to calculate the resilient modulus. Figures 4.15-4.17 show the resilient modulus values corresponding to each cycle. Research on unbound granular material for the effect of numbers of loads and a corresponding stress history on the resilient modulus value showed that this effect is not considerable as the resilient modulus value stabilises after around 100 to 1000 cycles (Lekarp et al., 2000). However for fine grained soils the result shows an increase in resilient modulus value with increase in the number of load repetitions as shown in Figures 4.15-4.17 for unstabilised soils. This trend was confirmed by Puppala et al. (2009). In their research sand, silt and clay soils were tested and the increase in resilient modulus value noticed with increase the number of loads. They applied 10000 cycles to the sample while in this research the number of applied loads was 50000 cycles. The decrease in resilient modulus values may occur only if aging and weathering effects are introduced to the test. This tendency can be seen at moisture content of 120% OMC at which these soils show stabilisation of resilient modulus value or a slight decrease for soils A-6. However for 80% OMC and 100% OMC the increase in resilient modulus is continuous for increase in number of load repetitions.

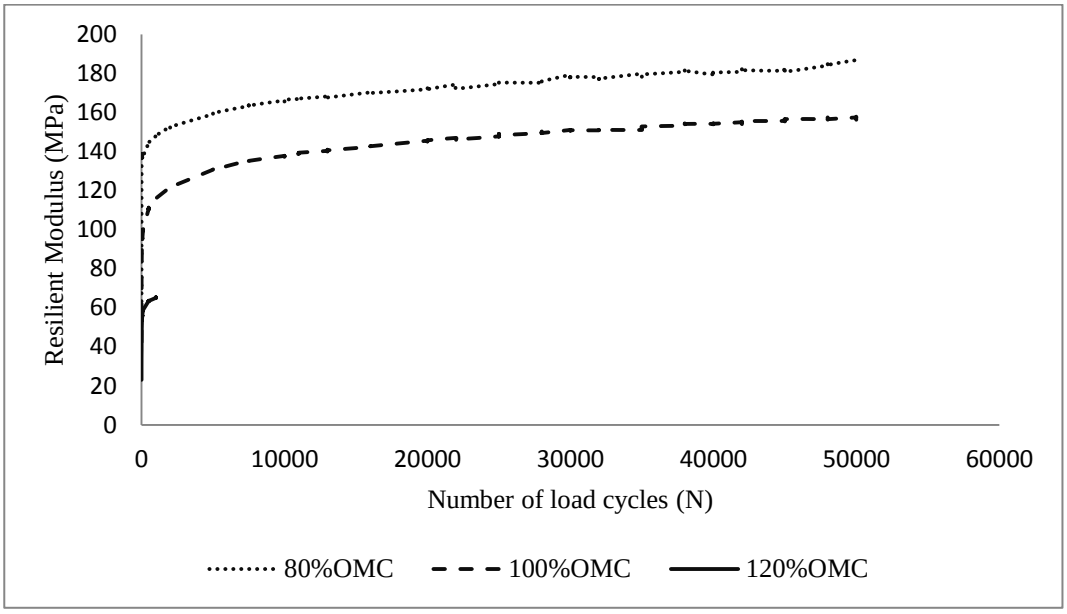

Figure 4. 15 Effect of number of loads on resilient modulus unstabilised A-4

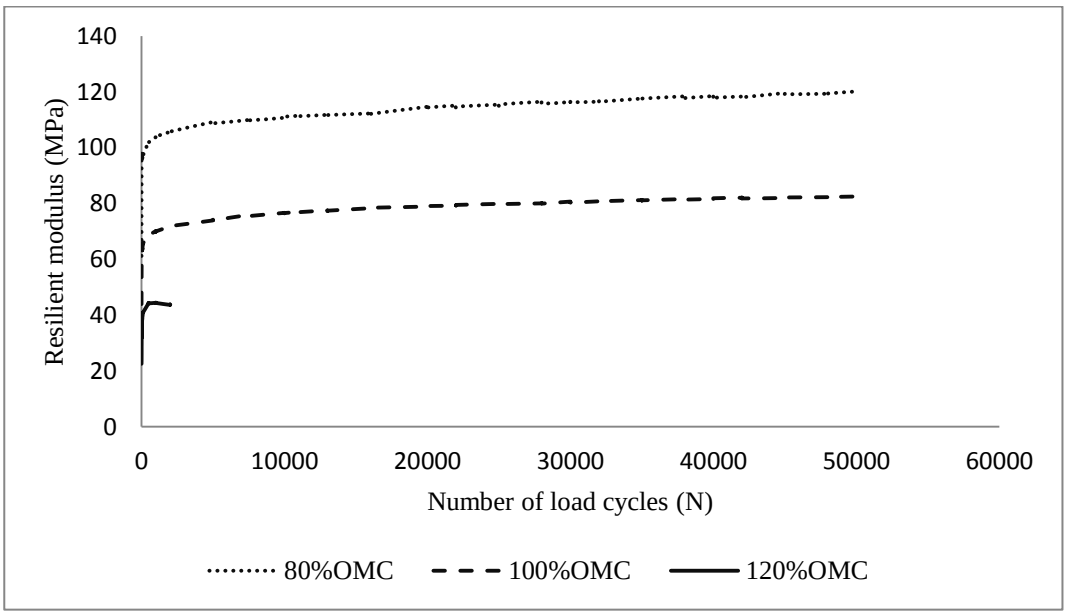

Figure 4. 16 Effect of number of loads on resilient modulus unstabilised A-6

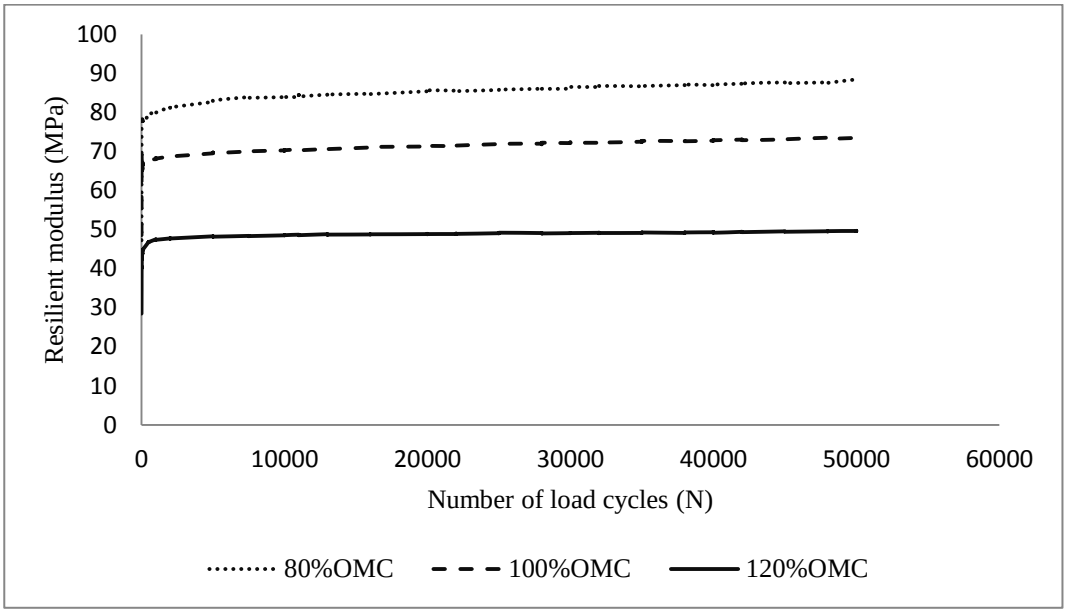

Figure 4. 17 Effect of number of loads on resilient modulus unstabilised A-7-5

The effect of the number of load repetitions on resilient modulus has different tendencies depending on the soil type. Figure 4.18 shows the resilient modulus values of these three soils at optimum moisture content from cycle 2000 to 50000. In AASHTO T307 test procedure 2000 cycles are applied to the sample for resilient modulus determination at 15 stress combination. Here the resilient modulus is shown after 2000 cycles of loads to assess the effect of number of load cycles on different soil types. It can be seen soil A-4 (which consists of 84% silt and sand) shows a higher rate of resilient modulus increase than soils A-6 and A-7-5 with 56% and 46% silt and sand content, respectively. This trend of soils was confirmed by Puppala et al (2009) that with increase in number of loads sandy soils show strain hardening.

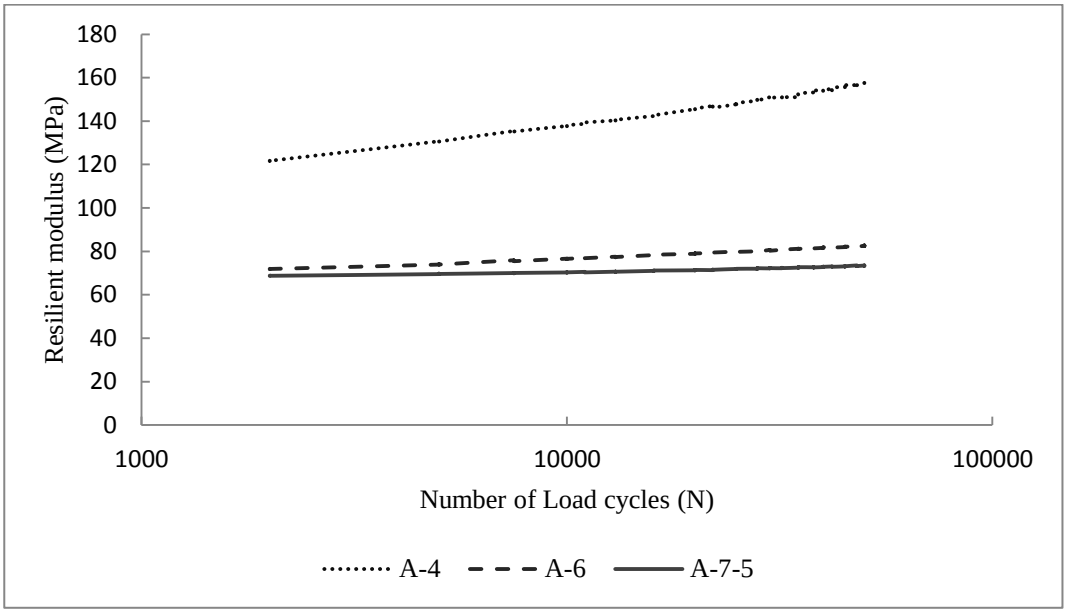

Figure 4. 18 Comparison of increase in resilient modulus value for different soil types after cycle 2000

For stabilised soils the trend is the same for all three compaction moisture contents. This may be due to a densification of the sample caused by the increase in the number of the load cycles. This can be seen in Figures 4.19-4.21 in which the three stabilised soils almost have the same rate of increase in resilient modulus while for unstabilised soils a higher increase can be observed for sand and silt soils than for the clay soil. The other conclusion is that the stabilisation not only increasing the resilient modulus value but also improves the mechanical trend and behaviour of the soils.

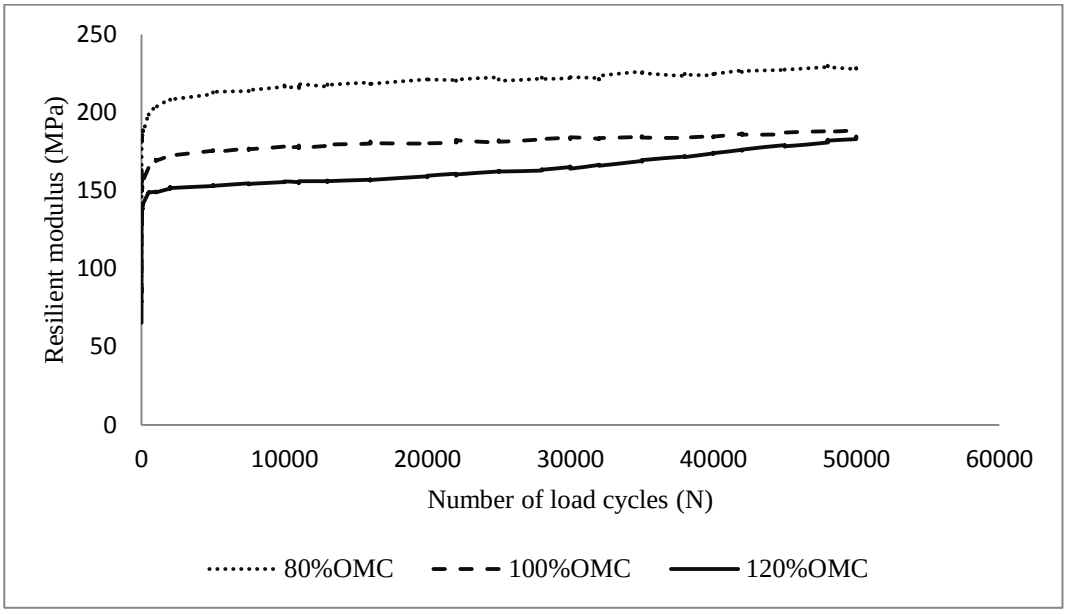

Figure 4. 19 Effect of number of loads on resilient modulus stabilised from single stage test for stabilised soil A-4

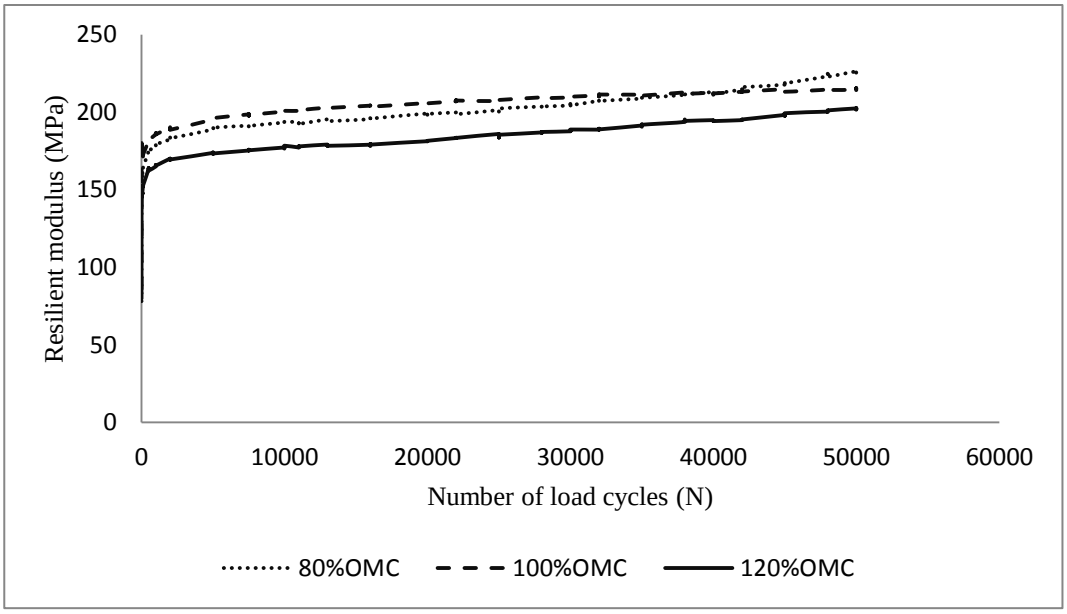

Figure 4. 20 Effect of number of loads on resilient modulus stabilised from single stage test for stabilised A-6

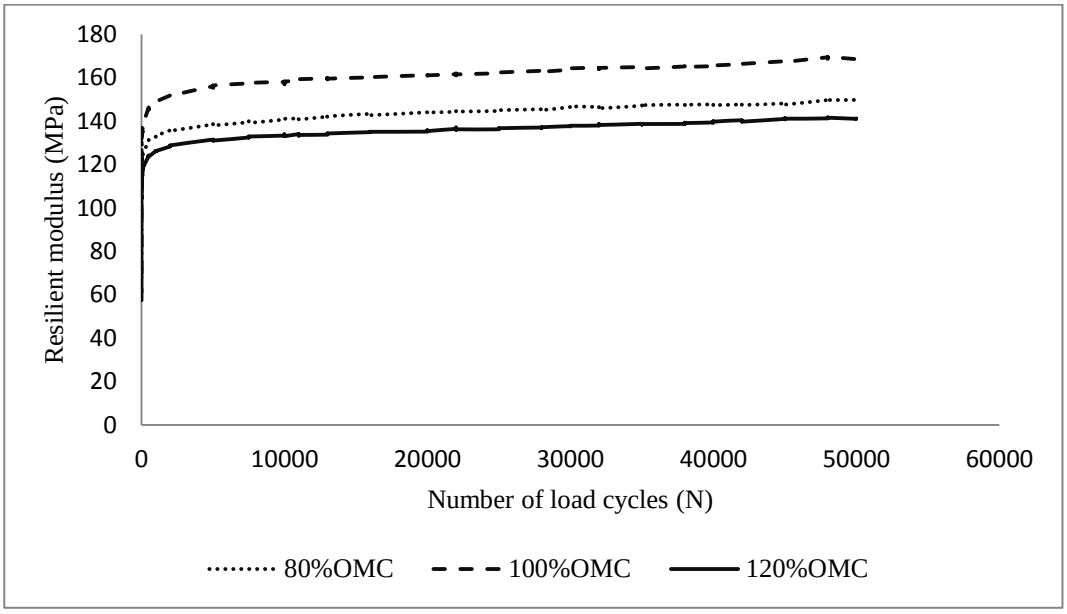

Figure 4. 21 Effect of number of loads on resilient modulus stabilised from single stage test for stabilised soil A-7-5

4.2.5 Effect of Type of Stabiliser and its Content

In order to compare these three soils for the effect of both stabiliser type and its content, they have been stabilised with 2%, 4% cement content and 2%+1.5% and 4%+1.5% combination of cement and lime. The effectiveness of soil stabilisation depends on the stabiliser type and ratio, soil type, curing time and many other factors. To account for these factors a wide range of soil type and stabiliser type and corresponding ratios are needed. However, due to the necessity of carrying out a huge number of tests of the resilient modulus and permanent deformation as well as the complexity and time constraints only lime and cement were selected in this research.

From Figure 4.22 the effect of stabilisation on soil A-4 with cement can be noticed as this soil contains 84% silt and sand and contains only 16% clay. Stabilisation with 4% cement content produced a higher resilient modulus value compared to the other proportions of stabiliser contents. At the time an addition of lime to the 2% cement content slightly increased the

resilient modulus, this lime does not contributed to the strength for 4% cement content plus 1.5% lime content. The lime content here is the minimum that obtained from initial lime consumption test. The other reason is that lime stabilised soils gain strength in long-term conditions. The same trend is confirmed by soil A-6 in Figure 4.23, this soil consisting of 18% gravel and 56% silt and sand.

A different trend has been obtained for soil A-7-5, as shown in Figure 4.24. The addition of lime showed a higher resilient modulus gain than that for stabilised with only cement. For example stabilisation with 2% cement content plus 1.5% lime content has a slightly higher resilient modulus value than stabilisation with 4% cement content of 6%, indicating the effectiveness of stabilisation with lime for clayey soils (as soil A-7-5 contains 54% clay).

For all investigated soils, the stabilisation resulted in increased in resilient modulus values of the native soil by 180%, 310% and 460% for soils A-4, A-6 and A-7-5, respectively when the highest resilient modulus value is considered for each soil type. Furthermore, the resilient modulus value of soil A-4 for stabilised and unstabilised conditions is higher than the two other soils; it is expected as it is more granular.

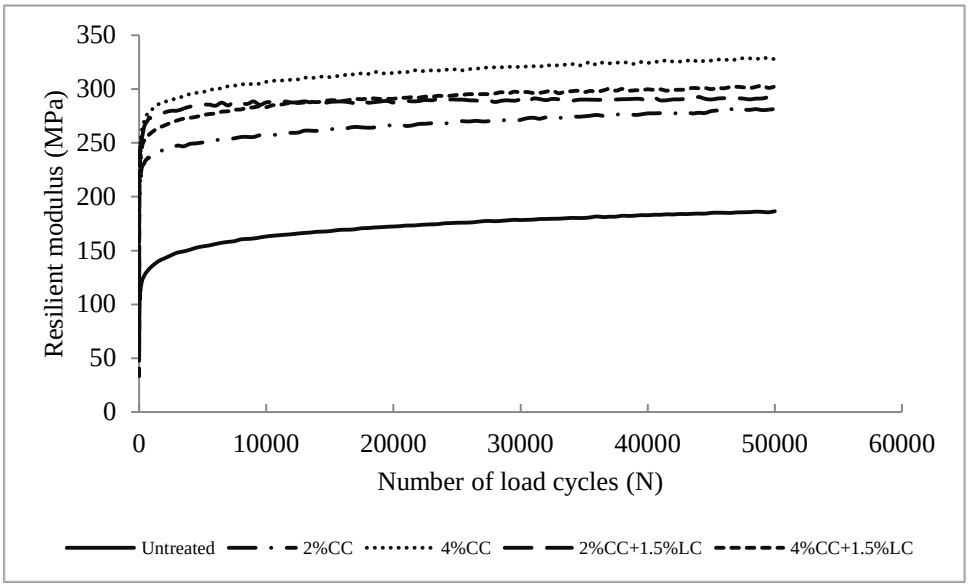

Figure 4. 22 Effect of stabilisation content on resilient modulus value for soil A-4

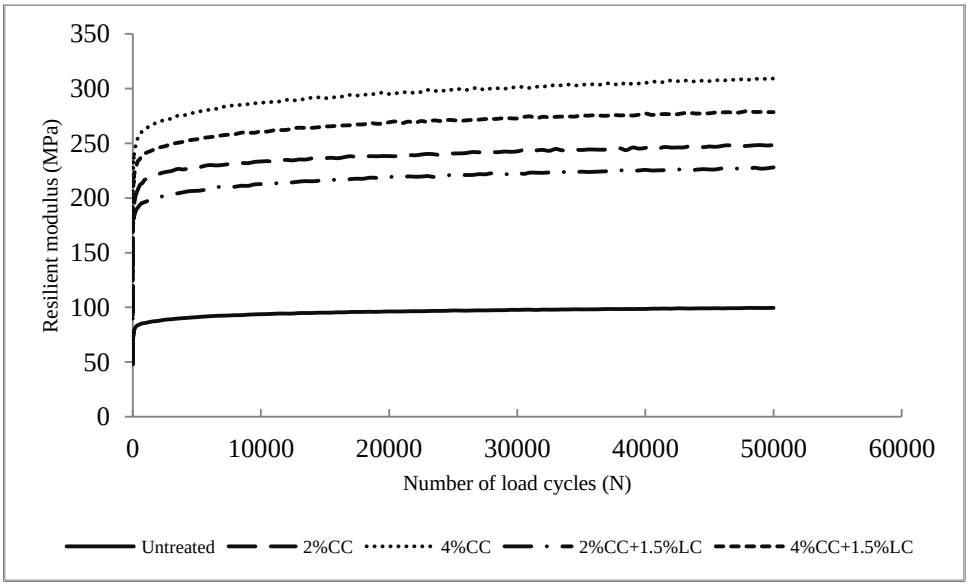

Figure 4. 23 Effect of stabilisation content on resilient modulus value for soil A-6

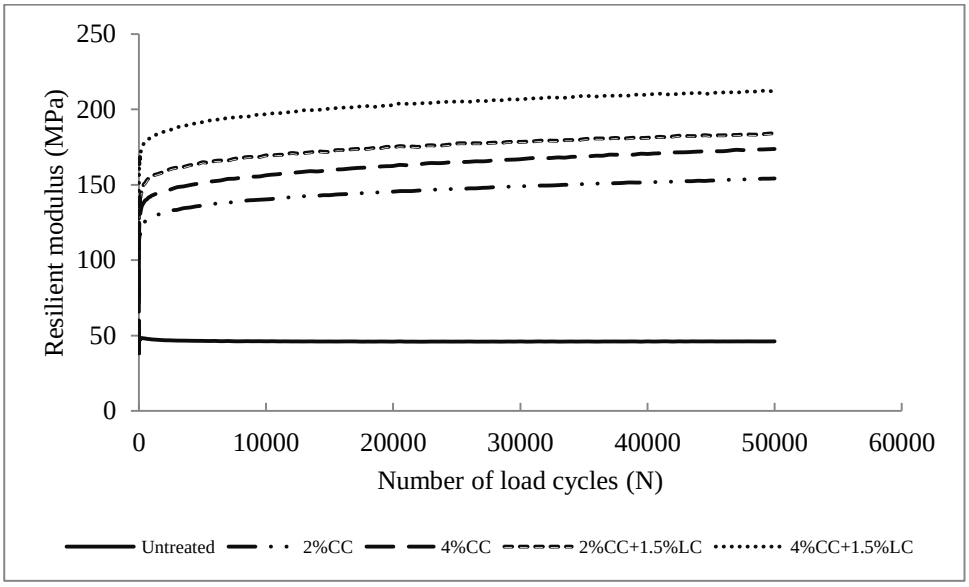

Figure 4. 24 Effect of stabilisation content on resilient modulus value for soil A-7-5

4.3 Measuring Resilient Modulus at Different Conditions

The resilient modulus of three types of soils was measured at various conditions: for unstabilised soil at three moisture contents, for stabilised soils at different stabiliser contents and after wetting and drying cycles for durability study. The effect of the moisture content and stabilisation on resilient modulus value has been explained in sections 4.2.1 and 4.2.5. However, in order to understand the performance of stabilised and unstabilised subgrade soils durability of stabilised soils need to be assessed. Freeze-thaw and wetting-drying tests are usually run to study the durability of pavement materials. The three soils (namely A-4, A-6 and A-7-5) were stabilised with 2% and 4% cement content and 2% cement plus 1.5% lime and 4% cement plus 1.5% lime respectively, see sections 1.2 and 3.2.2. Permanent deformation tests were carried out on samples using 120 kPa deviatoric stress and 12.4 kPa confining pressure for 50000 cycles. The resilient modulus test AASHTO T307 was then run directly after the permanent deformation test completion, and the resilient modulus values obtained from permanent deformation tests and the AASHTO T307 procedure was adapted.

The same samples were then submerged in water for 5 hours to start wetting and drying tests for durability study.

Soil samples of A-7-5 disintegrated at 2%CC, 4%CC and 2%CC+1.5%LC on first few cycles of wetting and only samples with 4%CC+1.5%LC endured the wetting, see for example Figure 4.25 in which the disintegration of the soil sample stabilised with 4%CC is presented. For soil A-6 only samples with 2%CC disintegrated and the other samples continued with the wetting and drying cycles see Figure 4.26 for soil A-6 with 2%CC after 20 cycles of wetting and drying. All samples of soil A-4 endured the wetting and drying cycles and tested for permanent deformation and resilient modulus tests. Table 4.3 presents all scenarios of these three soils and the cycles of wetting and drying that were carried out.

Figure 4. 25 Soil A-7-5 Stabilised with 4%CC at first cycle of wetting and drying

Figure 4. 26 Soil A-6 stabilised with 2%CC after 20 cycles of wetting and drying

Table 4. 3 Number of cycles for three types of soils stabilised with different stabiliser types and ratios

Soil type	Unstabilised	2%CC	4%CC	2%CC+1.5%LC	4%CC+1.5%LC
A-4	0	25	25	25	25
A-6	0	20	25	25	25
A-7-5	0	1	1	4	25

Resilient modulus values from permanent deformation tests after 7 days of curing and after cycles of wetting and drying are presented in Figures 4.27-4.31, which clearly show that the sandy silt soils stabilised with cement performed well compared with soils stabilised with cement and lime. In all scenarios the wetting and drying produced decreases in resilient modulus values, although in different ratios. For soils with a higher proportion of sand and silt the cement stabilisation resulted in higher resilient modulus values and the effect of wetting and drying was less than those stabilised with cement and lime such as soil A-4. On the other hand, for soils with a higher amount of clay content the effect of lime is apparent and endured well compared to cement stabilised cases, such as soil A-6 and A-7-5.

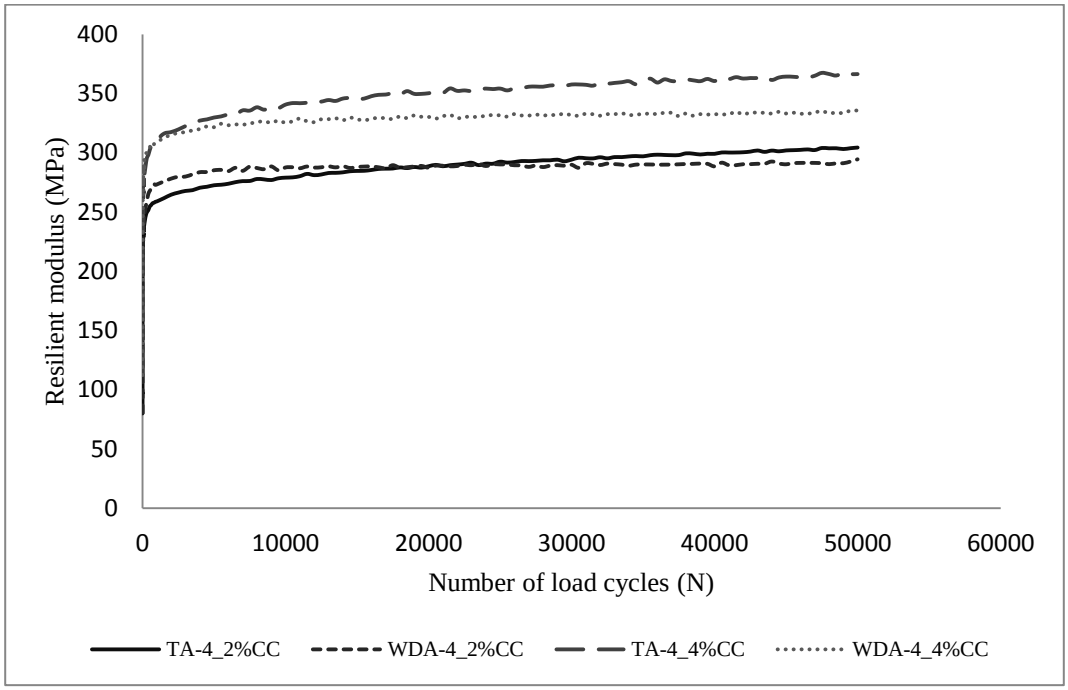

Figure 4. 27 Comparison of resilient modulus value after cycles of wetting & drying for 2%CC and 4%CC for soilA-4 (**TA** denotes for stabilised and **WD** denotes for wetting and drying)

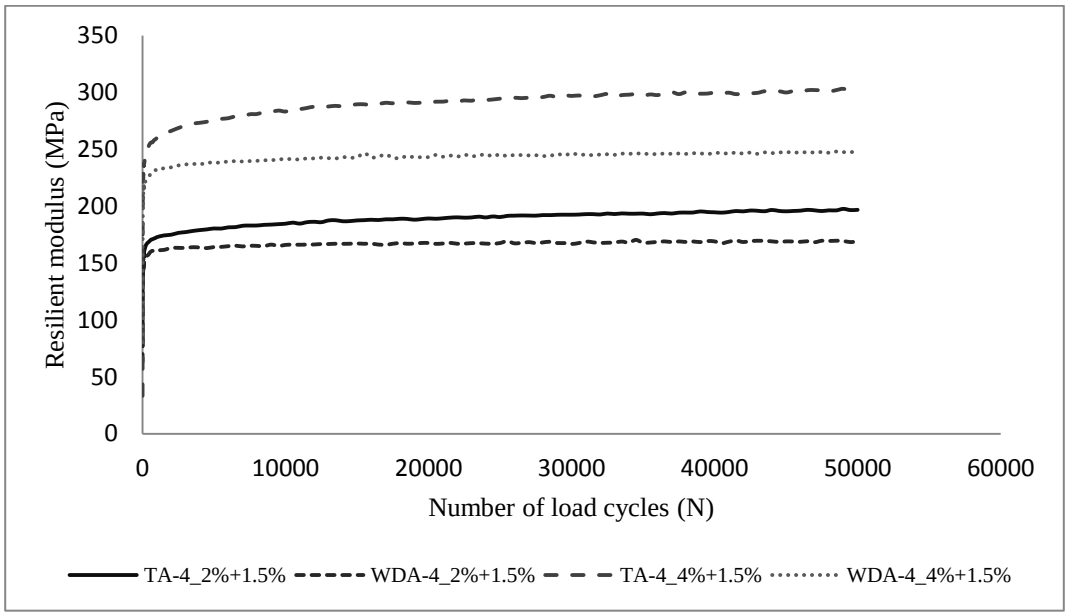

Figure 4. 28 Comparison of resilient modulus value after cycles of wetting & drying for 2%CC+1.5%LC and 4%CC+1.5%LC for soil A-4

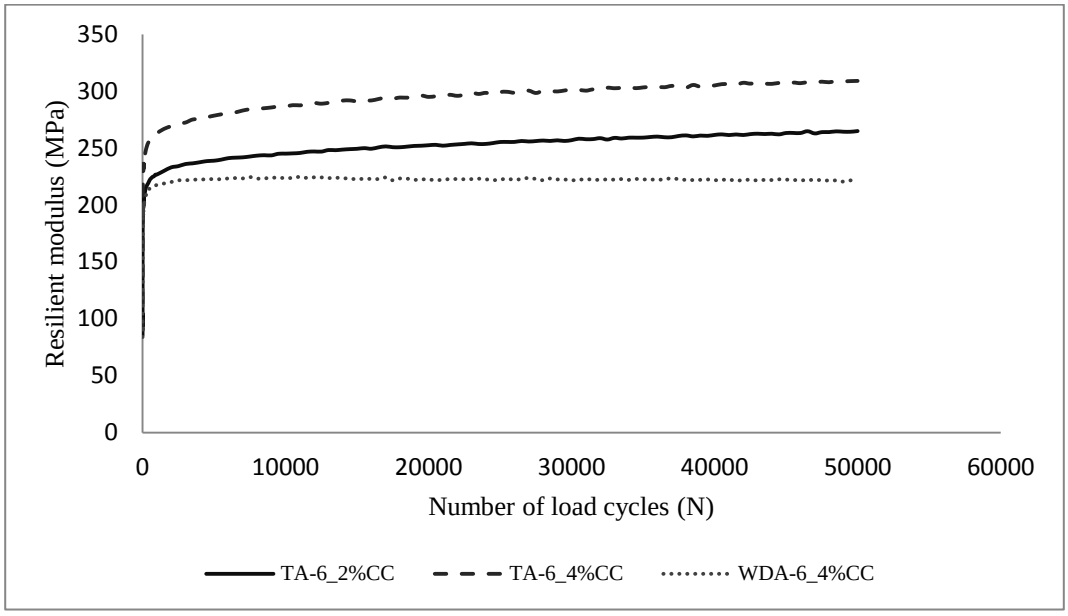

Figure 4. 29 Comparison of resilient modulus value after cycles of wetting & drying for 2%CC and 4%CC for soil A-6

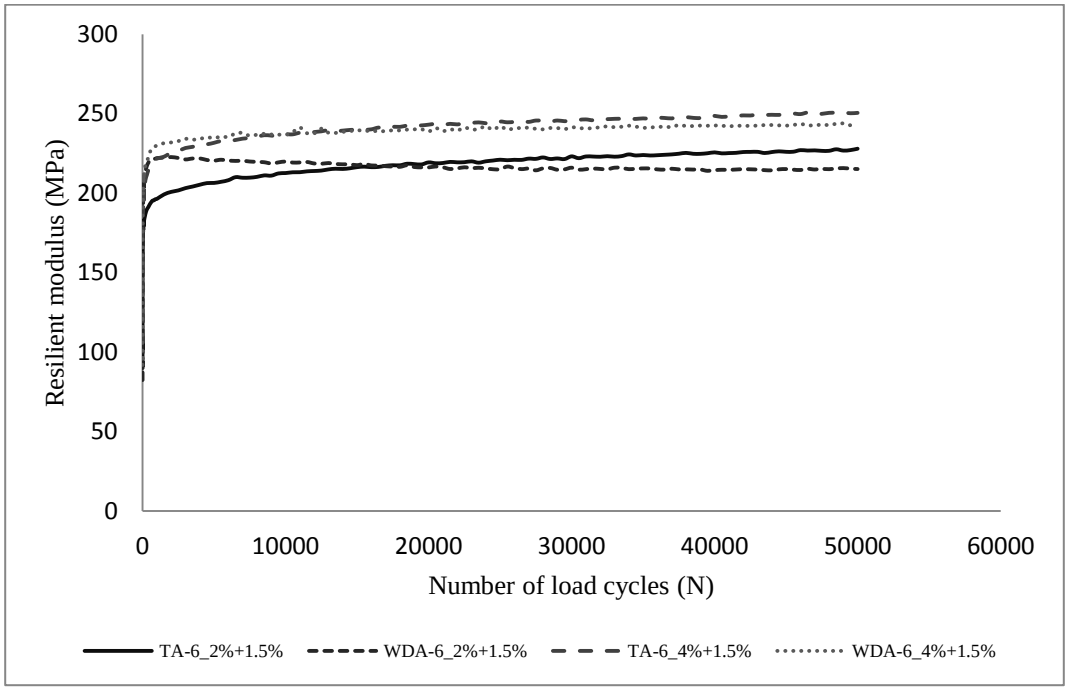

Figure 4. 30 Comparison of resilient modulus value after cycles of wetting & drying for 2%CC+1.5%LC and 4%CC+1.5%LC for soil A-6

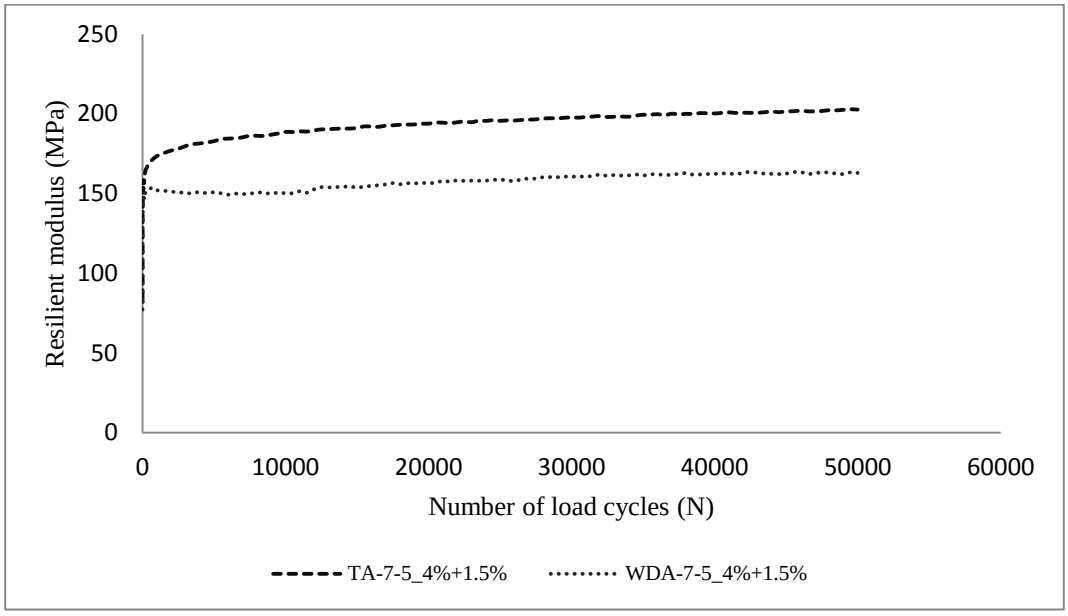

Figure 4. 31 Comparison of resilient modulus value after cycles of wetting & drying for 4%CC+1.5%LC for soil A-7-5

4.4 Nonlinear Behaviour of Subgrade Soils

As mentioned in Section 4.2.2 the intensity of the applied load affects the resilience response of both fine grained and granular materials. However, other materials such as lightly stabilised (modified) subgrade soils show this behaviour as the definition of nonlinear by MEPDG (2004) states:

'A material considered nonlinear if the value of elastic modulus depends on the state of the stress in the material. While many materials start to exhibit this behaviour at very high stress states, the only materials that are considered to be nonlinear in this Guide are unbound base/subbase and subgrade materials.'

Huang (1993) employed the K-θ model for nonlinearity of granular material in KENLAYER programme:

$$M_r = K_1 \theta^{K_2} \quad (4.2)$$

Where M_r is resilient modulus, θ is bulk stress or invariant stress $\theta = \sigma_1+\sigma_2+\sigma_3$ or $\theta = \sigma_x +\sigma_y +\sigma_z +\gamma z (1+2K_o)$ if the normal stresses and overlay weight is considered in which γ is average unit weight, z is the depth and K_o is the coefficient of earth pressure. K_1 and K_2 are material constants.

For fine grained soils Huang (1993) has incorporated bilinear equation in which the resilient modulus of fine grained soils decreases with increases of deviatoric stress in a deep slope up to a breakpoint. Thereafter the relation tends to have a flatter slope. Following equations represent two lines of the bilinear equation.

$$Mr = K_1 + K_3(K_2 - \sigma_d) \quad (4.3a)$$

$$Mr = K_1 - K_4(\sigma_d - K_2) \quad (4.3b)$$

In which σ_d is deviatoric stress = σ_1-σ_3 and K_i are material constants

ILLI-PAVE finite element programme by Raad and Figueroa (1980) also included the nonlinearity of unbound granular material through K-θ model for granular material and bilinear equation (equation 4.4) for fine-grained sand.

$$E_R = f\sigma_D \quad (4.4)$$

Where E_R is resilient modulus, σ_D is deviatoric stress and f is regression constant.

Researchers have defined Uzan and Witczak (1985) universal equation through the user defined subroutine (UMAT) in finite element models to account for unbound granular material nonlinearity. The Uzan and Witczak (1985) equation is appropriate for stabilised subgrade soils as shown in Table 4.4 and 4.5. Tables 4.4 and 4.5 present the parameters of this equation for unstabilised and stabilised soils, respectively. The coefficient of significance (R^2) of stabilised soils support the suitability of this equation for stabilised soils as it is more than 0.9 for all cases.

Table 4. 4 Parameters of Uzan and Witczak equation for unstabilised soil

Soil type	%OMC	K_1	K_2	K_3	R^2
A-4	80	0.867	0.088	0.102	0.87
	100	1	-0.524	0.964	0.853
	120	0.83	-0.292	0.342	0.921
A-6	80	1.079	-0.07	0.121	0.747
	100	0.427	0.137	-0.173	0.954
	120	0.303	0.127	-0.198	0.929
A-7-5	80	0.804	0.003	0.028	0.521
	100	0.655	-0.016	-0.015	0.202
	120	0.283	-0.1	-0.242	0.952

Table 4. 5 Parameters of Uzan and Witczak equation for stabilised soil

Soil type	%OMC	K_1	K_2	K_3	R^2
A-4	80	2.242	0.104	0.243	0.977
	100	2.555	0.13	0.294	0.983
	120	1.801	0.093	0.325	0.991
A-6	80	2.585	0.086	0.344	0.99
	100	2.829	0.088	0.38	0.991
	120	2.644	0.067	0.321	0.992
A-7-5	80	1.858	0.124	0.215	0.948
	100	2.272	0.068	0.359	0.98
	120	1.676	0.028	0.225	0.927

In this research the results from multistage permanent deformation tests are used to draw graphs representing the relationship between resilient modulus and deviatoric stress. The resilient modulus values were obtained by taking the average of the last four cycles at the end of each stress level stage. This is reasonable since the value is obtained after 10000 cycles of conditioning, which is the number of load repetitions for each stage. AASHTO T307 applies

500 to 1000 cycles for conditioning and 100 cycles for each stress combination (AASHTO, 2003) and then the last five cycles are averaged, while BS EN 13286-7 (BS, 2004) recommends taking the average of last 10 cycles after conditioning for 20000 cycles, however this number of load repetitions is much too big. Figures 4.32 and 4.33 are from the aforementioned procedure.

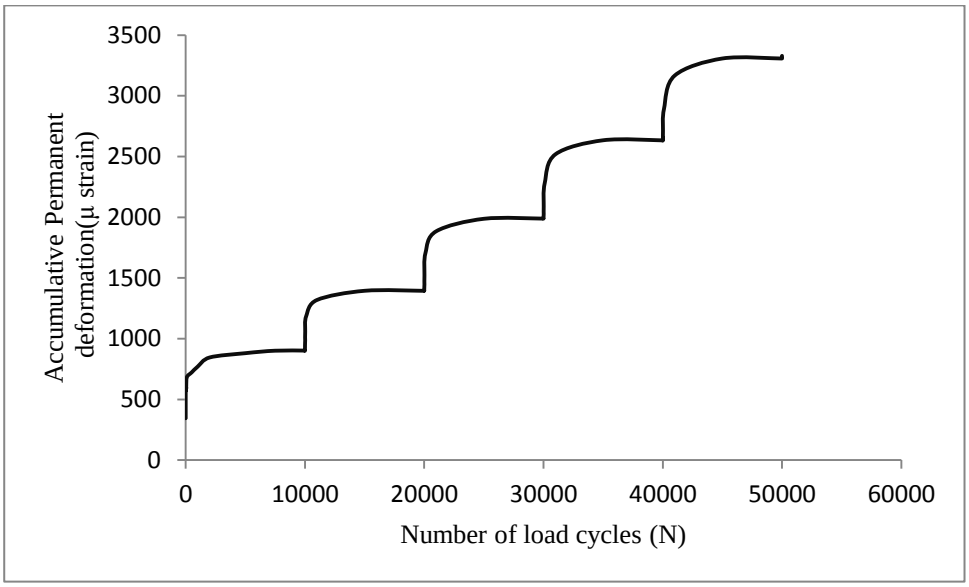

Figure 4. 32 Multistage permanent deformation test for unstabilised soil A-4 at optimum moisture content

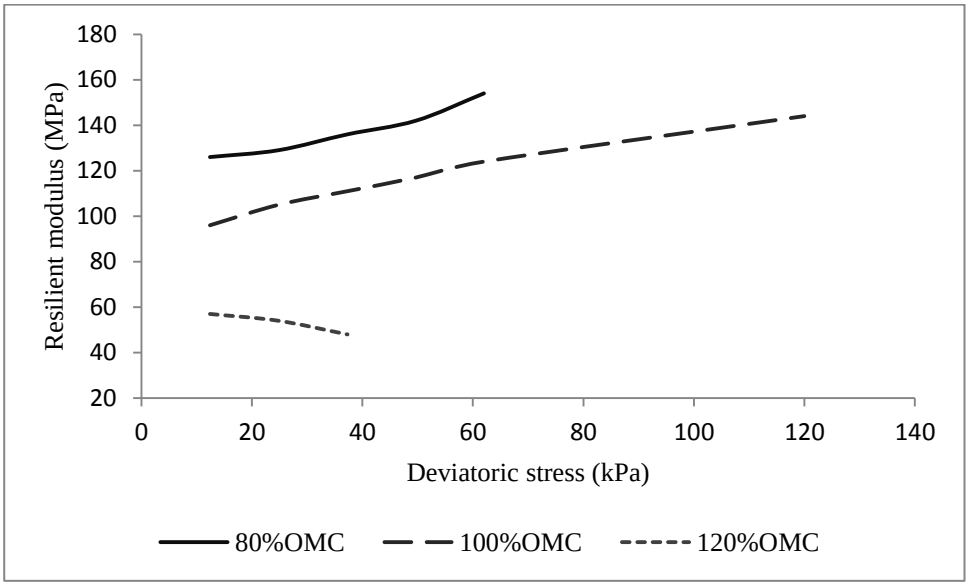

Figure 4. 33 Deviatoric to resilient modulus relation of unstabilised A-4 soil

Huang (1993) used an iterative method to determine the nonlinearity of granular material. First he determined the stresses from Burmister's layer theory. These stresses are then input to the elastic modulus equation, equation 4.5, with this elastic modulus used in the next analysis step to determine a new set of stresses. This procedure is continued until the differences between successive moduli are within tolerance.

$$E = E_o(1 + \beta\theta) \qquad (4.5)$$

Where E is elastic modulus under the applied stresses, E_o is the initial elastic modulus, θ is sum of stresses and β is a soil constant.

The following procedure was incorporated to take into account the nonlinearity of resilient response (to the applied load) in pavement design for stabilised and unstabilised subgrade soils:

i) A graph was plotted from the multistage permanent deformation test between deviatoric stress and resilient modulus.

ii) Pavement section with resilient modulus from the test result was then analysed for stress at the top of the subgrade or any required critical location (e.g. mid-depth of compacted subgrade layer). The resilient modulus was chosen such that the stress combination is close to the analysis results.

iii) From the resilient modulus/deviatoric stress graph (stage i above) determine the value of resilient modulus corresponding the relevant determined stress.

iv) The analysis is continued until the difference between successive stress values is negligible.

v) The next step is to use the resilient modulus determined from stage iv (above) in the analysis to find the stresses and strains at critical locations that can later be used in performance models.

The resilient modulus from this procedure is considered reliable as it represents the stress combination that was obtained through laboratory test. Examples demonstrating this procedure are presented in Chapter Seven.

Table 4.6 shows the difference between the converged resilient modulus and the compressive stress at the top of the subgrade soil from the KENLAYER programme (iteration process) and the procedure suggested in this research. As can be seen layers 3 and 4 have the same starting resilient modulus values, however with the depth the stress reduces and the resilient modulus values change consequently depending on the soil type. Previous sections show different trends of material behaviour to applied deviatoric stresses for the subgrade soils; it therefore appears to be more suitable to use the relationship of resilient modulus and deviatoric stress relations obtained from laboratory tests for nonlinearity of the subgrade soils (e.g. Figure 4.33). Furthermore the same sort of relationship can be used for stabilised subgrade soils.

Table 4. 6 the iteration progress in KENLAYER for resilient modulus nonlinearity

Iteration No.	Layer No./ Modulus (MPa)	Layer No./ Modulus (MPa)
At iteration 1	3 4.600E+04	4 4.600E+04
At iteration 2	3 4.936E+04	4 5.268E+04
At iteration 3	3 5.112E+04	4 5.602E+04
At iteration 4	3 5.203E+04	4 5.768E+04
At iteration 5	3 5.251E+04	4 5.851E+04
At iteration 6	3 5.275E+04	4 5.892E+04

4.5 Deterioration Factor

Mechanistic-Empirical Pavement Design Guide, MEPDG (2004) recommends a minimum compressive strength of 1724 kPa (250 psi) for stabilised subbases, selected material and subgrade soils for flexible pavements. However, analytical pavement design methods require the use of the resilient modulus, which is preferable. To obtain this important property for different conditions, especially after the material undergoing deterioration from environmental and loading conditions, a new model suggested here.

The ratio of the resilient modulus of a particular soil stabilised with a given amount and type of stabiliser is subject to weathering, M_rAWD to the resilient modulus of the stabilised soil not subject to weathering, M_rA, can be written as:

$$F_A = \frac{M_{rAWD}}{M_{rA}} \tag{4.6}$$

Where F_A is the deterioration factors of material A

Then assume that the ratios of the deterioration factors of the same soil, each with different amounts of the same stabiliser, is a function only of the resilient modulus values of the two materials and can therefore be written as:

$$\frac{F_A}{F_B} = \frac{M_{rA}}{M_{rB}} \quad (4.7)$$

$$F_B = \frac{M_{rBWD}}{M_{rB}} \quad (4.8)$$

this is the same as Equation (4.6) but for material B

Combining Equations 4.6, 4.7 and 4.8 and rearranging yields:

$$M_{rAWD} = M_{rBWD} * \left(\frac{M_{rA}}{M_{rB}}\right)^2 \quad (4.9)$$

Accordingly using Equation 4.9, the resilient modulus of material A subject to weathering can be determined from the values of the resilient modulus of material A prior to weathering together with the resilient modulus of material B both before and after weathering.

The significance of Equation 4.9 is that, by knowing the weathered resilient modulus of a soil with one stabiliser content and type, the weathered resilient modulus values for a range of stabiliser ratios and types can be predicted (estimated) without carrying out the respective laboratory tests.

To validate the equation the results of resilient modulus and permanent deformation tests were carried out on three soils at four different stabilisation ratios before and after cycles of wetting and drying, see Tables 4.7, 4.8, 4.9 and 4.10 showing these data. Figure 4.34 compares the measured values of resilient modulus versus those predicted using Equation 4.9 for soils A-4 and A-6. From Figure 4.34 it may be seen that there is a close agreement between the measured and predicted resilient modulus values with associated coefficient of significance (R^2) value of 0.77. Table 4.11 shows the resilient modulus values for soil A-7-5

found from equation 4.9 for three different stabiliser contents and ratios from results of stabilisation with 4%CC+1.5%LC.

Table 4. 7 Resilient modulus for stabilised and corresponding values after wetting and drying for soil A-4

Deviatoric Stress (kPa)	2%CCT* Mr (MPa)	2%CCWD# Mr (MPa)	4%CCT Mr (MPa)	4%CCWD Mr (MPa)	2%CC+1.5 %LCT Mr (MPa)	2%CC+1.5 %LCWD Mr (MPa)	4%CC+1.5 %LCT Mr (MPa)	4%CC+1.5 %LCWD Mr (MPa)
12.4	131	72	176	132	111	76	135	121
24.8	161	82	202	146	135	93	172	141
37.3	187	92	220	162	158	106	200	155
49.7	210	103	239	184	182	120	228	170
62.0	226	113	258	205	203	134	256	185
12.4	135	71	167	128	105	74	131	117
24.8	162	81	194	143	129	89	165	137
37.3	185	90	214	159	152	103	195	152
49.7	206	102	236	180	176	117	224	166
62.0	223	112	256	201	198	131	250	183
12.4	127	68	162	123	100	70	121	113
24.8	156	78	187	139	124	86	159	132
37.3	182	89	209	156	147	100	190	147
49.7	203	99	231	177	171	114	218	163
62.0	222	110	252	197	193	128	245	178
120.0	282	160	328	292	295	194	352	255

*T is the resilient modulus of stabilised soil before wetting and drying

#WD is the resilient modulus of stabilised soil after cycles of wetting and drying

Table 4. 8 Measured to predict from equation 4.9 resilient modulus values for soil A-4

Deviatoric Stress (kPa)	2%CC Mr (MPa)		4%CC Mr (MPa)		2%CC+1.5LC Mr (MPa)	4%CC+1.5%LC Mr (MPa)	
	Measured	Predicted	Measured	Predicted	Control	Measured	Predicted
12.4	72	54	132	189	76	121	111
24.8	82	65	146	207	93	141	150
37.3	92	76	162	205	106	155	170
49.7	103	90	184	206	120	170	188
62.0	113	108	205	216	134	185	212
12.4	71	44	128	186	74	117	114
24.8	81	56	143	201	89	137	146
37.3	90	70	159	204	103	152	170
49.7	102	85	180	210	117	166	189
62.0	112	103	201	219	131	183	208
12.4	68	43	123	183	70	113	102
24.8	78	54	139	194	86	132	141
37.3	89	65	156	202	100	147	167
49.7	99	81	177	207	114	163	185
62.0	110	97	197	218	128	178	205
120.0	160	212	292	238	194	255	276

Table 4. 9 Resilient modulus for unstabilised and stabilised and corresponding value after wetting and drying for soil A-6

Deviatoric Stress (kPa)	2%CC Mr (MPa)	4%CC Mr (MPa)	4%CCWD Mr (MPa)	2%CC+1.5%LC Mr (MPa)	2%CC+1.5%LCWD Mr (MPa)	4%CC+1.5%LC Mr (MPa)	4%CC+1.5%LCWD Mr (MPa)
12.4	139	122	93	113	78	121	99
24.8	160	151	107	133	89	156	116
37.3	174	177	120	149	97	177	133
49.7	187	199	136	162	107	195	148
62.0	200	221	152	175	117	213	167
12.4	136	117	91	110	77	115	94
24.8	156	146	103	129	85	148	111
37.3	171	173	117	145	94	170	127
49.7	185	195	132	159	104	189	145
62.0	198	217	149	172	116	209	164
12.4	133	110	87	106	74	109	91
24.8	153	140	100	126	83	142	108
37.3	168	166	114	141	93	166	125
49.7	182	190	129	156	103	186	142
62.0	196	212	145	170	113	205	161
120.0	248	309	221	228	167	279	243

Table 4. 10 Measured to predicted resilient modulus values for soil A-6

Confining pressure (kPa)	Deviatoric Stress (kPa)	4%CC Mr (MPa)		2%CC+ 1.5%LC Mr (MPa)	4%CC+1.5%LC Mr (MPa)	
		Measured	Predicted	Control	Measured	Predicted
41.4	12.4	93	91	78	99	89
41.4	24.8	107	115	89	116	122
41.4	37.3	120	137	97	133	138
41.4	49.7	136	161	107	148	155
41.4	62.0	152	187	117	167	174
27.6	12.4	91	88	77	94	85
27.6	24.8	103	108	85	111	111
27.6	37.3	117	134	94	127	129
27.6	49.7	132	157	104	145	148
27.6	62.0	149	185	116	164	171
12.4	12.4	87	80	74	91	79
12.4	24.8	100	103	83	108	106
12.4	37.3	114	130	93	125	129
12.4	49.7	129	153	103	142	147
12.4	62.0	145	176	113	161	164
12.4	120.0	221	307	167	243	249

Table 4. 11 Predicted resilient modulus values for different stabiliser combination for soil A-7-5

Deviatoric Stress (kPa)	2%CC Mr (MPa)		4%CC Mr (MPa)		2%CC+1.5LC Mr (MPa)		4%CC+1.5%LC Mr (MPa)	
	Before W&D	Predicted after W&D	Before W&D	Predicted after W&D	Before W&D	Predicted after W&D	Before W&D	Control
12.4	76	31	101	54	123	82	125	84
24.8	90	37	117	62	137	86	140	90
37.3	101	43	127	69	146	90	152	99
49.7	111	49	136	74	152	93	163	108
62.0	121	57	143	79	158	97	174	117
12.4	75	31	96	52	119	80	118	78
24.8	87	35	112	58	133	83	133	83
37.3	98	40	124	64	142	84	147	90
49.7	108	46	134	70	150	89	159	100
62.0	119	53	141	74	157	93	172	111
12.4	72	29	92	48	113	72	116	77
24.8	85	34	108	56	131	82	131	83
37.3	96	40	121	63	140	86	144	91
49.7	107	47	130	70	149	91	157	102
62.0	117	54	138	75	156	95	169	112
120.0	155	87	174	110	184	123	212	163

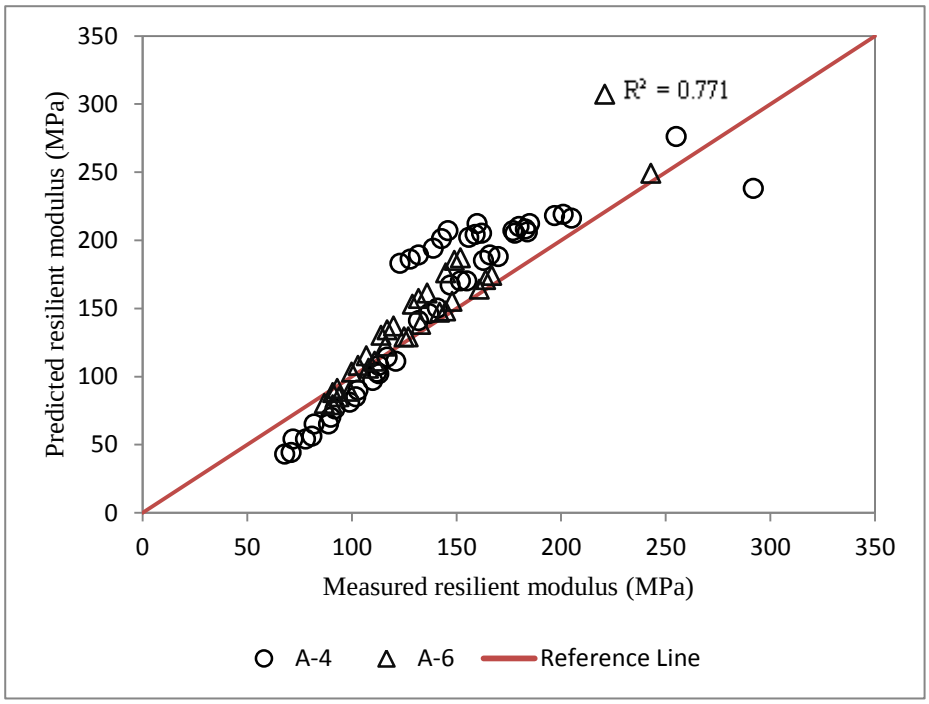

Figure 4. 34 Relationship between resilient modulus measured from tests and predicted from equation

4.6 Resilient Modulus Correlation Equations

In this section correlation between unconfined compressive strength (UCS) and resilient modulus is presented for stabilised subgrade soils. Unconfined compressive strength tests can be used to compare unstabilised soils at different moisture contents and to compare the strength properties of stabilised soils with different types and ratios of stabilisers. Correlations have been developed between UCS and resilient modulus. One such correlations for lime stabilised soils is given by Thompson (1970) (Little and Yusuf, 2001), Equation 4.10. See Table 4.13.

$$E_R = 0.124\ (UCS) + 9.98 \qquad (4.10)$$

Where E_R is resilient modulus given in Ksi and *UCS* is unconfined compressive strength in Psi

As discussed in previous sections many factors affect the resilient modulus value. Most have the same effects on both UCS and M_r. For example an increase in moisture content decreases both the UCS and M_r values. However, the effects that the changes in deviatoric stress make to the resilient modulus value cannot be expressed by UCS alone in Equation 4.10. Therefore, a correlation equation is suggested here taking into account the changes in deviatoric stress and UCS values to estimate the resilient modulus, $M_r\ \alpha\ (\sigma_d, p, UCS)$. In other words the resilient modulus is directly proportional to UCS and σ_d.

Equation 4.11 as suggested here is derived from analysis of permanent deformation and UCS tests. The dependency of the resilient modulus to the applied stress was presented in previous sections, particularly for stabilised soils in which the trend is principally constant as such any increase in deviatoric stress results in a corresponding increase in resilient modulus value.

Therefore, it is necessary to include this trend when correlating this property with other material properties such as UCS.

$$M_r = UCS^{a+b*\sigma_d} \quad (4.11)$$

Where M_r is resilient modulus in MPa, *UCS* is unconfined compressive strength in kPa, σ_d is deviatoric stress in kPa and *a* and *b* are regression parameters.

Table 4. 12 Unconfined compressive strength results after 7 days curing

Soil Type	Stabiliser content (%)	Average UCS (kPa)	Soil Type	Stabiliser content (%)	Average UCS (kPa)	Soil Type	Stabiliser content (%)	Average UCS (kPa)
A-4	Unstabilised	197	A-6	Unstabilised	178	A-7-5	Unstabilised	171
	2%CC	580		2%CC	579		2%CC	275
	4%CC	956		4%CC	874		4%CC	357
	2%CC+ 1.5%LC	618		2%CC+ 1.5%LC	557		2%CC+ 1.5%LC	427
	4%CC+ 1.5%LC	955		4%CC+ 1.5%LC	774		4%CC+ 1.5%LC	501

The resilient modulus values presented in Tables 4.7-4.11 and UCS in Table 4.12 are used for regression analysis for determining parameters, a and b, and validation of the model. For this purpose samples stabilised with 2%CC+1.5%LC and 4%CC+1.5%LC were used for regression analysis and samples stabilised with 2%CC and 4%CC were used for validation. From regression analysis values of a & b were found to be 0.737 and 0.001, respectively with an R^2 of 0.791. The validation of the calibrated equation is presented in Table 4.13, in which resilient modulus values obtained from the tests were compared with those obtained using Equation 4.11 and the comparison is depicted also in Figure 4.35 between measured and predicted. As can be seen the Mean Absolute Percentage Error (MAPE) (Hyndman and Koehler, 2006) of predicted is 19% indicating the reasonableness of the equation in predicting estimated value of resilient modulus of stabilised subgrade soils from unconfined compressive

strength tests (UCS) with a coefficient of significance (R^2) of 0.733. While the resilient modulus values obtained from Equation 4.10 have a Mean Absolute Percentage Error of 25%. This shows the accuracy of the correlation equation (Equation 4.11) in predicting the resilient modulus of lightly stabilised subgrade soils. At the same time in most cases the predicted resilient modulus values are lower than the measured resilient modulus values; therefore using these values secure a more conservative design.

Another correlation equation (Equation 4.12) has been developed in this research with a higher number of parameters including bulk stress and octahedral shear stress. These parameters were used in Uzan-Witczak (1985) model known as universal model for prediction of the resilient modulus of granular unbound materials from stress state of the applied load. However, in this research these parameters are used for correlation equation to predict the resilient modulus value of stabilised subgrade soils from UCS test results.

$$Mr = UCS^{[a*\left(\frac{\theta}{\sigma_{atm}}\right)^{b}*\left(\frac{\tau_{oct}}{\sigma_{atm}}\right)^{c}]} \quad (4.12)$$

In which θ = bulk stress = $\sigma_1+2\sigma_3$, τ_{oct}= octahedral shear stress = $(\sqrt{2}/3)(\sigma_1-\sigma_3)$, σ_{atm} = atmospheric pressure = 101 kPa and *a, b* and *c* are regression parameters

The same data for previous equation (Equation 4.11) were used in a nonlinear regression analysis in SPSS program from which these parameters were found to be; *a* = 0.882, *b* = 0.017 and *c* = 0.066 with R^2 = 0.833. The similar calculation carried out as for previous equation in Table 4.13 and a Mean Absolute Percentage Error (MAPE) of 15% obtained. A detailed cacluation and validation of this equation is presented in Table B.4 Appendix B. The comparison of measured to predicted resilient modulus values, using Equation 4.12, is

dicpicted in Figure 4.36 with an R^2 of 0.821, this shows this equation gives more accurate results and at the same time with lower conservative values.

4.7 Discussion

Using resilient modulus value as a key design parameter in road pavement design has been emphasised in literature and explained in this thesis (see Chapters Two to Seven). The factors affecting the resilient modulus property of unstabilised soils showed to include a wider range than lightly stabilised soils, especially the stress dependency of the soils. The discussion and example explanations in Chapter Six section 6.5 shows the diverse behaviour of unstabilised fine grained soils. While the resilient modulus of unstabilised soils may show decrease or increase with an increase in deviatoric stress depending on the soil type and clay content, the increase in resilient modulus with an increase in deviatoric stress is a constant trend for lightly stabilised soils. This constant trend of stress dependency of the lightly stabilised soils makes it easy for road designer to choose the correlation models of resilient modulus for stabilised soils more confidently. In other words the correlation equations developed between the resilient modulus value and other material properties for stabilised soils are more accurate than the same correlations developed for unstabilised soils. Therefore, using resilient modulus as a key design parameter for lightly stabilised subgrade soils is supported by this research.

Table 4. 13 Comparison of resilient modulus values of measured and predicted from equations 10 and 11

Soil Type	Stabilisation Ratio	Average UCS (kPa)	Deviatoric Stress (kPa)	Measured Mr (MPa)	Predicted Mr (MPa) eq. 4.11		Predicted Mr (MPa) eq. 4.10	
A-4	2%CC	580	12.4	131	118	0.101	141	0.074
			24.8	160	127	0.202	141	0.119
			37.3	185	138	0.253	141	0.238
			49.7	206	149	0.277	141	0.318
			62.0	224	161	0.278	141	0.371
			120.0	282	233	0.172	141	0.501
	4%CC	969	12.4	168	173	0.030	189	0.125
			24.8	194	188	0.030	189	0.027
			37.3	214	205	0.042	189	0.118
			49.7	235	224	0.049	189	0.196
			62.0	255	243	0.047	189	0.260
			120.0	328	362	0.107	189	0.423
A-6	2%CC	559	12.4	136	115	0.158	138	0.016
			24.8	156	124	0.208	138	0.116
			37.3	171	134	0.216	138	0.192
			49.7	185	145	0.215	138	0.252
			62.0	198	157	0.208	138	0.302
			120.0	248	226	0.088	138	0.443
	4%CC	845	12.4	116	156	0.344	174	0.494
			24.8	145	170	0.168	174	0.194
			37.3	172	185	0.075	174	0.011
			49.7	194	201	0.033	174	0.107
			62.0	217	218	0.007	174	0.198
			120.0	309	322	0.043	174	0.438
A-7-5	2%CC	275	12.4	74	67	0.090	103	0.391
			24.8	87	72	0.171	103	0.183
			37.3	98	77	0.211	103	0.048
			49.7	108	83	0.234	103	0.050
			62.0	119	89	0.253	103	0.135
			120.0	155	123	0.203	103	0.334
	4%CC	357	12.4	96	82	0.146	113	0.180
			24.8	112	88	0.214	113	0.010
			37.3	124	95	0.234	113	0.086
			49.7	133	102	0.234	113	0.150
			62.0	141	110	0.220	113	0.195
			120.0	174	154	0.115	113	0.350
					Mean Absolute Percentage Error (MAPE)	19	Mean Absolute Percentage Error (MAPE)	25

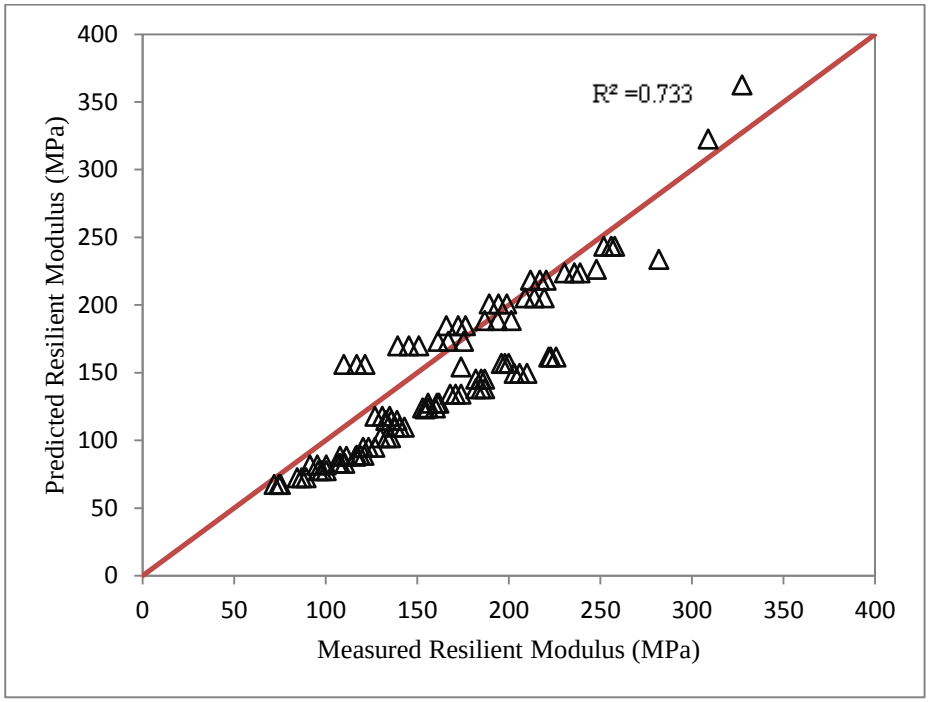

Figure 4. 35 measured resilient modulus from tests versus predicted resilient modulus from equation 4.11

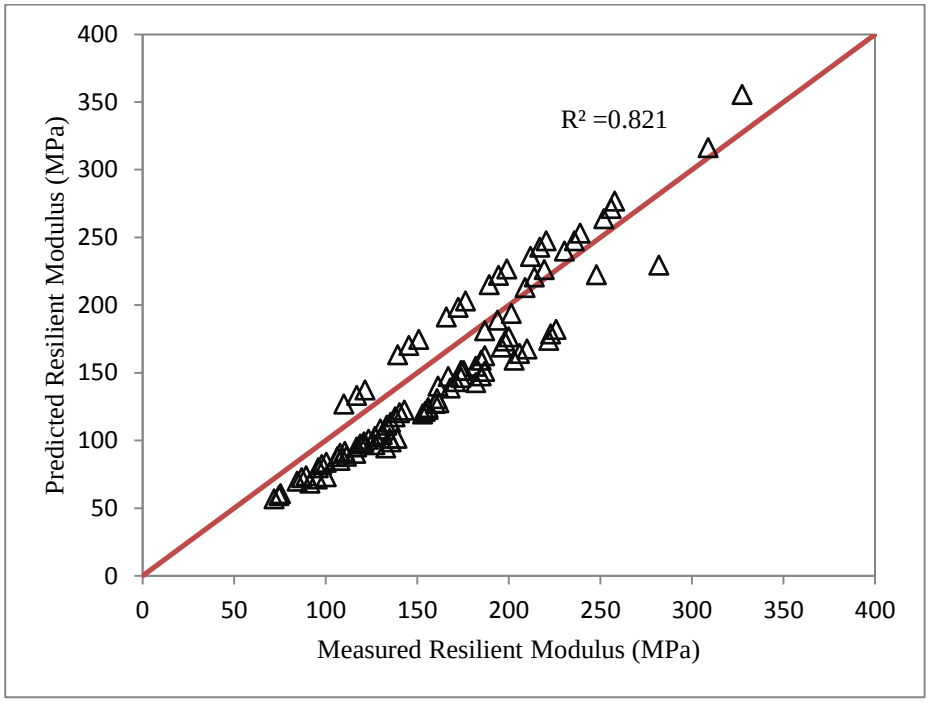

Figure 4. 36 measured resilient modulus from tests versus predicted resilient modulus from equation 4.12

4.8 Summary

The resilient modulus at different moisture and stress level conditions was determined from repeated load triaxial tests. The factors affecting the resilient modulus value and deterioration conditions that subgrade soils experience during their design life were assessed to show the changes to the mechanical properties of three types of soils for both stabilised and unstabilised cases. The susceptibility of soils to moisture, which is one of the factors affecting the pavement performance, is demonstrated. From the wide range of test results in this research a durability model was developed. Also two correlation equations were developed to predict the resilient modulus value from unconfined compressive strength results. Equation 4.12 which considers the octahedral shear strength and bulk stress can predict the resilient modulus from UCS more accurately. However, Equation 4.11 is simpler, which considers only the deviatoric stress. In order to demonstrate the outcome from the effect of these factors and conditions, their resilient modulus values were used in pavement section analysis. Finite element model and analytical techniques were used to compute compression stresses at the top of subgrade, which can then be used later in performance models to determine the life of the section. These calculations are presented in Chapter Seven.

CHAPTER FIVE

PERMANENT DEFORMATION

5.1 Introduction

One of the processes in an analytical pavement design procedure is the performance prediction of the road pavement's structure. Usually it is assessed from the number of load repetitions required to cause failure. Two most frequently used failure modes are fatigue cracking and rutting caused by repeated tyre loading. Typically a limit will be set on the top of the subgrade to control permanent deformation (rutting) distress. Therefore, a number of permanent deformation models were developed to incorporate this factor into road pavement design procedures. The permanent deformation in these models is dependent on the number of load repetitions in some of them and on the stress state and the number of load repetitions in others. The same factors affecting resilient modulus and conditions are applied to the permanent deformation and presented in this chapter.

5.2 Permanent Deformation Characterization

5.2.1 Effect of Moisture Content

From single-stage permanent deformation tests the effect of moisture change on permanent deformation is assessed and presented in Figures 5.1-5.4. As previously discussed in section 4.2.1 the change in moisture content affects the behaviour and performance of subgrade soils. In general an increase in moisture content is followed by a decrease in resilient modulus value and an increase in permanent deformation. Soils A-4 and A-6, which contain a high proportion of sand and silt, show large permanent deformation with an increase in moisture content from the optimum moisture content (OMC) to 120% OMC, as shown in Figures 5.1,

5.2 and 5.4. These two soils reached a high deformation close to failure in the first 1000 to 2000 cycles of the load applications. On the other hand, soil A-7-5, which is a clayey soil with a clay content of 52%, resisted permanent deformation with the same increase in moisture content as for the other two soils, see Figure 5.3. For stabilised soils A-4 and A-6, the increase in compacting moisture content results in an increase in permanent deformation; however for soil A-6, this increase was small compared to soil A-4. Furthermore, for stabilised soil A-7-5, the increase in compacting moisture content increased the permanent deformation and then started to decrease at 120% OMC as shown in Figures 5.5-5.7.

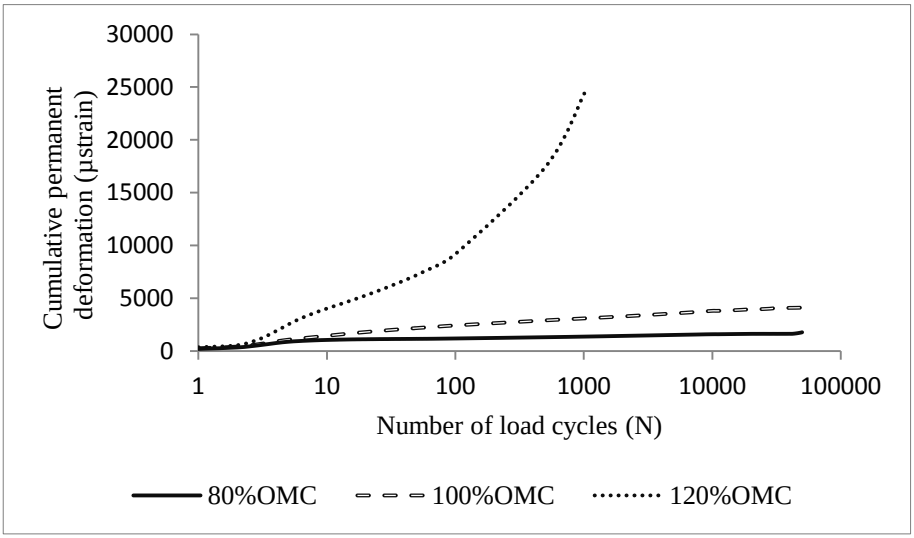

Figure 5. 1 Effect of moisture change on the permanent deformation for unstabilised soil A-4

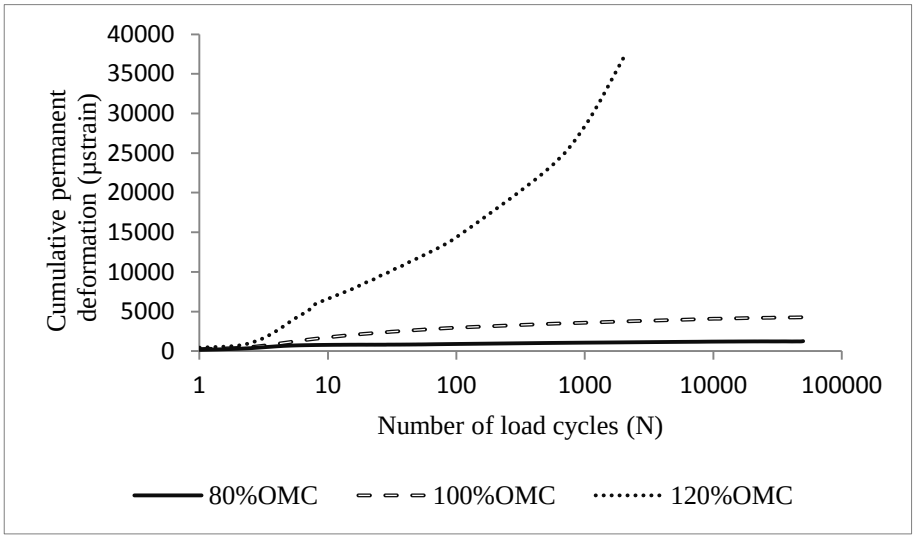

Figure 5. 2 Effect of moisture change on the permanent deformation for unstabilised soil A-6

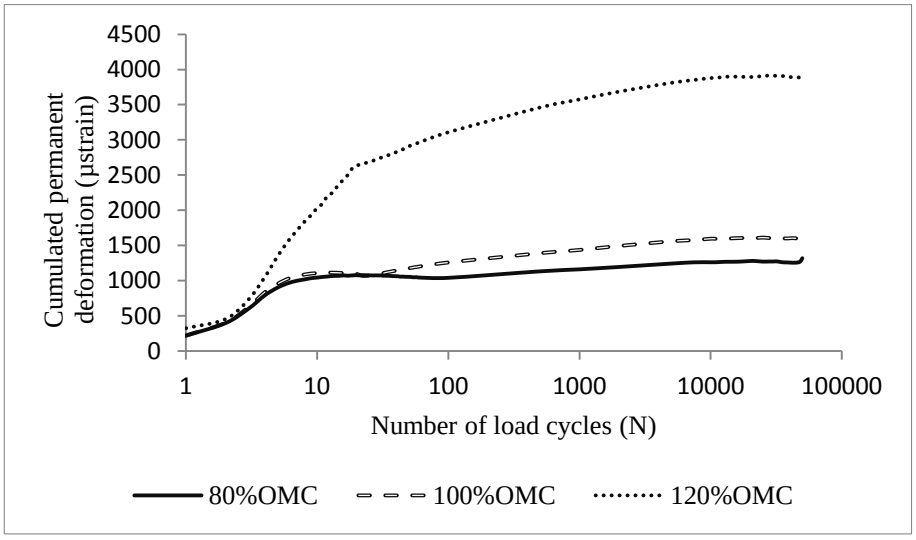

Figure 5. 3 Effect of moisture change on the permanent deformation for unstabilised soil A-7-5

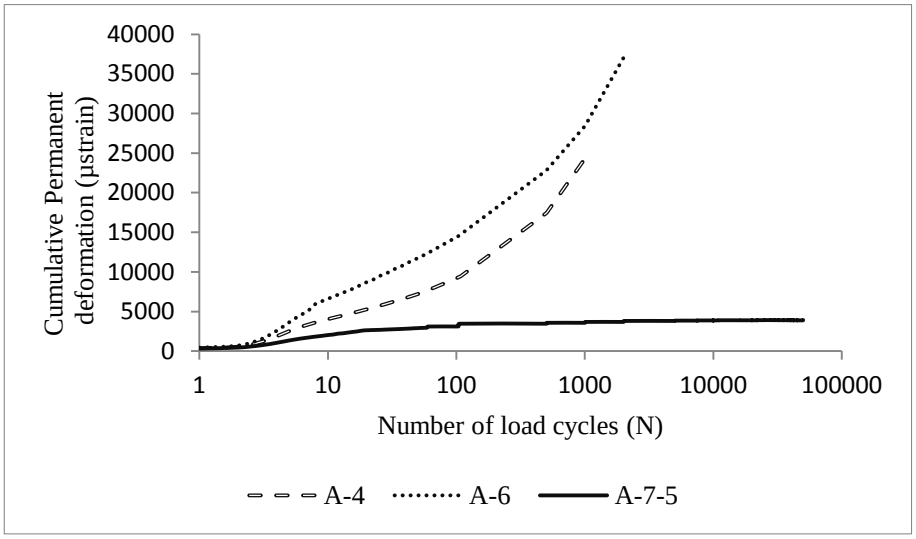

Figure 5. 4 Comparison of the three unstabilised soils for the effect of increase of the moisture up to 120% OMC

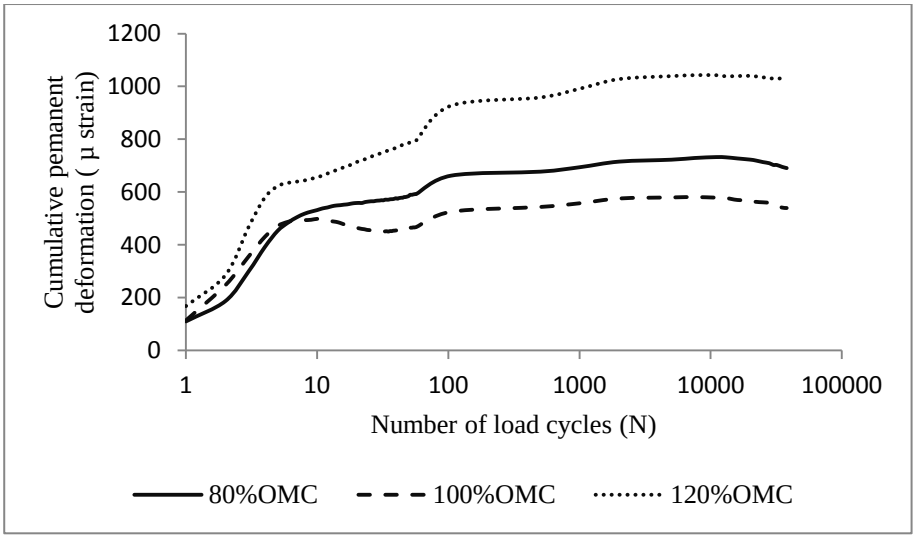

Figure 5. 5 Effect of compacting moisture content on the permanent deformation of stabilised soil A-4 with 4%CC+1.5%LC

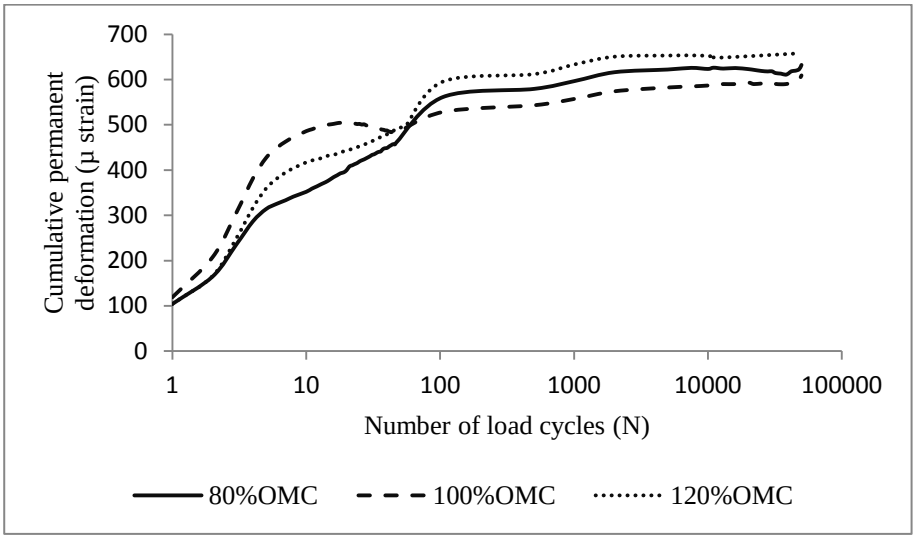

Figure 5. 6 Effect of compacting moisture content on the permanent deformation of stabilised soil A-6 with 4%CC+1.5%LC

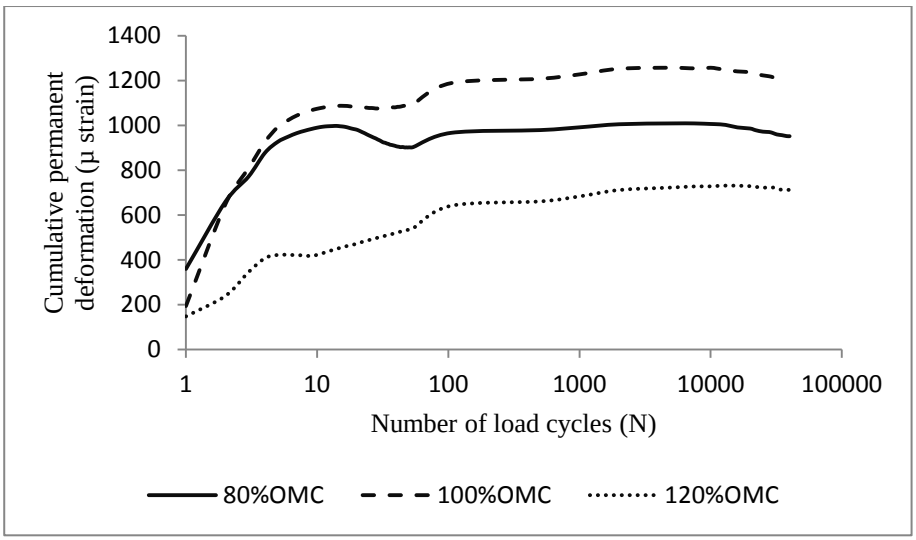

Figure 5. 7 Effect of compacting moisture content on the permanent deformation of stabilised soil A-7-5 with 4%CC+1.5%LC

5.2.2 Effect of the Stress Level

Multi-stage and single-stage permanent deformation tests were carried out to assess the effects of stress levels on the development of permanent deformation of the stabilised and unstabilised subgrade soils. Figures 5.8 and 5.9 show the progression of permanent deformation for unstabilised and stabilised subgrade soils, respectively. The increase in the deviatoric stress results in an increase in permanent deformation. Unstabilised soil A-4 exhibits higher permanent deformation than the other two soils; however, the stabilisation improved the resistance of this soil considerably compared with the other two soils. There is small change in permanent deformation for soil A-7-5 with stabilisation at a stress level of 12.4 kPa to 62.0 kPa (Figures 5.8 and 5.9), compared with soils A-4 and A-6; but the permanent deformation of this soil shows a high increase when the stress level is increased from 62.0 kPa to 120.0 kPa, as shown in Figures 5.10 and 5.11. In these two Figures the effect of the stress is demonstrated more clearly as the stress level increases from 62.0 kPa to 120.0 kPa, in a series of single-stage permanent deformation tests.

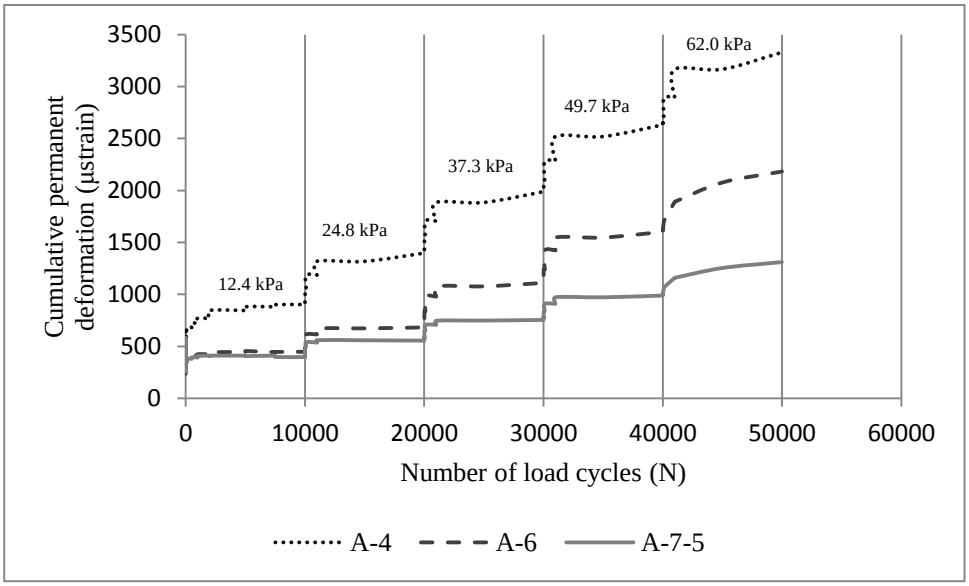

Figure 5. 8 Effect of stress level on the permanent deformation development for unstabilised subgrade soils at 100% OMC

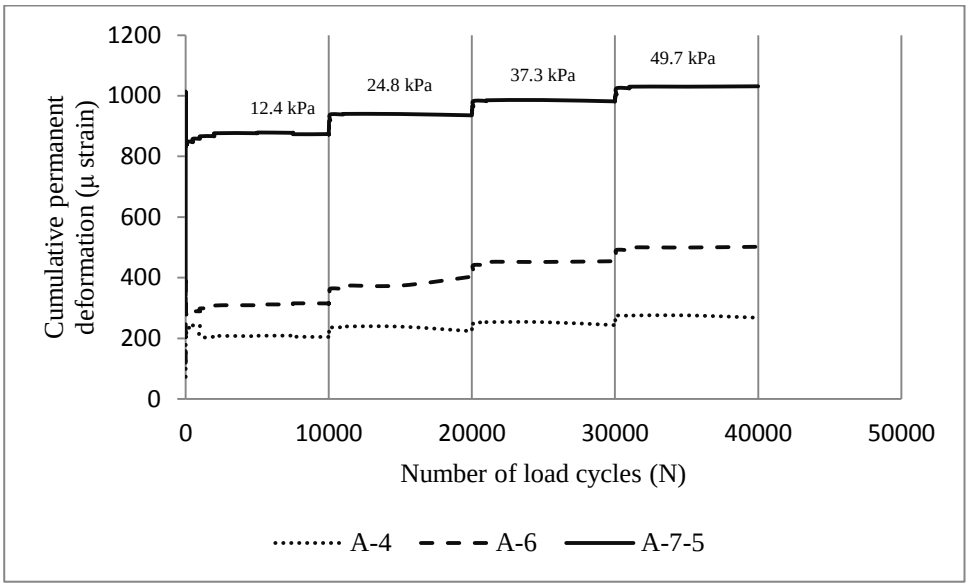

Figure 5. 9 Effect of stress level on the permanent deformation development for stabilised subgrade soils at 100% OMC

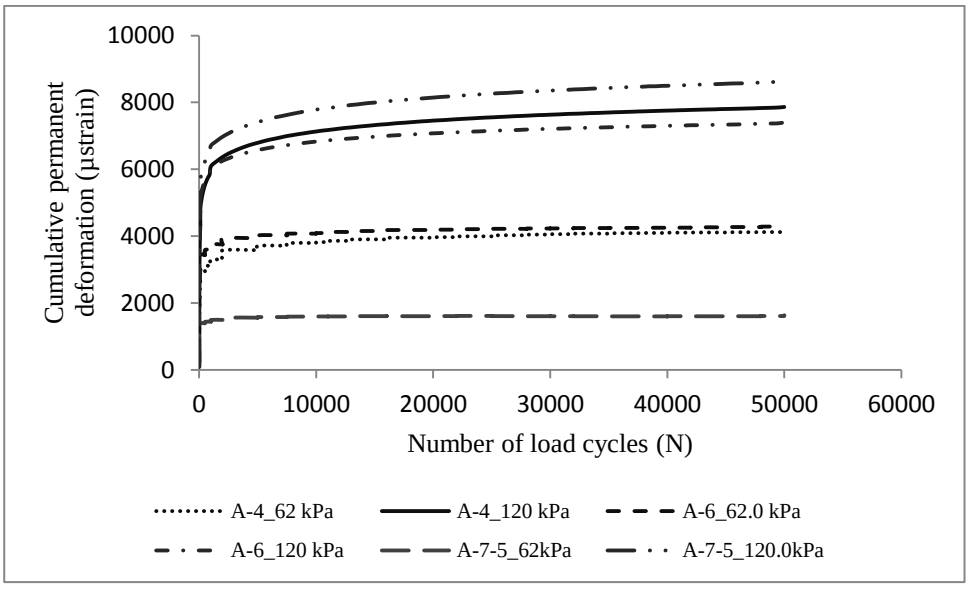

Figure 5. 10 Comparison of the permanent deformation progression for the three unstabilised soils for the deviatoric stresses of 62.0 and 120.0 kPa at 100% OMC

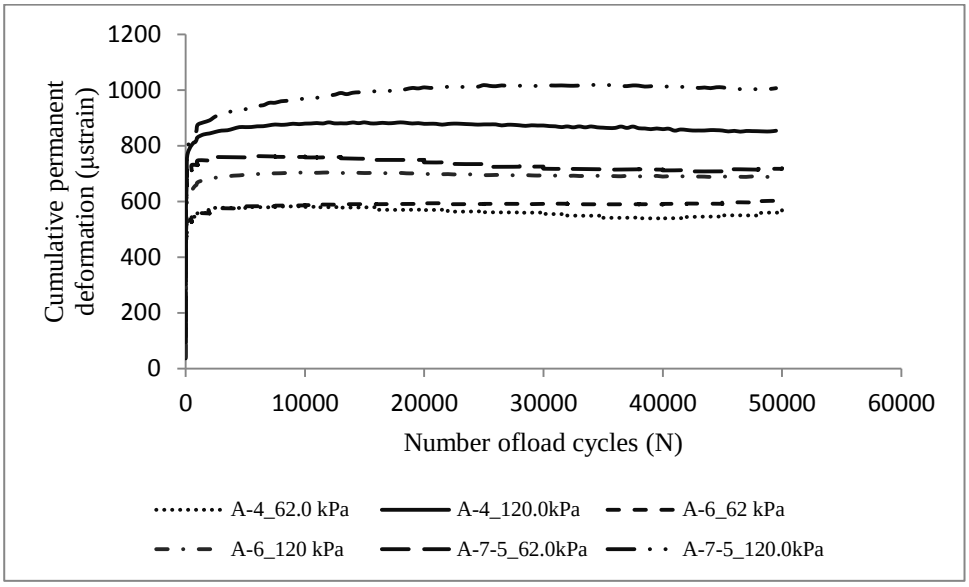

Figure 5. 11 Comparison of the permanent deformation progression for the three stabilised soils for the deviatoric stresses of 62.0 and 120.0 kPa at 100% OMC

5.2.3 Effect of Soil Type

The effect of the soil type on permanent deformation is demonstrated within the other effects. The difference between these three soils is depicted in Figures 5.12-5.17. For unstabilised soils with a high proportion of sand and silt content the accumulation of permanent deformation is higher than in the soil with clay contents, at different moisture contents ranging from 80% OMC to 120% OMC. In Figure 5.14 this difference is much clearer, where the increase of the moisture content significantly increased the permanent deformation. However, soil A-6, which contains a lower proportion of sand and silt, has a lower permanent deformation than soil A-4 at all the three moisture contents. This suggests the sensitivity of sandy silty subgrade soils to moisture changes. On the other hand, the stabilised subgrade soils have a completely different trend in which soils A-4 and A-6 undergo a very low permanent deformation compared to soil A-7-5; especially soil A-4 that shows a higher improvement in resistance to the permanent deformation. Compacting moisture content also

has a greater effect on the stabilised soil A-4; while this soil presents very good improvement it still undergoes increased deformation as the compacting moisture content increases to 120% OMC. Therefore, it is important to assess and quantify the effect of the compaction moisture content for different soil types during design and construction using stabilised subgrade soils.

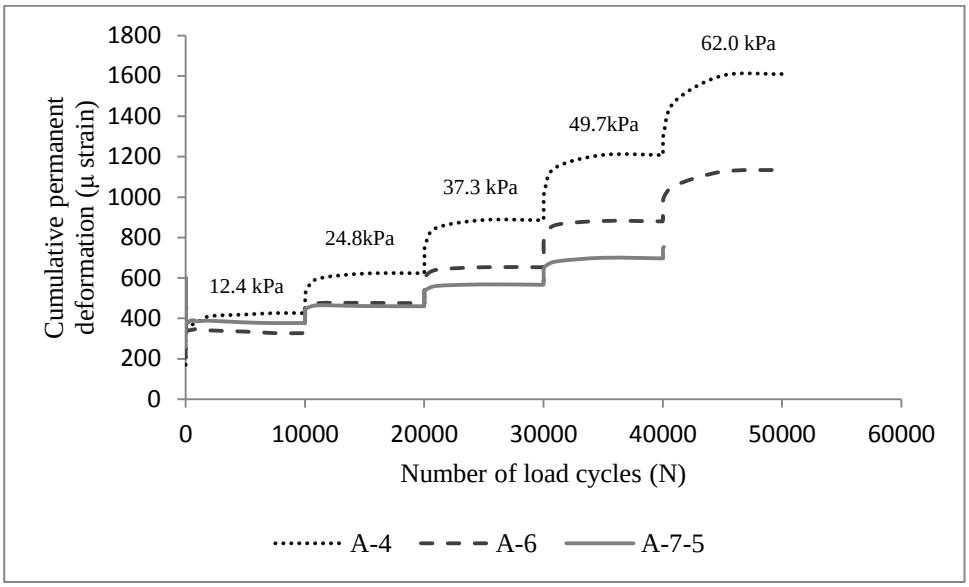

Figure 5. 12 Comparison of the permanent deformation of the three unstabilised soil types at moisture content of 80% OMC

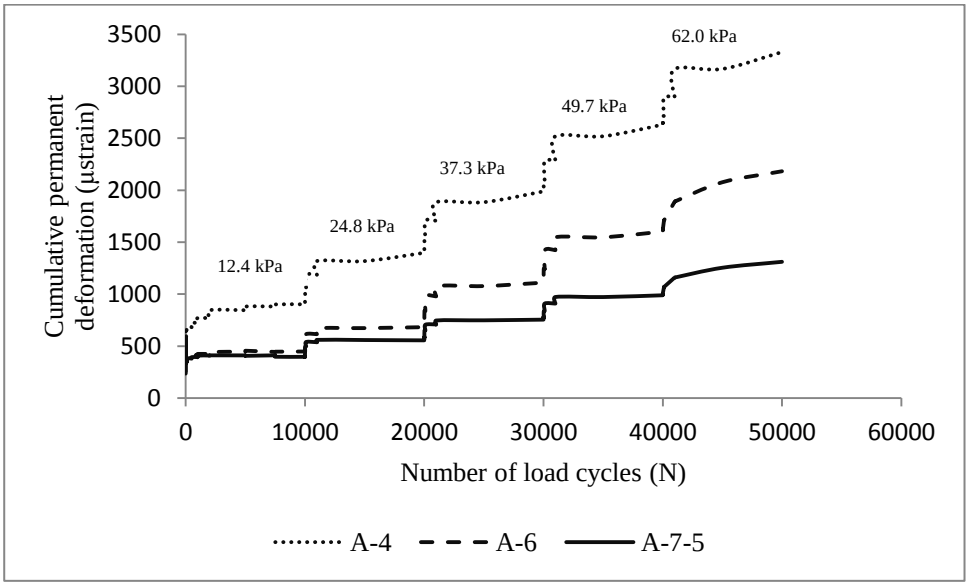

Figure 5. 13 Comparison of the permanent deformation of the three soil types at the moisture content of 100% OMC

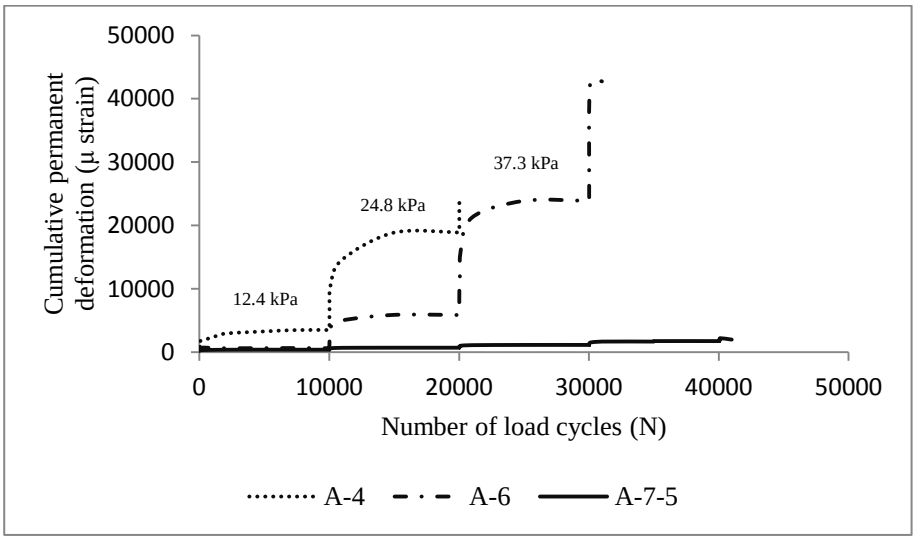

Figure 5. 14 Comparison of the permanent deformation of the three soil types for increase in moisture up to 120% OMC

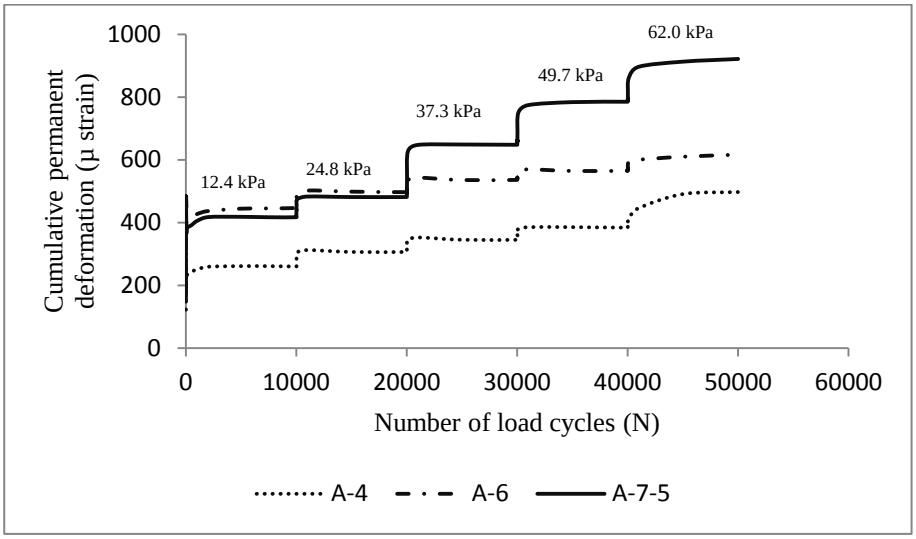

Figure 5. 15 Comparison of the permanent deformation of the three stabilised soils at the compacting moisture content of 80% OMC

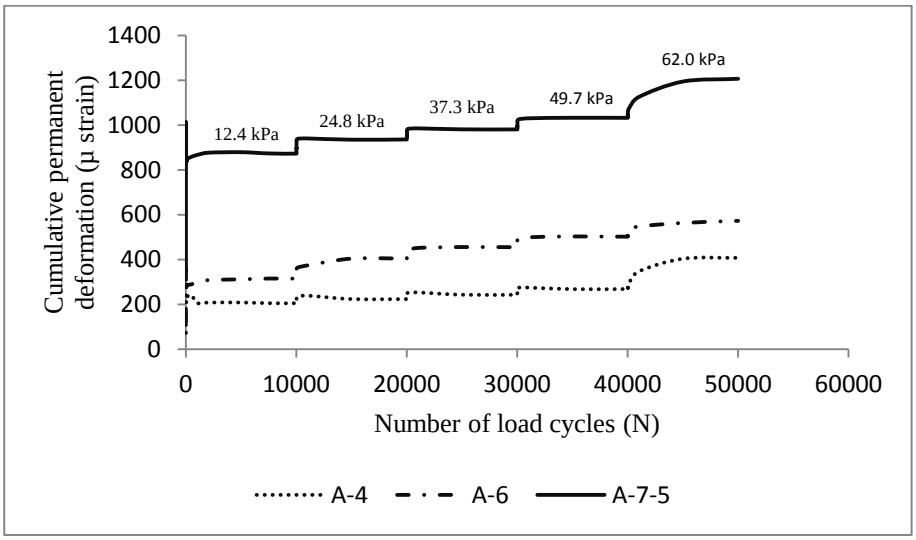

Figure 5. 16 Comparison of the permanent deformation of the three stabilised soils at the compacting moisture content of 100% OMC

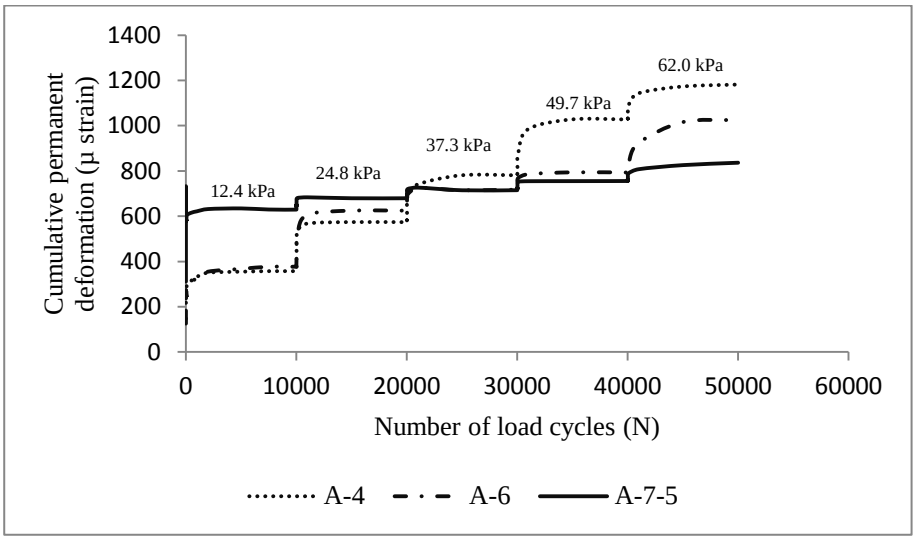

Figure 5. 17 Comparison of the permanent deformation of the three stabilised soils at the compacting moisture content of 120% OMC

5.2.4 Effect of the Number of Loads

The number of load repetitions has an influence on permanent deformation progression, as the number of load repetitions increases, the cumulative permanent deformation increases, however the rate of permanent deformation decreases and approaches zero. From the multi-stage test results in other sections (Sections 5.2.2 and 5.2.3) of this chapter, it is clear that the change in the stress level increases the rate of permanent deformation until it starts to decrease after a few hundreds of cycles. In Figures 5.10 and 5.11 the increase of permanent deformation with the increase in the number of load repetitions is also presented, in addition to the effect of the stress level. However, the increase in permanent deformation with the increase in the number of load repetitions is different for stabilised and unstabilised subgrade soils. For unstabilised soils the permanent deformation increases even though the rate decreases. However, for stabilised soils the rate of the permanent deformation progression decreases in the earlier cycles of the load repetitions and tends to stabilise and behave as an

elastic material if the stress level and environmental conditions remain constant. Yet, this constant rate changes dramatically after cycles of wetting and drying, as shown in Figures 5.23 and 5.24 in which the rate and the cumulative permanent deformation are increased with an increase in the number of load repetitions after cycles of wetting and drying.

5.2.5 Effect of Type of Stabiliser and Ratio

The soil type affects the permanent deformation for unstabilised and stabilised soils. In this section two different stabilisation agents and four ratios are used and the comparison is made between the permanent deformation progression, to assess the suitability and type of the stabiliser for different soil types. From Figure 5.18, cement stabilisation with 4% cement content for soil A-4 shows lower permanent deformation development than the other agent contents. The improvement in the soil strength and mechanical properties with cement stabilisation has been improved for soils containing a higher sand and silt content. The lime content in this soil seems to make no contribution to the strength, as previously presented for the resilient modulus value and unconfined compressive strength; this is because of the suitability of lime for the stabilisation of clayey soils rather than silty clay soils. The purpose of using this agent with this soil is to have a clearer comparison and understanding of the stabiliser types for different soil categories. The three soils were stabilised with the same agent content and ratios. In Figure 5.19 the effect of lime is increased because soil A-6 contains a higher ratio of clay, which is 26%; while soil A-4 contains only 16% clay. Stabilisation with 4% cement plus 1.5% lime content has a higher resistance to permanent deformation than the other stabilisation contents, indicating the suitability of cement-lime stabilisation for this type of soil. Soil A-7-5, which contains 52% clay content, showed a steady increase in its strength property with an increase in the stabiliser content and the addition of lime content, as demonstrated in Figure 5.20. The successive strength gain for

2%CC, 4%CC, 2%CC+1.5%LC and 4%CC+1.5%LC respectively, shows the increase in strength with the increase in cement ratio. At the same time, the addition of the lime appears to improve the property at a higher rate as the stabilisation with 2%CC+1.5%LC content has a greater effect than the stabilisation with 4% cement content without lime. From these results it easily can be concluded that the ratio of clay content has a considerable effect on the selection of the stabiliser type. Soils with higher clay content should be stabilised with lime and cement lime; while stabilisation with cement is more suitable for soils containing a higher proportion of sand and silt.

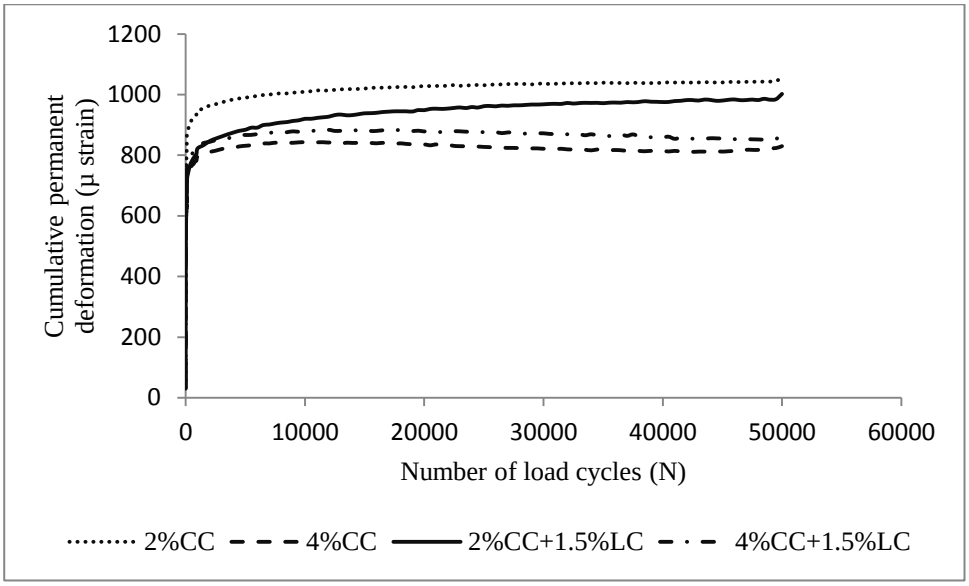

Figure 5. 18 Comparison of the permanent deformation for different stabiliser contents for soil A-4 at 100% OMC

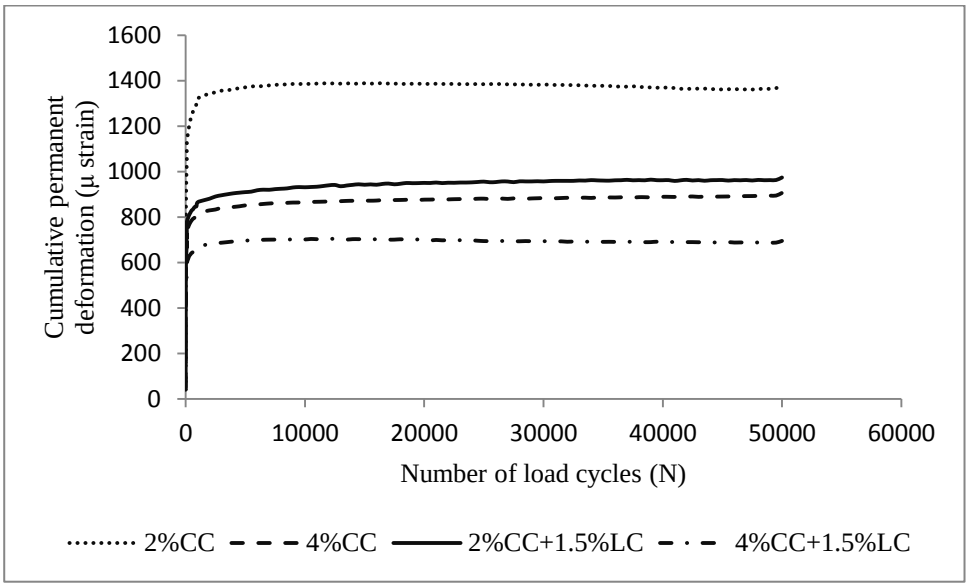

Figure 5. 19 Comparison of the permanent deformation for different stabiliser contents for soil A-6 at 100% OMC

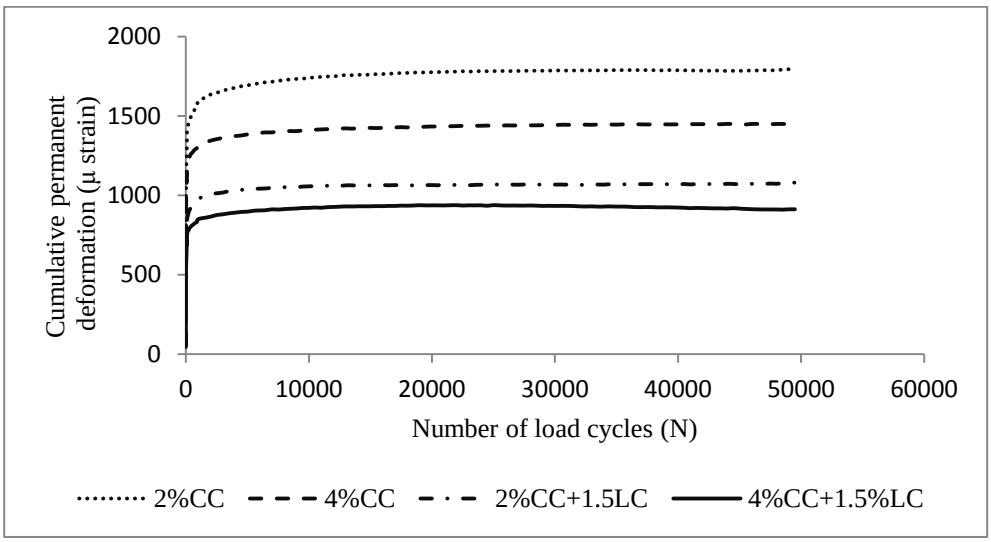

Figure 5. 20 Comparison of the permanent deformation for different stabiliser contents for soil A-7-5 at 100% OMC

5.2.7 Effect of Frequency and Load Sequence

Figures 5.21 and 5.22 show the accumulation of permanent deformation with the number of load repetitions for soils A-4 and A-7-5. The figures present the accumulation of permanent deformation for three types of load sequences: single-stage of 62.0 kPa deviatoric stress for 50,000 cycles; ascending deviatoric stress level from 12.4 kPa to 62.0 kPa in five stages; and descending deviatoric stress level from 62.0 kPa deviatoric stress to 12.4 kPa. As can be seen for the both soils, the single stage with the higher stress levels produces higher accumulated permanent deformation progression. The ascending stress level produces the increase in cumulative permanent deformation for both soils; while a decrease in the stress level from 62.0 kPa to 12.4 kPa gives different patterns for these two soils. Soil A-7-5, which is a clayey soil, tends to return to its previous shape; while the deformation of the soil A-4 does not change significantly with the decrease of the stress state. The ascending and descending although they have different pattern but the total permanent deformations were very close presumably because the total energy the sample has subjected to was the same however for constant stress the level the energy is higher therefore the permanent deformation was higher.

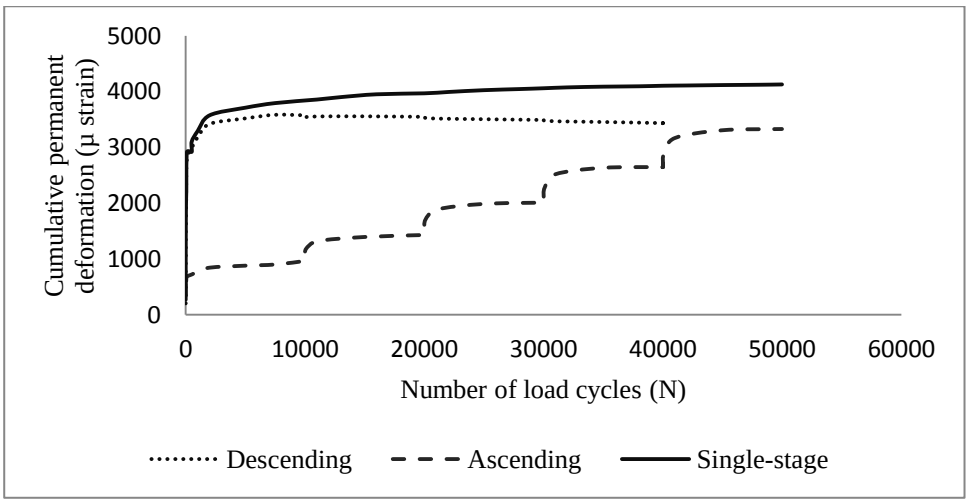

Figure 5. 21 Three different loading states for the permanent deformation accumulation of unstabilised soil A-4

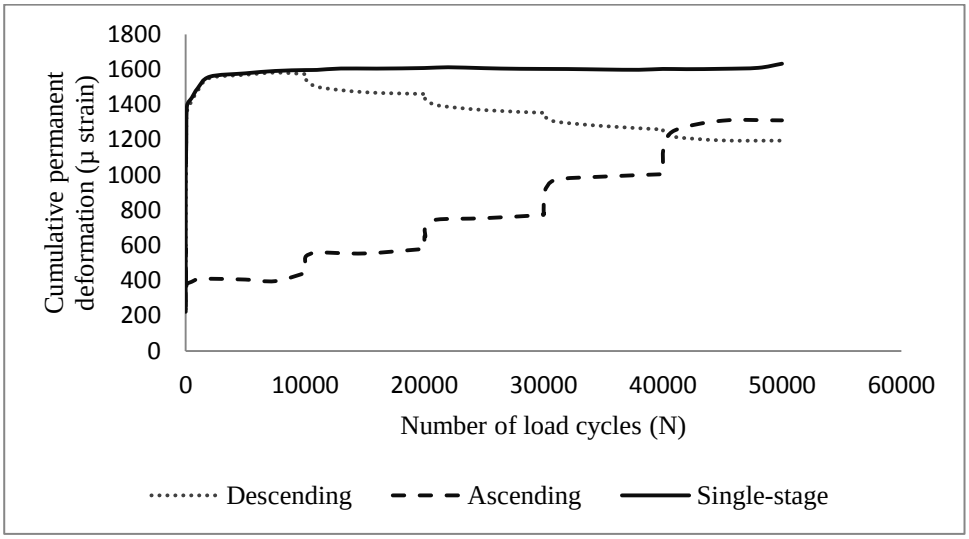

Figure 5. 22 Three different loading states for permanent deformation accumulation of unstabilised soil A-7-5

5.3 Measuring Permanent Deformation at Different Conditions

A range of stabilisation methods and agents are available to improve the properties of the subgrade soils. The stabiliser type and ratio of these stabilisers depend on many factors such as soil type, moisture conditions at construction, the required curing time and the required strength. To decide on the stabiliser ratio and its type, durability tests were carried out. Usually the property of the soils with stabilisation is assessed from an unconfined compressive strength (UCS) test. The stabiliser content is increased to achieve the required UCS values for a specified pavement section. The importance of the permanent deformation tests carried out in this research is indicated in that the mechanical properties, which are key designing inputs in analytical pavement design, were assessed and determined. From these test results, in addition to the permanent deformation, the resilient modulus values were determined as well for understanding of the behaviour of these stabilised soils. The durability equation and correlation equations developed in Chapter Four and the permanent deformation results in this section can help in deciding on the stabiliser ratio and its type. Figures 5.23-

5.24 show the permanent deformation development after seven days of curing (T) and the same samples after 25 cycles of wetting and drying (WD). Stabilisation with 2% for soil A-6 failed before the completion of the cycles; the results of other stabiliser contents are presented in Figure 5.23. Stabilisation with 4% cement content shows a better resistance to permanent deformation after cycles of wetting and drying, as it had the least deformation compared to the other stabiliser contents. On the other hand, stabilisation with 2% cement plus 1.5% lime shows a considerable reduction in resistance after wetting and drying. This demonstrates a high rate of deformation with the increase in the number of load repetitions, such that the failure is expected with more load cycles. It can be considered as range B of the failure conditions in the shakedown concept by Werkmeister et al. (2001), see Figure 5.25, these ranges are shown more clearly and the graphs are repeated in Chapter Seven section 7.9. For soil A-7-5 all stabilised samples failed after a few cycles of wetting and drying, except for those stabilised with 4% cement plus 1.5% lime, as presented in Figure 5.24. As it can be seen, the permanent deformation increases at a high rate and tends to reach failure. This tendency of the permanent deformation is considered as range C in Figure 5.25. From these durability tests it is clear that the decision on the stabiliser type and quantity needs more assessment and durability tests of permanent deformation to accurately design the subgrade layer in a road pavement section. Not all the route of a road pavement subgrade has the same soil type and it may differ from section to section. Therefore, it is important to decide on the type and quantity of the stabiliser for the whole project in such a way that it is commensurate with the required resistance to permanent deformation, embracing all types of soils expected to exist in the site.

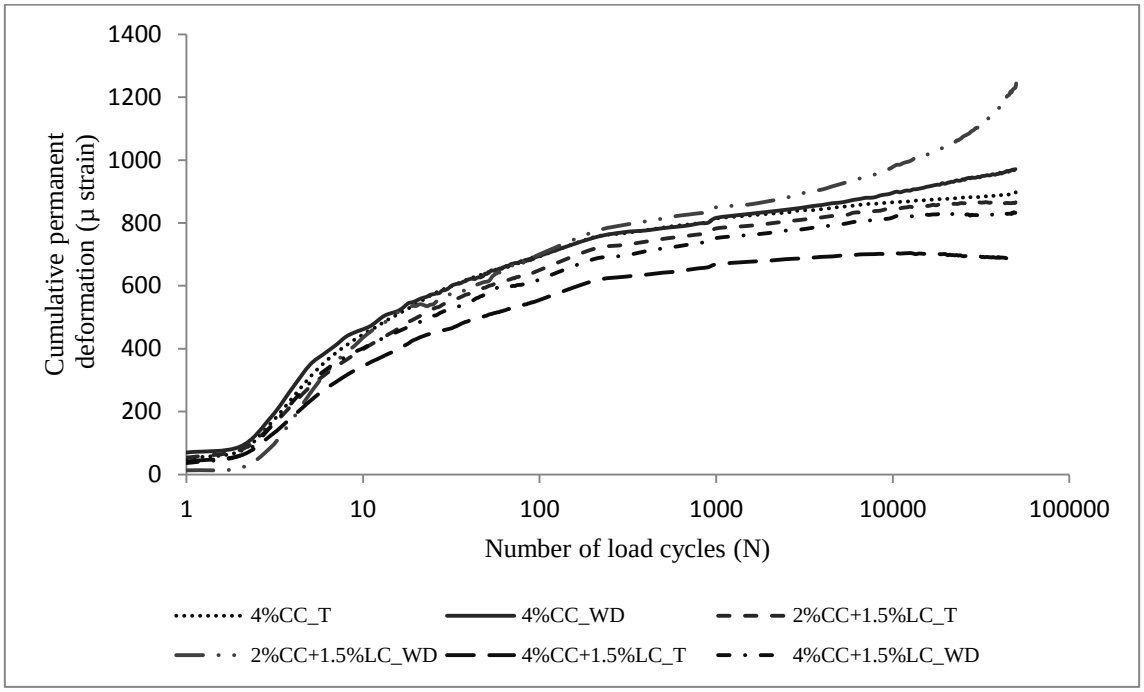

Figure 5. 23 Comparison of the permanent deformation after stabilisation and cycles of wetting and drying for soil A-6 (**T** denotes for before wetting and drying cycles and **WD** denotes for after wetting and drying cycles)

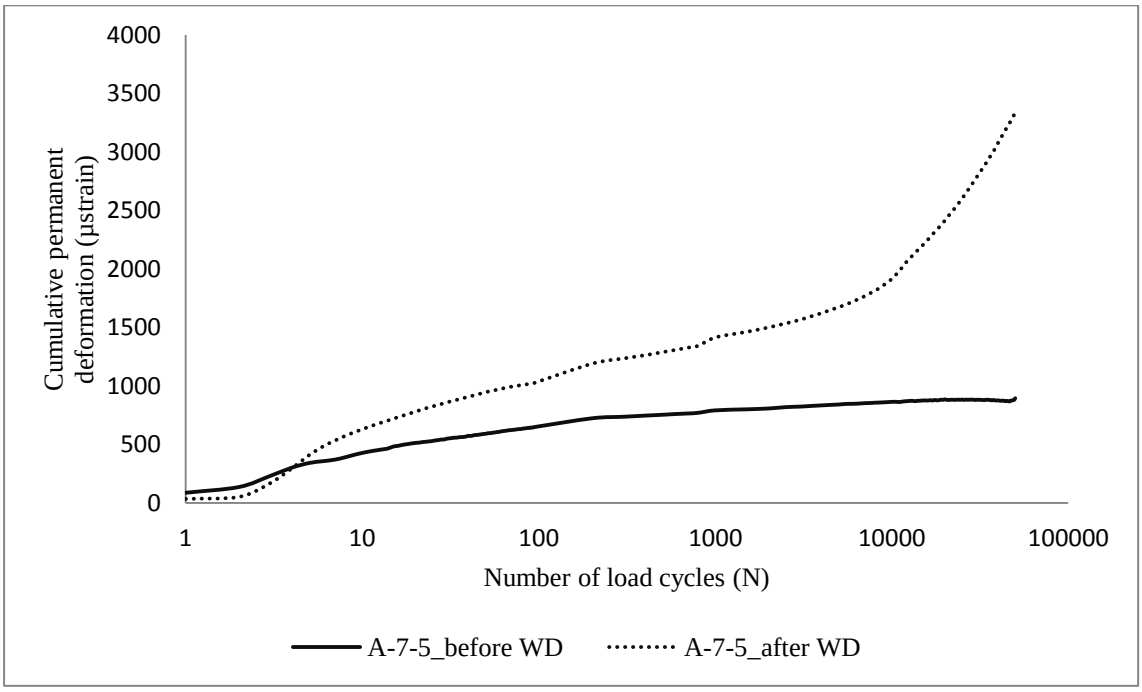

Figure 5. 24 Comparison of the permanent deformation after stabilisation and after cycles of wetting and drying for soil A-7-5 (**T** denotes for before wetting and drying cycles and **WD** denotes for after wetting and drying cycles)

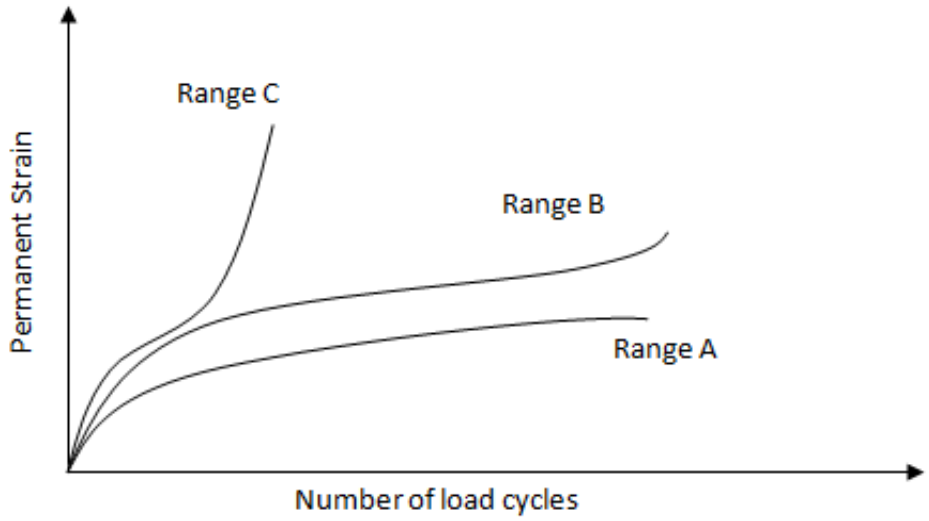

Figure 5. 25 Indicative permanent strain behaviour (After Werkmeister et al., 2001)

5.4 Permanent Deformation Models

The effect of the stress level on permanent deformation progression is presented and discussed in section 5.2.2. From these results the necessity of introducing the stress level in permanent deformation models is apparent. It is also clear from section 5.2.2 that the soil type and properties and the number of load repetitions have influence on the permanent deformation. To include as many as possible of these effects, the model may have a form such as Equation 5.1:

$$Vertical\ permanent\ deformation\ (\varepsilon_{p.1}) \propto [(Number\ of\ loads\ (N), Matrial\ property\ (Mr, ME\ or\ \sigma_s), Stress\ state(\sigma_d, \tau_{oct}\ and/or\ \Theta)] \quad (5.1)$$

Among the permanent deformation models mentioned in Chapter Two, six models were selected for further assessment, they described as below:

1) Veverka model (Lekarp and Dawson, 1998)

$$\varepsilon_{1,p} = a * \varepsilon_r * N^b \quad (5.2)$$

In which $\varepsilon_{1,p}$ is the accumulated permanent strain; ε_r is the resilient strain; N is the number of load repetitions; and a and b are regression parameters. This model relates the accumulated permanent deformation to the number of load repetitions and the resilient strain.

2) Khedr model (Lekarp and Dawson, 1998)

$$\frac{\varepsilon_{1,p}}{N} = A * N^{-m} \quad (5.3)$$

In which A and m are regression parameters.

3) Sweere model (Lekarp and Dawson, 1998)

$$\varepsilon_{1,p} = a * N^{b} \quad (5.4)$$

4) Ullidtz model (Ullidtz et al., 1999)

$$\varepsilon_{pz} = AN^{\alpha}[\frac{\sigma_z}{P}]^{\beta} \quad (5.5)$$

Where ε_{pz} is the vertical plastic strain in micro strains at depth z; σ_z is the vertical stress at depth z; P is a reference stress (atmosphere pressure); and A, α *and* β are constants.

5) Puppala model (Puppala et al., 2009)

$$\varepsilon_p = \alpha_1 N^{\alpha_2} \left(\frac{\sigma_{oct}}{\sigma_{atm}}\right)^{\alpha_3} \left(\frac{\tau_{oct}}{\sigma_{atm}}\right)^{\alpha_4} \quad (5.6)$$

Where $\sigma_{oct} = (\sigma_1 + 2\sigma_3)/3$; $\tau_{oct}\left(\sqrt{2}/3\right)(\sigma_1 - \sigma_3)$; σ_{atm} is the reference stress; and α_1, α_2, α_3 and α_4 are constants.

6) Li and Selig model (Li and Selig, 1996)

$$\varepsilon_{1,p} = a * (\frac{\sigma_d}{\sigma_s})^{m} * N^{b} \quad (5.7)$$

Where σ_d is the deviatoric stress; σ_s is the soil static stress; and the other parameters are as previously.

5.4.1 Integrating Resilient Modulus in a Permanent Deformation Model

Research by Rasul et al. (2015) presented the use of resilient modulus as a soil property and deviatoric vertical stress as a stress state with the number of load repetitions to predict the permanent deformation of stabilised and unstabilised subgrade soils. The suitability of the previously mentioned permanent deformation models for stabilised and unstabilised subgrade soils was assessed using a statistical procedure. Table 5.1 shows the results from a regression analysis of the permanent deformation tests with the permanent deformation models. From the table, the coefficient of significance (R^2) for unstabilised subgrade soils at optimum moisture content ranges from 0.875 to 0.989, regardless of whether the model contains a measure of the stress level or not. However, these coefficients are low for models which contain only the number of load repetitions and vary between 0.475 and 0.773 for stabilised subgrade soils. On the other hand, models with a measure of stress level have a higher R^2 ranging from 0.786 to 0.935. This shows the importance of including a stress parameter in permanent deformation models, especially for stabilised subgrade soils.

Table 5. 1 Parameters of permanent deformation models and coefficient of significance

Soil type and moisture content	Veverka			Sweere			Ullidtz			
	a	b	R^2	a	b	R^2	A	α	β	R^2
A-4 80% OMC U*	1.96	0.09	0.908	907.069	0.06	0.91	1433.858	0.05	0.757	0.983
A-4 100% OMC U	1.83	0.17	0.908	1407.35	0.1	0.95	2974.936	0.098	1.418	0.993
A-4 120% OMC U	1.24	0.44	0.969	1549.49	0.4	0.97	2098.81	0.393	0.561	0.974
A-6 80% OMC U	1.06	0.08	0.945	670.45	0.06	0.91	1021.733	0.052	0.694	0.973
A-6 100% OMC U	1.84	0.11	0.938	1805.01	0.08	0.9	7597.117	0.067	2.572	0.981
A-6 120% OMC U	2.03	0.34	0.965	3355.05	0.32	0.97	5972.695	0.308	1.052	0.979
A-7-5 80% OMC U	1.23	0.04	0.861	920.792	0.03	0.71	1407.552	0.023	0.681	0.939
A-7-5 100% OMC U	1.07	0.06	0.907	941.833	0.05	0.88	1447.777	0.044	0.706	0.961
A-7-5 120% OMC U	1.58	0.07	0.901	2145.54	0.06	0.8	5595.023	0.046	1.68	0.953
A-4 100% OMC TΔ	1.08	0.04	0.475	423.211	0.03	0.64	568.995	0.021	0.47	0.789
A-6 100% OMC T	1.23	0.05	0.773	425.139	0.03	0.75	620.169	0.024	0.604	0.935
A-7-5 100% OMC T	2.21	0.04	0.623	988.538	0.02	0.57	1414.698	0.014	0.567	0.858

*Unstabilised, Δ Stabilised

Continued

Soil type and moisture content	Puppala					Khedr			Li and Selig			
	α_1	α_2	α_3	α_4	R^2	b	A1	R^2	a	m	b	R^2
A-4 80% OMC U	0.401	0.05	1.93	0.096	0.985	0.94	907	0.911	0.326	0.757	0.05	0.983
A-4 100% OMC U	0.023	0.087	1.989	1.037	0.989	0.9	1405	0.954	0.986	1.418	0.098	0.988
A-4 120% OMC U	32.248	0.392	0.725	0.329	0.975	0.6	1549	0.974	0.289	0.559	0.394	0.975
A-6 80% OMC U	0.135	0.05	2.35	-0.138	0.976	0.94	670	0.912	0.196	0.694	0.052	0.973
A-6 100% OMC U	0.001	0.064	2.674	1.393	0.985	0.92	1805	0.897	6.187	2.572	0.067	0.981
A-6 120% OMC U	1405.2	0.313	-0.976	1.383	0.979	0.68	3355	0.972	1.087	1.052	0.308	0.979
A-7-5 80% OMC U	8.91	0.021	0.907	0.366	0.941	0.97	920	0.712	0.301	0.681	0.024	0.939
A-7-5 100% OMC U	0.171	0.044	2.351	-0.112	0.966	0.95	941	0.875	0.276	0.706	0.044	0.961
A-7-5 120% OMC U	0.508	0.043	1.094	1.266	0.953	0.94	2145	0.799	1.724	1.68	0.046	0.953
A-4 100% OMC T	0.179	0.018	2.33	-0.343	0.797	0.97	423	0.643				
A-6 100% OMC T	6.744	0.023	0.808	0.329	0.935	0.97	425	0.752				
A-7-5 100% OMC T	0.067	0.01	2.887	-0.438	0.872	0.98	988	0.571				

The effect of the stress level on permanent deformation progression has been presented in previous sections; therefore it is important to introduce this factor into permanent deformation models. The parameters of these equations are determined from single-stage permanent deformation tests with a deviatoric stress of 62.0 kPa.

In Li and Selig's model the effect of moisture on the permanent deformation has been accounted for using the static stress property of the soil for unstabilised subgrade soils. On the other hand, the model by (Ullidtz et al., 1999) uses the vertical stress and a reference stress at a specified depth for the vertical permanent strain calculation, in which the change in material quality cannot be taken into account. The suggested model (Equation 5.8) in this research combines the models by Ullidtz and Li and Selig's models to overcome the shortcomings of these two models by incorporating the stress level, material property and the number of load repetitions. At the same time, according to Huang (2004), the plastic and elastic strains are proportional, as in his words: 'The use of vertical compressive strain to control permanent deformation is based on the fact that plastic strains are proportional to elastic strains in paving

materials. Thus, by limiting the elastic strains on the subgrade, the elastic strains in other components above the subgrade will also be controlled; hence, the magnitude of permanent deformation on the pavement surface will be controlled in turn'.

$$\sum_{t=1}^{m} \varepsilon_p = a \times \left(\frac{\sigma_{dt}}{M_{rt}}\right) \times N_t^b \quad (5.8)$$

$\sum_{1}^{m} t$ = T

Where: ε_p is accumulated permanent strain in micro strains;

σ_{dt} is deviatoric stress in kPa during a period of time t;

M_{rt} is resilient modulus in MPa for a period of time t;

N_t is the number of load repetitions in the period of time t;

a and b are material parameters;

T is the design life of the road pavement.

The superiority of this model is shown in that the material property included is the resilient modulus, which is a mechanical property usually used in analytical pavement design procedures. The model is applied to stabilised and unstabilised subgrade soils; while the model by Li and Selig is applicable only to unstabilised subgrade soils. To validate the model, permanent deformation from the test results at 100% OMC for unstabilised subgrade soils with 50000 cycles and deviatoric stress of 120.0 kPa, is compared with the calculated permanent deformation from the model calibrated with 62.0 kPa deviatoric stresses. Table 5.2 shows the comparison between the measured permanent deformation from the test and the model. Soils A-4 and A-6 show good agreement between the measured and the predicted for unstabilised soils; while for soil A-7-5, there is underestimation for unstabilised soil. Regarding the stabilised soils, single-stage permanent deformation test results with 62.0 kPa deviatoric stress and 27.6 kPa confining pressure were used to find the permanent deformation equation parameters (Table 5.3). For validation of the model for stabilised soils,

multi-stage permanent deformation test results were used at five deviatoric stresses of 12.4, 24.8, 37.3, 49.7 and 62.0 kPa and 27.6 confining pressure at 80%OMC and 100%OMC. The measured permanent deformation at 10,000, 20,000, 30,000, 40,000 and 50,000 cycles compared with the calculated permanent deformation from the Equation 5.8 and presented in Figure 5.26. As can be seen there is a good agreement between the permanent deformation measured from the tests and predicted from the performance model with a coefficient of significance of R^2=0.85. Permanent deformation models by Uzan, Veverka and Tseng use the ratio of plastic deformation to resilient deformation; the developed model in this section has the same parameter (Mr) and deviatoric stress, as presented in section 2.5.3.

Table 5. 2 Comparison of permanent deformation of measured to predicted, from Equation 5.8

Soil type	Model parameters		Mr	σd	σd/Mr	Model ($\varepsilon_{\rho.1}$)	Measured ($\varepsilon_{\varrho.1}$)
	α	b	(Mpa)	(kPa)	(%)	(μ strain)	(μ strain)
A-4_Untreated	1707.794	0.171	187	120	0.642	6971	7864
A-6_Untreated	1842.765	0.107	100	120	1.200	7038	7401
A-7-5 _Untreated	1068.274	0.055	46	120	2.609	5053	8694

Table 5. 3 Permanent deformation model parameters for the three stabilised subgrade soils

Soil type	Model parameters	
	α	b
A-4_Stabilised	1075.348	0.042
A-6_Stabilised	1227.719	0.047
A-7-5 _Stabilised	2205.015	0.038

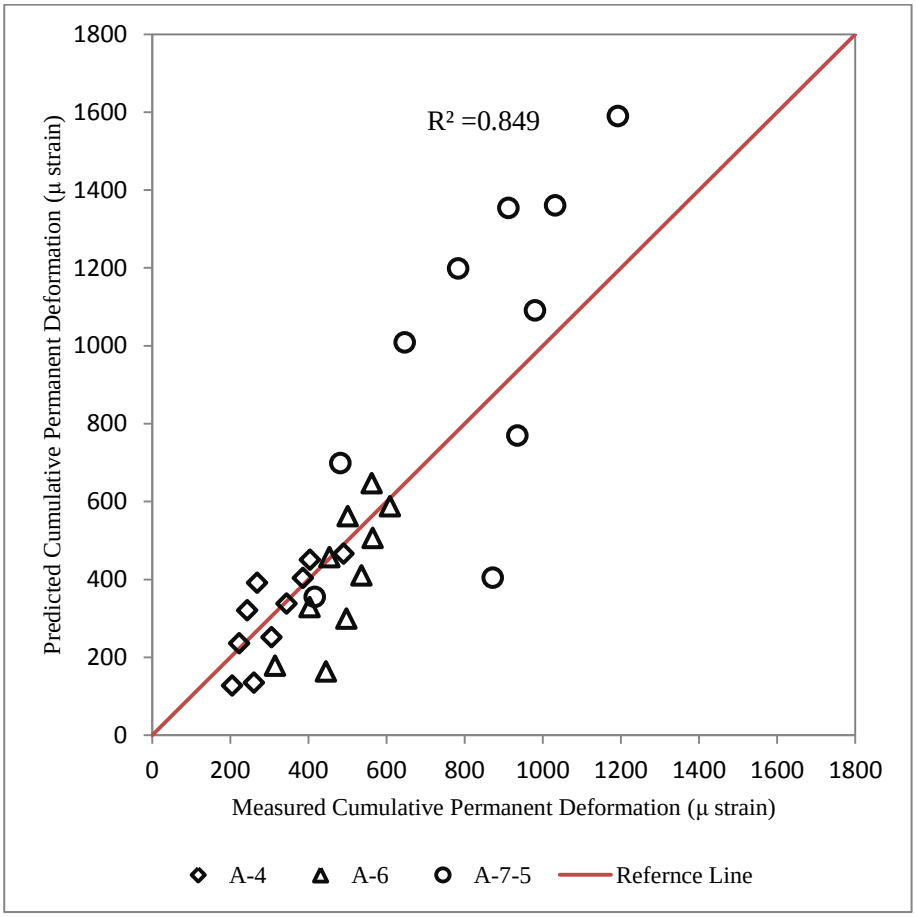

Figure 5. 26 Comparison of permanent deformation between measured from the test results and predicted from performance model (equation 5.8)

The developed performance model in this section combines most parameters that have an effect on permanent deformation progression in unstabilised and lightly stabilised subgrade soils. The importance and the use of the model are discussed in Chapter Seven. The importance of the model is more apparent where the deteriorated resilient modulus values are determined from durability tests and used in the model for incremental permanent deformation accumulation.

Modulus of elasticity is another property of the stabilised soils that has been determined in this research using BS EN 12390-13:2013; testing hardened concrete for the determination of

the secant modulus of elasticity in compression. A procedure for using this property in a performance model is presented in Appendix B. However, as presented in Chapter Seven, the resilient modulus was found to be a more suitable material property in permanent deformation prediction models.

5.5 Discussion

Although the use of the resilient modulus in pavement design and analysis is recommended and its superiority over the other material properties in the design procedure is confirmed in this thesis, the permanent deformation tests are still necessary. The results of permanent deformation tests in this chapter suggest the necessity of permanent deformation figures of the subgrade soils in addition to their resilient modulus properties. Since soils with high resilient modulus values may undergo high permanent deformations. Another important implementation of the permanent deformation tests is their use in calibrating of performance models of rut depth prediction. The performance model calibrated with one stress level can be used for different stress levels that are expected during the design life of the pavement, this is verified especially for lightly stabilised subgrade soils. Furthermore, lightly stabilised subgrade soils deteriorate with weathering and continuous traffic load applications, these conditions can be simulated through durability tests and then permanent deformation tests carried out to quantify the permanent deformation for a specified number of load repetitions.

5.6 Summary

Permanent deformation is one of the key design criteria that need to be calculated for a robust road pavement design procedure. This research showed the importance of permanent deformation; as an example, in unstabilised soils A-4 and A-6, while they have a high resilient modulus value still undergo high permanent deformation. However, soil A-7-5 has a consistent trend regarding the relation between resilient modulus and permanent deformation. To understand the behaviour of the stabilised and unstabilised subgrade soils, the factors affecting the permanent deformation were demonstrated from various methods of permanent deformation tests; single-stage for two different deviatoric stresses and multi-stage tests for five different stress levels. The importance of durability tests were verified using the wetting and drying cycles, mainly in deciding the stabiliser type and quantity for three stabilised subgrade soils. A permanent deformation model is developed to incorporate resilient modulus in permanent deformation calculation. The results from this chapter combined with the results in Chapter Four can be used to determine a suitable stabiliser, taking into account the compressive strains on the top of the subgrade calculated from a finite element model developed in the next chapter.

CHAPTER SIX

FINITE ELEMENT MODEL

6.1 Introduction

This chapter describes the development of a finite element model (FEM) of the road pavement structure which is used within the analytical pavement design procedure developed herein. As analytical pavement design procedures tend to replace empirical methods, obtaining accurate values of the pavements' responses to the applied traffic loads from finite element models is becoming more desirable. Historically computer programmes for analysing pavement responses such as KENLAYER programme (Huang, 1993) were developed using elastic multilayer solutions. However, to accurately determine a pavement's response to traffic load considering its constituent material behaviour to the applied load, researchers became interested in using finite element methods, among other methods, to model the road pavement layer. An example of such a model is ILLIPAVE (Raad and Figueroa, 1980). This process has been greatly facilitated by the increasing availability of computational power. It was decided to develop a FEM of the road pavement in ABAQUS^{TM} rather than use an existing tool such as KENLAYER programme for the following reasons:

i) The FEM allows for further development within the research project, which the use of off-the-shelf software such as KENLAYER programme included within the design procedures does not allow for example the incorporation of the iteration process described in Section 4.4.

ii) The FEM will allow further innovations to be incorporated in a pavement design process in Kurdistan.

6.2 Model Development

An important starting point of finite element modelling for a pavement section is to determine the domain size to obtain accurate results (Kim, 2007). Kim (2007) states "According to Duncan et al. (1968), to obtain a reasonable comparison of finite element analyses, it was necessary to move the fixed bottom boundary to a depth of 50-times the radius of the loading area and move the vertical roller boundary at a horizontal distance of 12-times the radius of the loading area from the centre of loading". Using this concept, a pavement section with the details shown in Table 6.1 was examined using the KENLAYER (Huang, 1993) Programme with a uniform tyre pressure of 550 kPa and a circular area of 152 mm radius. First the section was analysed for surface deflection at six horizontal distances of 0, 15, 20, 25, 30 and 35 times the radius, see Table 6.2. Then the section was analysed for compressive stress and strain at different depths as shown in Table 6.3. From these analyses a horizontal distance of 3,800 mm and a vertical depth of 21,180 mm were selected since the responses at these distances approach to zero, which are 25 and 140 times the radius of the loading area, respectively. Although the surface deflections and compressive stresses and strains are not zero, still these dimensions can be used. In KENLAYER programme it is assumed that the pavement section extends infinitely in horizontal and vertical direction, therefore there is no constraints on boundary conditions. While the finite element model will be fixed for horizontal and vertical movement through setting boundary conditions, this will be verified in the following sections.

Table 6. 1 Pavement section details

Layer type	Thickness (mm)	Modulus of Elasticity (MPa)	Poisson's ration (ν)	Material property
Asphalt Concrete	100	3000	0.3	Linear elastic
Base	200	300	0.35	Linear elastic
Comp. Subgrade	200	46	0.45	Linear elastic
Natural Subgrade	-	46	0.45	Linear elastic

Table 6. 2 Pavement section analysis in the KENLAYER Programme for the radial distance effect on surface deflection

Horizontal distance (mm) / Response	0	2280	3080	3800	4560	6080
Surface deflection (mm)	0.759	0.138	0.103	0.084	0.070	0.052
Tensile stress (kPa)	1367.125	4.393	2.265	1.463	1.017	0.587
Tensile strain (μ strain)	278.000	0.004	0.000	0.000	0.000	0.000
Compressive stress (kPa)	550.000	0.000	0.000	0.000	0.000	0.000
Compressive strain (μ strain)	-138.000	0.000	0.000	0.000	0.000	0.000

Table 6. 3 Pavement section analysis in the KENLAYER Programme for the vertical depth effect on stresses and strains' responses

Depth (mm) / Response	0	12160	15200	18240	21180	24320
Surface deflection (mm)	0.759	0.034	0.025	0.018	0.013	0.009
Tensile stress (kPa)	1367.125	-0.002	-0.008	-0.010	-0.010	-0.080
Tensile strain (μ strain)	278.000	-1.626	-1.245	-0.938	-0.697	-0.497
Compressive stress (kPa)	550.000	0.164	0.117	0.083	0.060	0.041
Compressive strain (μ strain)	-138.000	3.601	2.708	2.014	1.482	1.049

An 8-node bi-quadratic axisymmetric quadrilateral, reduced integration (CAX8R) was built with the above-mentioned dimensions. To achieve accurate and consistent results from a finite element model, the meshing should be adjusted into a size that ensures a balance between accuracy and speed (MEPDG, 2004). To investigate suitable mesh sizes, the surface deflection and compressive stress at the top of the subgrade of five different finite element meshes were compared (see Table 6.4 and Appendix C.1). The results of the analysis are presented in Figures 6.1 and 6.2. From these Figures it can be seen that convergence occurs after four trials in both the case of surface deflection and compressive strength on the top of the subgrade. Accordingly, model number 4 was selected since convergence is achieved and

the execution time using this mesh size was less than the finer meshes (options 5). The final axisymmetric finite element model is presented in Figure 6.3, which its characteristics described in more detail in section 6.4.

Table 6. 4 Mesh refinements for five different mesh sizes

	Refinement model number				
	1	2	3	4	5
Number of nodes	553	1034	1528	9997	27653
Number of elements	162	315	473	3240	9072
Vertical distance (mm)	21180	21180	21180	21180	21180
Horizontal distance (mm)	3800	3800	3800	3800	3800

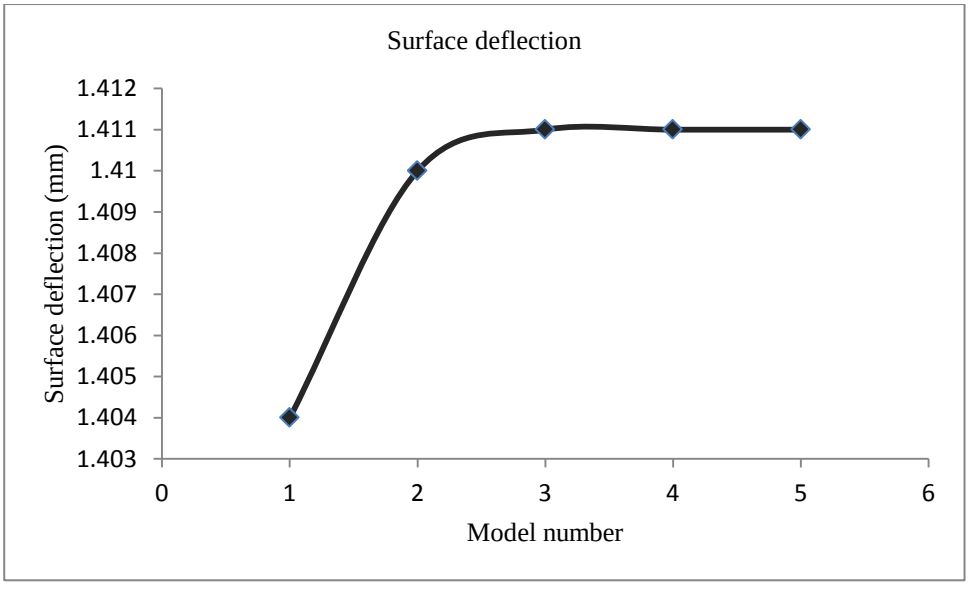

Figure 6. 1 Converge of surface deflection for different mesh refinements

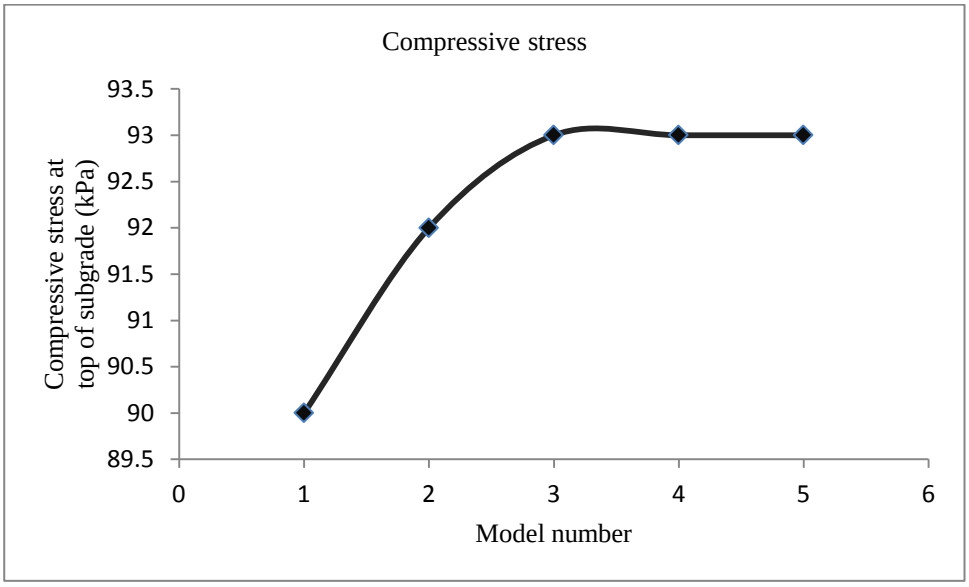

Figure 6. 2 Converge of compressive stress for different mesh refinements

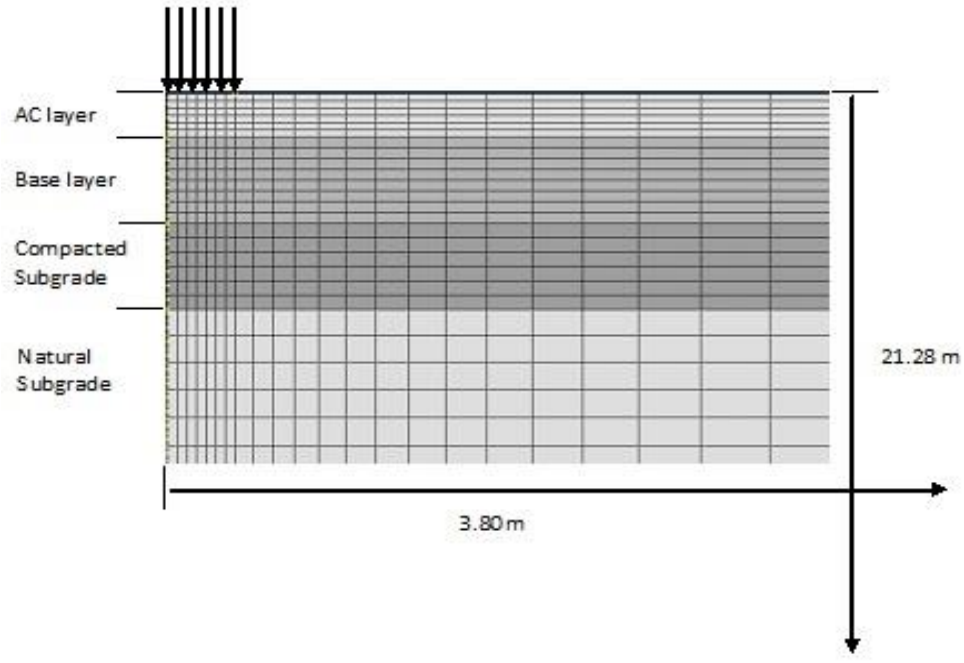

Figure 6. 3 The developed finite element model

6.3 Model Comparison

In order to verify the suitability of the model for this research some outputs of the developed model (with the characteristics given in Table 6.1) were compared with those achieved using the KENLAYER^{TM} (Huang, 1993). First, for the selected finite element model the comparison is made using the same details in Table 6.1. The surface deflection, tensile and compressive stresses and strains from both analyses are presented in Table 6.5.

Table 6. 5 The comparison of stresses, strains and deflections from the FEM model and KENLAYER

Response	Location	KENLAYER	Finite element model (FEM)
Surface deflection (mm)	TopL1	1.188	1.188
Tensile strain (μ strain)	Bottom L1	-426	-428
	Top L2	-426	-426
Tensile stress (kPa)	Bottom L1	-1662	-1665
	Top L2	7.5	6.4
Compressive stress (kPa)	Bottom L2	75	74
	Top L3	75	75
Compressive stress (kPa)	Bottom L3	43	43
	Top L4	43	43
Compressive strain (μ strain)	Bottom L2	863	858
	Top L3	1503	1502
Compressive stress (μ strain)	Bottom L3	872	869
	Top L4	872	868

As can be seen from Table 6.5, all the responses of the FEM developed herein and those from KENLAYER^{TM} (Huang, 1993) match very close in terms of surface deflection, tensile and compressive stresses and strains. A further comparison was undertaken using a lower tyre pressure of 860 kPa. The modulus of elasticity of the hot mix asphalt layer and base course were taken to be 3000 MPa and 300 MPa respectively and the resilient modulus of soil A-4 which is 187 MPa was used for compacted and natural subgrades. The results of the FEM model and KENLAYER analyses for three different sections' dimensions are given in Table

6.6. Furthermore, Figures 6.4 and 6.5 show the surface deflection to radial distance and compressive stress to vertical depth relationships for the section of 50×200×200 mm dimensions. As can be seen, the results are in acceptable agreement. The compressive stress (Figure 6.5) reduces with distance away from the load at a very similar rate for both the FEM model and KENLAYER^{TM} (Huang, 1993) analyses; while there is a slight difference in the surface deflection profile (Figure 6.4). The latter's may be due to the constraints set on the boundary conditions for the FEM model that are not considered in the KENALYER^{TM} (Huang, 1993) Programme. However, as the surface deflection is not a design criterion, this difference may be neglected (MEPDG, 2004).

Table 6. 6 Comparison of results from the FEM model and KENLAYER for different pavement section configurations

Pavement Sections		(50×200×200) mm		(50×150×150) mm		(100×150×0) mm	
Response	Location	KEN LAYER	Finite element model	KEN LAYER	Finite element model	KEN LAYER	Finite element model
Surface deflection (mm)	TopL1	0.497	0.482	0.513	0.499	0.374	0.364
Tensile stress (kPa)	Bottom L1	-806	-808	-848	-850	-941	-943
	Top L2	146	144	138	138	28	28
Tensile strain (μ strain)	Bottom L1	-235	-236	-245	-245	-246	-246
	Top L2	-235	-240	-244	-247	-246	-247
Compressive stress (kPa)	Bottom L2	149	149	195	195	117	117
	Top L3	149	149	195	195	117	116
Compressive stress (kPa)	Bottom L3	66	66	99	99	-	-
	Top L4	66	66	99	99	-	-
Compressive strain (μ strain)	Bottom L2	654	652	836	836	504	503
	Top L3	733	733	930	931	561	560
Compressive stress (μ strain)	Bottom L3	344	343	506	506	-	-
	Top L4	344	344	506	504	-	-

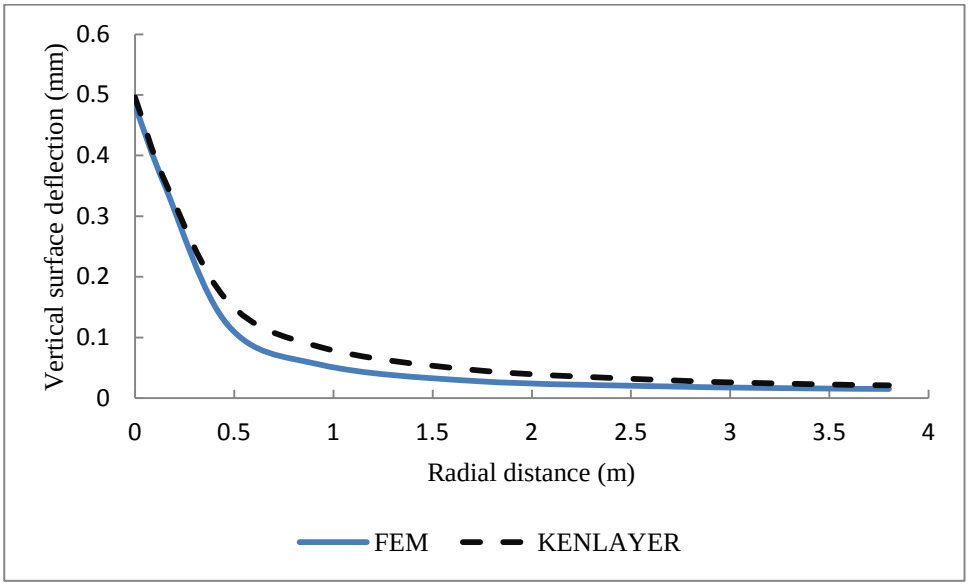

Figure 6. 4 Relationship between radial distance and surface deflection from the FEM and KENLAYER

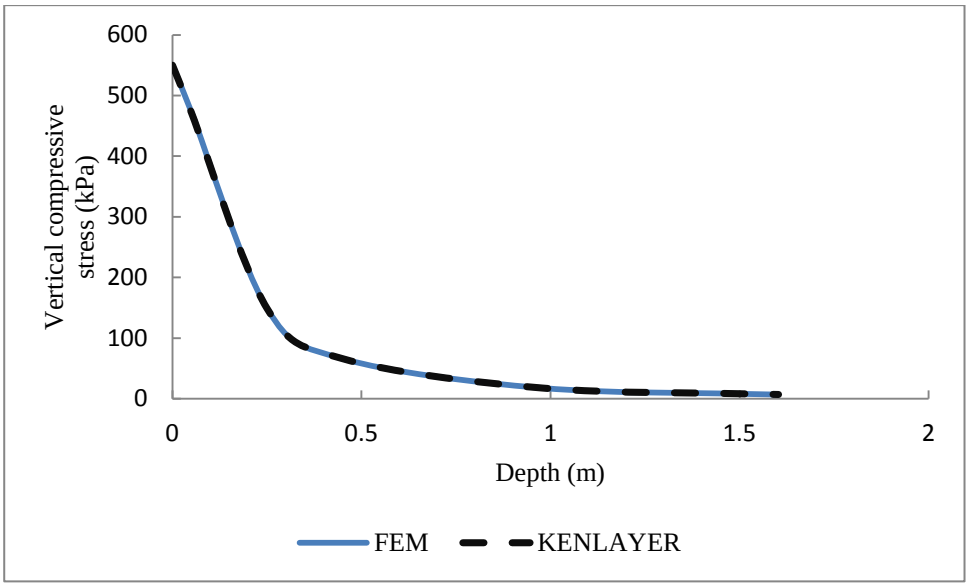

Figure 6. 5 Relationship between vertical depth and compressive stress from the FEM and KENLAYER

6.4 Model Characterization

6.4.1 Load Modelling

The traffic loads represented in the model were single axle loads of between 80 and 125 kN. If a standard axle load of 80 kN is taken to be a single axle with a single wheel and a contact pressure of 550 kPa is assumed, the radius of a circular contact area is 152 mm. In general the contact pressure is assumed to be equal to the tyre pressure (Huang, 2004). Evidently for 'constant inflation pressure the contact pressure increases with load' (O'Flaherty, 2002). In this research for different axle loads the same radius of circular contact area is used and the change in load translated to contact pressure in the KENLAYER and FEM model analysis.

6.4.2 Material Modelling

The materials were modelled using the Drucker-Prager model in the ABAQUS^{TM} material library by defining the parameters calculated from triaxial test results. Where the KENLAYER^{TM} (Huang,1993) programme was used, the materials were modelled using a k-θ model for materials where it was necessary to shown an increase in resilient modulus with deviatoric stress (e.g. soil A-4) and a bilinear equation to characterise materials which show a decrease in resilient modulus with an increase in deviatoric stress (e.g. soil A-7-5).

6.5 Discussion of Nonlinearity with Different Response Models

Representing the nonlinear relationship of stresses and strains of soils to the applied load is one of the important components in accurately modelling material behaviour. In section 4.4 a procedure has been suggested, which considers the stress dependency of the resilient modulus of stabilised and unstabilised subgrade soils. To show the suitability of this procedure a comparison was made of the approaches to modelling the non-linear behaviour of unstabilised subgrade soil using KENLAYER and the FEM developed herein. As explained in section 4.4,

the KENLAYER programme uses Equations 4.2, 4.3 and 4.4 via an iterative method to calculate the resilient modulus.

The results of the comparison are given in Table 6.7 are from the pavement section analysis with KENLAYER^{TM} for layers 3 and 4 which are compacted and natural subgrade layers of soil A-7-5. After six iterations the value of the resilient modulus has converged to 52.7 MPa and 58.9 MPa for these layers from a starting resilient modulus value of 46 MPa. It is necessary to mention that the KENLAYER programme stops the iteration when the difference between consecutive values is 1% or less. To carry out pavement section analysis in KENLAYER programme considering nonlinearity, k1 to k5 parameters in Equations 4.2, 4.3 and 4.4 were determined from resilient modulus test results. Since the three fine-grained subgrade soils in this research showed different behaviour to an increase in deviatoric stress, soil A-7-5 was modelled using a bilinear equation and soil A-4, which showed an increase in resilient modulus with an increase in deviatoric stress, was modelled using a k-θ model. Figure 6.6 shows the determination of the k parameters for soil A-7-5. These are: K1=57 MPa, K2= 60 kPa, K3= 500 and K4= 187.5. The geostatic stress calculation K_o, which is the coefficient of earth pressure in rest, was estimated from the literature to be 0.5(Huang, 2004; Austroads, 2008), K_o can also be calculated from the relationship: K_o =1- Sin (ϕ). Where ϕ is internal friction angle (Michalowski, 2005)

For the density of the asphalt layer and base course, default values were used. The density of the compacted and natural subgrade soils from the experimental results presented in Chapter Three and Four were used, these values were: 22.8 kN/m^3, 21.2 kN/m^3 and 14.8 kN/m^3 for asphalt concrete, base course and subgrade soils, respectively.

Table 6. 7 Iteration procedure in KENLAYER

Iteration NO.	Layer	Mr (MPa)	Layer	Mr (MPa)
1	3	46	4	46
2	3	49.36	4	52.68
3	3	51.12	4	56.02
4	3	52.03	4	57.68
5	3	52.51	4	58.51
6	3	52.75	4	58.92

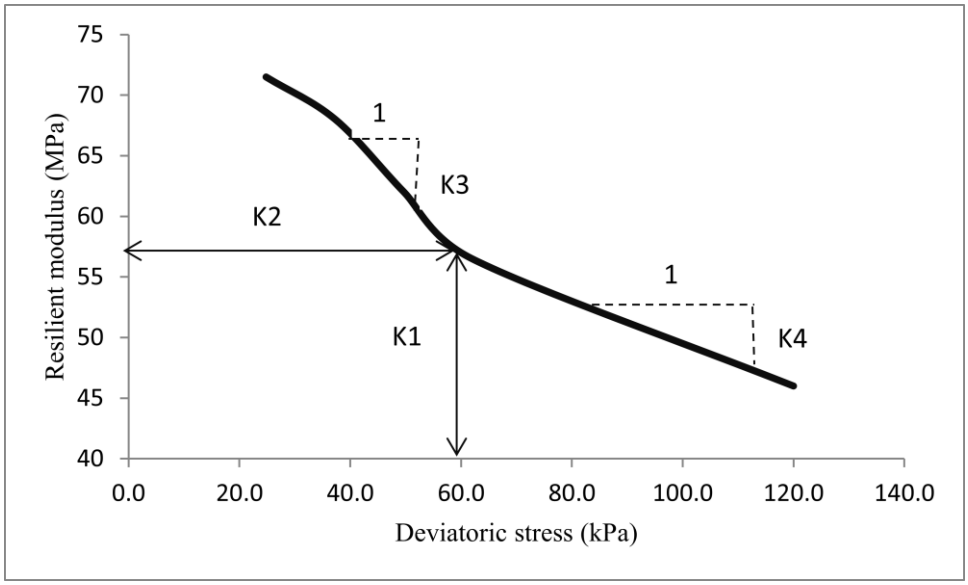

Figure 6. 6 Resilient modulus to deviatoric stress relationship for soil A-7-5 to determine the k parameters

Figure 6.7 shows the resilient modulus vs deviatoric stress relationship for soil A-4. As can be seen, the increase in deviatoric stress for this soil results in an increase in the resilient modulus value. Therefore, it was characterised via a K-θ model in the KENLAYER programme for granular material. This is one of the reasons that using the test results for nonlinearity may give more appropriate analysis results, especially for fine-grained soils. Via regression analysis of the laboratory results of soil A-4, values of K_1 and K_2 were determined to be 19.985 and 0.45 respectively, with a coefficient of significance (R^2) of 0.884. Table 6.8 shows the results of a pavement section with (100×200×200) mm dimensions. The results

compare the nonlinearity analysis for KENLAYER programme and method of using graphs; they agree very well from both analyses methods.

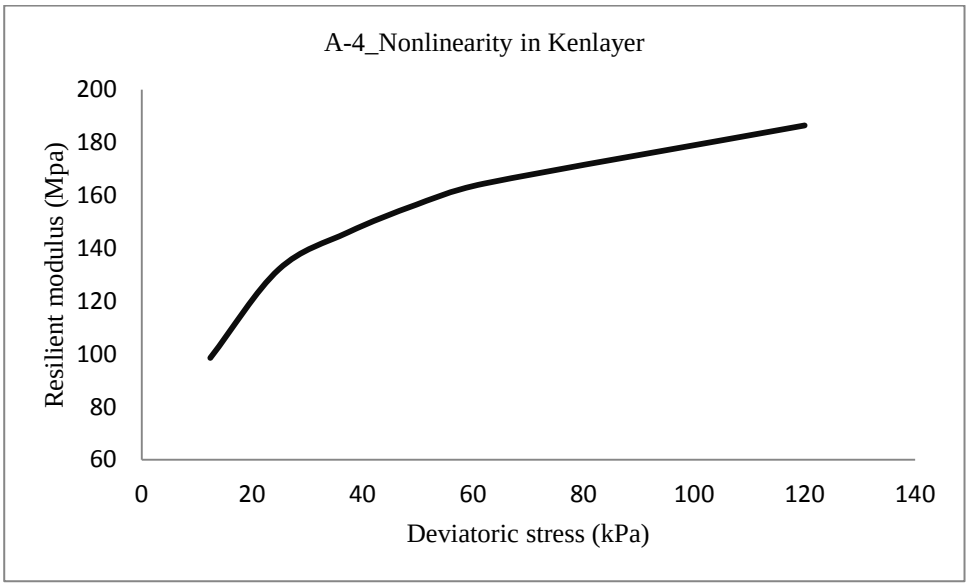

Figure 6. 7 Resilient modulus to deviatoric stress relationship for soil A-4 to determine the k parameters

Table 6. 8 Comparison of nonlinear analysis results from KENLAYER and using graphs

Response		Section (100X200X200) mm & 550 kPa tyre pressure					
		KENLAYER Linear		KENLAYER Nonlinear		Using Graphs Nonlinear	
		A-4	A-7-5	A-4	A-7-5	A-4 (t3)	A-7-5 (t3)
Surface deflection (mm)	TopL1	0.436	0.892	0.493	0.794	0.467	0.753
Tensile stress (μ strain)	Bottom L1	-875	-1017	-891	-986	-882	-994
	Top L2	42	13	38	19	40	17
Tensile strain (kPa)	Bottom L1	-348	-393	-353	-383	-349	-385
	Top L2	-348	-393	-353	-383	-352	-387
Compressive stress (kPa)	Bottom L2	109	60	101	68	105	68
	Top L3	109	60	101	68	105	68
Compressive stress (kPa)	Bottom L3	55	33	50	36	52	39
	Top L4	55	33	50	36	52	39
Compressive strain (μ strain)	Bottom L2	583	756	590	710	579	722
	Top L3	523	1208	588	1050	536	1106
Compressive strain (μ strain)	Bottom L3	282	677	334	589	304	573
	Top L4	282	677	346	598	314	539

The Drucker-Prager model (Drucker and Prager, 1952) in the ABAQUS^{TM} material library was used to represent the nonlinearity in the FEM. In the Drucker-Prager model (Drucker and Prager, 1952) the friction angle (β) and cohesion (d) were determined from triaxial tests using Equations 6-1 and 6-2 for non-dilatant flow (Systèmes, 2013). Table 3.10 of Chapter three is repeated here (Table 6.9) with the addition of the Drucker-Prager model parameters in the last two columns. The results of 100% OMC are used for the analysis in this chapter; while the analysis for the effect of moisture content using the finite element model is presented in Chapter Seven.

$$tan\,\beta = \sqrt{3}\,sin\,\phi \qquad (6\text{-}1)$$

$$\frac{d}{c} = \sqrt{3}\,cos\,\phi \qquad (6\text{-}2)$$

Table 6. 9 Calculation of Drucker-Prager model parameters from triaxial test results

UU Triaxial Test					Drucker-Prager parameters	
Soil type and MC%	Friction angle (ϕ)	Cohesion, C (kPa)	σs at 27kPa Confining pressure	τf	Friction angle (β)	Cohesion d
A-4 80% OMC	31	45	300	225	41.7	66.8
A-4 100% OMC	31	32	236	180	41.7	47.5
A-4 120% OMC	17	44	181	99	26.9	72.9
A-6 80% OMC	29	40	257	182	40	60.6
A-6 100% OMC	31	30	229	168	41.7	44.5
A-6 120% OMC	-	-	-	-	-	-

As the developed FEM will be used for the analytical pavement design procedure in Chapter Seven, its suitability for nonlinear analysis was assessed as described below. The outputs from modelling a pavement section with dimensions of 50×200×150 mm was compared when analysed using KENLAYER^{TM}, the graphical method (section 4.4) and the FEM incorporating the Drucker-Prager model as described above. The resilient modulus values of

the asphalt and granular base courses were taken to be 2000 MPa and 200 MPa, respectively. As mentioned previously, soil A-4 was found to exhibit stress hardening or increasing in the resilient modulus with an increase in deviatoric stress, therefore it was used for this analysis. Table 6.10 shows the results of the comparison for compacted and natural subgrade soils, using the graphical method described in section 4.4, KENLAYER and the FEM. The location of the response points were chosen to be at mid-depth of the compacted subgrade layer and 60 mm below the top of the natural subgrade (an explanation for selecting this depth is presented in section 7.5). Since the K-θ model in the KENLAYER Programme and the Drucker-Prager in the finite element model give an approximate solution for nonlinearity, the results differ by a small percentage. However, the results from using the graphical method may provide a more accurate figure as they are taken directly from the experimental results. From the results in Tables 6.8 and 6.10, it is clear that the procedure followed in section 4.4 can be used for consideration of stress dependency of the resilient modulus for unstabilised soil and consequently for stabilised soils, since the resilient modulus values are used directly in the analysis.

Table 6. 10 Comparison of nonlinear analysis results from KENLAYER, using graphs and FEM model for soil A-4

Location of response	KENLAYER Linear	KENLAYER Nonlinear	Graphical method Nonlinear				FEM Drucker-Prager
			Trial 1	Trial 2	Trial 3	Trial 4	
Comp. stress Mid-depth L3	118	102	118	109	107	107	112
6cm below top of subgrade	70	59	70	63	63	63	67
Comp. strain Mid-depth L3	658	719	658	667	694	696	757
6cm below top of subgrade	402	544	402	482	496	497	405

Soils A-4 and A-6 contain a high proportion of quarry fines as presented in Chapter Three. The fine particles are created artificially by crushing limestone; therefore their strengths are higher than that of a soil which exists naturally and has formed through years of weathering. This demonstrates the reason why these soils behave as granular material in terms of their resilient modulus values. However, as explained in Chapters Four and Five, although the soil A-4 has a high resilient modulus value it undergoes a high permanent deformation especially at higher moisture contents. Soil A-6 which contains 74% silt, sand and fine gravel exhibits a decrease in resilient modulus with an increase in deviatoric stress up to 62.0 kPa; after this value it showed the opposite trend (see Figure 6.8). To show the effect of moisture change on the behaviour of these two soils, a pavement section of 50×150×150 mm was analysed with the developed FEM using the Drucker-Prager model. The asphalt and granular base modulus were taken to be 2000 MPa and 200 MPa, respectively. The resilient modulus values of the compacted and natural subgrade soils were provided from the multi-stage permanent deformation test results. The effect of moisture on the performance of these soils is presented in Chapters Four and Five, however in this chapter the effect is translated to the structural analysis instead of test results. This comparison of soil types and the effect of moisture was one of the objectives of this research.

Figure 6. 8 Resilient modulus to deviatoric stress relationship for soil A-6 to determine the k parameters

Tables 6.11and 6.12 show the analysis results for surface deflection, compressive stress and strains for soils A-4 and A-6, respectively.

Table 6. 11 Responses of the pavement section for three different moisture contents to the applied tyre pressure of 860 kPa for soil A-4

Response	Location	Section (5×15×15) mm & 860 kPa tyre pressure		
		A-4 80% OMC	A-4 100% OMC	A-4 120% OMC
Surface Deflection (mm)	TopL1	1.093	1.264	2.089
Compressive Stress (kPa)	Mid-depth L3	205	177	134
Compressive Stress (kPa)	6cm below L4	124	112	84
Compressive Strain (μ strain)	Mid-depth L3	1714	2104	3229
Compressive Strain (μ strain)	6cm below L4	916	1169	1789

Table 6. 12 Responses of the pavement section for three different moisture contents to the applied tyre pressure of 860 kPa for soil A-6

Response	Location	Section (5×15×15) mm & 860 kPa tyre pressure		
		A-680%OMC	A-6100%OMC	A-6120%OMC
Surface deflection (mm)	TopL1	1.211	1.514	2.368
Compressive stress (kPa)	Mid-depth L3	189	156	125
Compressive stress (kPa)	6cm below L4	117	101	78
Compressive strain (μ strain)	Mid-depth L3	1972	2514	3526
Compressive strain (μ strain)	6cm below L4	1070	1437	2023

As can be seen the increase in moisture content from 80% OMC to 120% OMC has increased the surface deflection from 1.093 mm to 2.089 mm and from 1.211 mm to 2.368 mm for soils A-4 and A-6, respectively. Also, the resilient strains, for example at the mid-depth of layer three, increased from 1714 micro-strains to 3229 micro-strains and from 1972 micro-strains to 3526 micro-strains for soils A-4 and A-6, respectively. Figures 6.9 and 6.10 are showing the finite element output visualisation of the compressive strains for soils A-4 and A-6, respectively. For other response outputs see Appendix C.

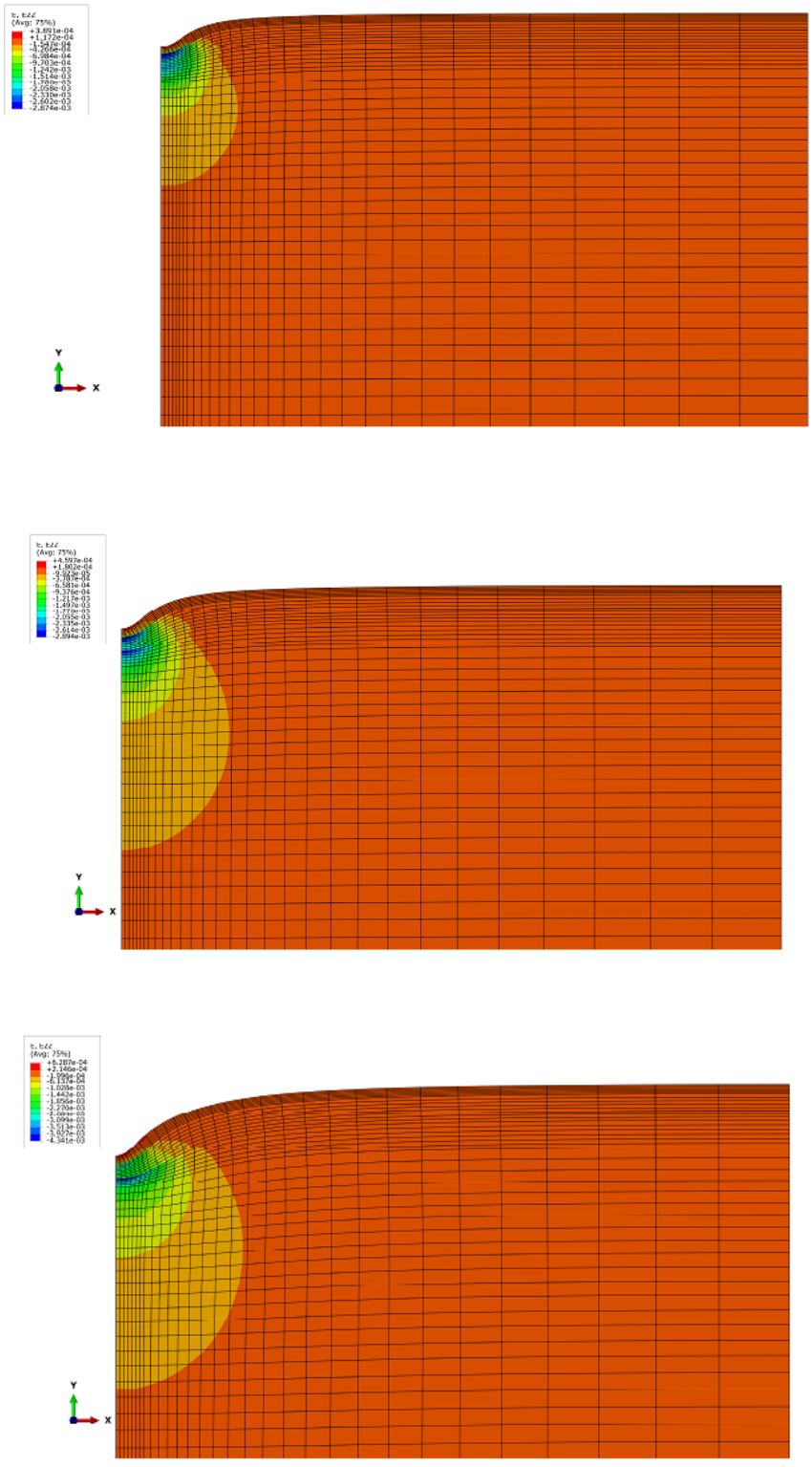

Figure 6. 9 Compressive strains' visualisation from finite element analysis for soil A-4 at 80% OMC, 100% OMC and 120% OMC, respectively

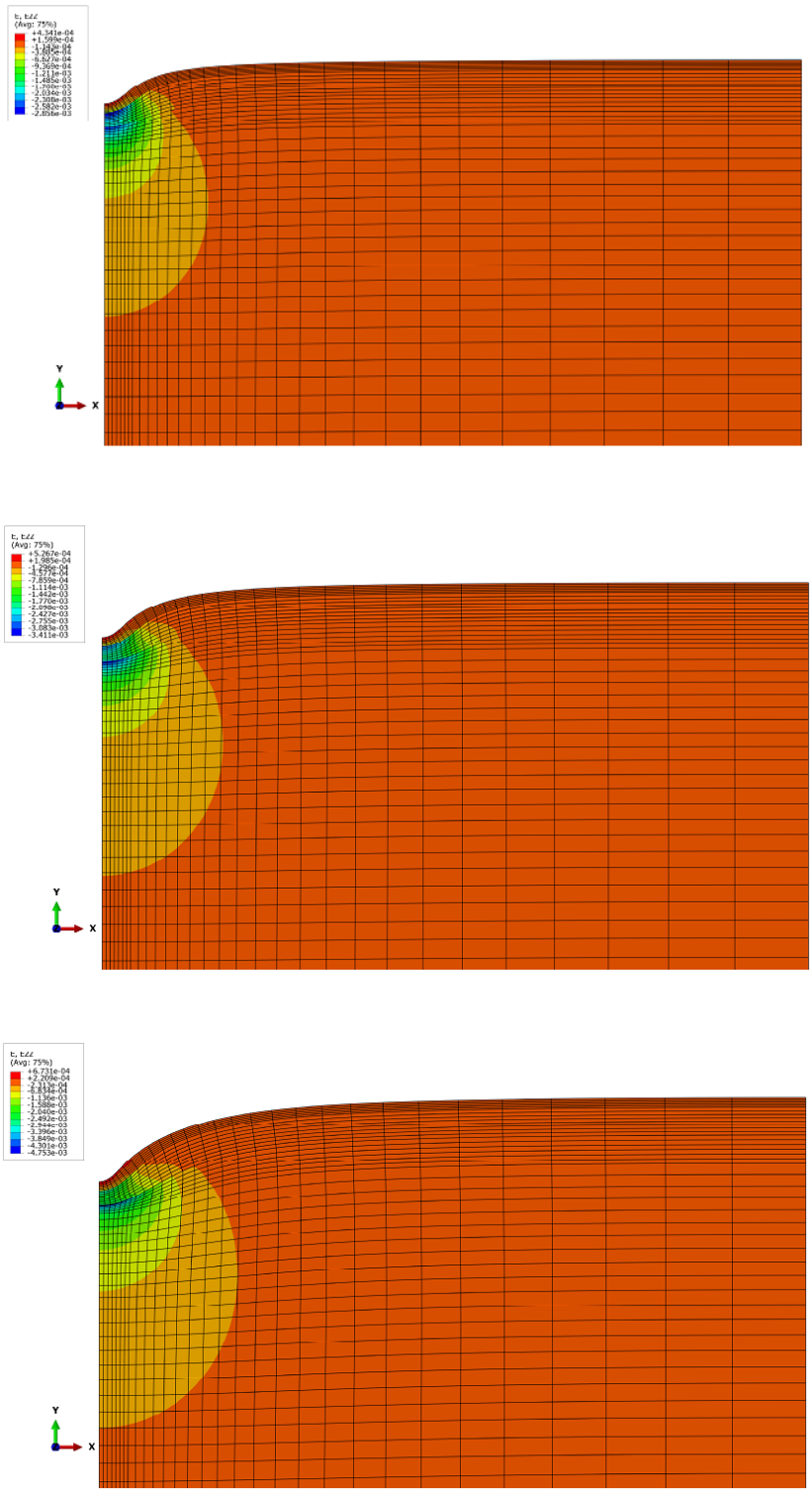

Figure 6. 10 Compressive strains' visualisation from finite element analysis for soil A-6 at 80% OMC, 100% OMC and 120% OMC, respectively

6.6 Summary

Analytical pavement design requires a pavement response model for determining the stresses and strains at critical locations. The responses obtained from such models are used in performance models to quantify the deteriorations occurring in a road pavement as a function of traffic and environmental load. For this purpose a finite element model (FEM) was developed in this research, and described in this chapter, to analyse different combinations of pavement sections, materials and loads. The developed model was compared using different pavement section configurations and loads to KENLAYER^{TM}, showing good agreement. The advantage of the finite element model developed in ABAQUS^{TM} for example, over other response models, is that it can benefit from the various material library models such as Cam-clay model, Mohr-Coulomb model and Drucker-Prager models and it enables the plastic strain and the boundary condition settings to be determined. The material characterisation was also discussed and the suitability of using graphs of deviatoric stress versus resilient modulus relationships for stabilised subgrade layer analysis was presented. The response of stabilised subgrade layer was determined using an iterative procedure and the natural subgrade layer, was represented via the Drucker-Prager model. In this way both layers can take into account the nonlinearity of the materials they represent. Examples are presented in Chapter Seven to include findings from this chapter and Chapters Four and Five in an analytical pavement design procedure for lightly stabilised subgrade layers.

CHAPTER SEVEN

ANALYTICAL PAVEMENT DESIGN FOR KURDISTAN

7.1 Introduction

This chapter utilizes the data and findings presented in Chapters Three to Six in a single analytical procedure to be followed for a successful subgrade design, considering the effect of moisture change during the pavement's design life. The analytical pavement design procedure is briefly presented with the main focus on the subgrade. All the pavement design procedures discussed in Chapter Two, whether they are empirical or analytical, include a clear requirement for subgrade characterisation, since the subgrade soil type and its sensitivity to environmental changes directly influence the materials and their thicknesses used for the upper pavement layers. However, the adequate characterisation of stabilised layers, especially the subgrade, in mechanistic-empirical pavement design procedures heretofore has not been considered. According to Velasquez et al. (2009), who carried out research for the implementation of the MEPDG (2004) for use in Minnesota State, the main drawback of the MEPDG in characterising stabilised layers is lack of consideration of the effect of moisture and temperature on stiffness. This research herein presents a procedure for considering the moisture effects on changes in resilient modulus and permanent deformation behaviour of lightly stabilised subgrade layers. Furthermore, an important aspect of pavement design considering the gradual deterioration of lightly stabilised subgrade soils is explained and incorporated into an analytical design procedure for a stabilised subgrade layer. These procedures for subgrade design are presented in two figures. Figure 7.1 is a method for examining the soil's suitability for use as subgrade without stabilisation and Figure 7.2 shows a method developed for stabilised subgrade soil.

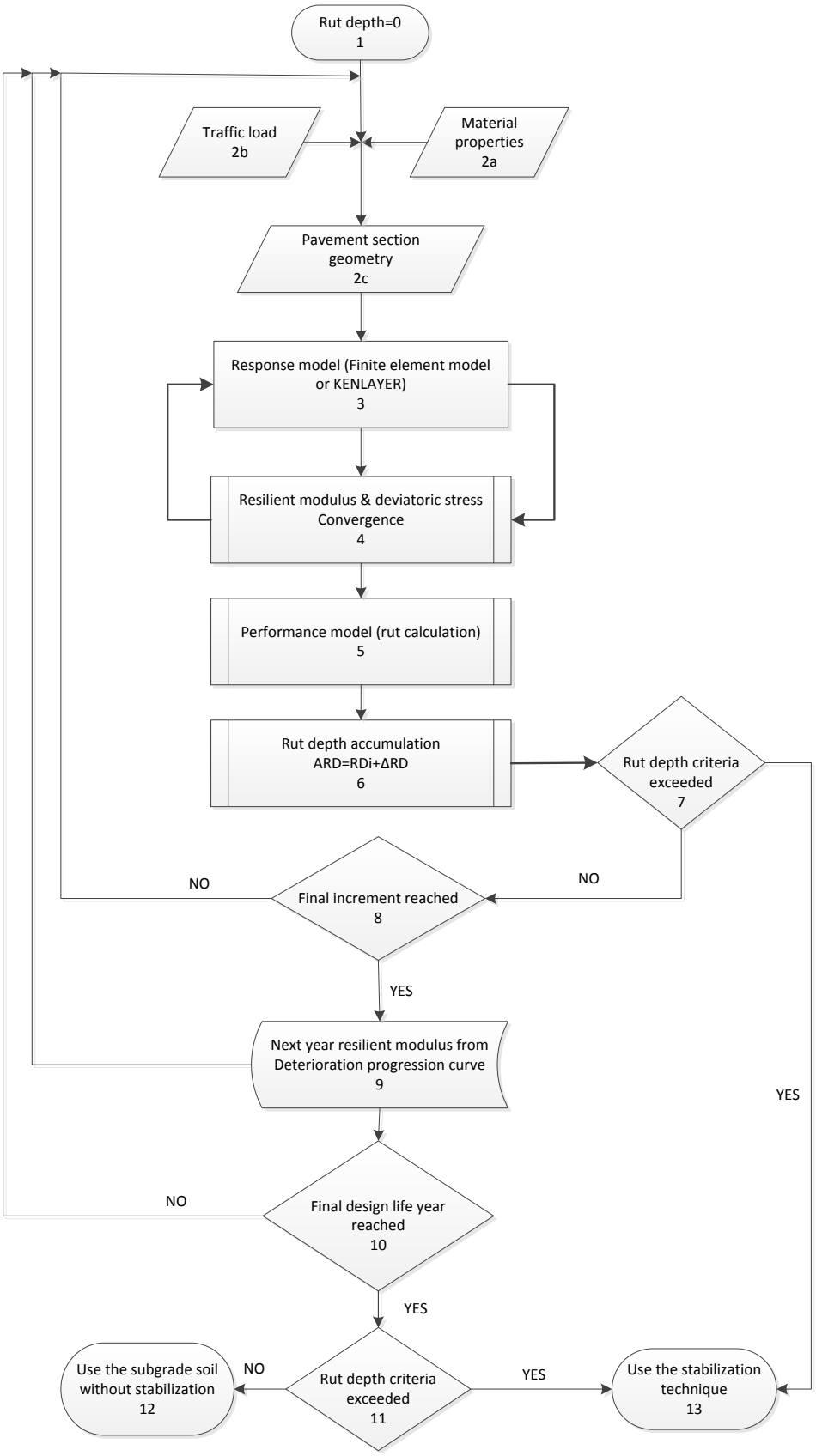

Figure 7. 1 Design procedure for unstabilised subgrade soil

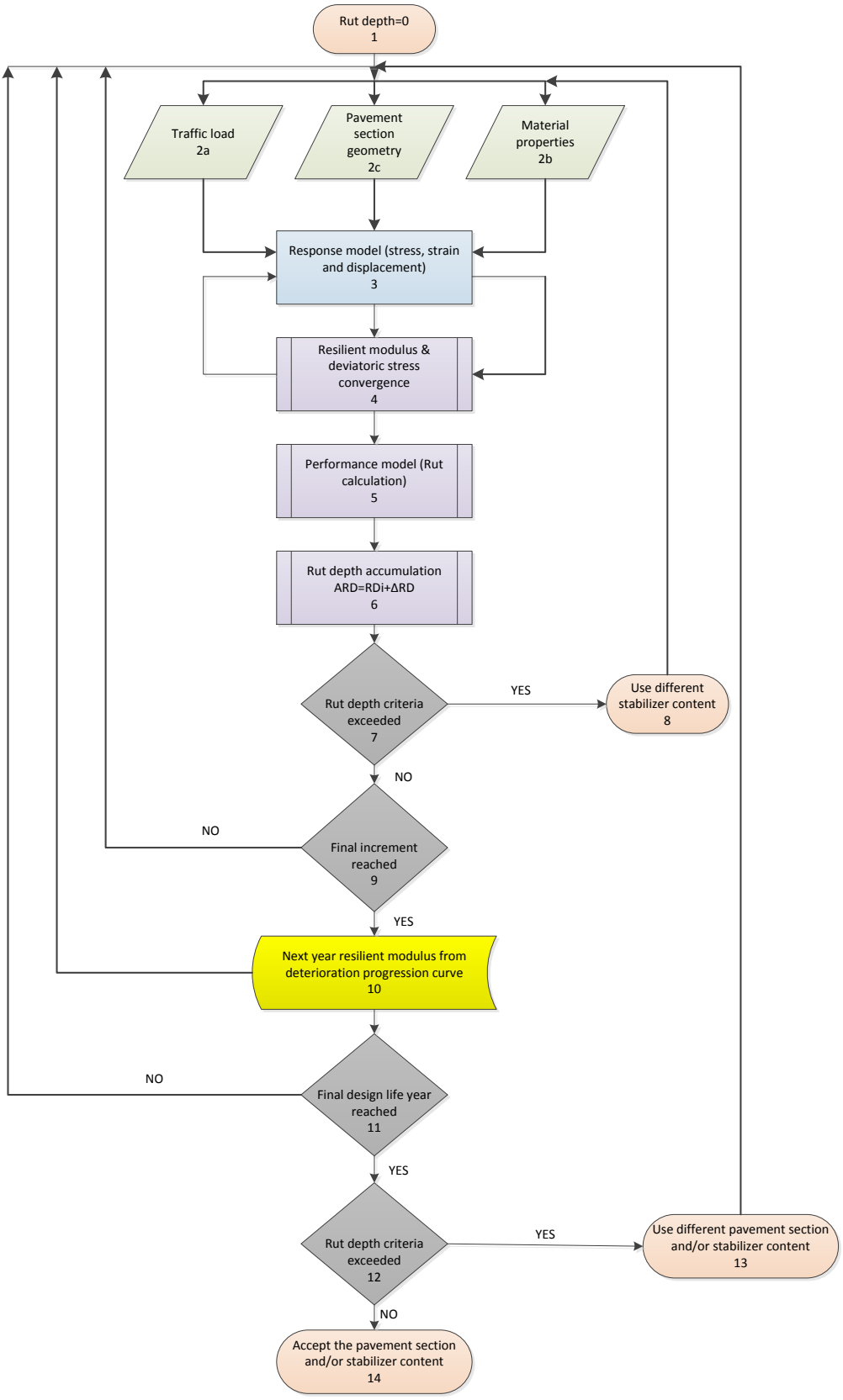

Figure 7. 2 Design procedure for stabilised subgrade soil

7.2 Progressive Deterioration of Resilient Modulus

Conventional analytical pavement design procedures use the same resilient modulus value of stabilised layers throughout the design life, while the deterioration of the asphalt is accounted for in the design through the selection of the appropriate stiffness from test results (MEPDG, 2004). The cumulative traffic load to which the road pavement is to be subjected (i.e. the designed traffic load) is typically based on current traffic loads plus an increment to account for future traffic growth. However, the deterioration of resilient modulus of the stabilised layers and unbound materials are not usually considered.

The deterioration progression in a pavement subgrade can be obtained from the durability tests and the procedure presented in Chapters Four and Five. The changes in resilient modulus values at different stages of deterioration are obtained from test results, or determined from the graphs that demonstrate the relationship between resilient modulus and age. Using this method the incremental damage to the pavement structure can be found and used for pavement design and management purposes. Steps 9 and 10 in Flowcharts 7.1 and 7.2, respectively, include this method to take into account the deterioration progression of the resilient modulus over time.

To include this characteristic within the pavement design process, a procedure has been developed herein as follows:

1) From durability tests described in Chapters Three to Five, the deterioration of the resilient modulus value can be determined. The durability test can include cycles of wetting/drying or freezing/thawing at different stages. For example at 0, 1, 5, 10, 15, 20 and 25 cycles; each cycle of these cycles can represent one year of the design life of the pavement.

2) The resilient modulus of unstabilised soils from tests at optimum moisture content was determined. For other expected moisture contents lower or higher than optimum moisture content, Equation (7.4) can be used. The permanent deformation for each increment or season was determined from Equation (7.5) and accumulated to obtain the first year's permanent deformation.

3) For the next period of analysis (e.g. after one year) the resilient modulus of the subgrade layer is modified. To determine the progressive deterioration, a matrix of the deviatoric stress and resilient modulus values was created and then converted to a series of curves for deterioration consideration of the resilient modulus of stabilised subgrade soils. To achieve this, the following steps were undertaken:

3-1) Firstly a graph was drawn between the deviatoric stress and resilient modulus before and after the durability test, see Figure 7.3. From the figure, the distance A-B is the decrease in resilient modulus value after 25 cycles of wetting and drying at a deviatoric stress of 12.4 kPa; and the distance C-D shows this change for a deviatoric stress of 120.0 kPa.

3-2) In the second step, a matrix of deviatoric stress and resilient modulus was created, considering the deterioration for each stress level and age (cycles of wetting and drying). Table 7.1 presents this matrix in which the first column (column 1) is the deviatoric stress, column 2 is the corresponding resilient modulus value before the durability test and column 3 is the resilient modulus value after the durability test. Column 4 is the Annual Deterioration Factor (ADF) which is determined from Equation (7.1).

$$ADF = \frac{Mr\ before\ durability\ test - Mr\ after\ durability\ test}{NDC} \quad (7.1)$$

Where: *ADF* is the annual deterioration factor; M_r is the resilient modulus and *NDC* is the number of durability cycles which can represent the number of years (25 in this research).

Columns 5 to 9 are the deteriorated resilient modulus values after 5, 10, 15, 20 and 25 wetting and drying cycles respectively.

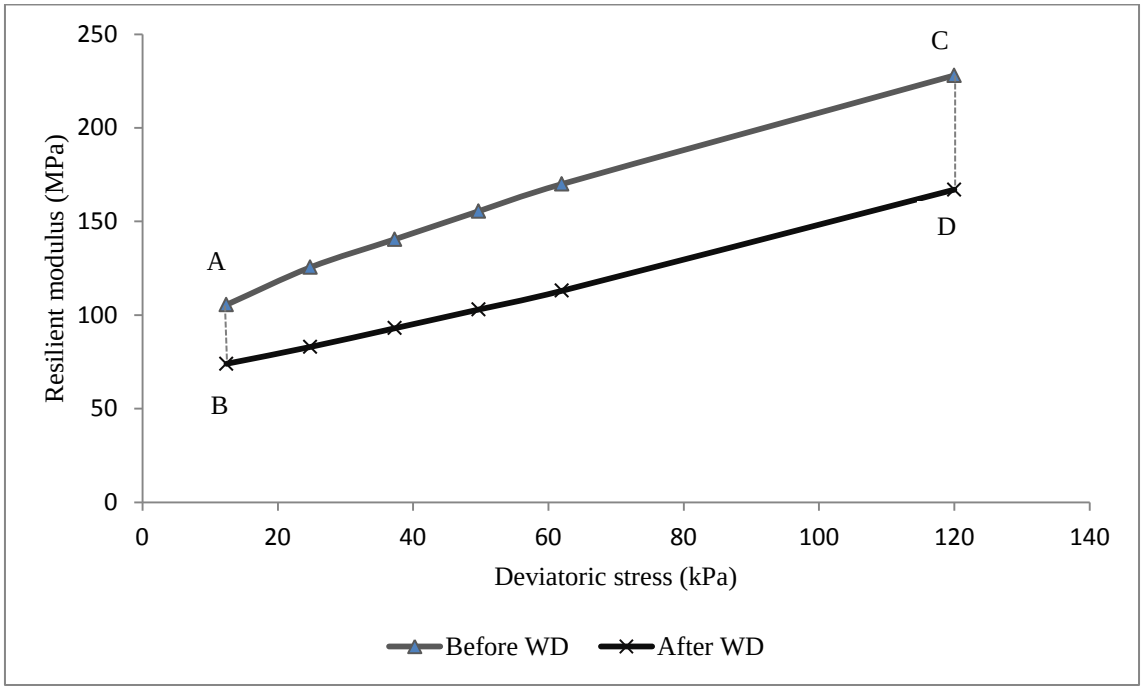

Figure 7. 3 Deviatoric stress to resilient modulus relationship for stabilised soil A-6 at 2%CC+1.5%LC before and after wetting and drying cycles

Table 7. 1 Matrix of deviatoric stress and resilient modulus after stages of deterioration progression for soil A-6 at 2%CC+1.5%LC

1	2	3	4	5	6	7	8	9
Deviatoric Stress (kPa)	Mr Before W&D (MPa)	Mr After W&D (MPa)	YDF	Mr after 5 years (MPa)	Mr after 10 years (MPa)	Mr after 15 years (MPa)	Mr after 20 years (MPa)	Mr after 25 years (MPa)
12.4	106	74	1.26	99	93	87	80	74
24.8	126	83	1.70	117	109	100	92	83
37.3	141	93	1.90	131	122	112	103	93
49.7	156	103	2.10	145	135	124	114	103
62.0	170	113	2.28	159	147	136	124	113
120.0	228	167	2.44	216	204	191	179	167

3-3) Finally from the results in Table 7.1, the deviatoric stresses against the resilient modulus values were plotted and are shown in Figure 7.4. This figure was then used in the pavement analysis as described in sections 4.4 and 5.4.1 to achieve the requirements for steps 9 and 10 in Flowcharts 7.1 and 7.2, respectively.

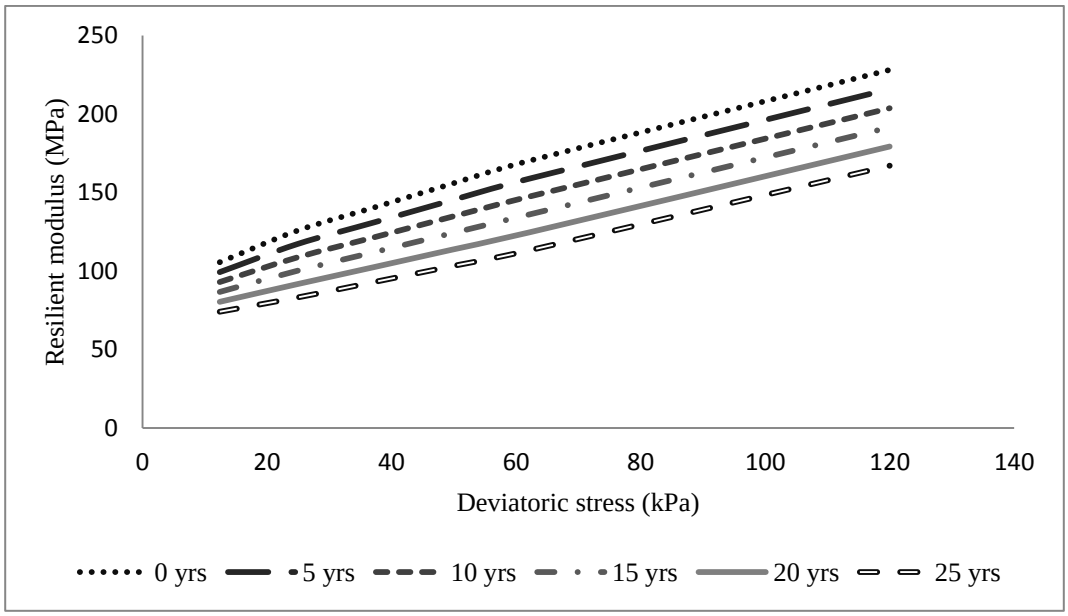

Figure 7. 4 Resilient modulus values at different stages of deterioration

4) Step 3 was repeated until the end of the design life of the pavement. It is important to mention that the number of load repetitions for each stage was calculated from the growth rate equation from the base year to the number of years to that stage. For the calculation of traffic forecasting, the MEPDG (2004) gives three equations presented below:

$AADTT_X = 1.0 * AADTT_{BY}$ For no growth (7.2a)

$AADTT_X = GR * AGE * AADTT_{BY}$ For linear growth (7.2b)

$AADTT_X = AADTT_{BY} * (GR)^{AGE}$ For compound growth (7.2c)

Where: $AADTT_X$ = annual average daily truck traffic at age X; $AADTT_{BY}$ = base year annual average daily truck traffic and GR = traffic growth rate.

Another simple procedure for forecasting the traffic load can be found in Austroads (2008) as presented in Equation (7.3):

$$\text{Cumulative Growth Factor (CGF)} = \frac{(1+0.01\text{R})^{\text{P}}-1}{0.01\text{R}} \quad (7.3)$$

Where: R= annual growth rate (%) of vehicles

P= design period in (years)

If the whole design life is divided into five stages the resilient modulus without deterioration is used for the first five years. The number of load repetitions was calculated from the growth rate equation; for example if the growth rate is 4% (R = 4) and the Average Annual Daily Traffic (AADT) for an ESAL of 80 kN is 300000, the forecasted number of loads for this stage (five years, or p = 5) will be 1,624,897 ESALs that is distributed through these five years.

5) In the absence of the equipment required to measure the resilient modulus or difficulty of obtaining resilient modulus values with a high ratio of stabiliser for example, the correlation equations (4.11 and 4.12) can be used. The advantage of these equations is that the resilient modulus value can be obtained for a range of deviatoric stresses from which graphs between resilient modulus and deviatoric stresses for nonlinearity can be plotted, as explained in the design examples of section 7.10. Also the durability tests (wetting and drying or freezing and thawing) on samples prepared for an unconfined compressive strength (UCS) test can be carried out and the above procedure followed. It is of note that the deterioration progression curve can be used for fatigue cracking of soil-stabilised layers as well.

The increase in moisture in this research from any of the different sources mentioned in Chapter Two is assumed to be 20% higher than the optimum moisture content for unstabilised soils and completely saturated and dried for stabilised soils. The sensitivity of the subgrade soils to the changes which occur in moisture contents is important in order to decide whether to stabilise the subgrade soils. To this end, the modular ratio (the resilient modulus ratio of two successive base/subbase/subgrade layers that should not exceed 2.5 for unbound granular materials and 5 for more cohesive soils (Jooste and Long, 2007)) should be considered to avoid decomposition, especially if the granular base course above the stabilised subgrade layer was not stabilised. This is demonstrated in the pavement design example given in Appendix F.

7.3 Design Inputs

Design inputs, as demonstrated in the design procedure Flowcharts 7.1 and 7.2 (item 2), are: traffic load, material properties and pavement section geometry. The geometry of the pavement section depends on the design life and the availability of the materials. The thicknesses are determined through structural pavement design and analysis procedures. Most of the pavement sections, found in Kurdistan, are conventional and deep strength flexible pavements (Figure 7.5). Regarding the traffic data, it must include the type of the vehicles and weight, number and configurations of their axles. It is also necessary to obtain the number of heavy vehicles and their growth rate, for future forecasting. From the data collected for the traffic, the number of the repetitions of each axle load, tyre pressure and tyre contact area are most essential; these are utilised within response models for stress, strain and displacement determination.

The properties of the road pavement materials are determined from laboratory tests or field measurements. These results give the highest level of data entry to the pavement analysis; however, not all the required data of this quality for a specified project can be obtained. Therefore, with a lower quality of data, correlation equations and default values as postulated in this thesis (see Section 4.6) can be used. These types of data classification is followed in the MEPDG 2004. The details of the material property requirements for asphalt and unbound granular materials are presented in many of the design guides (e.g. MEPDG, 2004; Austroads, 2008). The following section describes the resilient modulus of the stabilised and unstabilised subgrade soils.

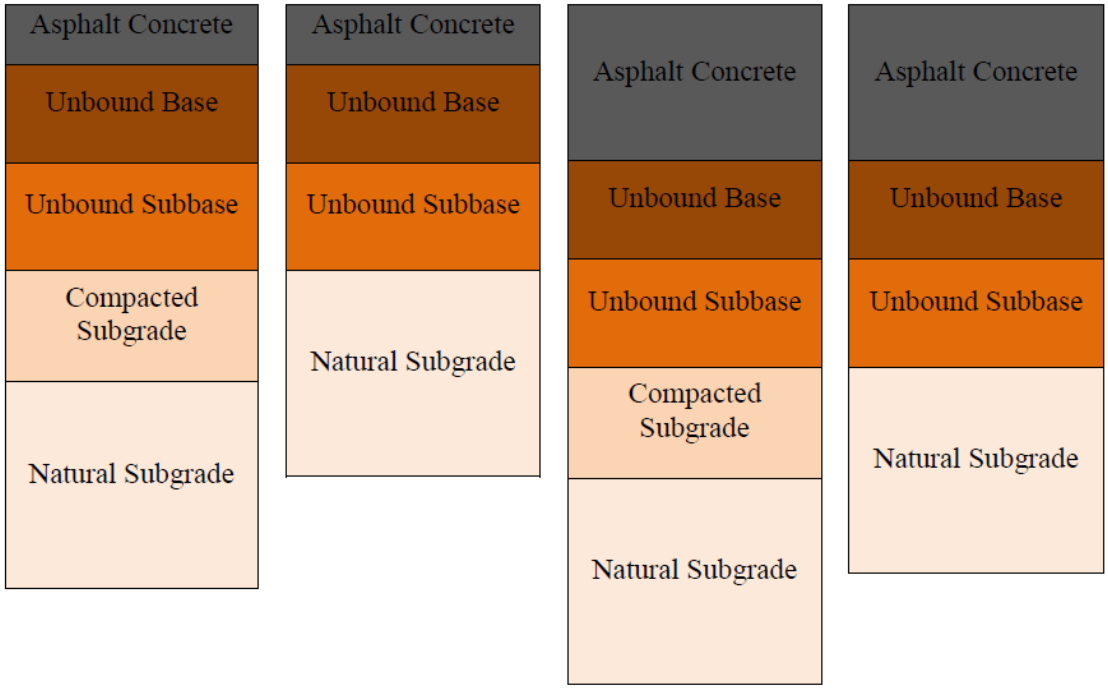

Figure 7. 5 Common flexible pavement systems found in Kurdistan

The resilient modulus is adjusted for the effect of moisture for the first year. The adjustment may be done for every single month or season according to the changes of moisture content and fluctuations that are expected through the whole year or the coming years of the design life. The effect of moisture is assessed through the tests of resilient modulus and permanent deformation at different moisture contents and the explanation of the moisture effect is discussed in detail in section 4.2.1. In particular, the effect of the degree of saturation on resilient modulus behaviour was demonstrated clearly. Based on this discussion, Equation 7.4 suggested by MEPDG (2004) for moisture effect on resilient modulus of unbound and subgrade layers, was utilised in the pavement design procedure in this research. This equation is used in example F.1 of Appendix F. However, where the resilient modulus value for different moisture contents of different seasons is available it can be used directly in the design procedure. Yet, if the resilient modulus is only available at optimum moisture content, equation 7.4 can be used (MEPDG, 2004).

$$log\frac{M_R}{M_{Ropt}} = a + \frac{b-a}{1+EXP[ln\frac{-b}{a}+k_m*(S-S_{opt})]} \quad (7.4)$$

Where: $\frac{M_R}{M_{Ropt}}$ = Resilient modulus ratio; M_R is the resilient modulus at a given time and M_{Ropt} is resilient modulus at a reference condition.

a = Minimum of $log\frac{M_R}{M_{Ropt}}$

b = Maximum of $log\frac{M_R}{M_{Ropt}}$

k_m = Regression parameter

$(S - S_{opt})$ = Variation in degree of saturation expressed in decimal.

The values suggested for a, b and k_m in the MEPDG (2004) are -0.3123, 0.3 and 6.8157 respectively, for coarse grained soils and -0.5934, 0.4 and 6.1324 respectively, for fine grained soils.

For stabilised subgrade soils, the resilient modulus can be found from Equations 4.11 and 4.12. Where the linear elastic method is used for analysis of the pavement section, the resilient modulus values obtained from these equations can be used. For nonlinearity considerations the procedure in Chapter Four section 4.4 can be followed.

7.4 Response Model

The response model in analytical pavement design procedures, step 3 in Figures 7.1 and 7.2, was used to determine the stresses, strains and deflections. The responses at critical locations in the pavement section were determined. These critical locations in most analytical pavement design procedures are: tensile strain at the bottom of the asphalt and cemented layers; and vertical strain at the top of the subgrade (Huang, 2004; MEPDG, 2004; Austroads, 2008). However, in this research the vertical stresses and strains within the compacted and natural subgrade layers were used instead since the absolute permanent deformation quantities of these layers was used for performance assessment. These responses were used later in the performance model to evaluate the pavement section's resistance to prevailing traffic and environmental conditions. These responses are influenced by the type and frequency of the traffic loads and environmental conditions. These environmental conditions concern the temperature that affects the asphalt concrete surface and the moisture that affects the subgrade and unbound granular layers.

The finite element model developed in Chapter Six was used to determine the response of a pavement layer to traffic loading. Where the nonlinearity of subgrade soil is considered, the Drucker-Prager model is applied to obtain the stress-dependent responses of the subgrade material, see section 6.5. However, there is no material property model in the finite element model to define stabilised subgrade soils for nonlinearity and therefore the procedure

described in Chapter Four section 4.4 was followed instead. By using this iterative procedure, the stress-dependent resilient modulus was determined and both the resilient modulus and vertical stress were used in the performance model. This iterative procedure is achieved by undertaking steps 3 and 4 in the Flowcharts 7.1 and 7.2. As the various materials' properties were determined from the laboratory test results which are presented in Chapters Three, Four, Five and Six, all required parameters for performance and response models were used for the pavement section analysis. The main reason behind developing a finite element model was its ability to consider the nonlinear behaviour of unbound materials used in a pavement structure. At the same time it can be used for linear elastic analysis as well. As explained in Chapter Six, Huang (2003) attempted an approximate solution for incorporating the nonlinearity of unbound material into a response model. However, the finite element model has the capability of simulating a variety of pavement material properties, especially by defining these properties with different codes and embedding them in the finite element model. It is worth mentioning that the KENLAYER (Huang, 1993) programme can be used for both linear and nonlinear analysis where the finite element model is not available.

7.5 Performance Prediction Model

The performance model (Equation 5.8) developed in section 5.4.1 was used for steps 5 and 6 in the Flowcharts 7.1 and 7.2. In section 5.4.1, the influence of the vertical stress and resilient modulus values in the permanent deformation progression of stabilised and unstabilised subgrade soils was verified. The importance of introducing these two parameters (resilient modulus and vertical stress) is that the resilient modulus of base course layer affected by the underlay layer material type; the resilient modulus of base course/subbase course material decreases if it is placed on a weak subgrade (Jooste and Long, 2007). Using the model, the deterioration can be accounted for in an incremental way. The change in resilient modulus

with aging and weathering can affect adversely the rutting progression; at the same time the change in the applied load was taken into account, where the increase in the applied load results in the progression of rutting.

An advantage of the proposed model is in its simplicity i.e. the parameters can be determined from one single permanent deformation test. The other advantage of the proposed model is that it can be used very straightforwardly with different load configurations and material properties. Section 2.5 presents the literature (Uzan, 2004; Tseng and Lytton, 1998; Veverka, 1979) concerning using permanent to resilient strains' ratios in performance models. A sensitivity analysis, described in Chapter Four and Five, using different moisture contents for unstabilised soils was carried out to find the factors affecting the pavement's performance at different moisture conditions. This would then make it easy to decide on the necessity of improving the pavement's performance. The results presented in Chapters Four and Five show the factors affecting the resilient modulus and permanent deformation values, especially the moisture content.

$$\sum_{t=1}^{m} \varepsilon_p = a \times \left(\frac{\sigma_{dt}}{M_{rt}}\right) \times N_t^b \qquad (7.5)$$

$\sum_{1}^{m} t$ = T

Where: ε_p is accumulated permanent strain in micro strain

σ_{dt} is deviatoric stress in kPa during a period of time t

M_{rt} is resilient modulus in MPa for a period of time t

N_t is the number of load repetitions in the period of time t

a and b are material parameters

T is the design life of the road pavement

In equation 7.5, the resilient modulus and deviatoric stress are calculated from the pavement section analysis and the nonlinearity is considered. The model can be written as the following for absolute rut depth if the limiting rut depth criterion is applied:

$$Rut\ Depth\ (mm) = \varepsilon_{1,p} * h \quad (7.6)$$

Where h is the thickness of the compacted subgrade layer in mm

For natural subgrades the thickness is selected according to the nature of the infinite layer; if the infinite layer is homogenous any depth can be selected and the permanent deformation is calculated. A model (Equation 7.7) suggested by the MEPDG (2004) can be used to determine absolute permanent deformation determination.

$$\varepsilon_p(z) = \left(\varepsilon_{p,z=0}\right) * e^{-kz} \quad (7.7)$$

Where: $\varepsilon_p(z)$ is the permanent deformation at the required depth; $\varepsilon_{p,z=0}$ is the permanent deformation at depth $z=0$; and k is a regression constant.

For all layers the stresses and strains were calculated at the mid-depth of the layer except for the subgrade layer, which was calculated at the top of the subgrade and a depth of 15.24 cm (6 inches).

Another method that is time consuming, but acceptable is to divide the subgrade into a number of sub-layers and calculate the permanent deformation at the mid-depth of each sublayer. The summation of the permanent deformation sublayers gives the permanent deformation of the subgrade layer.

The permanent deformation of stabilised layers is assumed to be zero in the MEPDG (2004). Also because of the unavailability of permanent deformation prediction equations for

stabilised subgrade layers, this model (Equation 7.5) is applicable primarily for lightly stabilised and unstabilised subgrade soils. The equation is supported by the concept of limiting the vertical compressive strain suggested by (Monismith et al., 1988) 'In pavement materials the magnitude of the plastic strain is directly proportional to the magnitude of the (vertical) elastic strain' (Austroads, 2008). Another reason supporting the use of equation 7.5 as a performance model (which uses the limiting vertical compressive strain concept) is provided by the Corps of Engineers (Janoo et al., 2003), in which the parameters of the performance model are related to the resilient modulus of the subgrade soil.

The criteria for permanent deformation according to the Corps of Engineers (COE) (Janoo et al., 2003):

$$Nd = 10{,}000 \times (a/\varepsilon v)^{b} \qquad (7.8)$$

Where $a = 0.000247 + 0.000245 \log (Mr)$

$b = 0.0658\ (Mr)^{0.559}$ and Mr is in psi

7.6 Performance Criteria

Road pavement design procedures require performance criteria to be determined for distress types of interest. As the focus of this research is on rutting as mentioned in Chapter One, the methods of design that are used to control rutting are discussed. In Huang's (2003) words: 'Two procedures have been used to limit rutting: one to limit the vertical compressive strain on top of the subgrade, the other to limit the total accumulated permanent deformation on the pavement surface based on the permanent deformation properties of each individual layer'. The limiting rut depth of 0.3 to 0.5 inches (7.62 to 12.7 mm) is normally used in analytical pavement design procedures (MEPDG, 2004). In the compressive strain on the top of the subgrade criterion, the resilient strain is related to the number (N) of load repetitions in an

equation; its parameters should be determined from a comparison of the predicted and field data. The following equations show the calibrated performance models used by different pavement design agencies.

$N_d = 1.365 * 10^{-9}(\varepsilon_c)^{-4.477}$ By Asphalt Institute (Shook et al., 1982) (7.9)

$N_d = 6.15 * 10^{-7}(\varepsilon_c)^{-4.0}$ By Shell (Claessen et al., 1977) (7.10)

$N_d = 6.18 * 10^{-8}(\varepsilon_c)^{-3.95}$ By UK TRRL (Brown et al., 1977) (7.11)

Where N_d is the allowable number of load repetitions and ε_c is the compressive strain on the top of the subgrade.

The same relationship of compressive strain and the number of load repetitions is expressed as the following in Austroads (2008):

$$N = \left[\frac{9300}{\mu\varepsilon}\right]^7 \quad (7.12)$$

Where *N* is the number of allowable load repetitions and $\mu\varepsilon$ is compressive strain at the top of the subgrade in micro-strains.

The Swedish National Road Administration (SNRA, 2001) uses an equation considering the moisture factor in addition to the compressive strain on the top of the subgrade (Agardh, 2005):

$$N_{te,i} = f_d \frac{8.06*10^{-8}}{\varepsilon_{te,i}^4} \quad (7.13)$$

Where $N_{te,i}$ = maximum number of standard axle loads at season *i*

f_d= correction factor for moisture

$\varepsilon_{te,i}$ = maximum vertical strain at the top of subgrade at season *i*

The Corps of Engineers (Janoo et al., 2003) included the resilient modulus of the subgrade material in the performance criteria equation to be as the following:

$$N_d = 10{,}000 * (\frac{a}{\varepsilon_v})^b \quad (7.14)$$

Where N_d = allowable number of load repetitions

ε_v= compressive strain on the top of the subgrade

a = 0.000247 + 0.000245 log (Mr)

b = 0.0658 (Mr) $^{0.559}$

Mr = resilient modulus in psi

All the above mentioned equations are used for specific locations and conditions; therefore their use for other sites may not be reliable. The other method of design to control the rutting is to limit the rutting to a tolerable quantity, for example 12.5 mm in 25 years (Huang, 2003). The performance model (Equation 5.8) developed in section 5.4.1was used in joint with this criterion (limiting rut depth) in this procedure design. This method allows the designer to use correlation equations derived experimentally in the laboratory. Steps 7 and 12 in the Flowcharts 7.1 and 7.2 can be applied to check if the material's final permanent deformation is reached.

7.7 Decision on Appropriate Scenario

The subgrade soil of a road project is not necessarily homogenous and could vary temporarily and spatially. It may therefore be neither appropriate nor applicable to stabilise different soil types with different stabiliser contents in one road construction project. The procedure presented in this chapter can be used for different soil types with different stabiliser contents. The results of analyses of different soil types with various stabiliser contents are then

tabulated, from which the most durable and most suitable economically can be used throughout the road project. This will provide a more robust subgrade design. It is of value to mention that the fatigue cracking analysis must be carried out for these trials to decide on the stabiliser type and content to compromise both rutting and cracking analyses.

7.8 Fatigue Cracking

The method of modulus of elasticity determination in Chapter Three can be employed for a fatigue cracking prediction model. Analytical pavement design procedures require a modulus of elasticity value for stabilised layers to be used in fatigue cracking performance models.

7.9 The Importance of Permanent Deformation Tests

Permanent deformation tests were carried out (see Chapter Five) to understand the behaviour of different types of subgrade soils, whether they are stabilised or unstabilised. MEPDG (2004) highlights the necessity of assessing the permanent deformation of different materials used in a pavement as follows:

"Regardless of the material type considered, there are generally three distinct stages for the permanent deformation behaviour of pavement materials under a given set of material, load and environmental conditions.

- *Primary stage: high initial level of rutting, with a decreasing rate of plastic deformation, predominantly associated with volumetric change.*
- *Secondary stage: small rate of rutting exhibiting a constant rate of change of rutting that is also associated with volumetric changes; however, shear deformation increase at increasing rate.*
- *Tertiary stage: high level of rutting predominantly associated with plastic (shear) deformation under no volume changes conditions."*

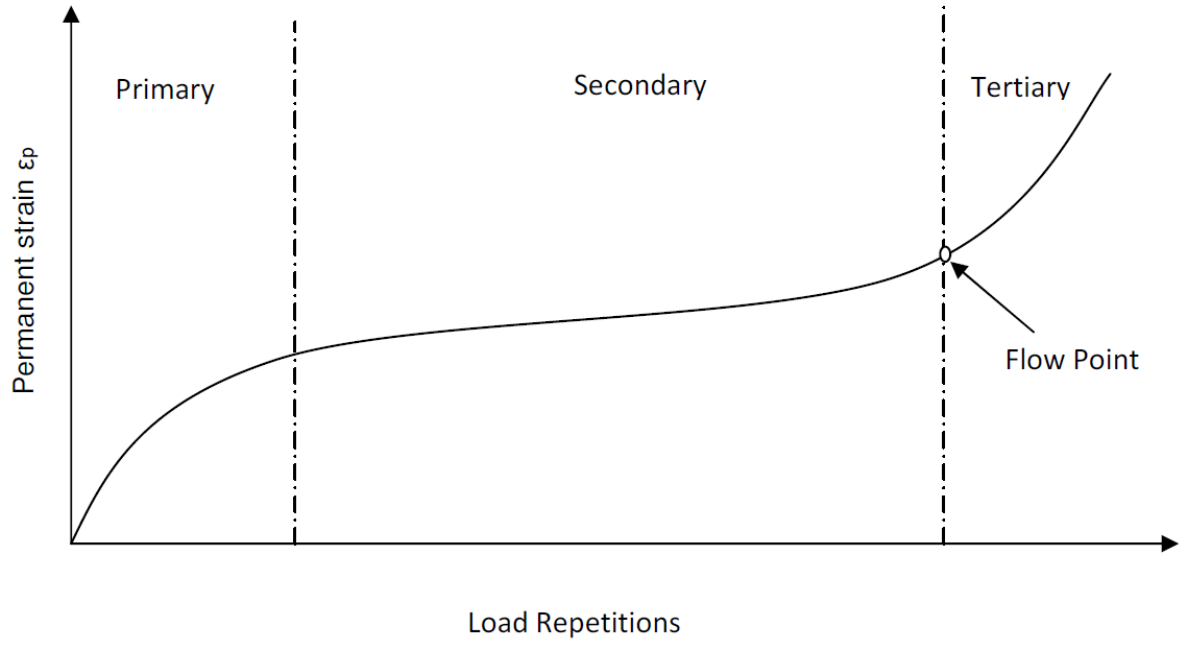

Figure 7. 6 Typical repeated load permanent deformation behaviour of pavement materials (After MEPDG, 2004)

The test results obtained in this research show that the stabilised subgrade soils undergo permanent deformation, especially after aging and weathering conditions, as shown in Figures 7.7 and 7.8.

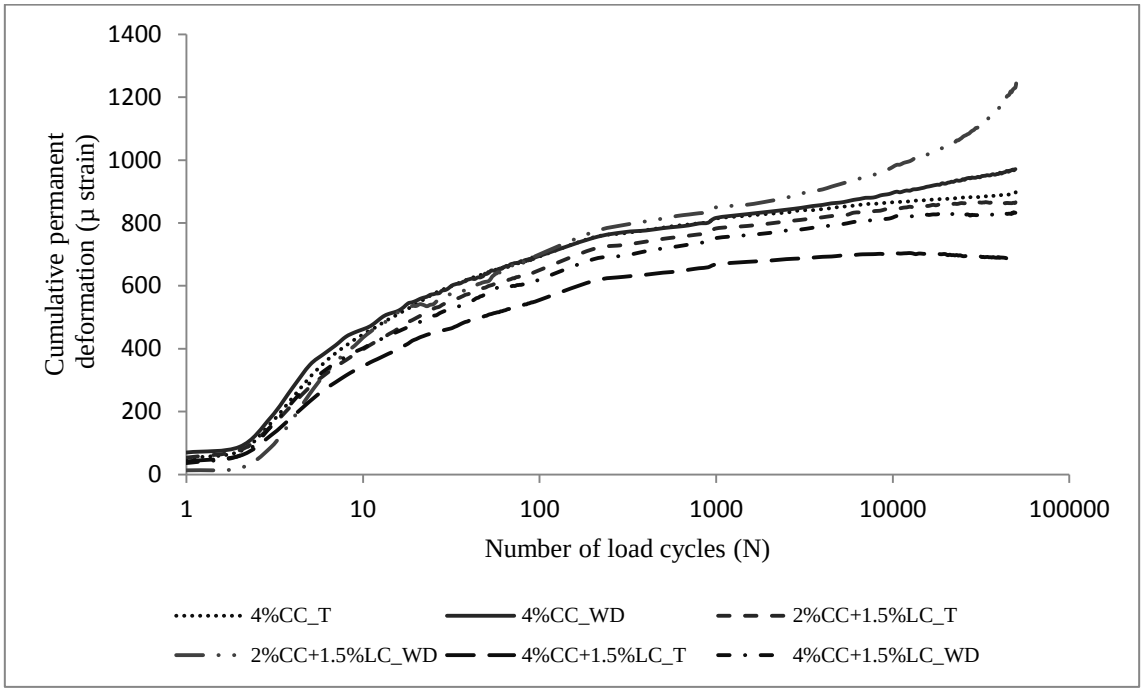

Figure 7. 7 Comparison of permanent deformation of stabilised, and stabilised after cycles of wetting and drying, for soil A-6

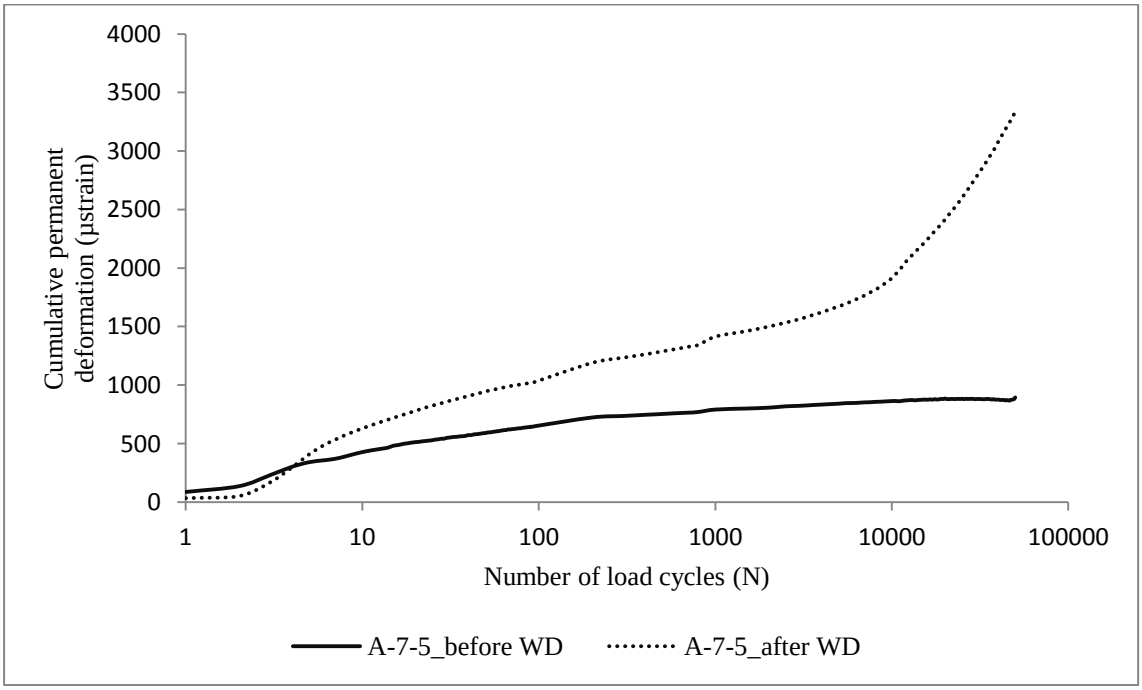

Figure 7. 8 Comparison of permanent deformation of stabilised, and stabilised after cycles of wetting and drying, for soil A-7-5

7.10 Design Examples

This section presents the design of road pavement sections using the developed analytical procedure. Three examples of using the equations and concepts developed and suggested in this research are presented. The first example presents the concept of deterioration progression in resilient modulus value of stabilised subgrade soils and the suitability of the performance model (Equation 5.8) developed in this research. The second example demonstrates the use of the correlation equations and the durability prediction equation (Equations 4.9, 4.11 and 4.12). The third example, which can be found in Appendix F, presents the use of this procedure in more detail.

Example 1:

Figure 7.9 shows a road pavement section consisting of a 100 mm asphalt concrete surface, a 200 mm granular base and a 200 mm stabilised subgrade layer over an infinite natural subgrade far away from the bedrock, see Tables 7.2 and 7.3.

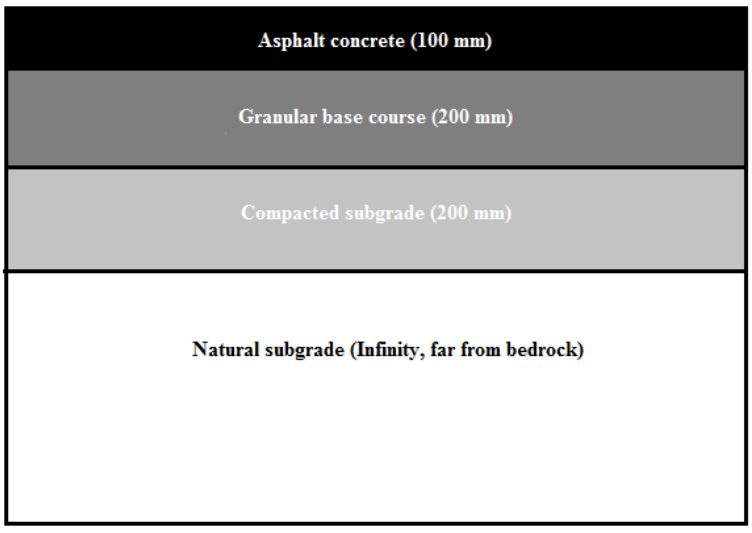

Figure 7. 9 Road pavement section configuration for analysis

Table 7. 2 Pavement section design parameters for example 1

Pavement section			
Layer type	Thickness (mm)	Resilient modulus (MPa)	Poisson's Ratio
Asphalt concrete	100	2500	0.3
Base course	200	300	0.35
Compacted subgrade	200	Variable	0.35
Natural subgrade	-	Variable	0.45
Traffic Data			
Traffic load for the base year	300000 Heavy Trucks		
Tyre pressure	550 kPa		
Loading radius area	152 mm		
Truck growth factor	4%		

The performance criterion for subgrade rutting was set to be 2 mm in 25 years. This is a portion of the rutting that occurs at the surface of the pavement section, since each layer of the pavement section contributes to the total rutting. The pavement section designed in this chapter assumes to have asphalt concrete and base course layers to behave elastically, as the data of these two materials is not available for nonlinearity consideration. In addition the focus of this research is on the subgrade layer.

Table 7. 3 Resilient modulus of the three soils unstabilised, and stabilised and after W/D with 2%CC

Deviatoric Stress (kPa)	A-4 Unstabilised Mr (MPa)	A-4 Stabilised/WD 2%CC Mr (MPa)		A-6 Unstabilised Mr (MPa)	A-6 Stabilised/WD 2%CC Mr (MPa)		A-7-5 Unstabilised Mr (MPa)	A-7-5 Stabilised/WD 2%CC Mr (MPa)	
12.4	99	127	68	85	133	118	70	72	29
24.8	132	156	78	100	153	123	72	85	34
37.3	146	182	89	102	168	133	68	96	40
49.7	157	203	99	101	182	141	62	107	47
62.0	165	222	110	100	196	150	57	117	54
120.0	187	282	160	100	248	198	46	155	87

Design

Assume a starting resilient modulus value for compacted and natural subgrade layers from the AASHTO T307 resilient modulus test results that consist of 15 stress combinations. In this example an initial seed resilient modulus of 30 MPa was used for both layers.

The number of soils in this analysis is three with 2% cement content for stabilisation.

Vertical stress is used in the performance model; see the note in Appendix D, in which the inclusion of horizontal and vertical geostatic stresses in the analysis procedure, is presented. The next step is to plot a graph of the resilient modulus against deviatoric stress (Figure 7.10). This graph is plotted from multistage permanent deformation tests for which the last four cycles were averaged to obtain the resilient modulus. Where only AASHTO T307 results are available, in which the resilient modulus values of subgrade layer are ranging from 12.4 kPa to 62.0 kPa, the graph may need an extrapolation, or a single-stage permanent deformation test is run for the highest stress level expected, for example 120.0 kPa. However, if a multi-stage permanent deformation test equipment and also the necessary testing time are available, the deviatoric stress levels can be set according to the expected stress levels. In this example the resilient modulus values of up to 62.0 kPa of deviatoric stress are from the AASHTO T307 test and the results of a single-stage permanent deformation test with 120.0 kPa deviatoric stress at 10000 cycles was used.

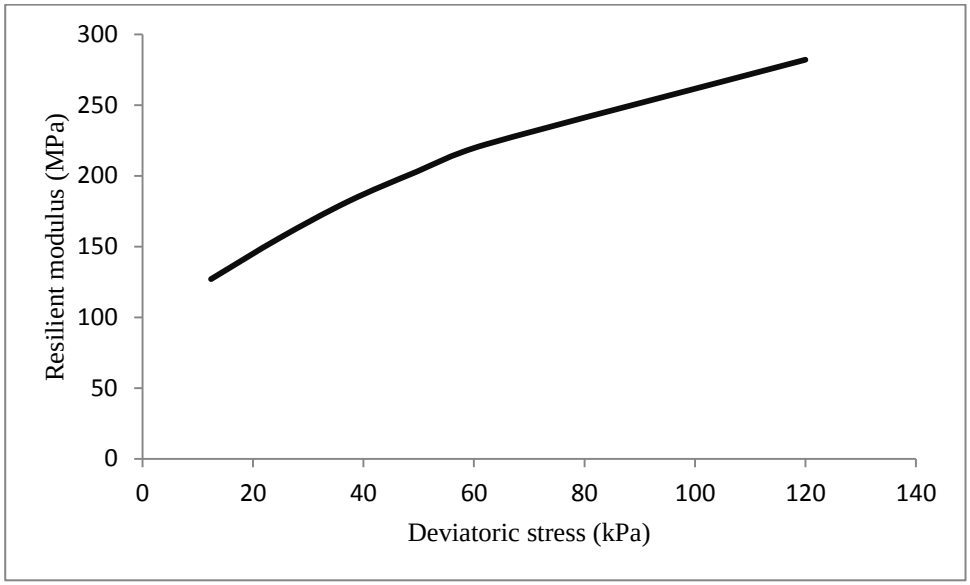

Figure 7. 10 Resilient modulus versus deviatoric stress for soil A-4 at 2%CC

The above pavement section configuration and material properties were input into the finite element model developed in this research (see Chapter Six). While a number of methods can be used to represent the stress dependency of the resilient modulus as disussed in section 6.5 the method used for the example was the linear analysis, resilient modulus and deviatoric stress curve in an iterative procedure to find the converged vertical stress and the resilient modulus values at critical locations.

Table 7.4 shows the trials used to obtain the deviatoric stress and resilient modulus values at convergence. Figures 7.11 and 7.12 show the iterative analysis to obtain converged resilient modulus and deviatoric stress. The first analysis trial using the resilient modulus values of 30 MPa for stabilised and natural subgrade layers, gives a vertical stress of 29 kPa at the mid-depth of the third layer (stabilised subgrade layer) and 20 kPa at 6 cm below the top of the natural subgrade layer. These values were used in the curves in Figures 7.11 and 7.12, respectively to obtain new resilient modulus values of 164 MPa and 120 MPa, respectively.

For trial number 2 these values were utilised for the stabilised and natural subgrade layers in the finite elment model. The subsequent analysis resulted in stresses of 57 kPa and 34 kPa at the mid-depth and top of the subgrade layer respectively. This procedure was repeated until the difference between two succesive trials was negligible. This can be seen from trials 3 and 4 in Table 7.4 in which the vertical stresses are 62 to 63 and 36 to 37 kPa.

Table 7. 4 Iterative trials for deviatoric and resilient modulus converge

	Trial 1	Trial 2	Trial 3	Trial 4
Mr (MPa)CS*	30	164	210	220
Mr (MPa)NS**	30	120	142	148
Stress MDL3 (kPa)	29	57	62	63
Stress L4 (kPa)	20	34	36	37
Strain MDL3 (μ strain)	992	393	333	323
Strain L4 (μ strain)	607	278	248	241

*CS=compacted subgrade, **NS=natural subgrade

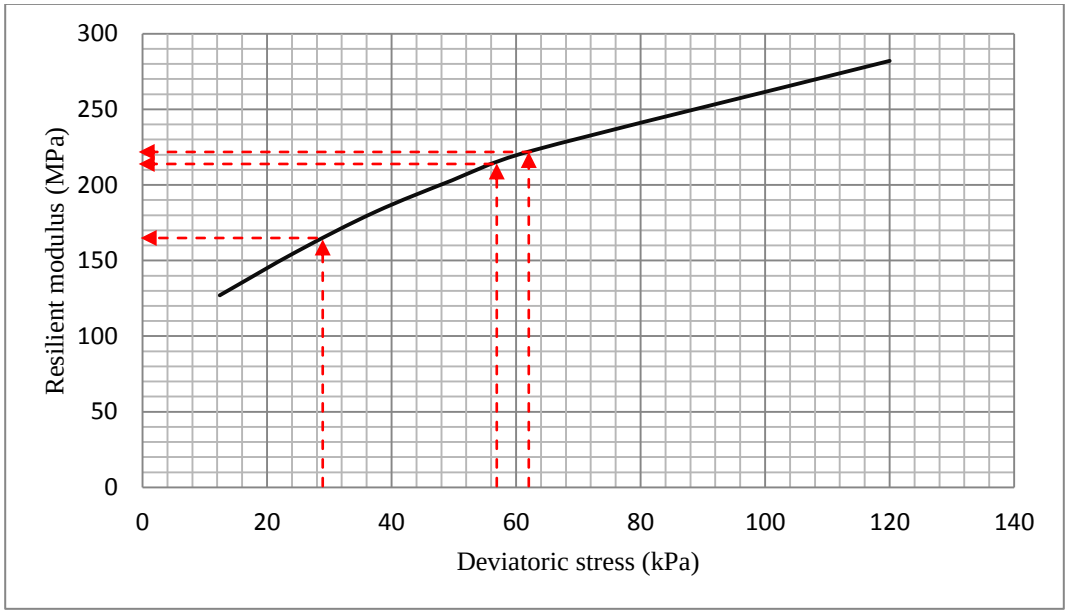

Figure 7. 11 Iterative trials on the deviatoric versus resilient modulus curve for unstabilised soil A-4 at 2%CC

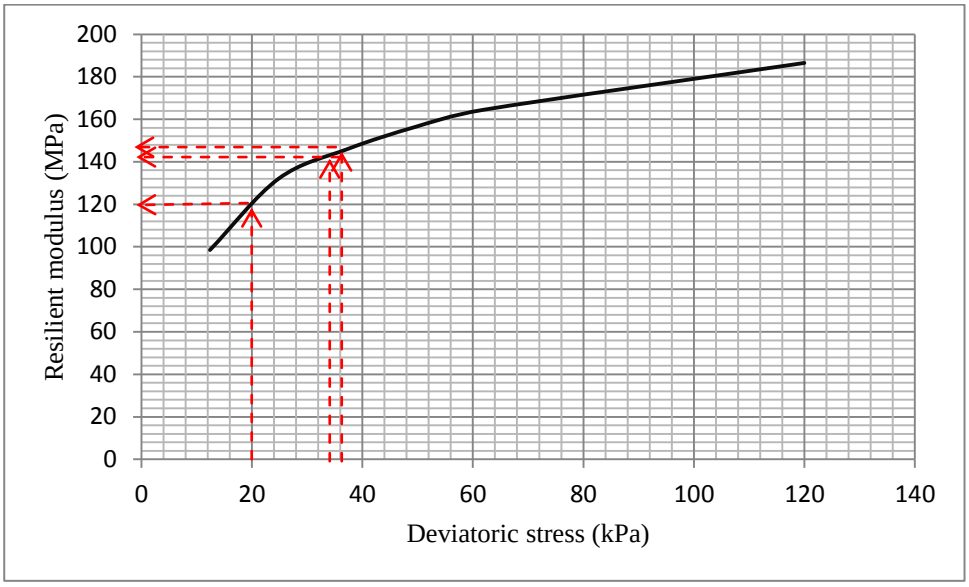

Figure 7. 12 Iterative trials on the deviatoric versus resilient modulus curve for unstabilised soil A-4

For the next stage the resilient modulus of the subgrade layer is changed over time. In this example the resilient modulus was changed every 5 years. According to the procedure described in section 7.2, see step 3 and the resilient modulus values in Table 7.3, a curve was plotted between deviatoric stress and resilient modulus values as in Figure 7.13, which depicts soil A-4 at 2%CC. In the next step the yearly deterioration factor (ADF) (Equation 7.1) was determined and the resilient modulus values for each stage were determined and tabulated in Table 7.5 (results of soil A-4 at 2%CC).

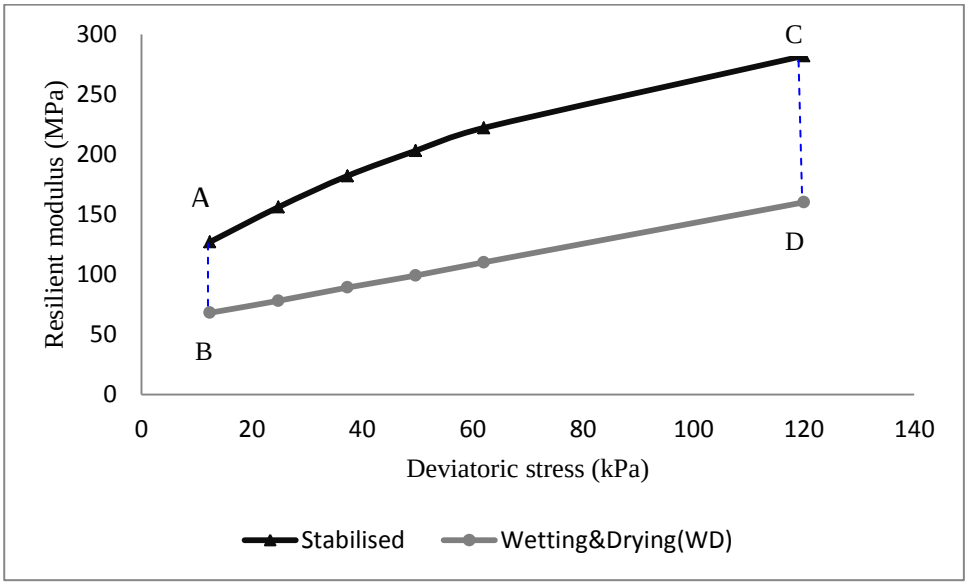

Figure 7. 13 Deviatoric to resilient modulus relationship for stabilised soil A-4 at 2%CC before and after wetting and drying cycles

Table 7. 5 Matrix of deviatoric stress and resilient modulus after stages of deterioration progression for soil A-4 at 2%CC

1	2	3	4	5	6	7	8	9
Deviatoric stress (kPa)	Mr Before W&D (MPa)	Mr After W&D (MPa)	YDF	Mr after 5 years (MPa)	Mr after 10 years (MPa)	Mr after 15 years (MPa)	Mr after 20 years (MPa)	Mr after 25 years (MPa)
12.4	127	68	2.360	115	103	92	80	68
24.8	156	78	3.120	140	125	109	94	78
37.3	182	89	3.720	163	145	126	108	89
49.7	203	99	4.160	182	161	141	120	99
62	222	110	4.480	200	177	155	132	110
120	282	160	4.880	258	233	209	184	160

- Finally from the results in Table 7.5, the deviatoric stresses to resilient modulus values were plotted and are shown in Figure 7.14 (for soil A-4 at 2%CC). This figure was then used in pavement analysis as described in the previous step (Table 7.4 and Figures 7.11 and 7.12) to achieve the requirements for steps 9 and 10 in the flowcharts shown in 7.1 and 7.2 in section 7.1 of this chapter, respectively.

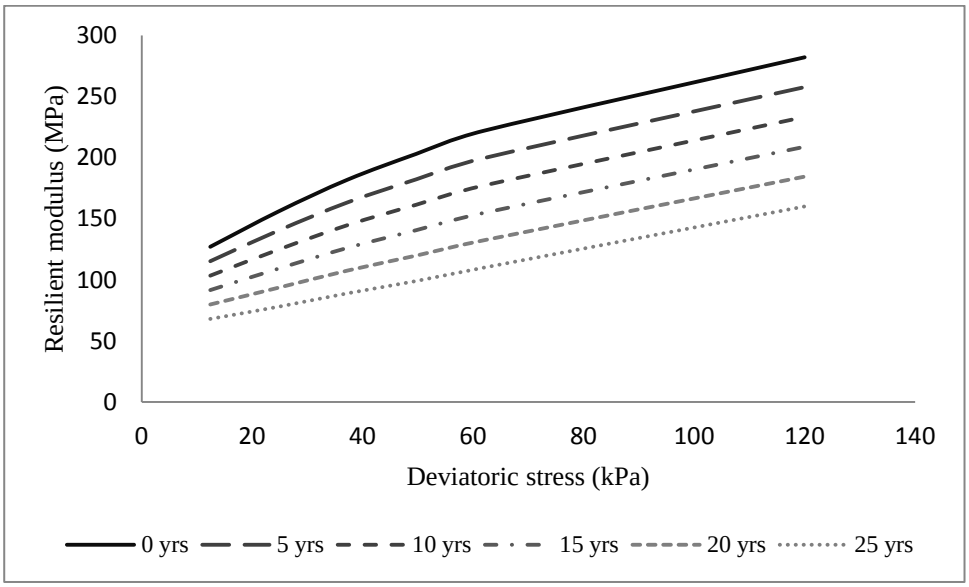

Figure 7. 14 Resilient modulus values at different stages of deterioration for soil A-4 at 2%CC

Table 7.6 shows the results of the analysis of the pavement section for soil A-4 at 2% cement content; using these values the permanent deformation can be predicted for each stage. The performance model (Equation 5.8) was used to determine the permanent deformation. For this purpose the permanent deformation test results were used to find the parameters of the model and are presented below:

$$\varepsilon_{1,p} = a * \left(\frac{\sigma_d}{M_r}\right) * N^b$$

$$\varepsilon_{1,p} = 1075.348 * \left(\frac{\sigma_d}{M_r}\right) * N^{0.042} \text{ (Soil A-4)}$$

$$\varepsilon_{1,p} = 1227.719 * \left(\frac{\sigma_d}{M_r}\right) * N^{0.047} \quad \text{(Soil A-6)}$$

$$\varepsilon_{1,p} = 2205.015 * \left(\frac{\sigma_d}{M_r}\right) * N^{0.038} \quad \text{(Soil A-7-5)}$$

Table 7. 6 The converged resilient modulus value and vertical stress for the five stages of resilient modulus deterioration

Stage 1		Stage 2		Stage 3		Stage 4		Stage 5	
Resilient Modulus (MPa)	Vertical Stress (kPa)	Resilient Modulus (MPa)	Vertical Stress (kPa)	Resilient Modulus (MPa)	Vertical Stress (kPa)	Resilient Modulus (MPa)	Vertical Stress (kPa)	Resilient Modulus (MPa)	Vertical Stress (kPa)
220	63	200	62	180	62	152	61	130	60
148	37	149	37	149	37	149	37	149	37

The results from Table 7.6 are repeated in Table 7.7 with the addition of the calculation of the growth factors and the number of heavy vehicles for each stage of the analysis; these results for soils A-6 and A-7-5 at 2% cement content are presented in Tables 7.8 and 7.9. The tables also contain the calculation of the permanent strain of each stage and the summation of the permanent deformation is presented in the last row. The resilient strain values corresponding to each stage of the analysis are presented, from which the number of load repetitions to failure can be determined from performance equations such as Equations 7.9 to 7.14 in section 7.6 of this chapter. Furthermore the growth factor is calculated using Equation 7.3 and multiplied by the number of heavy vehicles for the base year. Then the number of heavy vehicles of each stage is calculated by subtracting the number of heavy vehicles from the previous stage (except the first stage) from the current number.

Table 7. 7 Results of the road pavement section analysis with soil A-4 stabilised at 2% cement content

A-4_2%CC	Stage 1	Stage 2	Stage 3	Stage 4	Stage 5
Resilient modulus MDL3 (Mpa)	220	200	180	159	130
Vertical stress MDL3 (kPa)	63	62	62	61	60
Resilient modulus L4 (Mpa)	148	149	149	149	149
Vertical stress L4 (kPa)	37	37	37	37	37
Resilient strain MDL3 (μ strain)	323	346	373	421	470
Resilient strain L4 (μ strain)	241	241	241	241	240
Growth rate (%)	4	4	4	4	4
Years of the stage (years)	5	10	15	20	25
Number of heavy trucks of the base year	300000	300000	300000	300000	300000
Growth factor	5.4163226	12.006107	20.023588	29.778079	41.645908
Number of heavy trucks	53421.189	64995.045	79076.41	96208.544	117052.4
Parameter *(a)*	1075.348	1075.348	1075.348	1075.348	1075.348
Parameter *(b)*	0.042	0.042	0.042	0.042	0.042
Permanent strain MDL3 (μ strain)	486.44178	530.94764	594.82086	668.00039	810.2684
Permanent strain MDL3 (mm)	0.0972884	0.1061895	0.1189642	0.1336001	0.1620537
Total permanent deformation (mm)	0.62				

Table 7. 8 Results of the road pavement section analysis with soil A-6 stabilised at 2% cement content

A-6_2%CC	Stage 1	Stage 2	Stage 3	Stage 4	Stage 5
Resilient modulus MDL3 (Mpa)	190	180	170	160	152
Vertical stress MDL3 (kPa)	55	55	55	55	55
Resilient modulus L4 (Mpa)	102	102	102	102	102
Vertical stress L4 (kPa)	32	32	32	32	32
Resilient strain MDL3 (μ strain)	352	365	380	396	411
Resilient strain L4 (μ strain)	305	307	308	308	309
Growth rate (%)	4	4	4	4	4
Years of the stage (years)	5	10	15	20	25
Number of heavy trucks of the base year	300000	300000	300000	300000	300000
Growth factor	5.4163226	12.006107	20.023588	29.778079	41.645908
Number of heavy trucks	53421.189	64995.045	79076.41	96208.544	117052.4
Parameter *(a)*	1227.719	1227.719	1227.719	1227.719	1227.719
Parameter *(b)*	0.047	0.047	0.047	0.047	0.047
Permanent strain MDL3 (μ strain)	592.80329	631.5308	674.87129	723.69026	768.83289
Permanent strain MDL3 (mm)	0.1185607	0.1263062	0.1349743	0.1447381	0.1537666
Total permanent deformation (mm)	0.68				

Table 7. 9 Results of the road pavement section analysis with soil A-7-5 stabilised at 2% cement content

A-7-5_2%CC	Stage 1	Stage 2	Stage 3	Stage 4	Stage 5
Resilient modulus MDL3 (Mpa)	104	90	82	64	52
Vertical stress MDL3 (kPa)	46	45	45	43	42
Resilient modulus L4 (Mpa)	71	71	71	71	71
Vertical stress L4 (kPa)	28	28	28	28	28
Resilient strain MDL3 (μ strain)	516	565	599	698	793
Resilient strain L4 (μ strain)	388	387	386	378	368
Growth rate (%)	4	4	4	4	4
Years of the stage (years)	5	10	15	20	25
Number of heavy trucks of the base year	300000	300000	300000	300000	300000
Growth factor	5.4163226	12.006107	20.023588	29.778079	41.645908
Number of heavy trucks	53421.189	64995.045	79076.41	96208.544	117052.4
Parameter *(a)*	2205.015	2205.015	2205.015	2205.015	2205.015
Parameter *(b)*	0.038	0.038	0.038	0.038	0.038
Permanent strain MDL3 (μ strain)	1474.9903	1679.8519	1857.5307	2291.1955	2774.955
Permanent strain MDL3 (mm)	0.2949981	0.3359704	0.3715061	0.4582391	0.554991
Total permanent deformation (mm)	2.02				

Conclusions from Example 1:

The progress of the deterioration of stabilised subgrade soils was considered in this example from which the gradual deterioration of the stabilised subgrade material was calculated and used in the performance model.

From the analysis of the trial pavement section for the three soils stabilised with 2% cement content, it is clear that the stabilisation with this ratio of cement content is suitable for soils A-4 and A-6 with values of 0.62 mm and 0.68 mm, which is less than the criterion set at the beginning of the design. However, the permanent deformation for a design life of 25 years for soil A-7-5 stabilised with 2% cement content is not satisfactory. Therefore a different scenario of stabilisation should be tried, for example 2% cement plus 1.5% lime content.

The pavement section trial is found to be suitable with some necessary further stabilisation scenarios' examination. However, this analysis was carried out for a single axle load with a tyre pressure of 550 kPa. For other expected tyre pressures further analysis required. For this purpose the analysis may consist of different analysis increments, the summation of all these increments would be the final predicted rut depth in the stabilised subgrade layer.

Example 2

A pavement section was assumed with the dimensions and properties shown in Table 7.10. This example was taken to illustrate the use of the correlation equations developed in (sections 4.4 and 5.4.1) the performance model (Chapter Five) and the overall design procedure developed in this research.

Table 7. 10 Road pavement section dimensions, traffic data and material properties

Soil properties			
Soil type	Stabilisation ratio and type	UCS* (kPa)	UCS** (kPa)
A-7-5	2% CC	275.0	?
	4% CC	357.0	?
	2% CC + 1.5% LC	427.0	?
	4% CC + 1.5% LC	501.0	350.0
Pavement section			
Layer type	Thickness (mm)	Resilient modulus (MPa)	Poisson's Ratio
Asphalt concrete	100	2500	0.3
Base course	150	300	0.35
Compacted subgrade	150	Variable	0.35
Natural subgrade	-	47	0.45
Traffic Data			
Traffic load for the base year	300000 Heavy Trucks		
Tyre pressure	860 kPa		
Loading radius area	152 mm		
Truck growth factor	4%		

*****Stabilised soil before the durability test

** Stabilised soils after the durability test

Design

Step 1:

From Equation 4.11 the resilient modulus values for the following deviatoric stresses were determined. Table 7.11 shows the results of resilient modulus values from Equation 4.11in page 138 using the given values of UCS in the example in Table 7.10. See section 4.6 for the value of the equation parameters.

$$M_r = UCS^{0.737+0.001*\sigma_d}$$

Table 7. 11 Resilient modulus values for a range of deviatoric stresses from UCS test results

Deviatoric Stress (kPa)	4%CC+ 1.5%LC		4%CC+ 1.5%LC W&D		2%CC+ 1.5%LC		4%CC		2%CC	
	UCS (kPa)	Mr (MPa)	UCS (kPa)	Mr (MPa)	UCS (kPa)	Mr (MPa)	UCS (kPa)	Mr (MPa)	UCS (kPa)	Mr (MPa)
12.4	501	106	350	81	427	94	357	82	275	67
24.8		114		87		101		88		72
37.3		123		93		109		95		77
49.7		133		100		117		102		83
62.0		144		108		126		110		89
120.0		206		151		180		154		123
160.0		264		191		229		195		154
200.0		339		242		292		247		193

Step 2:

From Equation (4.9) the deteriorated (WD) resilient modulus values for different scenarios stabilised with 2%CC+1.5%LC, 4%CC and 2%CC were determined and tabulated in Table 7.12.

Table 7. 12 Deteriorated resilient modulus values for three stabiliser contents from Equation 4.8

Deviatoric Stress (kPa)	4%CC+ 1.5%LC	4%CC+ 1.5%LC W&D	2%CC+ 1.5%LC	2%CC+ 1.5%LC W&D	4%CC	4%CC WD	2%CC	2%CC WD
	Mr (MPa)	Mr (MPa)	Mr (MPa)	Mr (MPa)	Mr (MPa)	Mr (MPa)	Mr (MPa)	Mr (MPa)
12.4	106	81	94	63	82	49	67	33
24.8	114	87	101	68	88	52	72	35
37.3	123	93	109	73	95	55	77	37
49.7	133	100	117	78	102	59	83	39
62.0	144	108	126	84	110	63	89	41
120.0	206	151	180	115	154	85	123	54
160.0	264	191	229	144	195	104	154	65
200.0	339	242	292	179	247	128	193	79

Step 3:

From the resilient modulus values obtained for different stabiliser ratios and corresponding deteriorated resilient modulus values, a series of graphs were plotted between deviatoric stress and resilient modulus. See Figures 7.15-7.18.

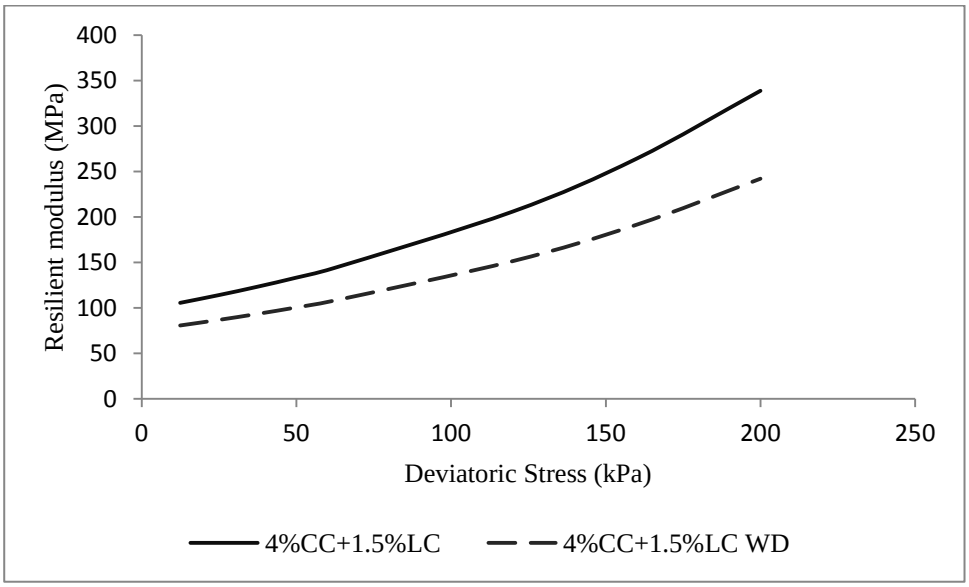

Figure 7. 15 Deviatoric to resilient modulus value relationship for stabilised soil before and after durability test at 4%CC+1.5%LC

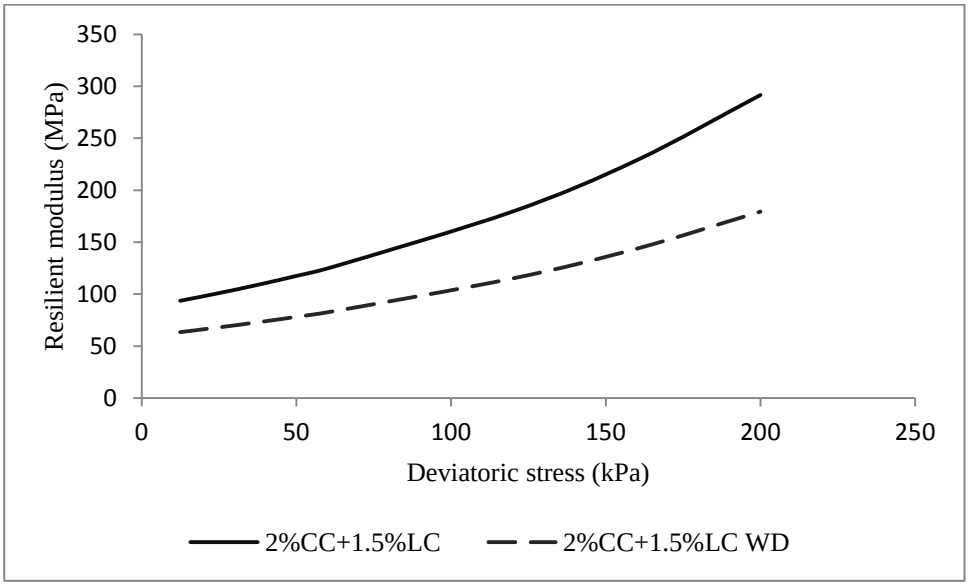

Figure 7. 16 Deviatoric to resilient modulus value relationship for stabilised soil before and after durability test at 2%CC+1.5%LC

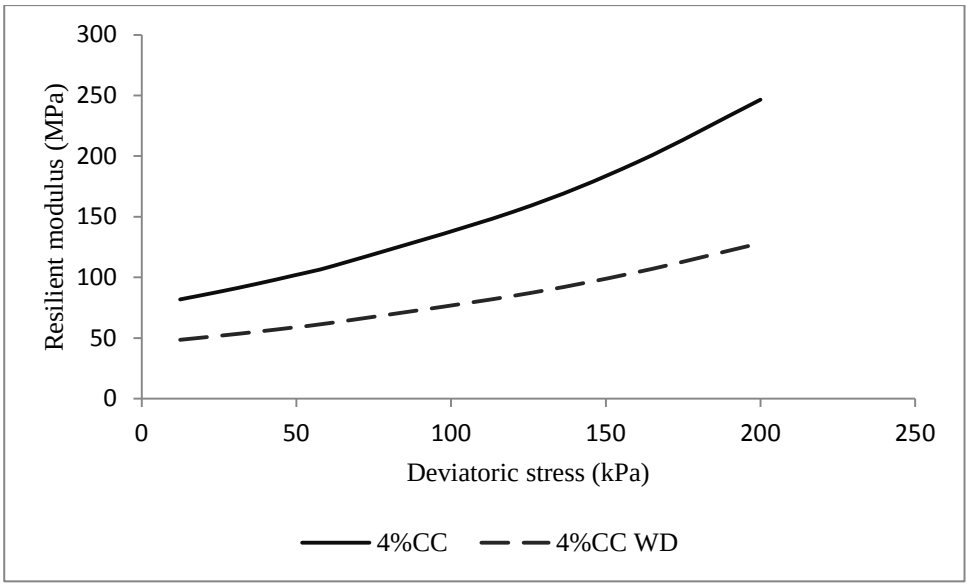

Figure 7. 17 Deviatoric to resilient modulus value relationship for stabilised soil before and after durability test at 4%CC

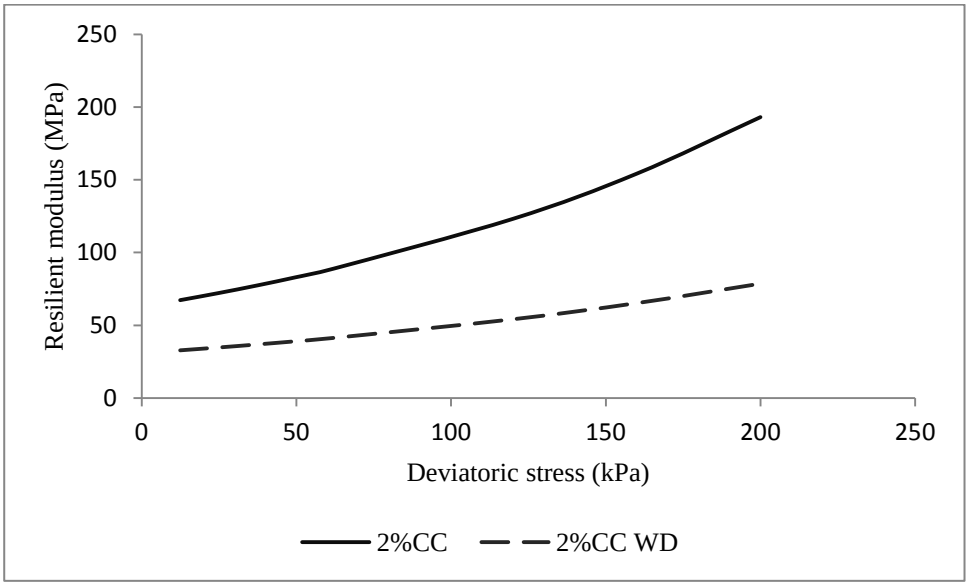

Figure 7. 18 Deviatoric to resilient modulus value relationship for stabilised soil before and after durability test at 2%CC

To account for the deterioration of resilient modulus the design life was divided into five stages (increments), each of five years (in this example). Then the deteriorated resilient modulus for each year was calculated. Next the Annual Deterioration Factor (ADF) was determined.

The resulting deteriorated resilient modulus values for these four stabilisation scenarios at five different stages are tabulated in Tables 7.13 to 7.16.

Table 7. 13 Deteriorated resilient modulus for five stages for soil A-7-5 stabilised with 2%CC

1	2	3	4	5	6	7	8	9
Deviatoric Stress (kPa)	Mr Before W&D (MPa)	Mr After W&D (MPa)	YDF	Mr after 5 years (MPa)	Mr after 10 years (MPa)	Mr after 15 years (MPa)	Mr after 20 years (MPa)	Mr after 25 years (MPa)
12.4	67	33	1.38	60	54	47	40	33
24.8	72	35	1.50	65	57	50	42	35
37.3	77	37	1.62	69	61	53	45	37
49.7	83	39	1.76	74	65	57	48	39
62	89	41	1.90	79	70	60	51	41
120	123	54	2.76	109	96	82	68	54
160	154	65	3.56	136	119	101	83	65
200	193	79	4.58	170	147	124	102	79

Table 7. 14 Deteriorated resilient modulus for five stages for soil A-7-5 stabilised with 4%CC

1	2	3	4	5	6	7	8	9
Deviatoric Stress (kPa)	Mr Before W&D (MPa)	Mr After W&D (MPa)	YDF	Mr after 5 years (MPa)	Mr after 10 years (MPa)	Mr after 15 years (MPa)	Mr after 20 years (MPa)	Mr after 25 years (MPa)
12.4	82	49	1.33	75	69	62	55	49
24.8	88	52	1.45	81	74	66	59	52
37.3	95	55	1.58	87	79	71	63	55
49.7	102	59	1.72	93	85	76	67	59
62	110	63	1.87	100	91	81	72	63
120	154	85	2.77	140	126	112	99	85
160	195	104	3.63	177	159	140	122	104
200	247	128	4.73	223	199	176	152	128

Table 7. 15 Deteriorated resilient modulus for five stages for soil A-7-5 stabilised with 2%CC+1.5%LC

1	2	3	4	5	6	7	8	9
Deviatoric Stress (kPa)	Mr Before W&D (MPa)	Mr After W&D (MPa)	YDF	Mr after 5 years (MPa)	Mr after 10 years (MPa)	Mr after 15 years (MPa)	Mr after 20 years (MPa)	Mr after 25 years (MPa)
12.4	94	63	1.21	88	82	76	69	63
24.8	101	68	1.32	94	88	81	75	68
37.3	109	73	1.44	102	94	87	80	73
49.7	117	78	1.57	109	102	94	86	78
62	126	84	1.71	118	109	101	92	84
120	180	115	2.58	167	154	141	128	115
160	229	144	3.40	212	195	178	161	144
200	292	179	4.49	269	247	224	202	179

Table 7. 16 Deteriorated resilient modulus for five stages for soil A-7-5 stabilised with 4%CC+1.5%LC

1	2	3	4	5	6	7	8	9
Deviatoric Stress (kPa)	Mr Before W&D (MPa)	Mr After W&D (MPa)	YDF	Mr after 5 years (MPa)	Mr after 10 years (MPa)	Mr after 15 years (MPa)	Mr after 20 years (MPa)	Mr after 25 years (MPa)
12.4	106	81	0.99	101	96	91	86	81
24.8	114	87	1.09	109	103	98	92	87
37.3	123	93	1.19	117	111	105	99	93
49.7	133	100	1.31	126	120	113	107	100
62	144	108	1.43	136	129	122	115	108
120	206	151	2.18	195	184	173	162	151
160	264	191	2.91	250	235	220	206	191
200	339	242	3.87	319	300	281	261	242

Step 4:

In this step the pavement section was analysed with the data given in this example. Any resilient modulus value can be used to commence the iteration between resilient modulus and deviatoric stress; however a resilient modulus value of 47.0 kPa was used for the first trial. From the first trial, the deviatoric stress was found to be 75.0 kPa and then from the curve, resilient modulus corresponding to this stress was found to be 98.0 MPa, see Figure 7.19. This new resilient modulus was used within the FEM and a deviatoric stress of 81.0 kPa was obtained. This value was then used to obtain a resilient modulus of 102.0 MPa. Finally the use of a resilient modulus of 102.0 MPa in the FEM resulted in a deviatoric stress of 82.0 kPa. The resilient modulus matching this stress was 103.0 MPa. In this way the stress dependency of the stabilised soil was introduced to the analysis. In Figure 7.19 two iterations are presented for stabilised soil with 2%CC. This procedure was repeated for the five increments of soil stabilised with 2%CC and then for the four stabilisation ratios of soil A-7-5. The incremental calculation of deterioration was then followed to determine the permanent deformation for a design life of 25 years.

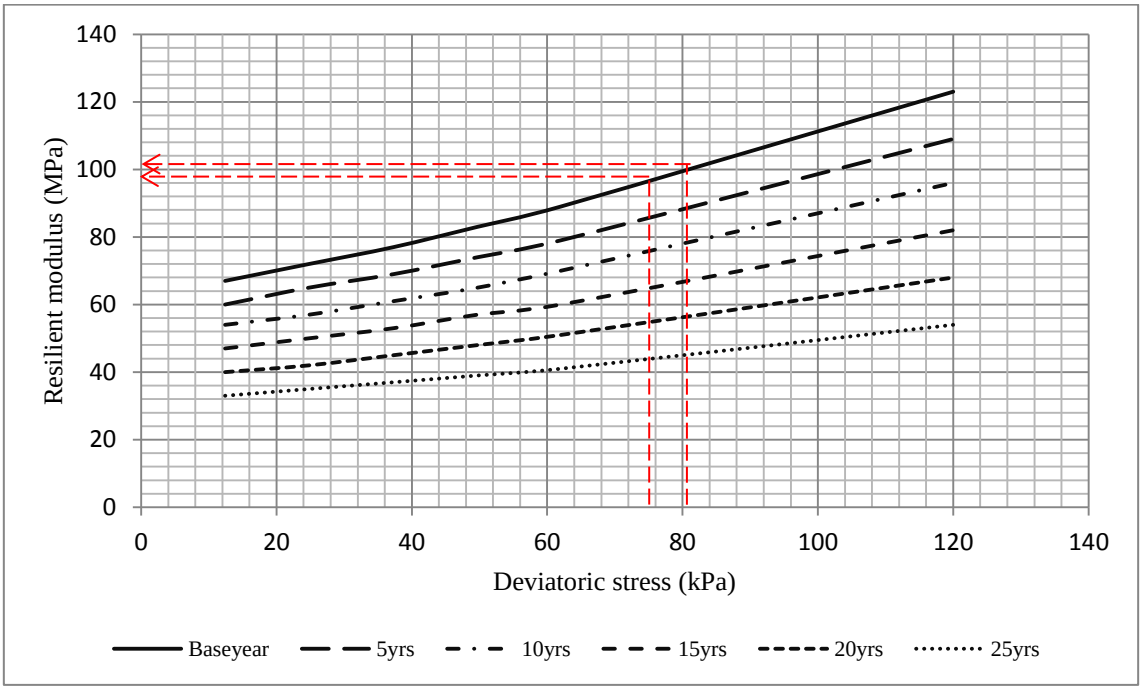

Figure 7. 19 Iteration analysis of resilient modulus and deviatoric stress convergence for soil A-7-5 stabilised with 2%CC and for five stages of 5 years each

Step 5:

For the incremental permanent deformation, the performance model (Equation 5.8) was used. In equation 5.8 the parameters, a and b, were found from regression analysis. The parameters were found in a previous work on the same soil stabilised with 4%CC+1.5%LC, with a deviatoric stress and confining pressure of 62.0 kPa and 27.5 kPa, respectively (Rasul et al, 2015); these values were a = 2205.015 and b = 0.038.

For the calculation of the number of the heavy vehicles, Equation 7.3 was used.

Table 7.17 shows the results of the pavement section analysis for the four stabiliser ratios at five increments and the summation of permanent deformation at the mid-depth of the stabilised layer is presented at the end of each analysis for these four stabiliser contents.

Table 7. 17 Pavement section analysis for stabilised subgrade soil with four different stabiliser contents

A-7-5_2%CC	Increment (1)	Increment (2)	Increment (3)	Increment (4)	Increment (5)
Resilient modulus MDL3 (Mpa)	103	90	79	67	53
Tensile strain beneath L1 (μ strain)	-454	-461	-467	-474	-485
Vertical stress MDL3 (kPa)	82	81	80	79	77
Resilient strain MDL3 (μ strain)	1063	1150	1240	1364	1564
Vertical stress L4 (kPa) Top	59	60	60	60	60
Resilient strain L4 (μ strain) Top	1246	1249	1247	1237	1209
Growth rate (%)	4	4	4	4	4
Years of the stage (years)	5	10	15	20	25
Number of heavy trucks of the base year	300000	300000	300000	300000	300000
Growth factor	5.416	12.006	20.024	29.778	41.646
Number of heavy trucks	1,624,897	1,976,935	2,405,244	2,926,347	3,560,349
parameter *(a)*	2205.015	2205.015	2205.015	2205.015	2205.015
parameter *(b)*	0.038	0.038	0.038	0.038	0.038
Permanent strain MDL3 (μ strain)	3023	3443	3903	4578	5683
Permanent strain MDL3 (mm)	0.453	0.516	0.585	0.687	0.852
Total permanent deformation (mm)	3.09				
A-7-5_4%CC	(1)	(2)	(3)	(4)	(5)
Resilient modulus MDL3 (Mpa)	127	113	104	92	80
Tensile strain beneath L1 (μ strain)	-444	-450	-454	-460	-466
Vertical stress MDL3 (kPa)	83	82	82	81	80
Resilient strain MDL3 (μ strain)	939	1006	1056	1135	1231
Vertical stress L4 (kPa) Top	58	59	59	60	60
Resilient strain L4 (μ strain) Top	1230	1241	1246	1249	1248
Permanent strain MDL3 (μ strain)	2481	2776	3039	3418	3912
Permanent strain MDL3 (mm)	0.372	0.416	0.456	0.513	0.587
Total permanent deformation (mm)	2.34				
A-7-5_2%CC+1.5%LC	(1)	(2)	(3)	(4)	(5)
Resilient modulus MDL3 (Mpa)	148	135	124	114	104
Tensile strain beneath L1 (μ strain)	-437	-441	-445	-450	-454
Vertical stress MDL3 (kPa)	84	83	83	82	82
Resilient strain MDL3 (μ strain)	857	906	953	1001	1056
Vertical stress L4 (kPa) Top	57	58	58	59	59
Resilient strain L4 (μ strain) Top	1211	1223	1233	1240	1246
Permanent strain MDL3 (μ strain)	2155	2352	2580	2793	3084
Permanent strain MDL3 (mm)	0.323	0.353	0.387	0.419	0.463
Total permanent deformation (mm)	1.94				
A-7-5_4%CC+1.5%LC	(1)	(2)	(3)	(4)	(5)
Resilient modulus MDL3 (Mpa)	172	158	150	140	130
Tensile strain beneath L1 (μ strain)	-429	-433	-436	-439	-443
Vertical stress MDL3 (kPa)	85	84	84	84	83
Resilient strain MDL3 (μ strain)	783	824	850	886	926
Vertical stress L4 (kPa) Top	57	57	57	58	58
Resilient strain L4 (μ strain) Top	1186	1202	1209	1218	1227
Permanent strain MDL3 (μ strain)	1876	2034	2158	2330	2497
Permanent strain MDL3 (mm)	0.281	0.305	0.324	0.349	0.375
Total permanent deformation (mm)	1.63				

Conclusions from Example 2:

The example included all the equations developed in this research. The example also showed the advantage of these equations to achieve an analytical pavement design procedure for a stabilised subgrade layer. If it is assumed that the performance criterion for the stabilised subgrade layer is 2 mm for 25 years, thus the soil stabilisation in this example suggests using 2%CC+1.5%LC as a minimum requirement for a durable stabilised subgrade layer. However, for a more comprehensive stabilised subgrade design, different soils with different stabiliser types and contents can be examined. From these alternatives the more appropriate stabiliser content and type thus can be selected.

The example shows that from a simple stabilised subgrade material property, which is unconfined compressive strength (UCS), an analytical pavement design procedure can be followed. This simplifies the design of pavement sections with lightly stabilised subgrade soils.

7.11 Summary

This chapter presented the main steps involved in using the research findings presented in the thesis to undertake an analytical design for road pavements in Kurdistan. These steps are associated with: obtaining the design inputs, the use of a response model, pavement performance modelling and setting appropriate design criteria. The overall design approach is demonstrated using two examples which utilize simulated data representing conditions in Kurdistan to demonstrate the practical use of the developed approach. The importance of the permanent deformation tests before and after the durability tests for deterioration consideration of the material properties with environmental and loading conditions were demonstrated.

CHAPTER EIGHT

CONCLUSIONS AND RECOMMENDATIONS FOR FUTHER RESEARCH

The research described in this thesis has investigated the development of an analytical pavement design procedure for Kurdistan which considers stabilised subgrade soils.

The implementation of such an analytical pavement design procedure requires:

- Necessary data and tools.
- A numerical model of the pavement structure to determine the stresses and strains at any point within the model.
- Equations of material performance for predicting the distresses.

To this end, the key contribution of the research is associated the development of a rational design of asphalt road pavement with modified subgrade soils. The work accomplishments, findings and conclusions drawn from the research are presented in the following categories:

8.1 Accomplished Work

8.1.1 Durability Equation

A durability equation has been developed, from which the weathered resilient modulus values for a range of stabiliser ratios and types can be predicted. This equation does away with the need to carry out the required laboratory tests. The resilient modulus values can be calculated by knowing the weathered resilient modulus of a soil with one stabiliser content and type. See Section 4.5 of Chapter Four.

$$M_{rAWD} = M_{rBWD} * \left(\frac{M_{rA}}{M_{rB}}\right)^2$$

8.1.2 Correlation Equations

Two correlation equations were developed in this research for lightly stabilised subgrade soils. The importance of these two equations is that they accurately predict the resilient modulus value from unconfined compressive strength (UCS). Therefore, it is possible to implement an analytical pavement design procedure using only UCS test results as demonstrated in Chapter Seven. See Section 4.6 of Chapter Four.

$$M_r = UCS^{a+b*\sigma_d}$$

$$Mr = UCS^{[a*\left(\frac{\theta}{\sigma_{atm}}\right)^b*\left(\frac{\tau_{oct}}{\sigma_{atm}}\right)^c]}$$

8.1.3 Performance Equation

A model of material performance for unstabilised and lightly stabilised subgrade soils was developed to include a large number of the parameters that have an effect on permanent deformation. The model calculates the incremental accumulation of the permanent deformation for different stages of a pavement's design life, see Section 5.4.1.

$$\sum_{t=1}^{m} \varepsilon_p = a \times \left(\frac{\sigma_{dt}}{M_{rt}}\right) \times N_t^b$$

$\sum_{1}^{m} t$ = T

8.1.4 Deterioration Progression of Resilient Modulus Value

A method was developed to include deteriorated resilient modulus value of a stabilised subgrade layer in the analytical pavement design procedure. To this end, the resilient modulus and permanent deformation of stabilised subgrade soils are determined before and after the durability tests. Section 7.2 of Chapter Seven explains the method in detail and it is clearly demonstrated in the design examples of Chapter Seven.

8.1.5 Nonlinearity of Stabilised and Unstabilised Subgrade Soils

The use within a numerical model of the pavement structure of resilient modulus values which are a function of the stress state was found from the literature to be an important consideration for analytical pavement design procedures for unbound materials. To account for this stress dependency of the resilient modulus values a novel procedure was developed. In the suggested procedure, by carrying out one multi-stage permanent deformation test, the resilient modulus values at the end of each stage are determined and a graph relating the deviatoric stress and resilient modulus is plotted. The procedure was consisted of selection a seed resilient modulus value and utilising this within FEM to determine the relevant deviatoric stress. This deviatoric stress is then used, via the graph, to obtain a new corresponding resilient modulus value. The resilient modulus value is utilised within the FEM to obtain a new deviatoric stress. This procedure is continued until the resilient moduli between two iterations converge. These values are later used in the performance model to determine the incremental accumulation of permanent deformation. See Section 4.4 of Chapter Four and the design examples in Chapter Seven.

8.2 Findings

8.2.1 Experimental Work

The mould fabricated in this research was found to be very compatible with the static compaction presented in ASSHTO T307 ANNEX C. Especially for obtaining an even and uniform sample surface that may be difficult to obtain with dynamic compaction in split moulds. In permanent deformation tests it is important to have an even surface of the sample.

In simulating soils, to guarantee homogenous and repeatable samples, the soils need to be separated into individual and different particle size ranges and remixed according to the required particle size distribution of a specified soil type for testing. Regarding the selection

of the deviatoric stress level an unconsolidated undrained triaxial (UU) test was found to be useful in deciding the threshold stress of different soil types. In this research a standard testing procedure was attempted to determine the modulus of elasticity of stabilised subgrade soils, the procedure of testing hardened concrete in BS EN 12390-13: 2013 method B for determining the secant modulus of elasticity in compression was found to be suitable for this purpose and it can be used in fatigue cracking distress equations.

8.2.2 Resilient Modulus

The effect of the moisture change on mechanical behaviour such as resilient modulus is a complex mechanism. However, from test results and the literature it was demonstrated that an increase in the degree of saturation results in a decrease in the resilient modulus value. Therefore, the equations that relate the change in degree of saturation to the change in resilient modulus can be used for determining the resilient modulus value at different seasons. The number of load repetitions found to affect the resilient modulus value; the resilient modulus values of stabilised and unstabilised soils obtained after a high number of cycles of permanent deformation test were higher than those obtained with a lower number of cycles.

The general trend regarding resilient modulus of unbound materials is that the resilient modulus of coarse grained soils increases with an increase in deviatoric stress, while for fine-grained soils the trend is the reverse. The clay content may have a dominant role in this trend; while soil A-4 in this research is a fine-grained soil it showed a different trend where any increase in deviatoric stress resulted in an increase in the resilient modulus value. The soil had a clay content of 16% and 84% of silt and sand.

It was also found that there is an inter-relation between stress level and moisture content regarding the resilient modulus value, in such a way that a change in moisture content changes the stress dependency of these soils in their stress levels. For example, soil A-4

exhibits an increase in the resilient modulus value with an increase in deviatoric stress at moisture contents lower than the optimum. However, the soil showed a decrease in resilient modulus with an increase in deviatoric stress at moisture contents higher than optimum moisture content.

8.2.3 Permanent Deformation

Soils with higher resilient modulus values do not necessarily show a higher resistance to the permanent deformation. Rather, permanent deformation was found to be dependent on the soil type, moisture content and stress level. For example, consider soil A-4, which has a higher proportion of sand and silt than soil A-7-5 and had higher resilient modulus values than soil A-7-5; However soil A-4 undergoes higher permanent deformations than soil A-7-5 at a stress level of 62.0 kPa, but exhibits lower permanent deformation at a stress level of 120.0 kPa.

Regarding the stabilised soils, stabilisation with cement and lime has improved the resilient modulus and permanent deformation properties of subgrade soils significantly. It is also found that measuring permanent deformation at different moisture and stress level conditions, especially in weathered environments can be simulated by a wetting and drying test or any other durability test that reflects the influence of environmental conditions, such as a freeze and thaw test.

8.2.4 Subgrade Soil Type

The improvement of different types of soils unifies the response trend (increase or decrease of resilient modulus value with increase in deviatoric stress) of stabilised subgrade soils to the applied load. For example, the increase in deviatoric stress results in an increase in resilient modulus values for all soil types and conditions; while for unstabilised soils, the trend varies among different soil types.

8.2.5 Response Model

Fine-grained subgrade soils in this research show varied trends regarding nonlinearity in response to the applied loads. Therefore it was found appropriate to use the suggested procedure in this research for nonlinearity considerations of fine-grained subgrade soils. The procedure uses graphs plotted between deviatoric stress and resilient modulus values in an iterative analysis procedure to obtain nonlinear resilient modulus values. Currently the KENLAYER programme offers two different models: the k-θ model for coarse-grained soils and the bilinear model for fine-grained soils. The graphical procedure was also found suitable for nonlinearity of modified subgrade soils, since there is no material model in the ABAQUS finite element material library for stabilised soils. The Drucker-Prager model in the ABAQUS^{TM} material library can be used for nonlinearity considerations of silty sandy soils (such as soil A-4) in the finite element model (FEM).

8.3 Conclusions

8.3.1 Experimental Work

For the characterisation of stabilised and unstabilised subgrade soils, only permanent deformation tests (without need of resilient modulus tests) can be run, from which the required data and information on resilient modulus and permanent deformation can be obtained. However, if resilient modulus test is followed the conditioning of the sample for up to 20,000 cycles, as recommended by BS EN 13286-7: 2004, is more reliable than the resilient modulus obtained from AASHTO T307, in which the sample conditioning takes place from 500 to 1000 cycles.

An unconfined compressive strength (UCS) test can be used to determine the compression strength of stabilised and unstabilised soils. In addition to this, the test is used to find the

modulus of elasticity by applying two cycles of unloading and loading and then the straight line drawn through these two cycles is averaged.

8.3.2 Resilient Modulus

The effect of different stress states and stress history can be quantified using only one multi-stage permanent deformation test. The resilient modulus of the soil at a range of stress combinations can be determined correspondingly.

It is reasonable for practical purposes to use the models relating resilient modulus to the degree of saturation for unsaturated soils in predicting the changes in resilient modulus with changes in moisture content. Therefore, it can be said that the clay content affects the rate of change of the resilient modulus value differently depending on the degree of saturation.

8.3.3 Permanent Deformation

The permanent deformation tests after cycles of wetting and drying in this research contributed significantly to understanding the conditions of the stabilised subgrade soils exposed to weathering. It is from these tests that the correct stabiliser content can be selected for a robust subgrade design.

8.3.4 Subgrade Soil Type

It is important to assess the conditions of stabilised subgrade soils after wetting and drying in terms of the resilient modulus. The resilient modulus is an important property required to characterise the soils and its use in the pavement design procedure is fundamental.

8.3.5 Response Model

The finite element model developed in this research is suitable for different pavement section thicknesses and load configurations and also different material properties.

8.3.6 Performance Model

Equations of permanent deformation that consider the stress state in addition to the number of load repetitions are better able to predict permanent deformation. For example, if they have been calibrated for a specified stress combination of an identified load, they can be used for different load levels.

8.3.7 Durability Considerations

Stabilised soils can improve the performance of the subgrade layers of road pavements. However, in order to capture such improvements in performance within analytical pavement design procedures it is important for appropriate durability tests and the development of associated relationships to quantify likely in situ soil performance.

8.4 Recommendations for Further Research

In the case of applying different stabilisation methods to the subgrade, the proposed subgrade design procedure provides a robust methodology to achieve an appropriate performance based solution for the required pavement design life. It is particularly useful where the subgrade soil is susceptible to moisture and the ingress of water is not controllable. Therefore, the design procedure presented in this thesis for stabilised and unstabilised subgrade soils is recommended to be merged into an analytical pavement design procedure.

The following future research is recommended for each section of the subgrade design within an analytical pavement design procedure:

- The durability test used in this research was a wetting and drying test specified by ASTM D559. In order, to simulate other environmental conditions, such as freezing and thawing other durability tests need to be carried out. This test (ASTM D559) may

be regarded to model only a part of the environmental effect to which a soil may be subjected. It is therefore recommended that further research investigates the potential of modifying ASTM D559 to represent additional environmental effects.

- A wider range of deviatoric stresses and confining pressures than those utilised in the experimental procedure proposed herein are recommended to obtain the design curves associated with stress dependency of resilient modulus of stabilised and unstabilised soils. This will allow for a greater range of loads transmitted to the subgrade layers to be considered.
- A wider range of soil types are recommended to be used for calibration of the equations developed in this research.
- Performance models are a major part of the mechanistic-empirical pavement design procedures. Therefore, the research on the new models relating the progression of distresses such as rutting to the material properties and loading conditions remain of great importance.

References

ABU-FARSAKH, M., DHAKAL, S. & CHEN, Q. 2014. Performance Evaluation of Cement Treated/Stabilized Very Weak Subgrade Soils. *Geo-Congress 2014 Technical Papers@ sGeo-characterization and Modeling for Sustainability.* ASCE.

ABUSHOGLIN, F. & KHOGALI, W. 2006. Resilient Modulus and Permanent Deformation Test for Unbound Materials. Institute for Research in Construction, National Research Council Canada.

AGARDH, S. 2005. *Rut Depth Prediction on Flexible Pavements-Calibration and Validation of Incremental-Recursive Models*, Lund University.

ARMY, T. 1994. TM 5-822-14 and Air Force AFJMAN 32-1019,". *Soil stabilization for pavements," Department of the Army, the Navy, and the Air force*.

ARNOLD, G. K. 2004. *Rutting of granular pavements.* PhD thesis, University of Nottingham;.

BARKSDALE, R. D. Laboratory evaluation of rutting in base course materials. Presented at the Third International Conference on the Structural Design of Asphalt Pavements, Grosvenor House, Park Lane, London, England, Sept. 11-15, 1972., 1972.

BELL, F. 1996. Lime stabilization of clay minerals and soils. *Engineering geology,* 42**,** 223-237.

BODHINAYAKE, B. C. 2008. A study on nonlinear behaviour of subgrades under cyclic loading for the development of a design chart for flexible pavements. *University of Wollongong Thesis Collection***,** 868.

BOWERS, B. F., DANIELS, J. L. & ANDERSON, J. B. 2013. Field considerations for calcium chloride modification of soil-cement. *Journal of Materials in Civil Engineering,* 26**,** 65-70.

BROWN, S., BRUNTON, J. & STOCK, A. THE ANALYTICAL DESIGN OF BITUMINOUS PAVEMENTS. ICE Proceedings, 1985. Thomas Telford, 1-31.

BROWN, S.F. & DAWSON, A.R., 1992. Two-stage mechanistic approach to asphalt pavement design. In *International Conference on Asphalt Pavements, 7th, 1992, Nottingham, United Kingdom* (Vol. 1).

BROWN, S.F., 1996. Soil mechanics in pavement engineering. Geotechnique,46(3), pp.383-426.

BROWN, S., PELL, P. & STOCK, A. The application of simplified, fundamental design procedures for flexible pavements. Volume I of proceedings of 4th International Conference on Structural Design of Asphalt Pavements, Ann Arbor, Michigan, August 22-26, 1977., 1977.

BROWN, S. F. Achievements and challenges in asphalt pavement engineering. Proc. of 8th Int. Conf. on Asphalt Pavements, Seattle, 1997.

BURMISTER, D. Theory of Stress and Displacement in Layered System and Applications to the Design of Airport. Proceedings of Annual Meeting of the Transportation Research Board, Highway Research Board, Washington, DC, 1943.

BURMISTER, D. M. 1945. The general theory of stresses and displacements in layered systems. I. *Journal of applied physics,* 16**,** 89-94.

CHANDRA, S., VILADKAR, M. & NAGRALE, P. P. 2008. Mechanistic approach for fiber-reinforced flexible pavements. *Journal of Transportation Engineering,* 134**,** 15-23.

CHAUHAN, M. S., MITTAL, S. & MOHANTY, B. 2008. Performance evaluation of silty sand subgrade reinforced with fly ash and fibre. *Geotextiles and Geomembranes,* 26**,** 429-435.

CHAZALLON, C., KOVAL, G., HORNYCH, P., ALLOU, F. & MOUHOUBI, S. 2009. Modelling of rutting of two flexible pavements with the shakedown theory and the finite element method. *Computers and Geotechnics,* 36**,** 798-809.

CHEN, D.-H. & LIN, H.-H. Development of an Equation to Predict Permanent Deformation. Accelerated Pavement Testing Conference, 1999.

CHEN, D.-H., ZAMAN, M., LAGUROS, J. & SOLTANI, A. 1995. Assessment of computer programs for analysis of flexible pavement structure. *Transportation Research Record***,** 123-133.

CHEN, J.-S., LIN, C.-H., STEIN, E. & HOTHAN, J. 2004. Development of a mechanistic-empirical model to characterize rutting in flexible pavements. *Journal of transportation engineering,* 130**,** 519-525.

CHITTOORI, B., PUPPALA, A. J., WEJRINGSIKUL, T., HOYOS, L. R. & LE, M. 2012. Numerical Modeling of the Impact of Deteriorating Treated Subgrade Modulus due to Seasonal Changes on Pavement Performance. *GeoCongress 2012: State of the Art and Practice in Geotechnical Engineering.*

CHITTOORI, B. C. S. 2008. *Clay mineralogy effects on long-term performance of chemically treated expansive clays.* PhD thesis, THE UNIVERSITY OF TEXAS AT ARLINGTON.

CHRISTOPHER, B., SCHWARTZ, C. & BOUDREAU, R. 2006. Geotechnical Aspects of Pavements FHWA NHI-05-037. *National Highway Institute, Federal Highway Administration, US Department of Transportation, Washington, DC*.

CLAESSEN, A., EDWARDS, J., SOMMER, P. & UGE, P. Asphalt Pavement Design--The Shell Method. Volume I of proceedings of 4th International Conference on Structural Design of Asphalt Pavements, Ann Arbor, Michigan, August 22-26, 1977, 1977.

DRUCKER, D. & PRAGER, W. 1952. Soil mechanics and plasticity analysis of limit design, Q. *Appl. Math*, 10.

DUNCAN, J. M. & CHANG, C.-Y. 1970. Nonlinear analysis of stress and strain in soils. *Journal of the soil mechanics and foundations division*, 96**,** 1629-1653.

ELLIOTT, R., DENNIS, N. & QIU, Y. 1998. Permanent deformation of subgrade soils (Phase I: A test protocol). USA: University of Arkansas.

FOSTER, C. & AHLVIN, R. Stresses and deflections induced by a uniform circular load. Highway Research Board Proceedings, 1954.

FROST, M. W., FLEMING, P. R. & ROGERS, C. D. 2004. Cyclic triaxial tests on clay subgrades for analytical pavement design. *Journal of transportation Engineering,* 130**,** 378-386.

FWA, T. F. 2006. *The handbook of highway engineering,* 6000 Broken Sound Parkway NW, Suite 300 Boca Raton, FL 33487-2742, Taylor & Francis Group, LLC.

GALLIPOLI, D., GENS, A., SHARMA, R. & VAUNAT, J. 2003. An elasto-plastic model for unsaturated soil incorporating the effects of suction and degree of saturation on mechanical behaviour. *Géotechnique.*, 53**,** 123-136.

GUPTA, S., RANAIVOSON, A., EDIL, T., BENSON, C. & SAWANGSURIYA, A. 2007. Pavement design using unsaturated soil technology USA: National Technical Information Services, Springfield, Virginia 22161.

HAN, D., HUANG, X.-M. & HU, H.-M. New Constitutive Model Implementation of the Geogrid Using UMAT. 11th International Conference of Chinese Transportation Professionals (ICCTP), 2011.

HARICHANDRAN, R., BALADI, G. & YEH, M. 1989. Development of a computer program for design of pavement systems consisting of bound and unbound materials. *Department of Civil and Environmental Engineering, Michigan State University*.

HELWANY, S., DYER, J. & LEIDY, J. 1998. Finite-element analyses of flexible pavements. *Journal of Transportation Engineering,* 124**,** 491-499.

HICKS, R. G. 2002. Alaska soil stabilization design guide. USA: Alaska DOT&PF Research and Technology Transfer Fairbanks, AK 99709-5399.

HIGHWAY, A. A. O. S. & OFFICIALS, T. 1993. *AASHTO Guide for Design of Pavement Structures, 1993,* AASHTO.

HJELMSTAD, K. & TACIROGLU, E. 2000. Analysis and implementation of resilient modulus models for granular solids. *Journal of Engineering Mechanics,* 126**,** 821-830.

HORNYCH, P., KERZRÉHO, J.-P. & SALASCA, S. 2002. Prediction of the behaviour of a flexible pavement using finite element analysis with non-linear elastic and viscoelastic models. *Proceedings of the Ninth International Conference on the Structural Design of Asphalt Pavements, Copenhagen, Denmark.*

HUANG, Y. H. 1993. *Pavement analysis and design,* 1st edition,USA, Pearson Education Inc.

HUANG, Y. H. 2004. *Pavement analysis and design,* 2nd edition,USA, Pearson Education Inc.

HYNDMAN, R.J. & KOEHLER, A.B. Another look at measures of forecast accuracy. *International journal of forecasting*, *22*(4), pp.679-688, 2006.

JAMESON, G. 2008. *Guide to pavement technology: part 2: pavement structural design,* Australia, Austroads Incorporated.

JANOO, V., IRWIN, L. & HAEHNEL, R. 2003. Pavement Subgrade Performance Study: Project Overview. US Army Corps of Engineers, DTIC Document, ERDC/ITL TR-03-5.

JONES, D., RAHIM, A., SAADEH, S. & HARVEY, J. T. 2010. Guidelines for the Stabilization of Subgrade Soils in California. USA: California Department of Transportation, Division of Research and Innovation, Office of Roadway Research, UCD-ITS-RR-10-38.

JOOSTE, F. & LONG, F. 2007. A knowledge based structural design method for pavements incorporating bituminous stabilized materials. Gauteng Department of Public Transport, Roads and Works and Southern Africa Bitumen Association (SABITA) Pinelands, South Africa.

KHEDR, S. 1985. *Deformation characteristics of granular base course in flexible pavements*.

KHOURY, N., MUSHARRAF, Z., NEVELS, J. & MANN, J. 2003. Effect of soil suction on resilient modulus of subgrade soil using the filter paper technique. *CD-ROM, Transportation Research Board, National Research Council, Washington, DC.*

KIM, D.-G. 2004. *Development of a constitutive model for resilient modulus of cohesive soils.* PhD thesis, The Ohio State University.

KIM, M. 2007. *Three-dimensional finite element analysis of flexible pavements considering nonlinear pavement foundation behavior.* PhD thesis, University of Illinois at Urbana-Champaign.

KNAPTON, J. The Romans and their roads-The original small element pavement technologists. 5th International Concrete Block Paving Conference, Tel-Aviv, Israel, 1996.

LASHINE, A. 1971. *Some aspects of the behaviour of Keuper Marl under repeated loading.* PhD, University of Nottingham.

LEKARP, F. & DAWSON, A. 1998. Modelling permanent deformation behaviour of unbound granular materials. *Construction and building materials,* 12**,** 9-18.

LEKARP, F., ISACSSON, U. & DAWSON, A. 2000a. Permanent strain response of unbound aggregates. *J. Transp. Engng.-ASCE,* 126**,** 66-83.

LEKARP, F., ISACSSON, U. & DAWSON, A. 2000b. State of the art. I: Resilient response of unbound aggregates. *Journal of transportation engineering,* 126**,** 66-75.

LEKARP, F., ISACSSON, U. & DAWSON, A. 2000c. State of the art. II: Permanent strain response of unbound aggregates. *Journal of transportation engineering,* 126**,** 76-83.

LENTZ, R. W. & BALADI, G. Y. 1981. Constitutive equation for permanent strain of sand subjected to cyclic loading. *Transportation Research Record***,** pp 50-54.

LI, D. & SELIG, E. T. 1996. Cumulative plastic deformation for fine-grained subgrade soils. *Journal of geotechnical engineering,* 122**,** 1006-1013.

LIANG, R. Y., RABAB'AH, S. & KHASAWNEH, M. 2008. Predicting moisture-dependent resilient modulus of cohesive soils using soil suction concept. *Journal of Transportation Engineering,* 134**,** 34-40.

LITTLE, D. & YUSUF, M. 2001. Example Problem Illustrating the Application of the National Lime Association Mixture Design and Testing Protocol (MDTP) to Ascertain Engineering Properties of Lime Treated Subgrades for Mechanistic Pavement Design/Analysis. The National Lime Association, Federal Highway Administration and the Mississippi Department of Transportation, FHWA/MS-DOT-RD-01-129.

LITTLE, D. N. 1987. Evaluation of structural properties of lime stabilized soils and aggregates. Available: https://lime.org/documents/publications/free_downloads/soils-aggregates-vol-3.pdf [Accessed 18 July 2012].

LITTLE, D. N. 1995. *Stabilization of pavement subgrades and base courses with lime*.

LITTLE, D. N. & NAIR, S. 2009. Recommended practice for stabilization of subgrade soils and base materials. Available: http://onlinepubs.trb.org/onlinepubs/nchrp/nchrp_w144.pdf [Accessed 18 July 2012].

LUO, Z., 2005. Flexible pavement condition model using cluster wise regression and mechanistic-empirical procedure for fatigue cracking modelling (Doctoral dissertation, University of Toledo).

LYTTON, R. L. 1987. Concepts of pavement performance prediction and modeling. *Proc., 2nd North American Conference on Managing Pavements.*

MCELVANEY, J. & SNAITH, M. 2002. Analytical design of flexible pavements. *Highways the location design construction and maintenance of pavements. Oxford: Butterworth-Heine-mann*.

MCMANIS, K. 2003. Identification and stabilization methods for problematic silt soils: A laboratory evaluation of modification and stabilization additives. USA: louisiana transportation research center, No. 99-4GT.

MICHALOWSKI, R. L. 2005. Coefficient of earth pressure at rest. *Journal of geotechnical and geoenvironmental engineering*, 131**,** 1429-1433.

MILBURN, J. P. & PARSONS, R. 2004. Performance of soil stabilization agents. Kansas Department of Transportation, Bureau of Materials and Research, Research Unit, K-TRAN: KU-01-8.

MILLER, J. & BELLINGER, W. 2003. DISTRESS IDENTIFICATION MANUAL FOR THE LONG-TERM PAVEMENT PERFORMANCE PROGRAM. USA: Federal Highway Administration, FHWA-RD-03-031.

MINER, M. A. 1945. Cumulative damage in fatigue. *Journal of applied mechanics*, 12**,** 159-164.

MOKWA, R. & AKIN, M. 2009. Measurement and evaluation of subgrade soil parameters: phase 1-synthesis of literature. Tech. Rep. FHWA/MT-09-006/8199, Western Transportation Institute, Montana State University, Bozeman, Mont, USA.

MONISMITH, C. L., SOUSA, J. & LYSMER, J. 1988. Modern pavement design technology including dynamic load conditions. SAE Technical Paper.

MULUNGYE, R., OWENDE, P. & MELLON, K. 2007. Finite element modelling of flexible pavements on soft soil subgrades. *Materials & design*, 28**,** 739-756.

NINOUH, T. & ROUILI, A. 2013. The Protection and Enhancement of the Roman Roads in Algeria. International Journal of Social, Behavioural, Educational, Economic and Management Engineering 7**,** 1772-1775.

NOWAK, P. and GILBERT, P., 2015. *Earthworks: a guide*. London, UK: ICE Publishing.

O'FLAHERTY, C. 2002. Highways: The Location, Design, Construction and Maintenance of Pavements. Butterworth-Heinemann, Oxford, United Kingdom.

PAIGE-GREEN, P. 2008. A reassessment of some road material stabilization problems. *SATC 2008*.

PAPPIN, J. W. 1979. *Characteristics of a granular material for pavement analysis*. PhD, University of Nottingham.

PAUTE, J. 1988. A MODEL FOR THE STRUCTURAL DESIGN CALCULATION OF FLEXIBLE PAVEMENTS. *BULLETIN DE LIAISON DES LABORATOIRES DES PONTS ET CHAUSSEES*.

PAVEMENTINTERACTIVE. 6 May 2008. *Rutting* [Online]. http://www.pavementinteractive.org/article/rutting/. [Accessed 1st March 2015].

PAVEMENTINTERACTIVE. 7 April 2009. *Fatigue Cracking* [Online]. http://www.pavementinteractive.org/article/fatigue-cracking/. [Accessed 25 January 2015].

PUNTHUTAECHA, K., PUPPALA, A. J., VANAPALLI, S. K. & INYANG, H. 2006. Volume change behaviors of expansive soils stabilized with recycled ashes and fibers. *Journal of materials in Civil Engineering*.

PUPPALA, A. J. 2008. *Estimating stiffness of subgrade and unbound materials for pavement design*, Transportation Research Board.

PUPPALA, A. J., HOYOS, L. R. & POTTURI, A. K. 2011. Resilient moduli response of moderately cement-treated reclaimed asphalt pavement aggregates. *Journal of Materials in Civil Engineering,* 23**,** 990-998.

PUPPALA, A. J., MOHAMMAD, L. N. & ALLEN, A. 1999. Permanent deformation characterization of subgrade soils from RLT test. *Journal of Materials in Civil Engineering,* 11**,** 274-282.

PUPPALA, A. J., SARIDE, S. & CHOMTID, S. 2009. Experimental and modeling studies of permanent strains of subgrade soils. *Journal of geotechnical and geoenvironmental engineering,* 135**,** 1379-1389.

PUTRI, E.E., RAO, N.K. & MANNAN, M.A., 2012, August. Threshold Stress of the Soil Subgrade Evaluation for Highway Formations. In *Proceedings of World Academy of Science, Engineering and Technology* (No. 68). World Academy of Science, Engineering and Technology.

RAAD, L. & FIGUEROA, J. L. 1980. Load response of transportation support systems. *Journal of Transportation Engineering,* 106.

RASUL, J., GHATAORA, G. & BURROW, M. 2015. Permanent deformation of stabilized subgrade soils. *Bituminous Mixtures and Pavements VI***,** 41.

READ, J. & WHITEOAK, D. 2003. *The shell bitumen handbook,* UK, Thomas Telford Ltd.

ROLT, J. 1995. THE DESIGN OF BITUMEN-SURFACED ROADS IN TROPICAL AND SUB-TROPICAL COUNTRIES-THE 4TH EDITION OF OVERSEAS ROAD NOTE 31. *TRL ANNUAL REVIEW 1994*.

ROSCOE, K. 1968. On the generalised stress-strain behaviour of wet clay. *Engineering Plasticity***,** 535-609.

ROUT, R. K., RUTTANAPORMAKUL, P., VALLURU, S. & PUPPALA, A. J. Resilient Moduli Behavior of Lime-Cement Treated Subgrade Soils. Geo Congress, ASCE, 2012. 1428-1437.

SAAD, B., MITRI, H. & POOROOSHASB, H. 2005. Three-dimensional dynamic analysis of flexible conventional pavement foundation. *Journal of transportation engineering,* 131**,** 460-469.

SADRNEJAD, S., GHANIZADEH, A. & FAKHRI, M. 2011. Evaluation of three constitutive models to characterize granular base for pavement analysis using finite element method. *Australian Journal of Basic and Applied Sciences,* 5**,** 2011.

SCHAEFER, V. R., WHITE, D. J., CEYLAN, H. & STEVENS, L. J. 2008. Design Guide for Improved Quality of Roadway Subgrades and Subbases. USA: Iowa Highway Research Board (IHRB Project TR-525).

SCHWARTZ, C. W. 2002. Effect of stress-dependent base layer on the superposition of flexible pavement solutions. *The International Journal Geomechanics,* 2**,** 331-352.

SHARMA, R. S. & MOHAMED, M. H. Evolution of Degree of Saturation and Suction Relationships under Dynamic Flow. Unsaturated Soils 2006, 2006. ASCE, 1494-1502.

SHERWOOD, P. & TRL, T. R. L. 1993. *Soil stabilization with cement and lime,* London : HMSO.

SHOOK, J., FINN, F., WITCZAK, M. & MONISMITH, C. 1982. Development of the Asphalt Institute thickness design manual (MS-1). Research Report.

SISSAKIAN, V.K., 1997. Geological map of Erbil and Mahabad Quadrangle, sheet no. NJ-38-14 and NJ-38-15 (1:250,000) GEOSURV Library.

SOARES, R. F., ALLEN, D. H., KIM, Y.-R., BERTHELOT, C., SOARES, J. B. & RENTSCHLER, M. E. 2008. A computational model for predicting the effect of tire configuration on asphaltic pavement life. *Road Materials and Pavement Design,* 9**,** 271-289.

SOLANKI, P., KHOURY, N. N., ZAMAN, M., JEFF DEAN, P. & SCOTT SEITER, P. 2009. Engineering Properties of Stabilized Subgrade Soils for Implementation of the AASHTO 2002 Pavement Design Guide. School of Civil Engineering and Environmental Science, University of Oklahoma.

SOLANKI, P., ZAMAN, M. & DEAN, J. 2010. Resilient modulus of clay subgrades stabilized with lime, class c fly ash, and cement kiln dust for pavement design. *Transportation Research Record: Journal of the Transportation Research Board***,** 101-110.

SOLIMAN, H., SHALABY, A., ENG, P., KASS, S. & NG, T. N. Characterizing the soil resilient modulus for typical Manitoba soils. The 2009 Annual Conference of the Transportation Association of Canada, Vancouver, British Columbia, 2009.

SUKUMARAN, B., WILLIS, M. & CHAMALA, N. Three dimensional finite element modeling of flexible pavements. 2004 FAA Worldwide Airport Technology Transfer Conference. Atlanta, 2004.

SWEERE, G. T. H. 1990. *Unbound granular bases for roads.* PhD thesis, TU Delft, Delft University of Technology.

SYSTÈMES, D. 2013. ABAQUS User's & Theory Manuals—Release 6.13-1. *Providence, RI, USA.*

THEYSE, H. Mechanistic-empirical modelling of the permanent deformation of unbound pavement layers. 8th International Conference on Asphalt Pavements, Federal Highway Administration, Washington DC, 1997.

THEYSE, H., DE BEER, M. & RUST, F. 1996. Overview of South African mechanistic pavement design method. *Transportation Research Record: Journal of the Transportation Research Board***,** 6-17.

THEYSE, H., STEYN, W., SADZIK, E. & HENDERSON, M. 2006. Heavy Vehicle Simulator and laboratory testing of a light pavement structure for low-volume roads.

TSENG, K.-H. & LYTTON, R. L. 1989. Prediction of permanent deformation in flexible pavement materials. *Implication of aggregates in the design, construction, and performance of flexible pavements, ASTM STP,* 1016**,** 154-172.

TUTUMLUER, E. & KIM, M. Considerations for nonlinear analyses of pavement foundation geomaterials in the finite element modeling of flexible pavements. Symposium on the Mechanics of Flexible Pavements, 2007.

TXDOT, T. D. O. T. 2005. Guidelines for Modification and Stabilization of Soils and Base for Use in Pavement Structures USA: Construction Division Materials & Pavements Section Geotechnical, Soils & Aggregates Branch

ULLIDTZ, P. 1987. *Pavement Analysis. Developments in Civil Engineering, 19*.

ULLIDTZ, P. 1993. *Mathematical model of pavement performance under moving wheel load (No. 1384).*

ULLIDTZ, P. Analytical tools for design of flexible pavements. Keynote Address delivered at the 8th ISAP Conference held in Copenhagen, 2002.

UTHUS, L., HERMANSSON, Å., HORVLI, I. & HOFF, I. 2006. A study on the influence of water and fines on the deformation properties and frost heave of unbound aggregates. *Cold Regions Engineering, Norway*.

UZAN, J. 2004. Permanent deformation in flexible pavements. *Journal of Transportation Engineering,* 130**,** 6-13.

UZAN, J. & WITCZAK, M. Composite Subgrade Modulus for Rigid Airfield Pavement Design Based upon Multilayer Theory. Third International Conference on Concrete Pavement Design and Rehabilitation, 1985.

VELASQUEZ, R., HOEGH, K., YUT, I., FUNK, N., COCHRAN, G., MARASTEANU, M. & KHAZANOVICH, L. 2009. Implementation of the MEPDG for new and rehabilitated pavement structures for design of concrete and asphalt pavements in Minnesota.

VOROBIEFF, G. & MURPHY, G. 2003. A new approach to pavement design using lime stabilised subgrades. *Publication of: ARRB Transport Research, Limited*.

WERKMEISTER, S., DAWSON, A. & WELLNER, F. 2001. Permanent deformation behavior of granular materials and the shakedown concept. *Transportation Research Record: Journal of the Transportation Research Board***,** 75-81.

WERKMEISTER, S., NUMRICH, R., DAWSON, A. & WELLNER, F. 2003. Design of granular pavement layers considering climatic conditions. *Transportation Research Record: Journal of the Transportation Research Board***,** 61-70.

WHITE, D., HARRINGTON, D. & THOMAS, Z. 2005. Fly ash soil stabilization for non-uniform subgrade soils, Volume I: Engineering properties and construction guidelines. *Iowa Highway Research Board Report: IHRB Projectc TR-461*.

WOLFF, H., VISSER, A. & COULOMB, M. 1994. Incorporating elasto-plasticity in granular layer pavement design. *Proceedings of the ICE-Transport,* 105**,** 259-272.

WU, Z., CHEN, X. & YANG, X. 2011a. Finite element simulation of structural performance on flexible pavements with stabilized base/treated subbase materials under accelerated loading. Louisiana Transportation Research Center.

WU, Z., GAUTREAU, G. & ZHANG, Z. Performance Evaluation of Lime and Cement Treated Soil Layers under Laboratory and Full Scale Accelerated Pavement Testing. Reston, VA: ASCEProceedings of the First Transportation and Development Institute Congress; March 13-16, 2011, Chicago, Illinois| d 20110000, 2011b. American Society of Civil Engineers.

YANG, S.-R., LIN, H.-D., KUNG, J. H. & HUANG, W.-H. 2008. Suction-controlled laboratory test on resilient modulus of unsaturated compacted subgrade soils. *Journal of Geotechnical and Geoenvironmental Engineering,* 134**,** 1375-1384.

YODER, E. J. & WITCZAK, M. W. 1975. *Principles of pavement design*, John Wiley & Sons.

ZAGHLOUL, S. M. & WHITE, T. 1993. Use of a three-dimensional, dynamic finite element program for analysis of flexible pavement. *Transportation Research Record; 1388:60–69.*

ZAMAN, M. & KHOURY, N. 2007. Effect of soil suction and moisture on resilient modulus of subgrade soils in Oklahoma, (No. ORA 125-6662). *ORA.*

Appendices

Appendix A

A.1 Data Sheet for Preparing Resilient Modulus and Permanent Deformation Tests

Sample Preparation Sheet for Mr-PD Test of Cohesive Materials										
Specimen Number		2								
Material type	A-4 untreated	*Comment*		100% of OMC				Date:	12/03/2014	
Specimen ID	PDA-4100%OMC2			Multi-Stage			*Stress test conditions*			
MTS specimen #							σ_d=	kPa and σ_3=	kPa	
Max dry density (g/cm^3)		1.841		Weight of porous-stone saturated (g)				Porous stone thickness (mm)		
Water content (%)		11				Upper				
Mould diameter (cm)		10				Bottom				
Mould height (cm)		20								
Mould volume (cm^3)		1571.4286		Weight of the Membrane (g)					Factor for extra	1.08
Weight of dry material (g)		2893							material and water	
Weight of water (g)		318		Total weight of dry material (g)			3124		for moisture content	
Number of layers		5		Total weight of water in mix (g)			344			
Weight of soil mix/ layer (g)		642		Material for moistur content			257			
Sample for actual water content should be min. 200 gms										
		Before M$_r$ test		After M$_r$ test	Bulk density computation after M$_r$ test					
Wieght of container empty (g)		393.7		493.8			Wet weight (gm)	3232.7	Dry weight (gm)	2896.6
Wet weight + container (g)		634.3		3726.5	Volume of wet sample (cm^3)			1612.879	Water weight (gm)	336.1
Dry weight + container (g)		611.1		3390.4			δ_b (gm/cm^3)	2.004		
Water content (%)		10.67		11.60			**δd (gm/cm^3)**	1.772		
sample diameter mm		Before M$_r$ test		After M$_r$ test			M.C (%)	11.603		
	D1	100.84		101.14						
	D2	100.92		101.17						
	D3	101		101.33	D=	101.07	mm	R=	50.53	mm
	D-avg. (mm)	100.92		101.21	H=	200.64	mm			
sample diameter mm		Before M$_r$ test		After M$_r$ test	Total weight of sample immediately after compaction					
	H1	200.78		200.37	*(sample+2porous stone+membrane)*				3203.7	(gm)
	H2	200.96		200.49	Total weight of sample immediately after test					
	H3	200.96		200.29	*(sample+2porous stone+membrane)*				3232.7	(gm)
	H-avg. (mm)	200.90		200.38	**For comments during test**					

Figure A. 1 Data sheet for resilient modulus and permanent deformation tests (After Abushoglin and Khogali, 2006)

A.2 Moisture-Density Relationships for Stabilised Subgrade Soils

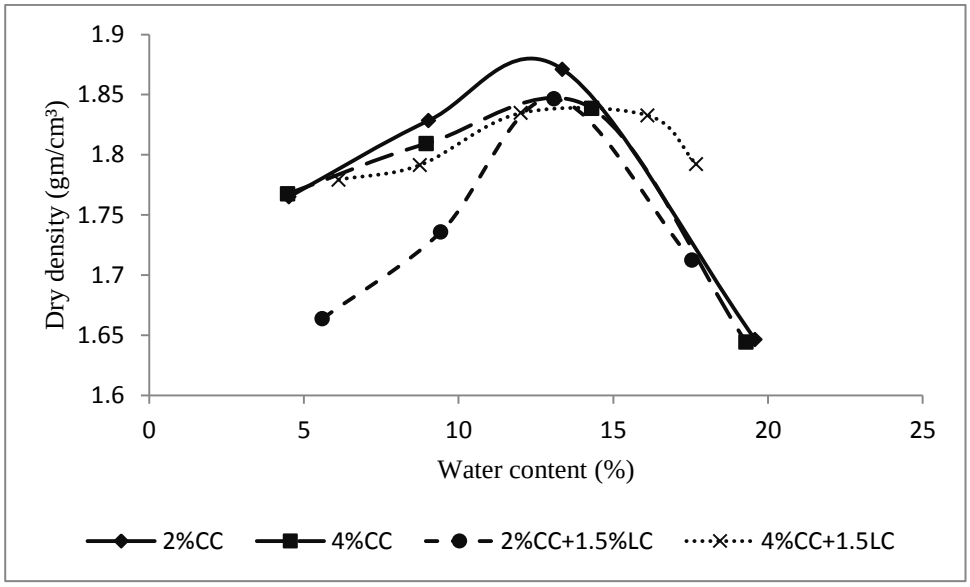

Figure A. 2 Moisture to density relationship for stabilised soil A-4 at four different stabiliser contents

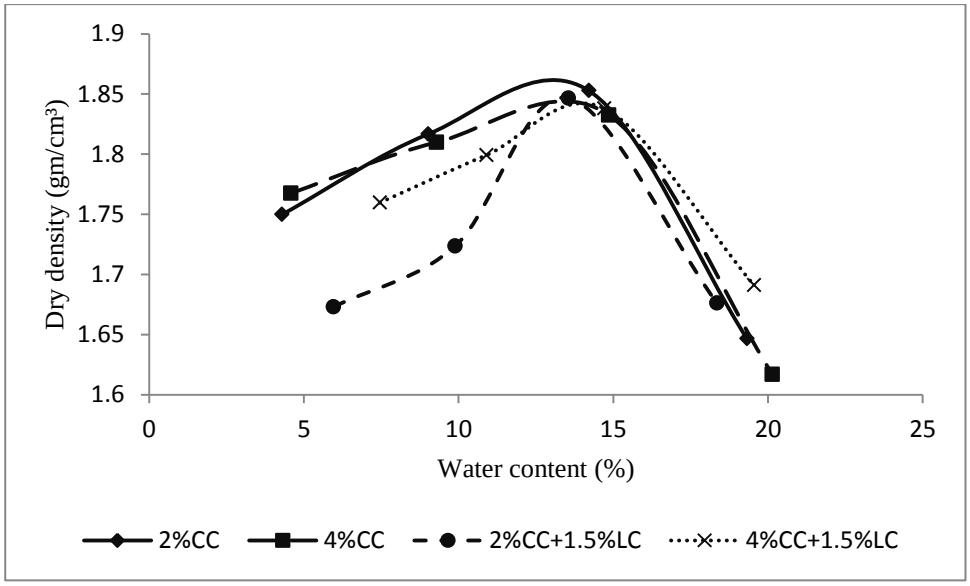

Figure A. 3 Moisture to density relationship for stabilised soil A-6 at four different stabiliser contents

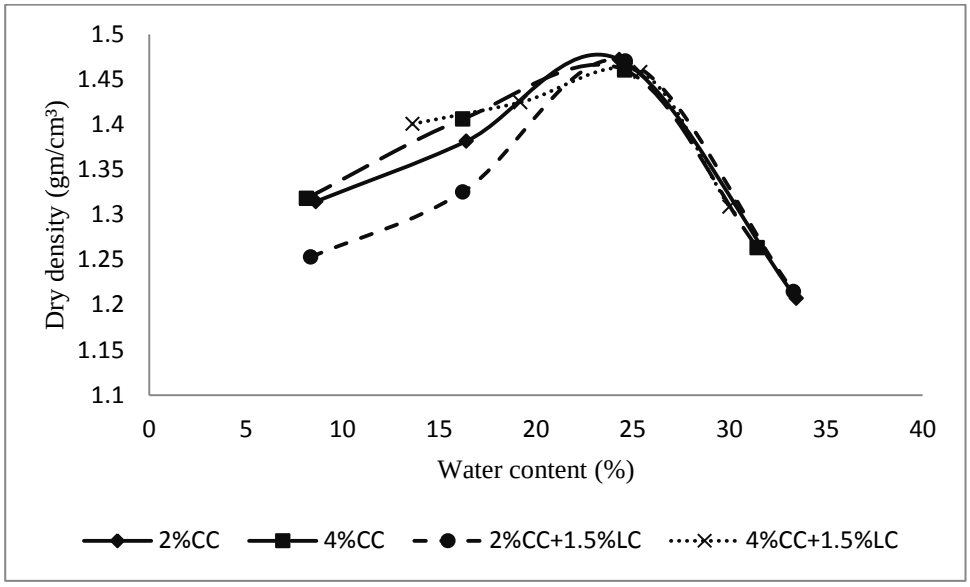

Figure A. 4 Moisture to density relationship for stabilised soil A-7-5 at four different stabiliser contents

A.3 Unloading and Loading Cycles in UCS Test for Modulus of Elasticity Determination

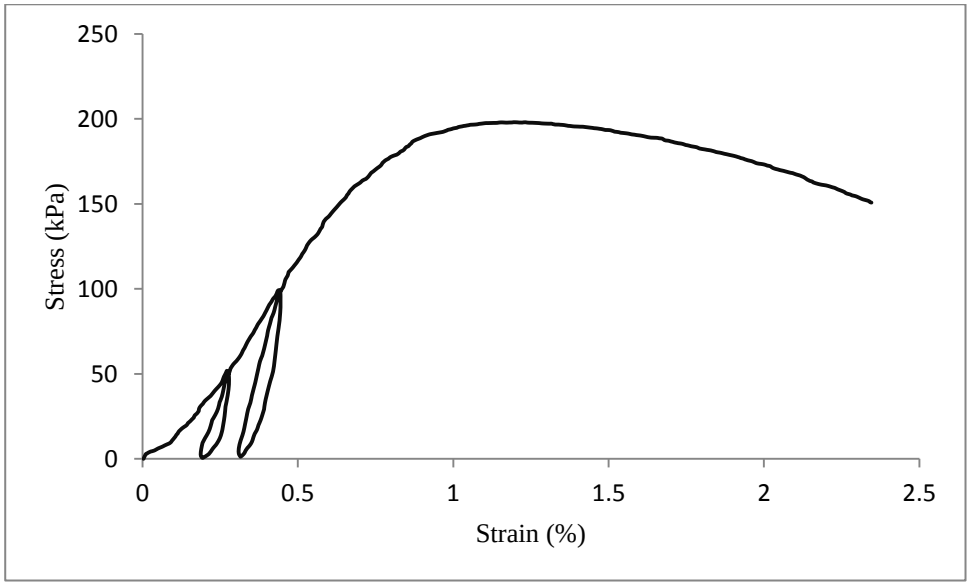

Figure A. 5 Modulus of elasticity from the slope of two cycles for unstabilised soil A-4

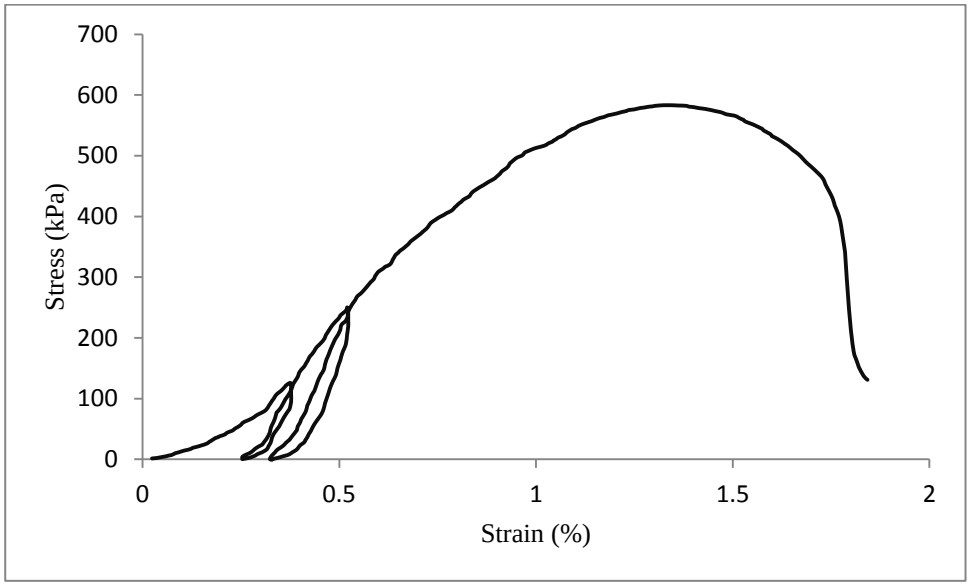

Figure A. 6 Modulus of elasticity from the slope of two cycles for stabilised soil A-4 at 2%CC

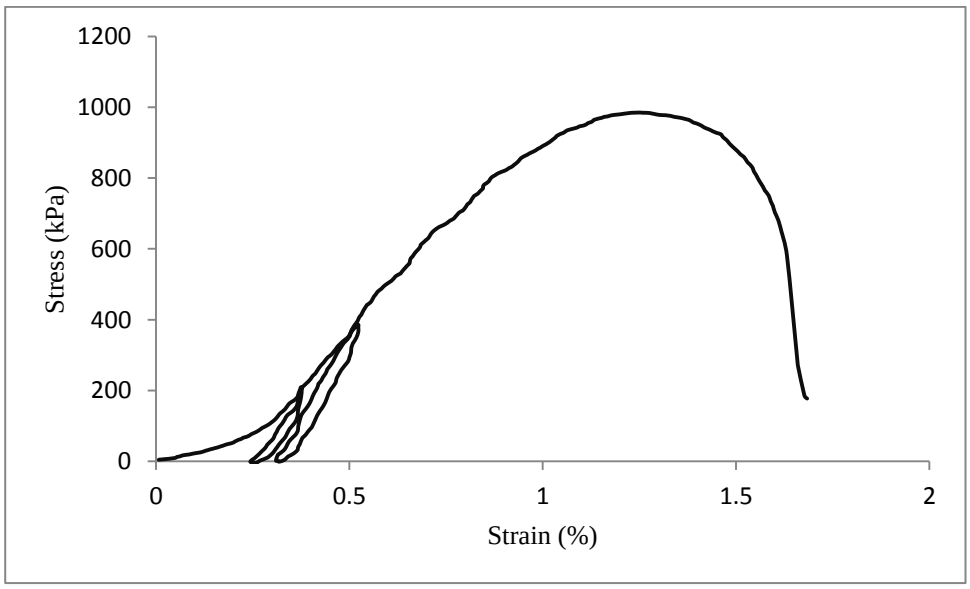

Figure A. 7 Modulus of elasticity from the slope of two cycles for stabilised soil A-4 at 4%CC

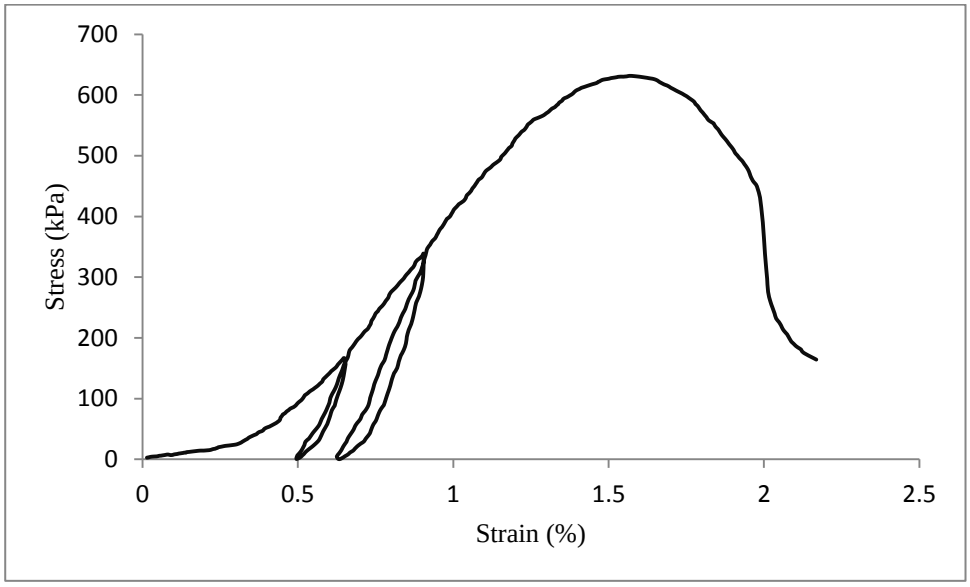

Figure A. 8 Modulus of elasticity from the slope of two cycles for stabilised soil A-4 at 2%CC+1.5%LC

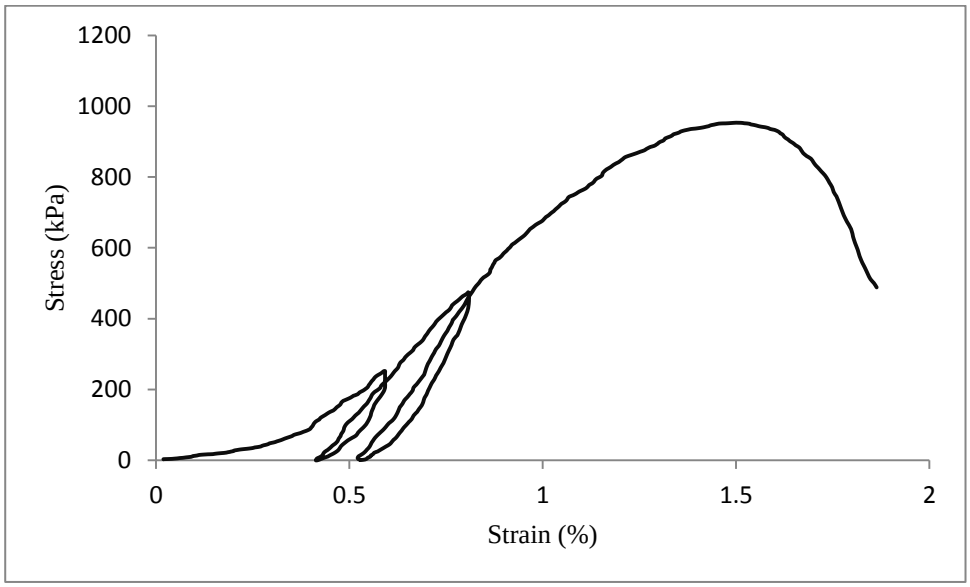

Figure A. 9 Modulus of elasticity from the slope of two cycles for stabilised soil A-4 at 4%CC+1.5%LC

Table A. 1 Unconfined compressive strength tests for the three soil types at three moisture contents

	%OMC	Samples	Untreated UCS (kPa)	Average (kPa)
A-4	80	1	254	268
		2	262	
		3	288	
	100	1	214	228
		2	234	
		3	237	
	120	1	103	120
		2	99	
		3	157	
A-6	80	1	321	323
		2	339	
		3	310	
	100	1	292	274
		2	275	
		3	256	
	120	1	193	189
		2	187	
		3	187	
A-7-5	80	1	281	281
		2	275	
		3	286	
	100	1	160	211
		2	226	
		3	247	
	120	1	186	195
		2	207	
		3	193	

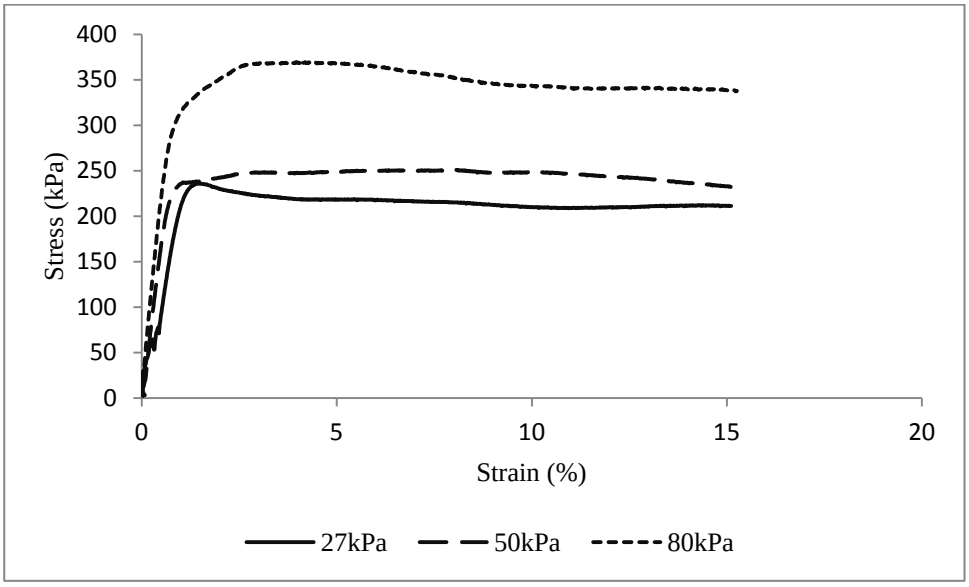

Figure A. 10 Stress-strain relationship for soil A-4 at 27, 50 and 80 kPa in unconsolidated untrained triaxial test

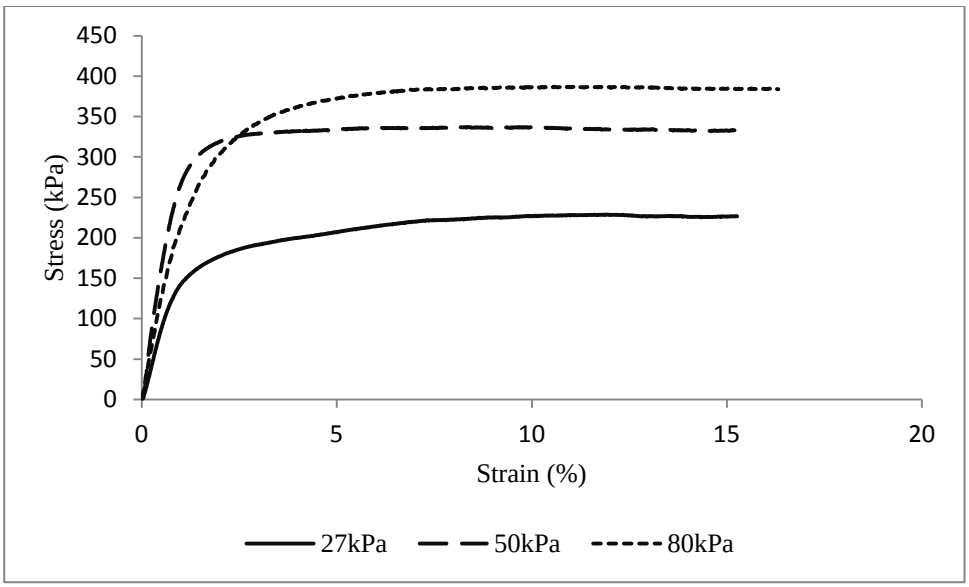

Figure A. 11 Stress-strain relationship for soil A-6 at 27, 50 and 80 kPa in unconsolidated untrained triaxial test

Appendix B

B.1 Integrating Modulus of Elasticity in Permanent Deformation Model

Modulus of elasticity is one of the stabilised subgrade properties that have been determined in this research using BS EN 12390-13:2013; testing hardened concrete for determination of secant modulus of elasticity in compression. Table 1 shows results of these tests and unconfined compressive strength for these three soils at different stabiliser contents and unstabilised soils. The values obtained from these tests can be used to determine the fatigue cracking of the compacted subgrade layer using performance models such as the one in Austroads 2008 (equation 5.9).

$$N = RF\left[\frac{\left(\frac{113000}{E^{0.804}}+191\right)}{\mu\varepsilon}\right]^{12} \quad \text{(B.1)}$$

Where: N = allowable number of repetitions of the load, με = tensile strain produced by the load (micro strain), E = cemented material modulus (MPa), RF = reliability factor for cemented materials fatigue.

This equation will give an indication of the performance of the stabilised subgrade layer for fatigue resistance, from which the comparison can be made with the performance from permanent deformation as the designed stabilised subgrade layer should satisfy both fatigue cracking and permanent deformation criteria.

To demonstrate the appropriateness of using modulus of elasticity in permanent deformation determination the same model parameters in section 5.4.1 are used and repeated here to compare the differences between introducing the modulus of elasticity and resilient modulus. The values of unstabilised and stabilised with 4% cement plus 1.5% lime are used as the

parameters of the equation are determined for these group of the samples, the equation can be expressed as shown in equation 5.10.

$$\varepsilon_{1,p} = a * \left(\frac{\sigma_d}{ME}\right) * N^b \quad \text{(B.2)}$$

Where: $\varepsilon_{1,p}$ is vertical permanent deformation in micro strains, σ_d is deviatoric stress in kPa, ME is modulus of elasticity in Mpa, N is the number of loads and *a* and *b* model parameters found from regression.

Table 2 shows the results of the permanent deformation determination from both equations 5.8 and B.2, in which the nonlinearity is not counted for, the results from equation with modulus of elasticity are too conservative than the values with the equation with resilient modulus. However where the nonlinearity is considered the results are more realistic especially for stabilised soils as presented in Table 3. These results show the suitability of using a property of the stabilised subgrade soil whether the introduced property is the modulus of elasticity or resilient modulus. It is of a great advantage if the disintegration or deterioration of the pavement materials could be counted for. In other words it is important to determine the gradual loss of strength and property of materials and use it in pavement design and management. Durability tests were carried out in this research for resilient modulus value and permanent deformation, however these tests are not available here for UCS and modulus of elasticity.

Table B. 1 Modulus of elasticity and corresponding unconfined compressive strength (UCS) values

Soil Type	Stabilizer	No.	Treated UCS (kPa)	Average (kPa)	ME	ME ave.
A-4	Untreated	1	198	197	63	70
		2	201		74	
		3	186		74	
		4	201			
	2%CC	1	583	580		160
		2	570		124	
		3	579		170	
		4	589		186	
	4%CC	1	985	969		199
		2	957		183	
		3	1016		215	
		4	917		199	
	2%CC+1.5%LC	1	631	618		152
		2	582		119	
		3	611		155	
		4	646		183	
	4%CC+1.5%LC	1	953	955		186
		2	973		162	
		3	950		193	
		4	942		203	
A-6	Untreated	1	223	189	59	70
		2	172		61	
		3	186		90	
		4	175			
	2%CC	1	600	559	113	154
		2	585		156	
		3	552		160	
		4	500		147	
	4%CC	1	903	845		181
		2	907		165	
		3	811		173	
		4	757		204	
	2%CC+1.5%LC	1	537	574	133	167
		2	532		154	
		3	601		179	
		4	625			
	4%CC+1.5%LC	1	800	774		171
		2	758		174	
		3	778		173	
		4	759		165	
A-7-5	Untreated	1	176	171	37	41
		2	177		36	
		3	163		49	
		4	166		40	
	2%CC	1	276	275	78	83
		2	278		83	
		3	270		81	
		4	276		88	
	4%CC	1	357	357	91	98
		2	342		93	
		3	355		95	
		4	374		113	
	2%CC+1.5%LC	1	430	427	133	124
		2	427		109	
		3	418		130	
		4	434			
	4%CC+1.5%LC	1	512	501		137
		2	509		109	
		3	482		173	
		4	417		129	

Table B. 2 comparison of permanent deformation from equation 5.8 and 5.10 and measured

Soil type	Model parameters		Mr	σd	σd/Mr	Model 5.8 ($\varepsilon_{p.1}$)	Measured ($\varepsilon_{p.1}$)	ME	Model 5.10 ($\varepsilon_{p.1}$)
	α	b	(Mpa)	(kPa)	(%)	(μ strain)	(μ strain)	(Mpa)	(μ strain)
A-4_Untreated	1707.794	0.171	187	120	0.642	6971	7864	70	18623
A-6_Untreated	1842.765	0.107	100	120	1.200	7038	7401	70	10054
A-7-5 _Untreated	1068.274	0.055	46	120	2.609	5053	8694	41	5669
A-4_Treated	1075.348	0.042	301	120	0.399	675	869	186	1093
A-6_Treated	1227.719	0.047	279	120	0.430	878	695	171	1433
A-7-5_Treated	2205.015	0.038	225	120	0.533	1774	976	137	2914

Table B. 3 the comparison of permanent deformation from equation 5.8 and 5.10 when the nonlinearity is considered

Soil type	Model parameters		Mr	σd	σd/Mr	Model ($\varepsilon_{p.1}$)	ME	Model ($\varepsilon_{p.1}$)
	α	b	(Mpa)	(kPa)	(%)	(μ strain)	(Mpa)	(μ strain)
A-4_Untreated	1707.794	0.171	130	78	0.600	6518	70	12105
A-6_Untreated	1842.765	0.107	86	67	0.779	4569	70	5614
A-7-5 _Untreated	1068.274	0.055	73	62	0.849	1645	41	2929
A-4_Treated	1075.348	0.042	248	91	0.367	622	186	829
A-6_Treated	1227.719	0.047	200	83	0.415	847	171	991
A-7-5_Treated	2205.015	0.038	145	75	0.517	1721	137	1821

B.2 Post-Cracking Secant Modulus Calculation

A test carried out in this research to show the decrease in secant modulus of stabilised subgrade soil. These values can be used in the pavement design procedure for different stages of the pavement design life. The test was carried out in triaxial frame used for UCS tests. The stabilised subgrade soil sample is subjected to a series of loading and unloading cycles, the loading is continues to the failure point of the material and then the sample is unloaded to zero stress value and the sample is reloaded to failure again. This procedure is continued until the sample fails or the test is terminated according to the number of cycles required. See Figure B.1.

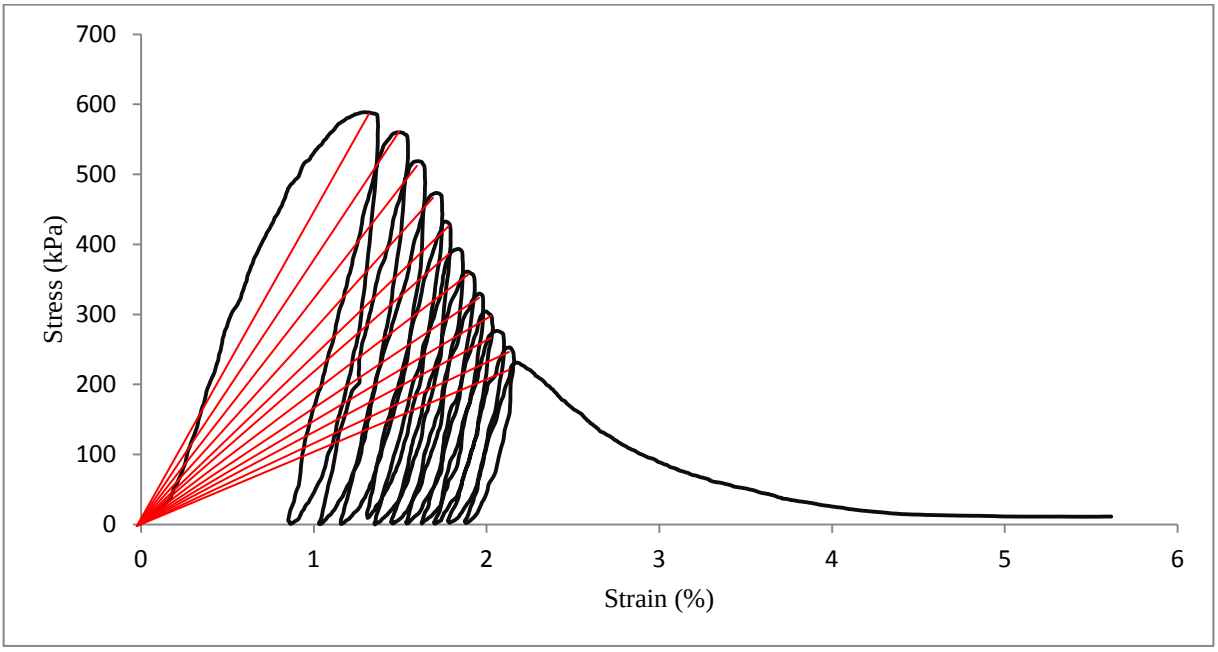

Figure B. 1 Secant modulus determination at different failure points for soil A-4 stabilised with 2%CC

From the definition of the secant modulus, which is the slope of the line drawn from the stress-strain curve origin point to a required point on the curve, a range of secant modulus can be calculated. From these secant values at different failure points it is possible to incorporate the post-cracking (as suggested by Austroads, 2008 for degradation of cemented layer). The importance of this procedure is the modulus of elasticity at different stages of deterioration can be predicted in incorporated into the pavement design for fatigue cracking and permanent deformation if equation B.2 is used. Following figures (Figures 2-7) are examples of this type of figures for the three soil types. The UCS test results are also presented through figures 8-10.

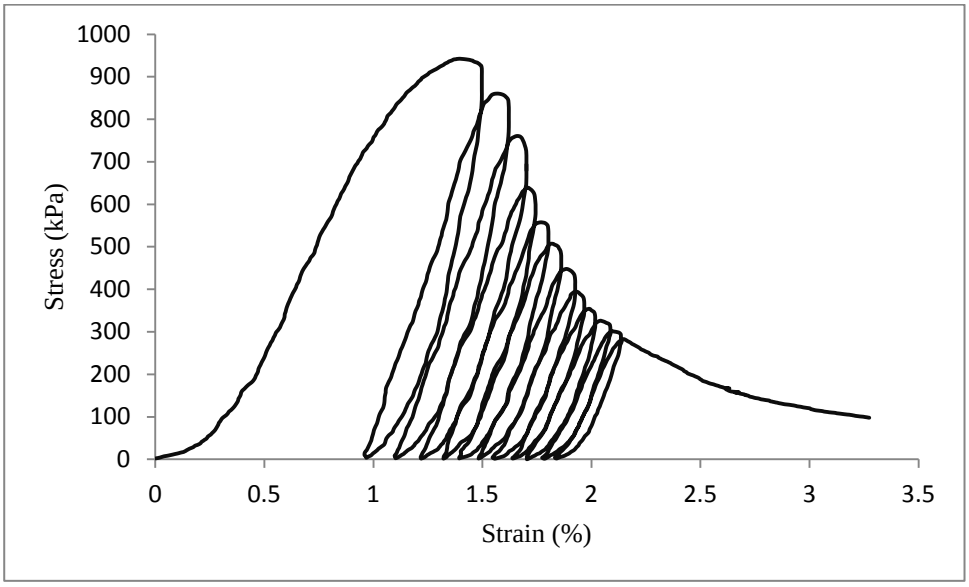

Figure B. 2 Secant modulus determination at different failure points for soil A-4 stabilised with 4%CC+1.5%LC

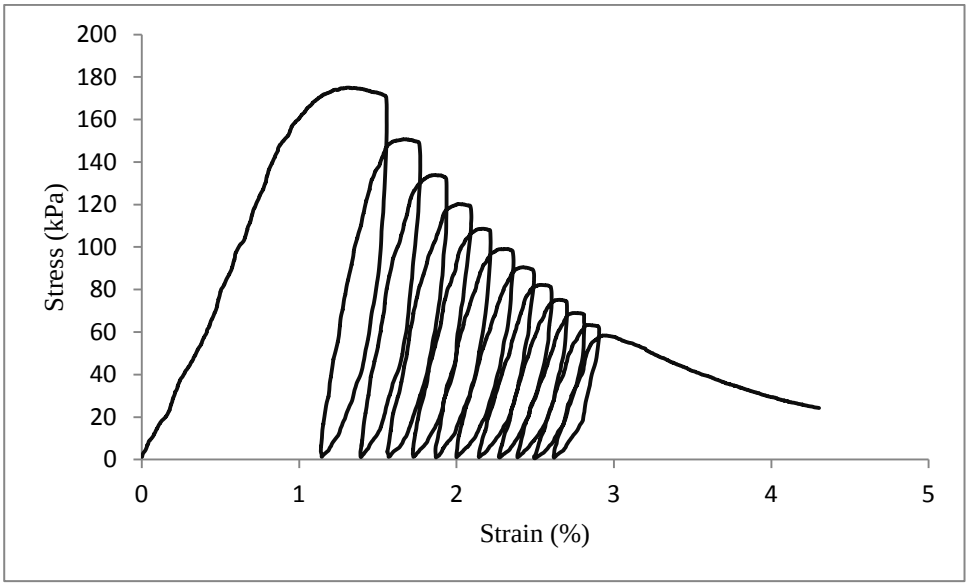

Figure B. 3 Secant modulus determination at different failure points for unstabilised soil A-6

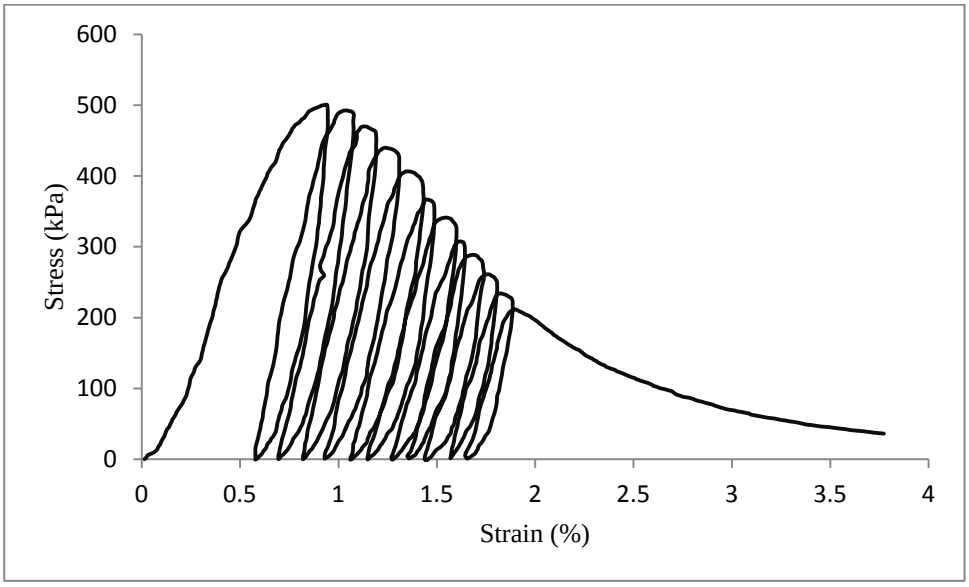

Figure B. 4 Secant modulus determination at different failure points for soil A-6 stabilised with 2%CC

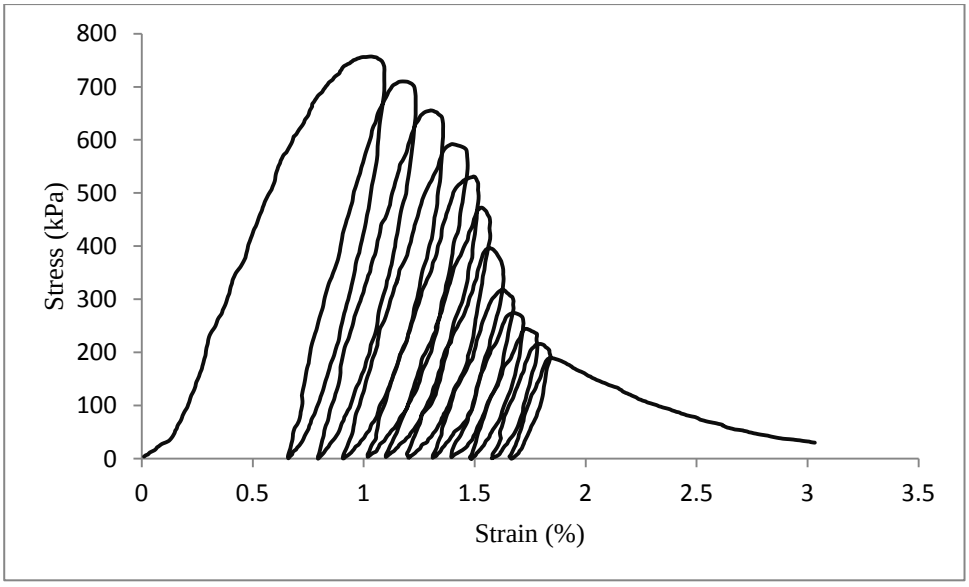

Figure B. 5 Secant modulus determination at different failure points for soil A-6 stabilised with 4%CC

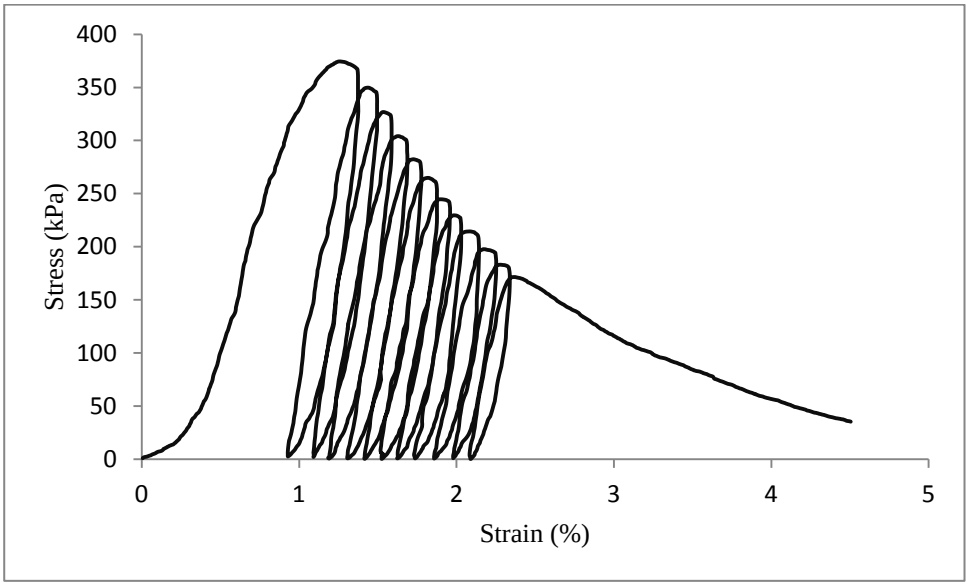

Figure B. 6 Secant modulus determination at different failure points for soil A-7-5 stabilised with 4%CC

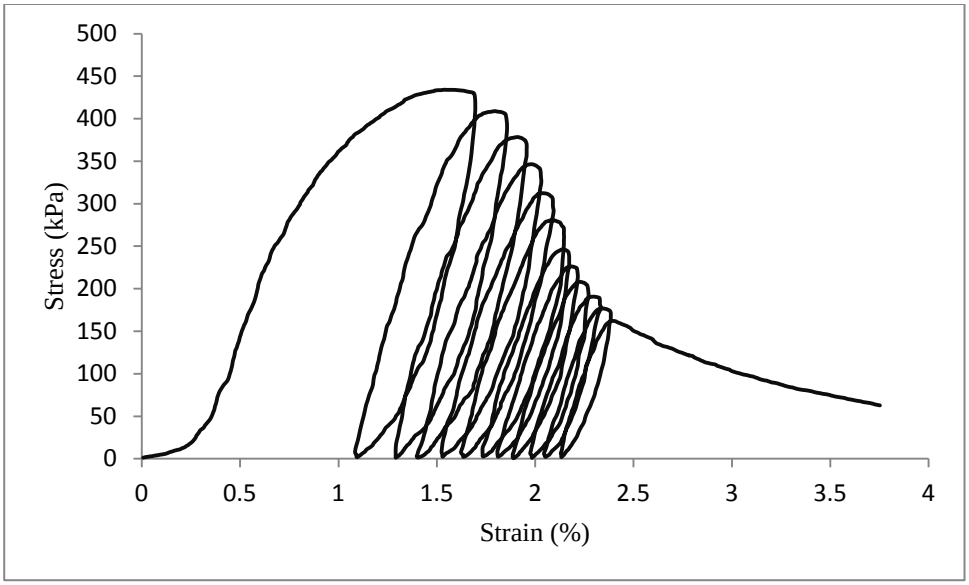

Figure B. 7 Secant modulus determination at different failure points for soil A-7-5 stabilised with 2%CC+1.5%LC

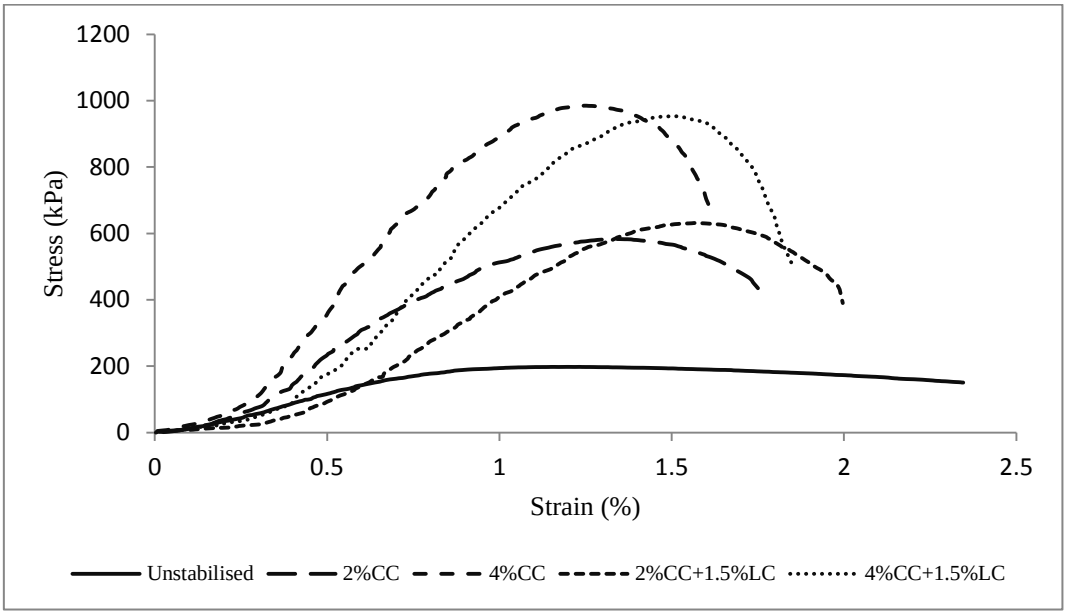

Figure B. 8 Stress-strain relationships from UCS tests for soil A-4 at different stabiliser contents

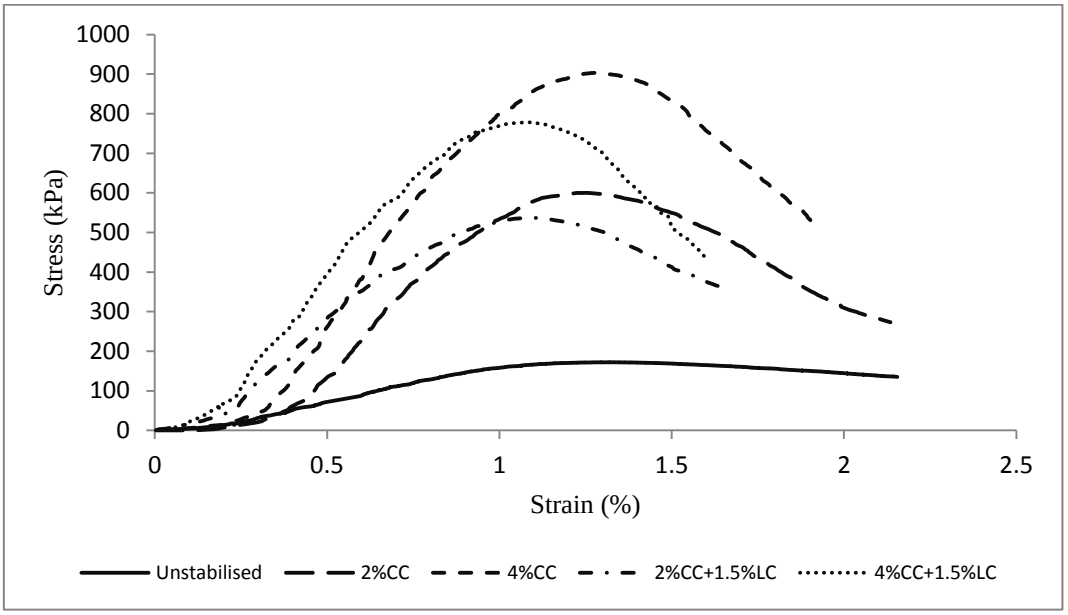

Figure B. 9 Stress-strain relationships from UCS tests for soil A-6 at different stabiliser contents

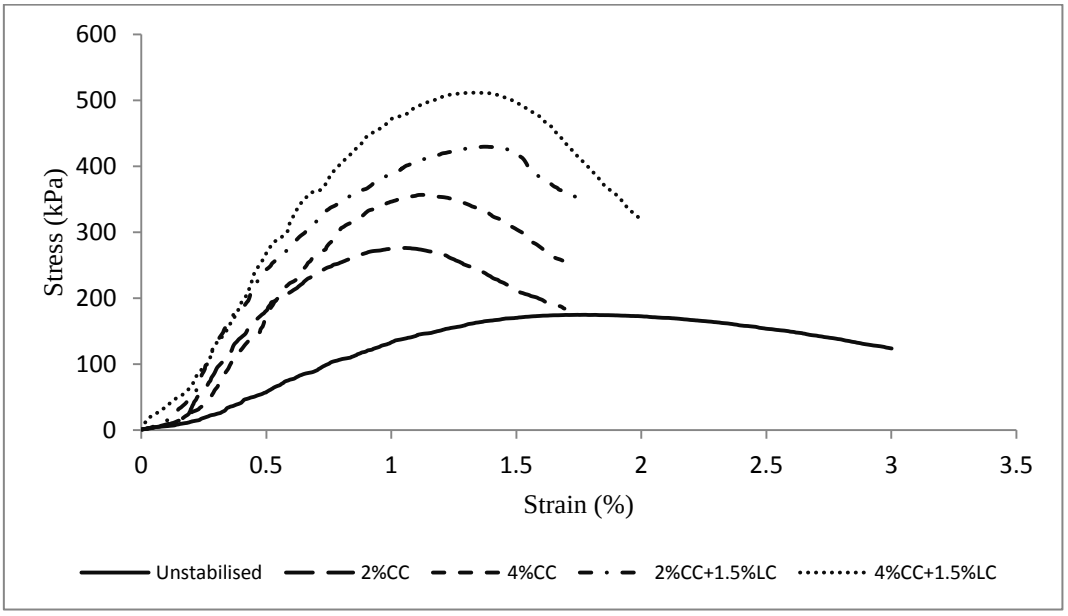

Figure B. 10 Stress-strain relationships from UCS tests for soil A-7-5 at different stabiliser contents

Table B. 4 Results for validation of model 4.11

Soil Type	Stabilization Ratio	Average UCS (kPa)	Confining Stress (kPa)	Deviatoric Stress (kPa)	θ (kPa)	τ_{oct} (kPa)	Measured Mr from tests (MPa)	Predicted Mr from Eq. 4.14 (MPa)	
A-4	2%CC	580	41.4	12.4	95.2	5.8	131	104	0.205
			41.4	24.8	107.6	11.7	161	131	0.188
			41.4	37.3	120.1	17.6	187	151	0.194
			41.4	49.7	132.5	23.4	210	167	0.203
			41.4	62.0	144.8	29.2	226	182	0.196
			27.6	12.4	67.6	5.8	135	101	0.249
			27.6	24.8	80.0	11.7	162	128	0.213
			27.6	37.3	92.5	17.6	185	147	0.203
			27.6	49.7	104.9	23.4	206	164	0.204
			27.6	62.0	117.2	29.2	223	178	0.200
			12.4	12.4	37.2	5.8	127	97	0.238
			12.4	24.8	49.6	11.7	156	123	0.214
			12.4	37.3	62.1	17.6	182	143	0.217
			12.4	49.7	74.5	23.4	203	159	0.216
			12.4	62.0	86.8	29.2	222	174	0.217
			12.4	120.0	144.8	56.6	282	229	0.187
	4%CC	969	41.4	12.4	95.2	5.8	176	151	0.137
			41.4	24.8	107.6	11.7	202	194	0.039
			41.4	37.3	120.1	17.6	220	226	0.029
			41.4	49.7	132.5	23.4	239	253	0.058
			41.4	62.0	144.8	29.2	258	277	0.072
			27.6	12.4	67.6	5.8	167	147	0.119
			27.6	24.8	80.0	11.7	194	189	0.028
			27.6	37.3	92.5	17.6	214	220	0.030
			27.6	49.7	104.9	23.4	236	247	0.048
			27.6	62.0	117.2	29.2	256	271	0.059
			12.4	12.4	37.2	5.8	162	140	0.134
			12.4	24.8	49.6	11.7	187	181	0.033
			12.4	37.3	62.1	17.6	209	213	0.017
			12.4	49.7	74.5	23.4	231	240	0.039
			12.4	62.0	86.8	29.2	252	263	0.045
			12.4	120.0	144.8	56.6	328	355	0.085

Continued

Soil Type	Stabilization Ratio	Average UCS (kPa)	Confining Stress (kPa)	Deviatoric Stress (kPa)	θ (kPa)	τ_{oct} (kPa)	Measured Mr from tests (MPa)	Predicted Mr from Eq. 4.14 (MPa)	
A-6	2%CC	559	41.4	12.4	95.2	5.8	139	101	0.271
			41.4	24.8	107.6	11.7	160	127	0.206
			41.4	37.3	120.1	17.6	174	146	0.159
			41.4	49.7	132.5	23.4	187	162	0.131
			41.4	62.0	144.8	29.2	200	176	0.118
			27.6	12.4	67.6	5.8	136	99	0.275
			27.6	24.8	80.0	11.7	156	124	0.205
			27.6	37.3	92.5	17.6	171	143	0.163
			27.6	49.7	104.9	23.4	185	159	0.140
			27.6	62.0	117.2	29.2	198	173	0.125
			12.4	12.4	37.2	5.8	133	94	0.292
			12.4	24.8	49.6	11.7	153	119	0.220
			12.4	37.3	62.1	17.6	168	138	0.176
			12.4	49.7	74.5	23.4	182	155	0.151
			12.4	62.0	86.8	29.2	196	169	0.139
			12.4	120.0	144.8	56.6	248	222	0.104
	4%CC	845	41.4	12.4	95.2	5.8	122	137	0.128
			41.4	24.8	107.6	11.7	151	174	0.155
			41.4	37.3	120.1	17.6	177	203	0.149
			41.4	49.7	132.5	23.4	199	226	0.138
			41.4	62.0	144.8	29.2	221	247	0.122
			27.6	12.4	67.6	5.8	117	133	0.138
			27.6	24.8	80.0	11.7	146	170	0.168
			27.6	37.3	92.5	17.6	173	198	0.148
			27.6	49.7	104.9	23.4	195	222	0.140
			27.6	62.0	117.2	29.2	217	242	0.117
			12.4	12.4	37.2	5.8	110	127	0.152
			12.4	24.8	49.6	11.7	140	163	0.168
			12.4	37.3	62.1	17.6	166	191	0.151
			12.4	49.7	74.5	23.4	190	215	0.134
			12.4	62.0	86.8	29.2	212	236	0.112
			12.4	120.0	144.8	56.6	309	316	0.023

Continued

Soil Type	Stabilization Ratio	Average UCS (kPa)	Confining Stress (kPa)	Deviatoric Stress (kPa)	θ (kPa)	τ_{oct} (kPa)	Measured Mr from tests (MPa)	Predicted Mr from Eq. 4.14 (MPa)	
A-7-5	2%CC	275	41.4	12.4	95.2	5.8	76	60	0.200
			41.4	24.8	107.6	11.7	90	74	0.175
			41.4	37.3	120.1	17.6	101	84	0.167
			41.4	49.7	132.5	23.4	111	92	0.169
			41.4	62.0	144.8	29.2	121	99	0.184
			27.6	12.4	67.6	5.8	75	59	0.209
			27.6	24.8	80.0	11.7	87	72	0.170
			27.6	37.3	92.5	17.6	98	82	0.163
			27.6	49.7	104.9	23.4	108	90	0.165
			27.6	62.0	117.2	29.2	119	97	0.184
			12.4	12.4	37.2	5.8	72	57	0.214
			12.4	24.8	49.6	11.7	85	70	0.174
			12.4	37.3	62.1	17.6	96	80	0.170
			12.4	49.7	74.5	23.4	107	88	0.175
			12.4	62.0	86.8	29.2	117	95	0.189
			12.4	120.0	144.8	56.6	155	121	0.216
	4%CC	357	41.4	12.4	95.2	5.8	101	73	0.273
			41.4	24.8	107.6	11.7	117	90	0.226
			41.4	37.3	120.1	17.6	127	103	0.190
			41.4	49.7	132.5	23.4	136	113	0.164
			41.4	62.0	144.8	29.2	143	122	0.145
			27.6	12.4	67.6	5.8	96	71	0.254
			27.6	24.8	80.0	11.7	112	88	0.210
			27.6	37.3	92.5	17.6	124	101	0.184
			27.6	49.7	104.9	23.4	134	111	0.168
			27.6	62.0	117.2	29.2	141	120	0.145
			12.4	12.4	37.2	5.8	92	68	0.254
			12.4	24.8	49.6	11.7	108	85	0.213
			12.4	37.3	62.1	17.6	121	98	0.190
			12.4	49.7	74.5	23.4	130	108	0.168
			12.4	62.0	86.8	29.2	138	117	0.150
			12.4	120.0	144.8	56.6	174	151	0.130
								Mean Absolute Percentage Error (MAPE)	15.0

Appendix C

C.1 Refinement of Selected Finite Element Model Mesh

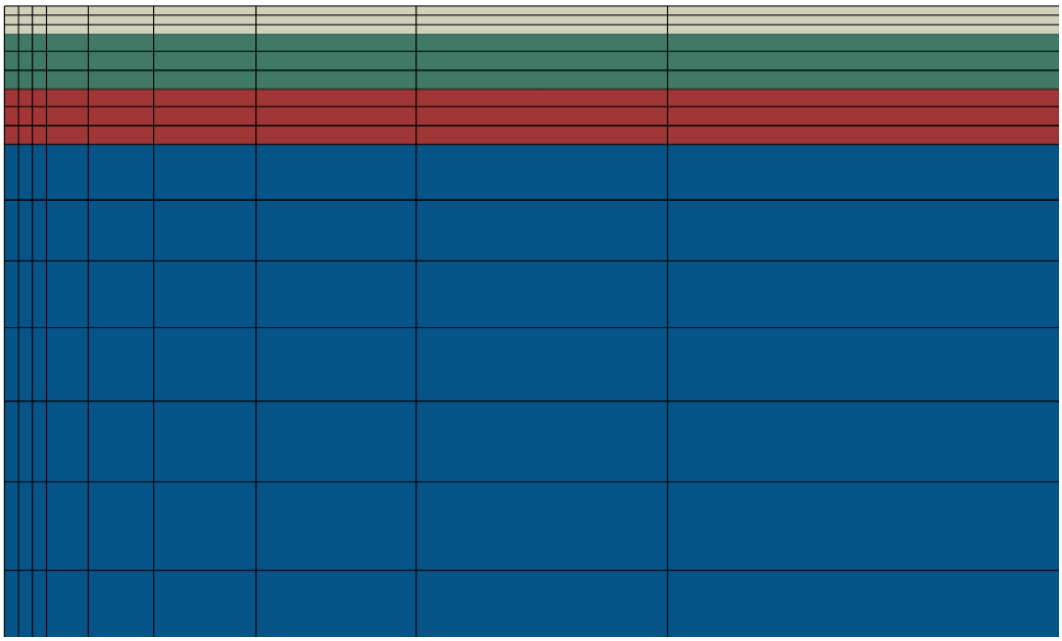

Figure C. 1 trial No. 1 for finite element model refinement

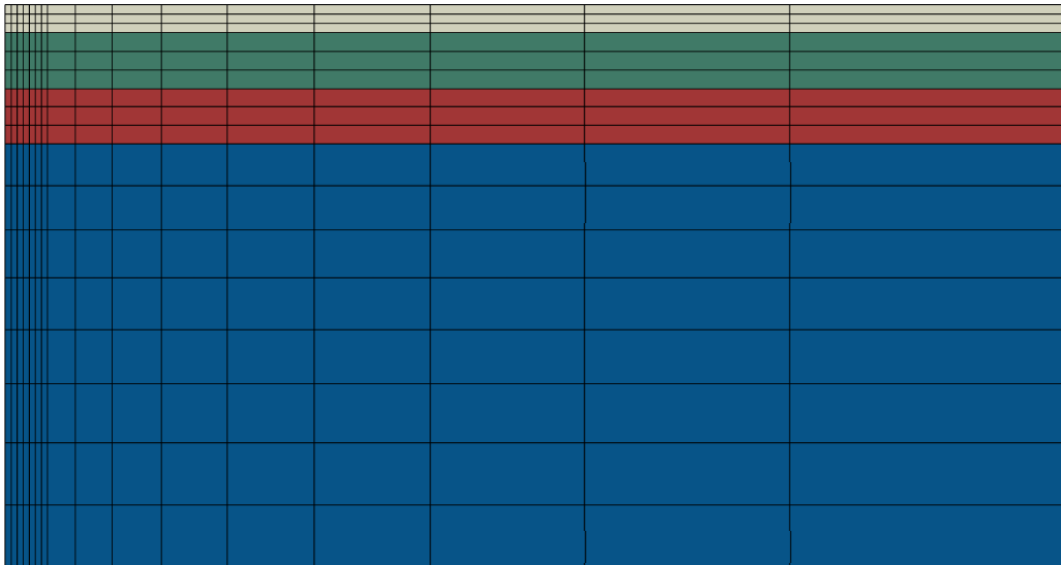

Figure C. 2 trial No. 2 for finite element model refinement

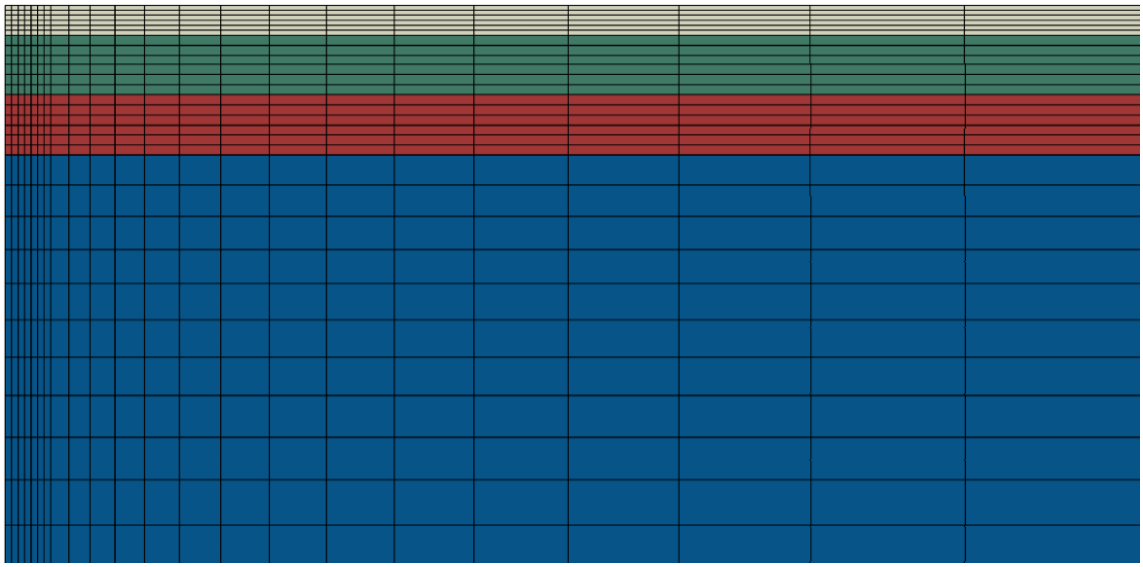

Figure C. 3 trial No. 3 for finite element model refinement

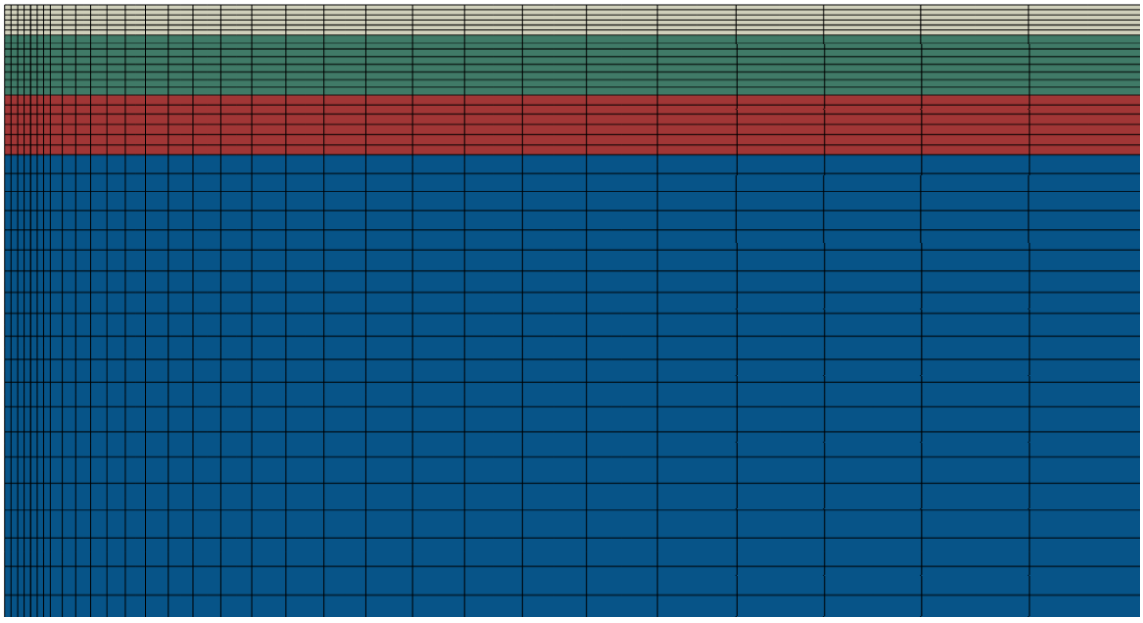

Figure C. 4 trial No. 4 for finite element model refinement

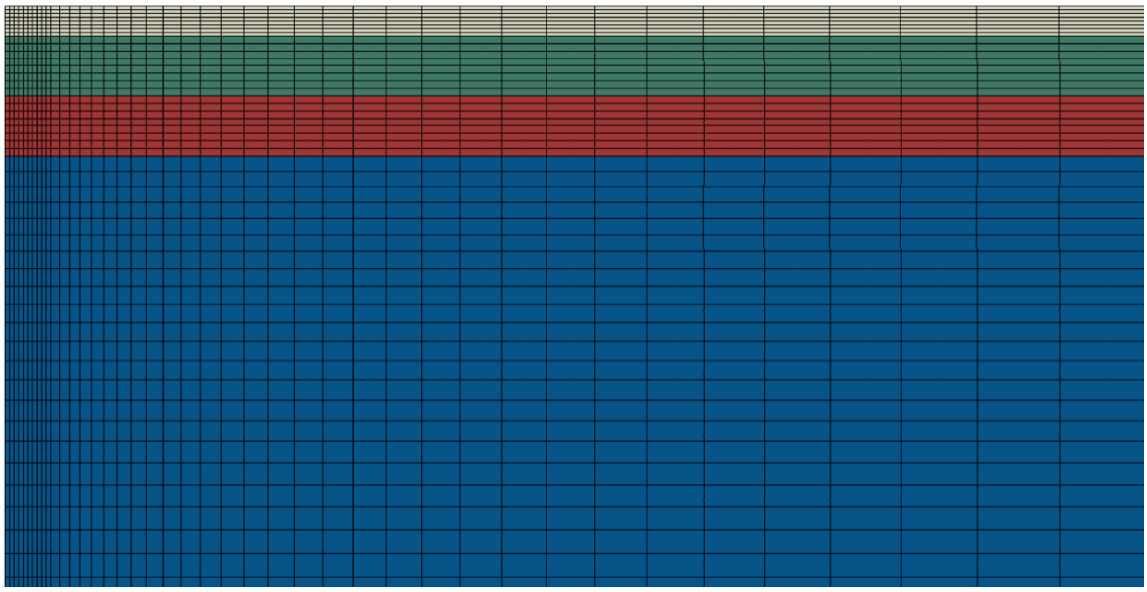

Figure C. 5 trial No. 5 for finite element model refinement

C.2 Visualization of Different Responses from FEM

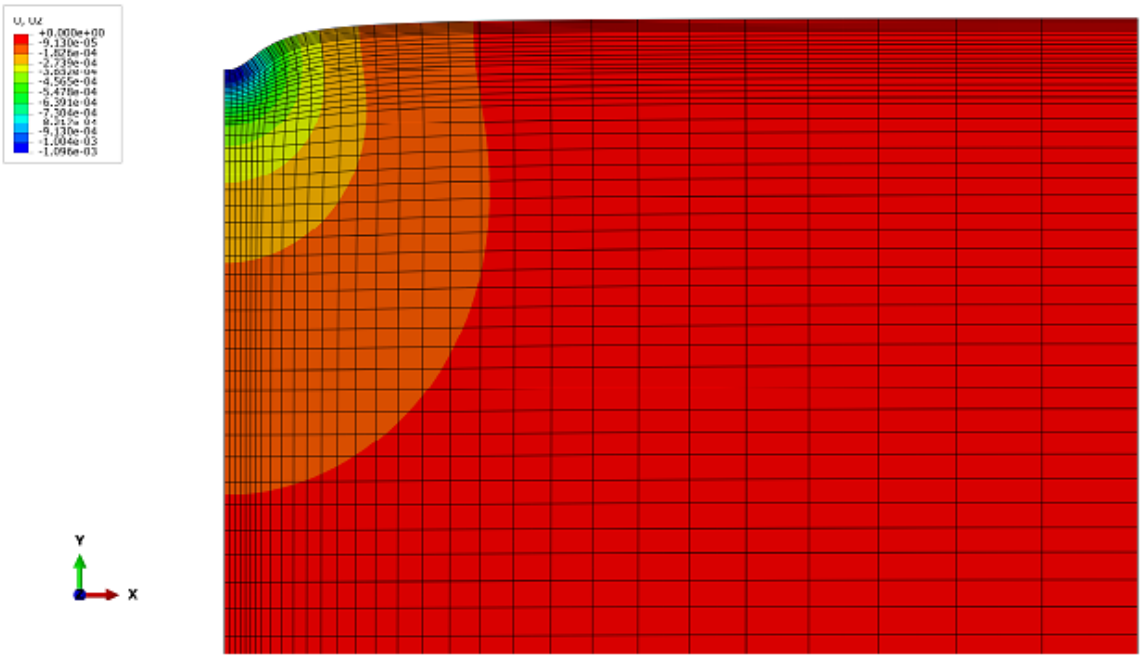

a)

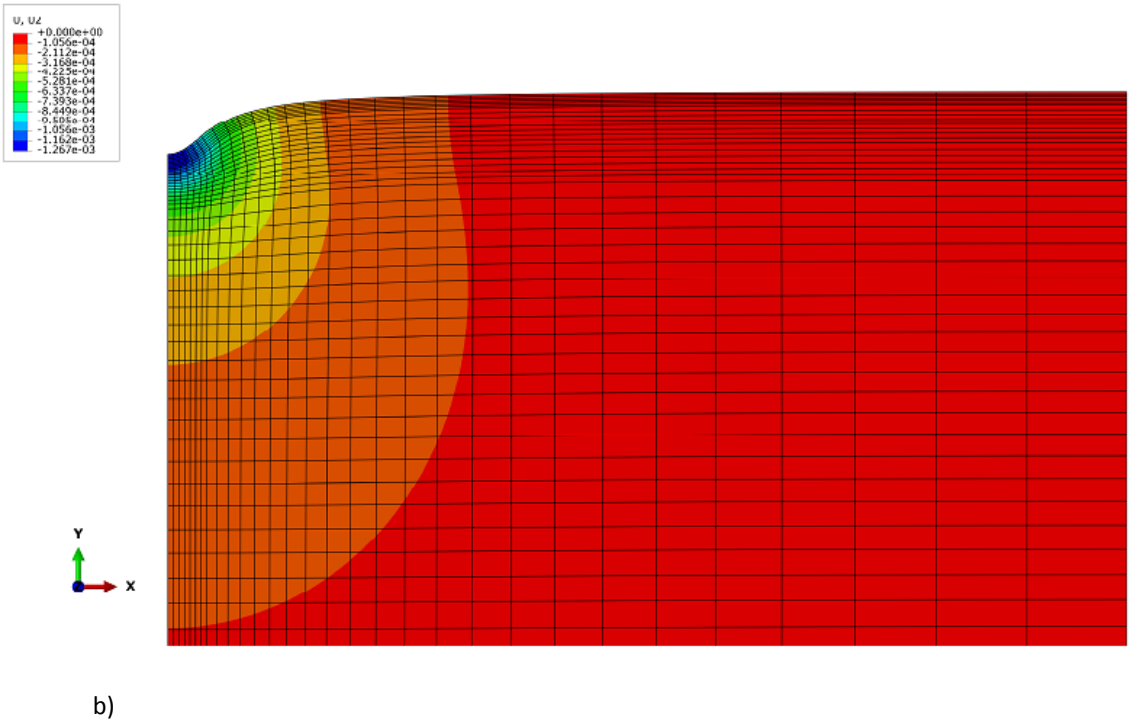

b)

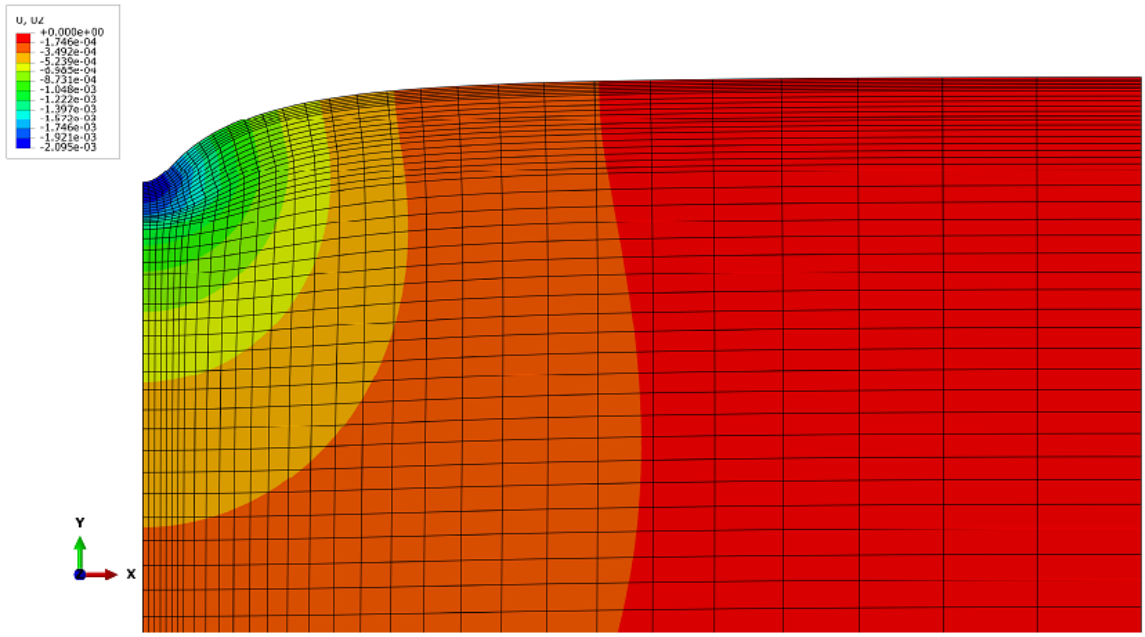

c)

Figure C. 6 surface deflection visualization from finite element analysis for soil A-4 at a) 80%OMC, b) 100%OMC and c) 120%OMC, respectively

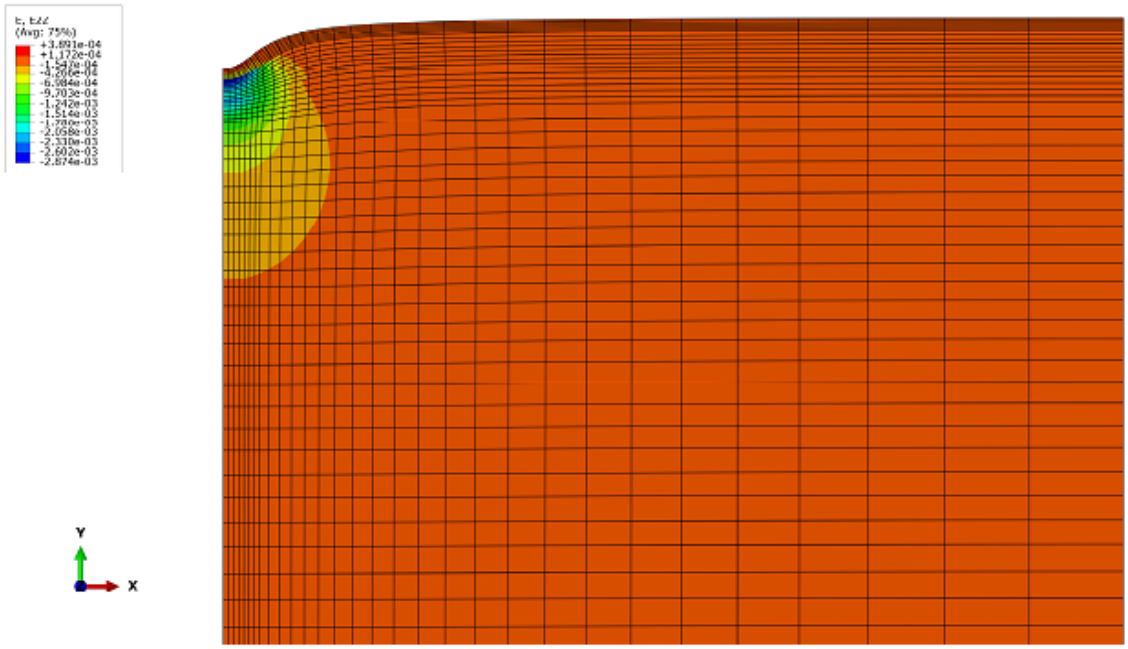
E, E22
(Avg: 75%)
+3.891e-04
+1.172e-04
-1.547e-04
-4.266e-04
-6.984e-04
-9.703e-04
-1.242e-03
-1.514e-03
-1.786e-03
-2.058e-03
-2.330e-03
-2.602e-03
-2.874e-03
Y
X

a)

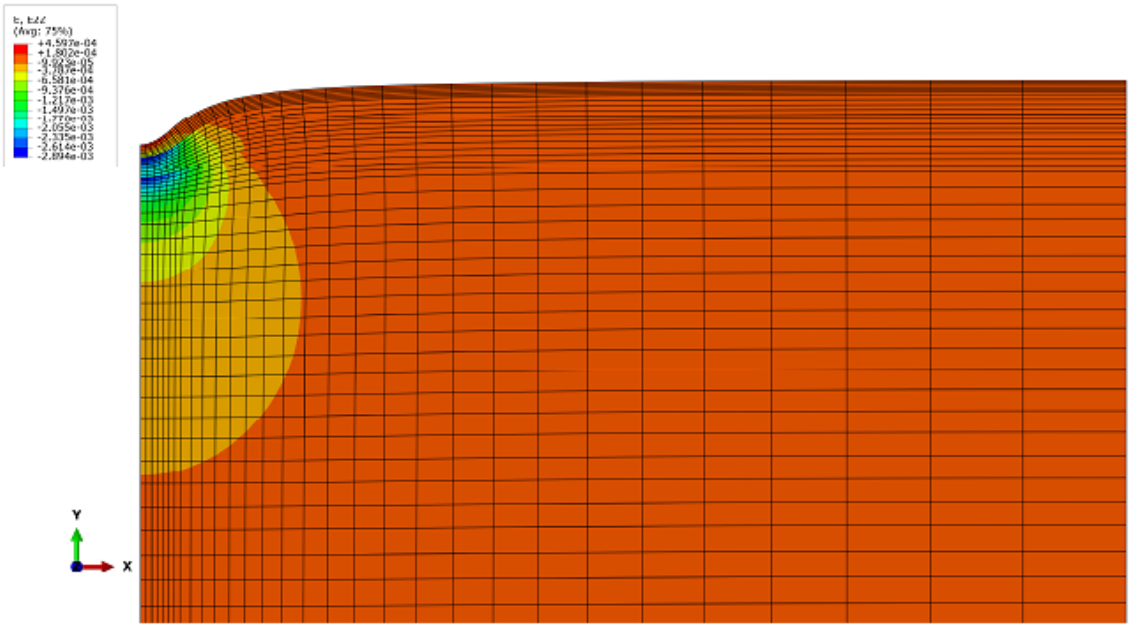
E, E22
(Avg: 75%)
+4.597e-04
+1.802e-04
-9.969e-05
-3.787e-04
-6.581e-04
-9.376e-04
-1.217e-03
-1.497e-03
-1.777e-03
-2.055e-03
-2.335e-03
-2.614e-03
-2.894e-03
Y
X

b)

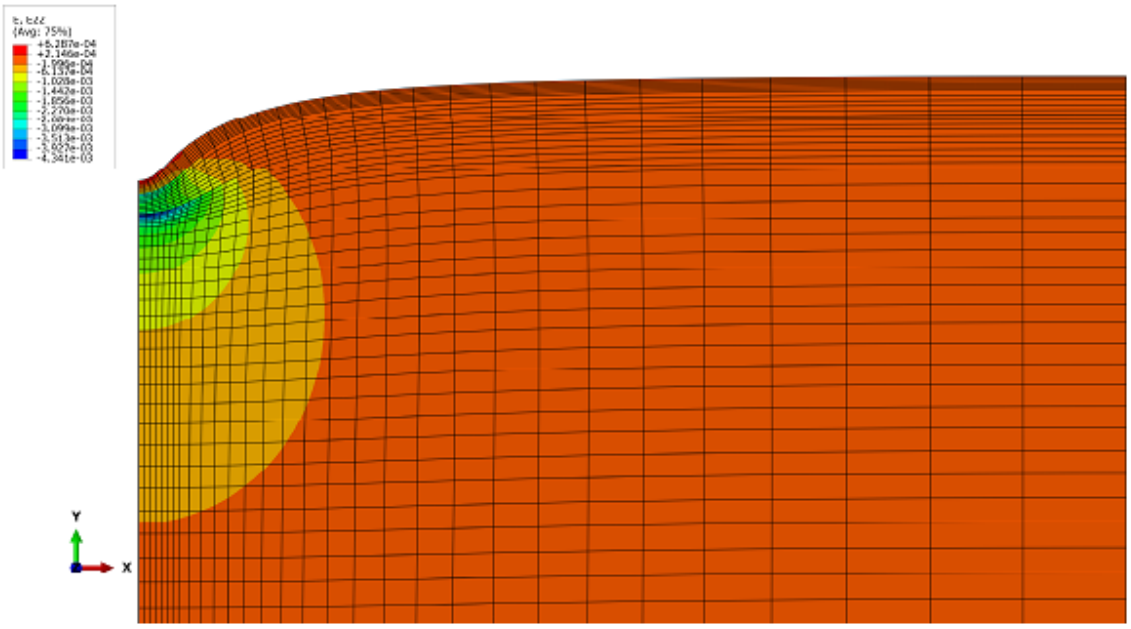

c)

Figure C. 7 compressive strain visualization from finite element analysis for soil A-4 at a) 80%OMC, b) 100%OMC and c) 120%OMC, respectively

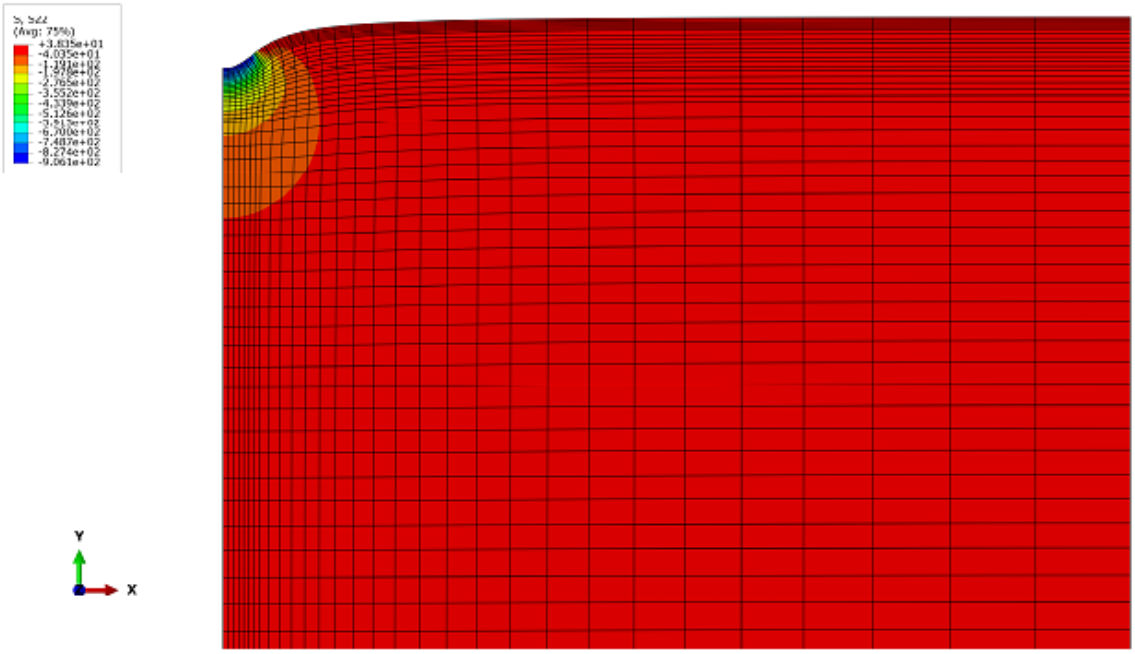

a)

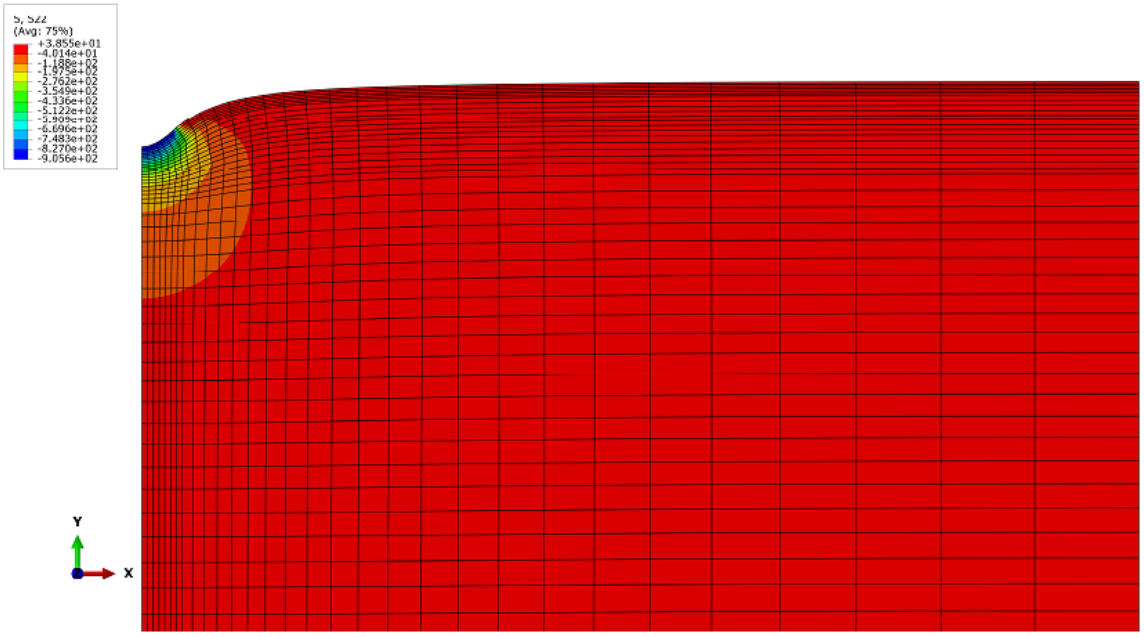

b)

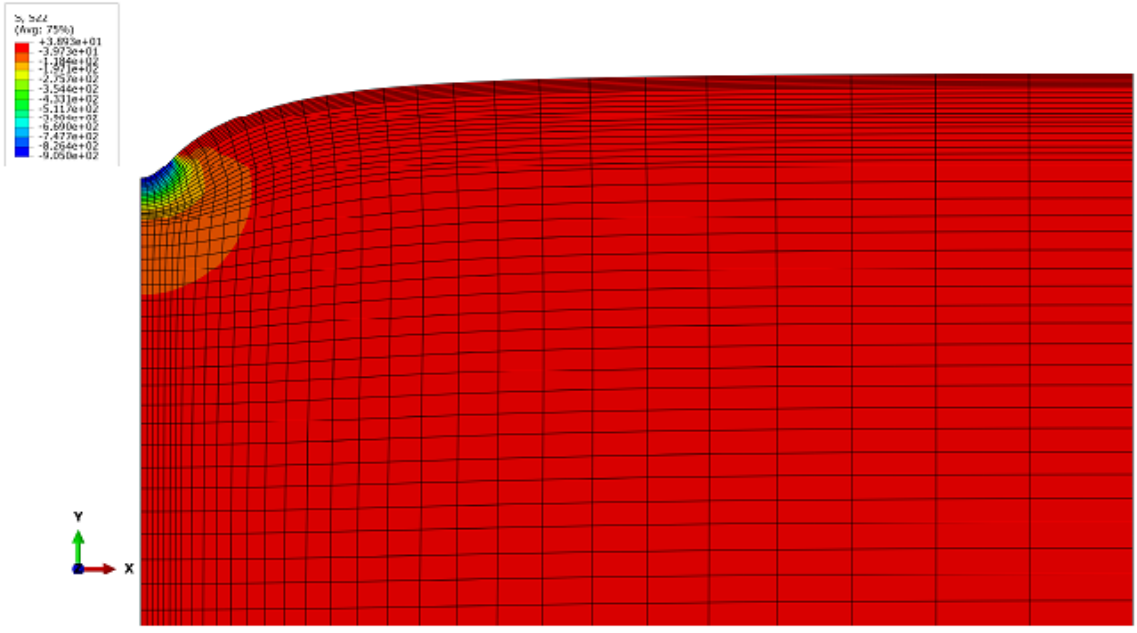

c)

Figure C. 8 compressive stress visualization from finite element analysis for soil A-4 at a) 80%OMC, b) 100%OMC and c) 120%OMC, respectively

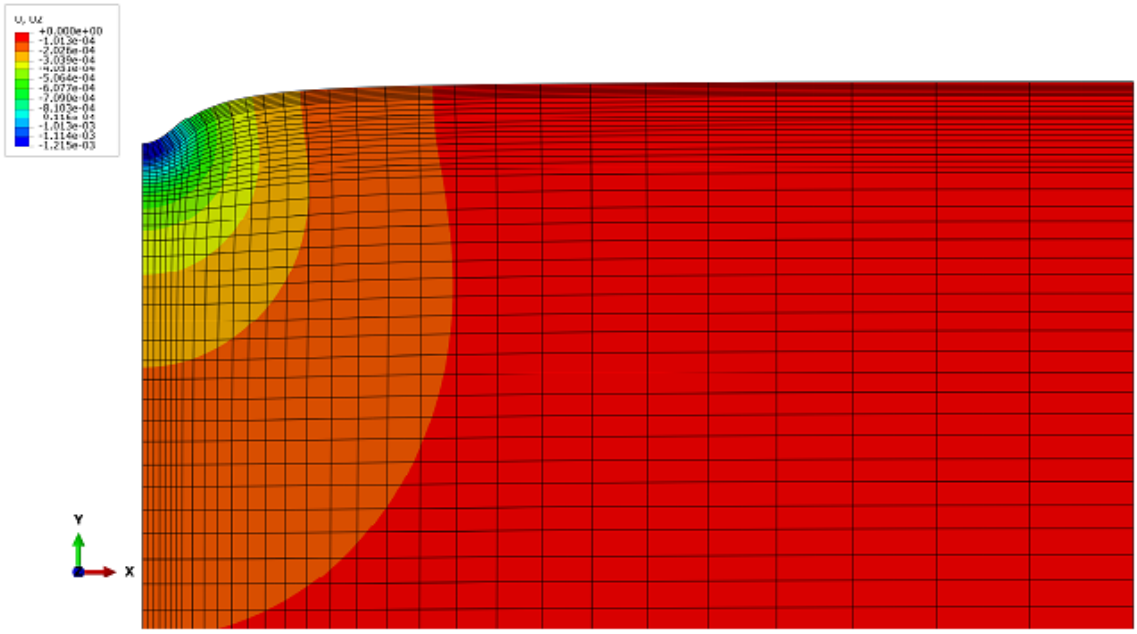
U, Uz
+0.000e+00
-1.013e-04
-2.026e-04
-3.039e-04
-5.064e-04
-6.077e-04
-7.090e-04
-8.103e-04
-1.013e-03
-1.114e-03
-1.215e-03
Y
X

a)

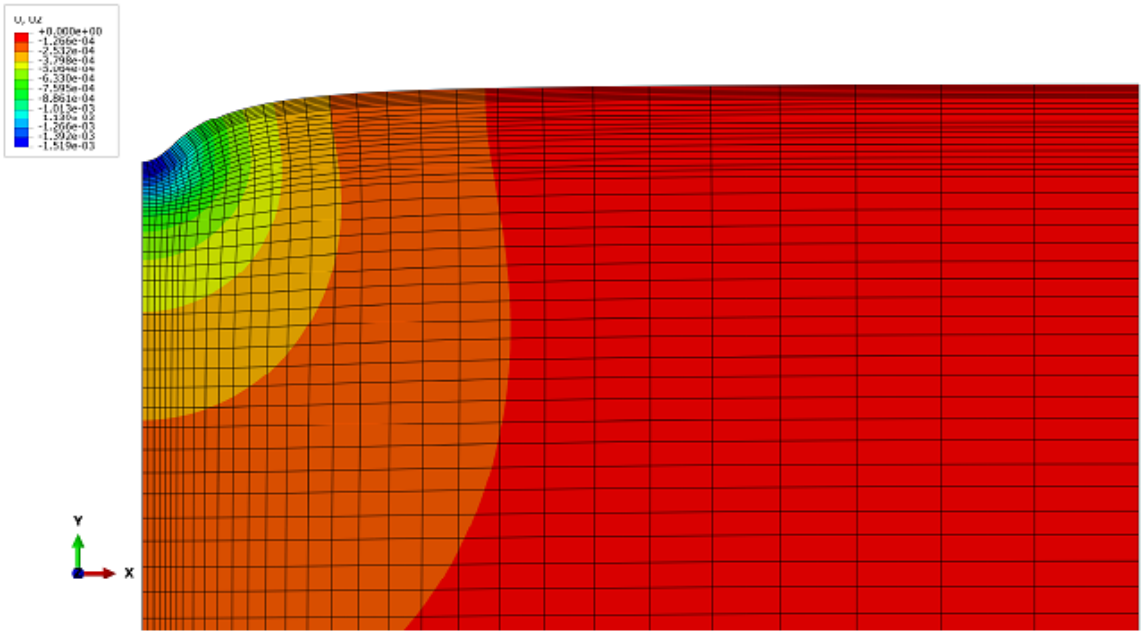
U, Uz
+0.000e+00
-1.266e-04
-2.532e-04
-3.798e-04
-6.330e-04
-7.595e-04
-8.861e-04
-1.013e-03
-1.266e-03
-1.392e-03
-1.519e-03
Y
X

b)

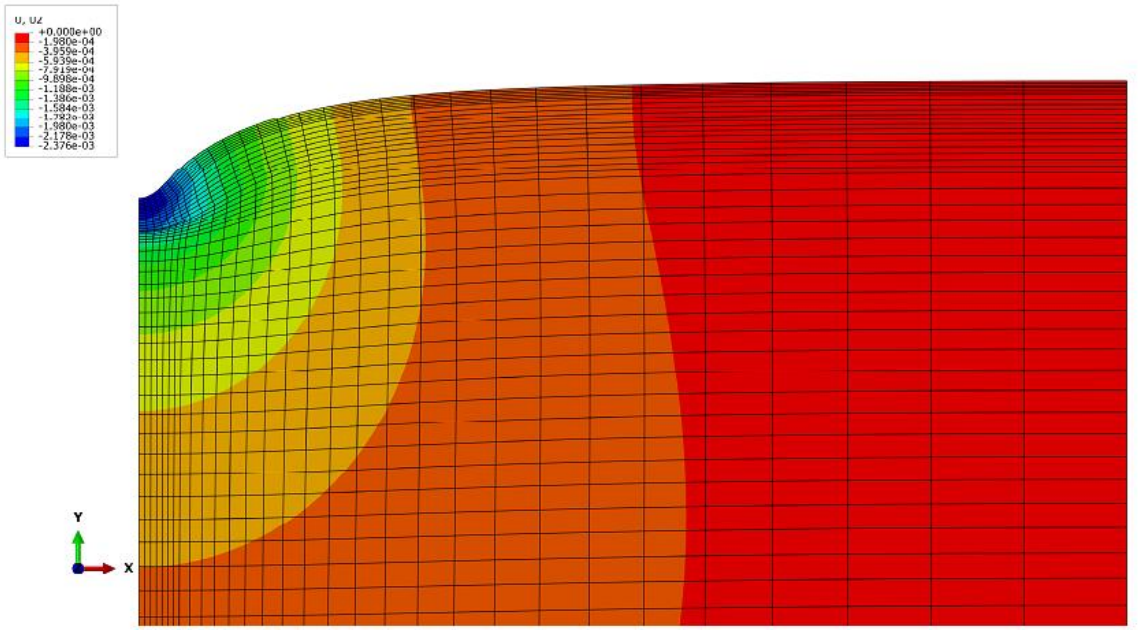

c)

Figure C. 9 surface deflection visualization from finite element analysis for soil A-6 at a) 80%OMC, b) 100%OMC and c) 120%OMC, respectively

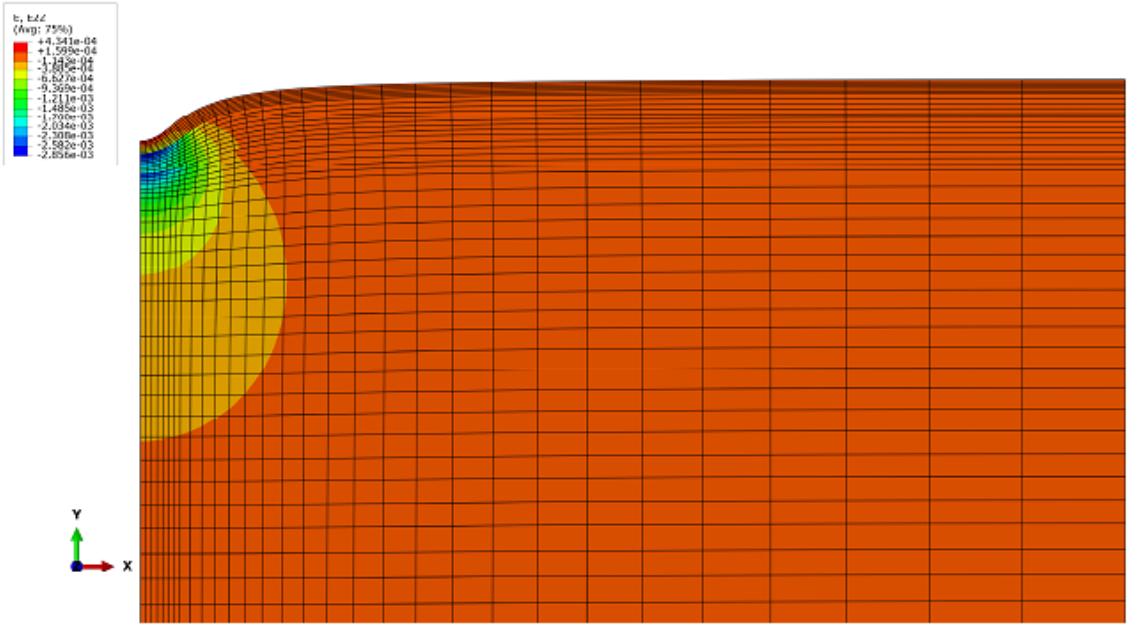

a)

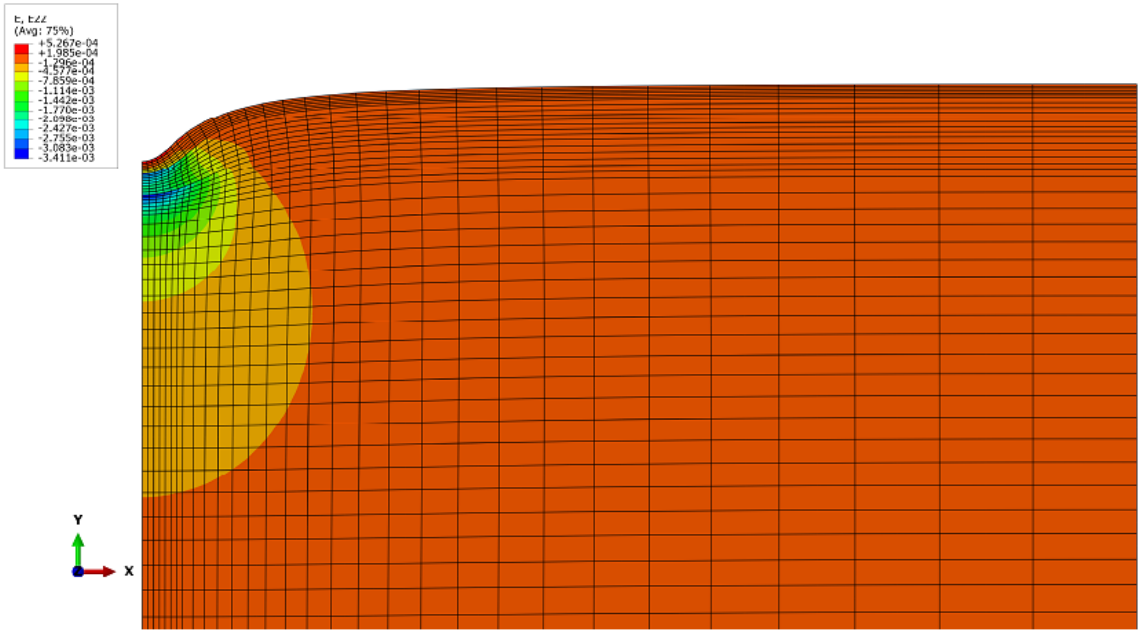

b)

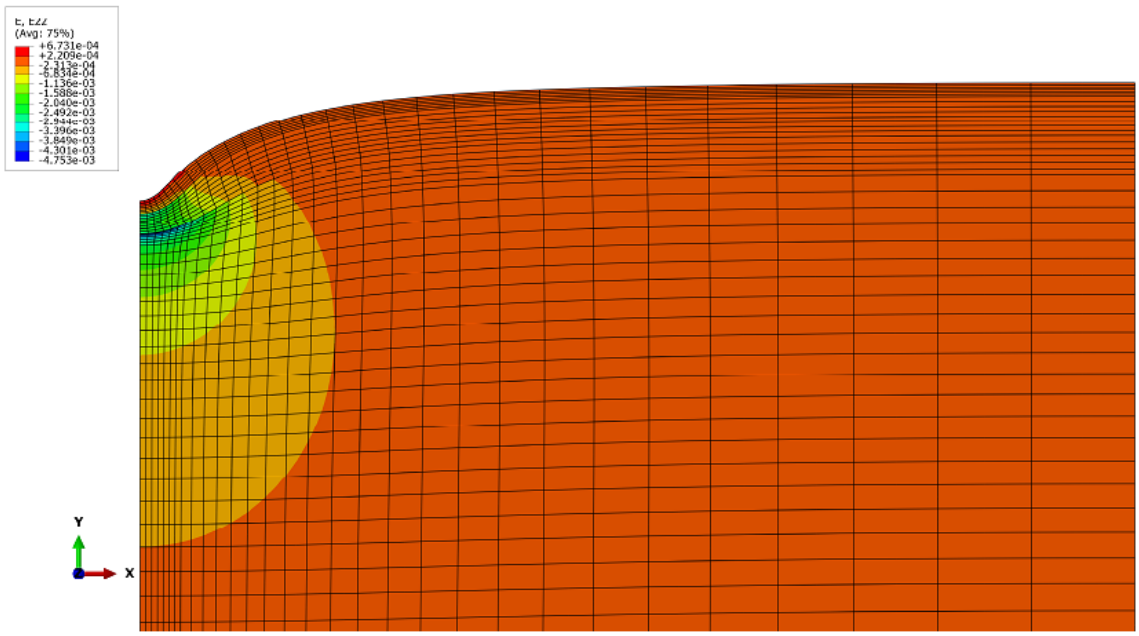

c)

Figure C. 10 compressive strain visualization from finite element analysis for soil A-4 at a) 80%OMC, b) 100%OMC and c) 120%OMC, respectively

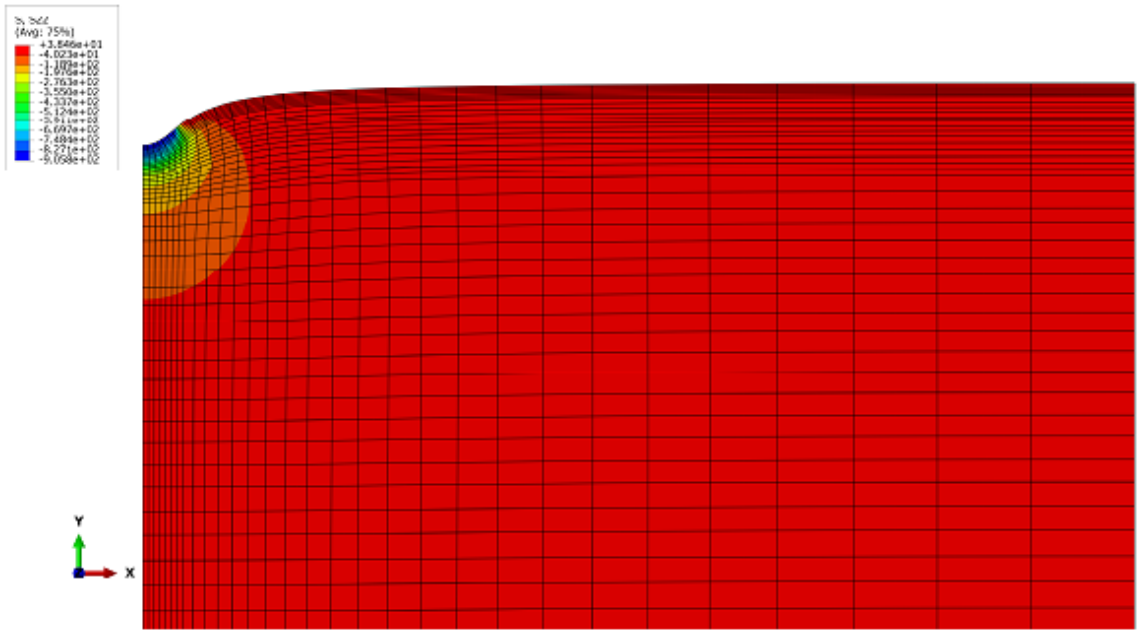

a)

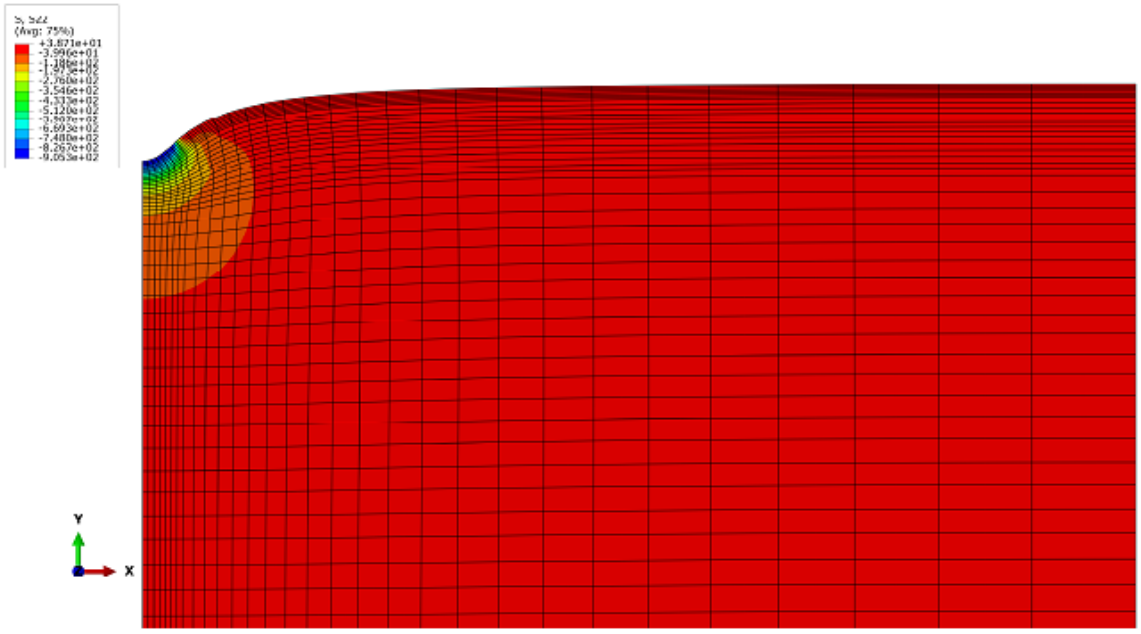

b)

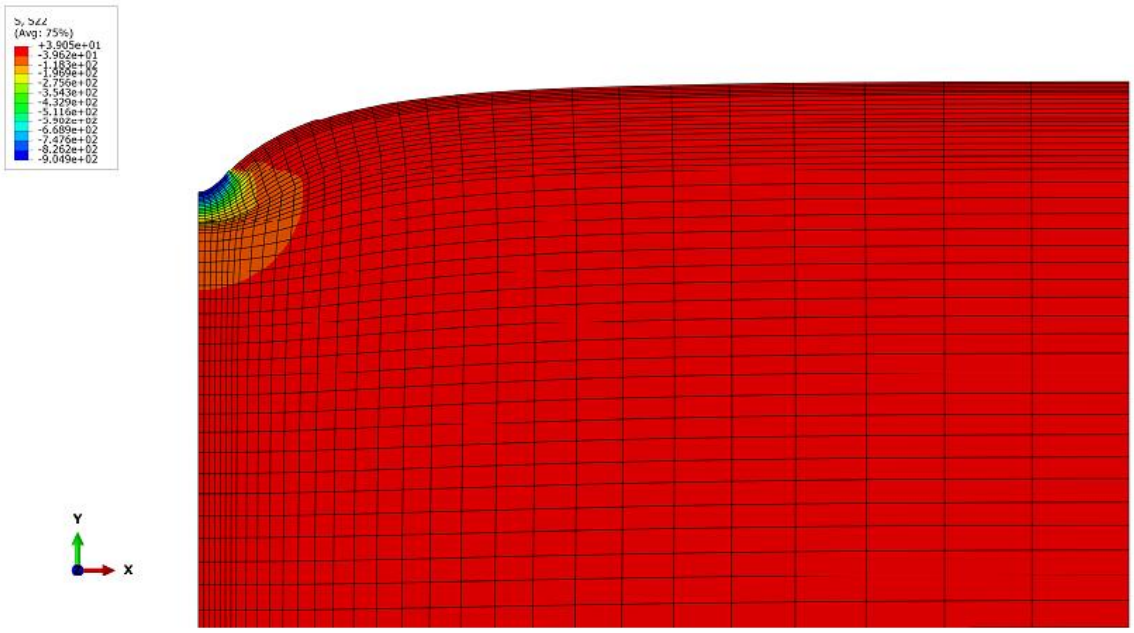

c)

Figure C. 11 compressive strain visualization from finite element analysis for soil A-4 at a) 80%OMC, b) 100%OMC and c) 120%OMC, respectively

Appendix D

D.1 NOTE: Example for Geostatic Consideration

K_o (A-4= 1-Sin (ϕ) = 1- Sin (31) = 0.45, A-6 = 0.48, A-7-5 = 1- Sin (23) = 0.61)

γ (A-4) = 1.76 g/cm^3, (A-6) = 1.769 g/cm^3, (A-7-5) = 1.406 g/cm^3

γ Asphalt =2.33 g/cm^3, γ Base = 2.16

γ pavement = [(2.33×10)+(2.16×20)+(1.753×20)]/(10+20+20) = 2.0312 g/cm^3

σ_3Pavement = K_o ×(γ $_{pavement}$×(tasphalt+tbase+tsubgrade) = 0.48 ×[2.0312×(10+20+20)] = 48.7488 g/cm^2= 4.781 kPa

σ_3Load = 2.759 kPa [(10×20×20) cm, A-4, Mr= 2500, 300, 260, 220 Mpa, 550 kPa tyre pressure]

σ_3 Total = 4.781+2.759 = 7.54 kPa

σ_d Load = $\sigma_1$load -σ_3 load = 50.194-2.759 = 47.435 kPa (from KENLAYER analysis of Chapter7_10×20×20_A-4.DAT)

σ_d Pavement = σ_d pavement - σ_3 pavement

σ_3 Pavement/ σ_1 pavement =K_o

σ_d Pavement= (σ_d pavement/K_o) - σ_3 pavement = (4.781/0.48)- 4.781 = 5.179 kPa

σ_d Total = σ_d load + σ_d pavement = 47.435 + 5.179 = 52.614 kPa

σ_1 Load ≈ σ_d total (50.194, 52.614)

D.2 Deterioration Progression Curves

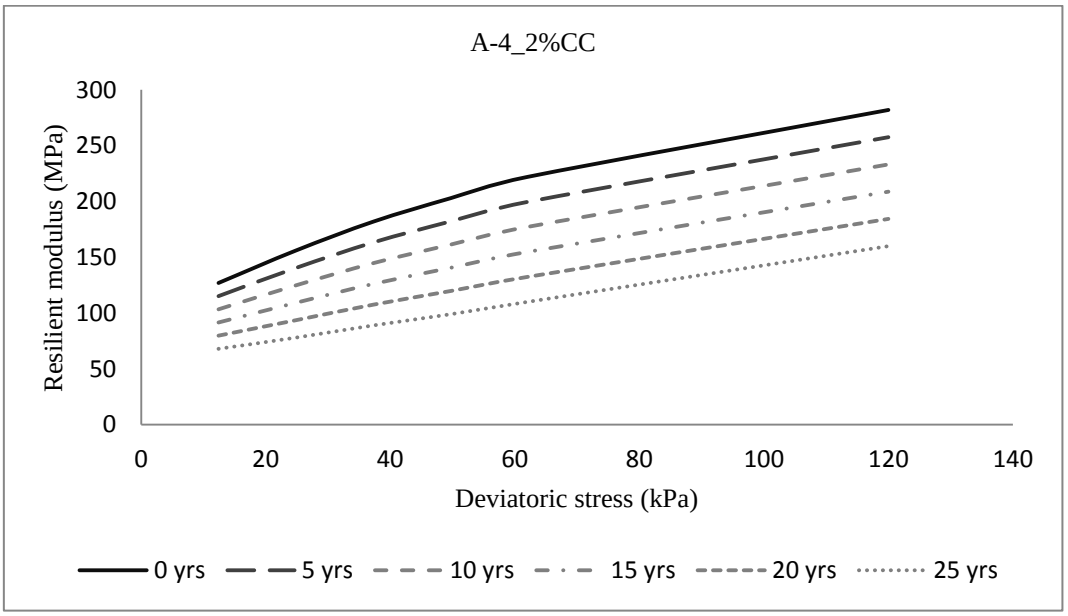

Figure D. 1 Deviatoric stress to resilient modulus values at different stages of deterioration for soil A-4 at 2%CC

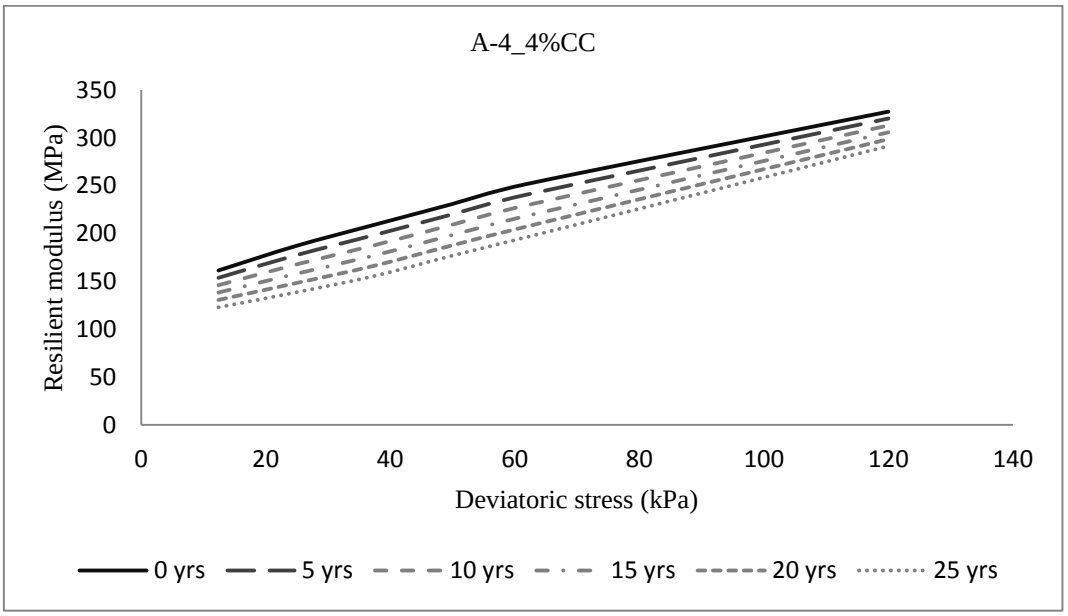

Figure D. 2 Deviatoric stress to resilient modulus values at different stages of deterioration for soil A-4 at 4%CC

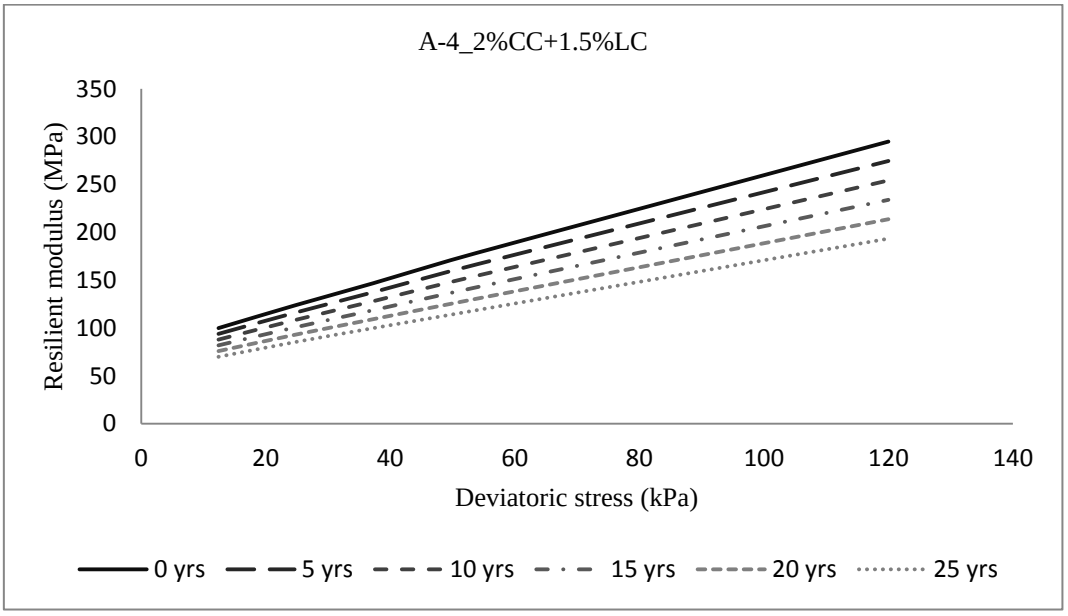

Figure D. 3 Deviatoric stress to resilient modulus values at different stages of deterioration for soil A-4 at 2%CC+1.5%LC

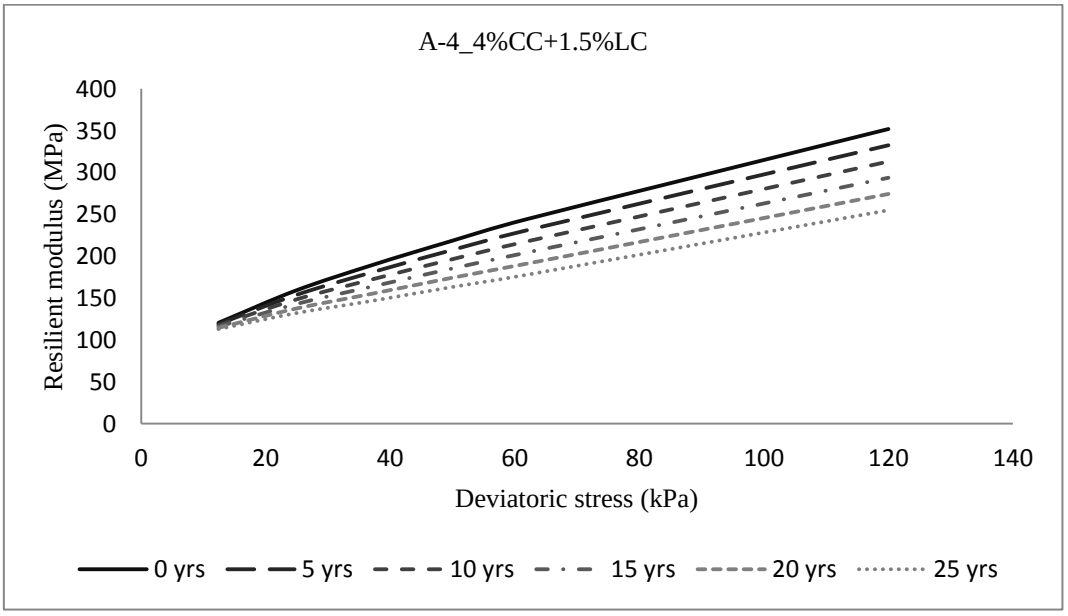

Figure D. 4 Deviatoric stress to resilient modulus values at different stages of deterioration for soil A-4 at 4%CC+1.5%LC

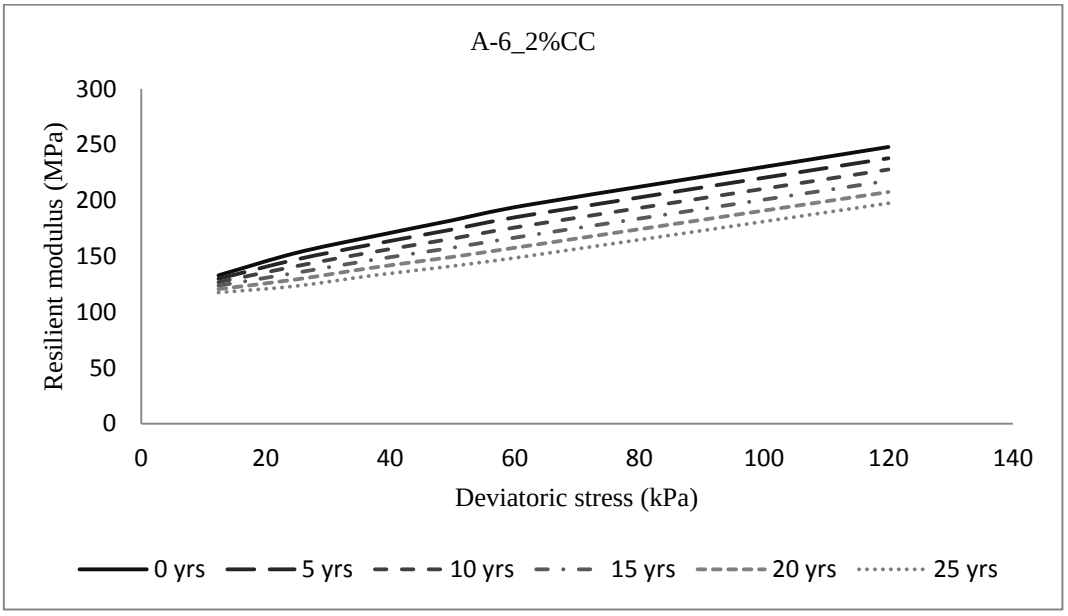

Figure D. 5 Deviatoric stress to resilient modulus values at different stages of deterioration for soil A-6 at 2%CC

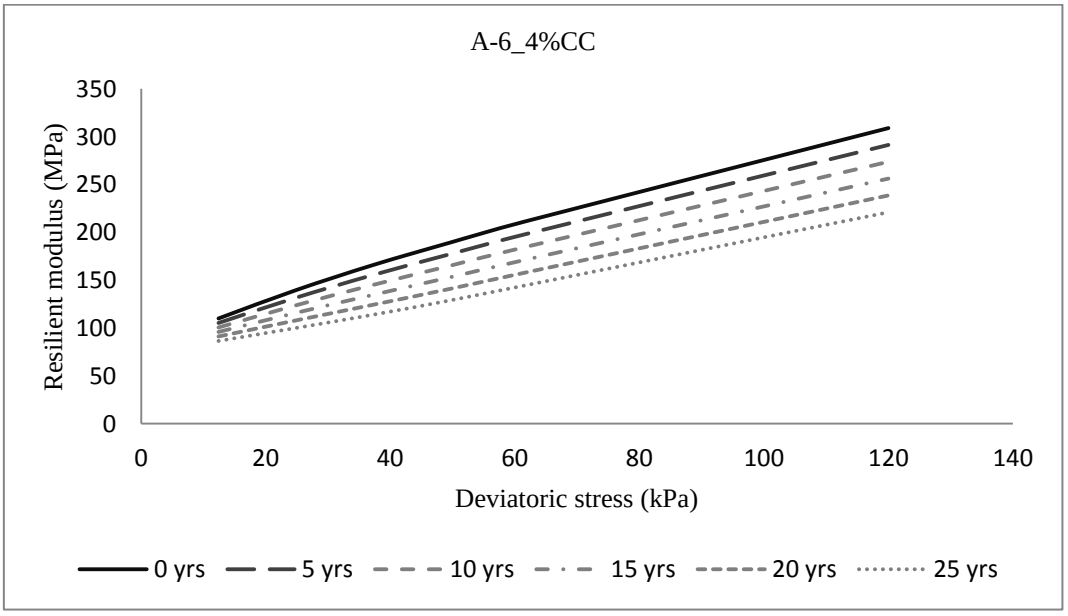

Figure D. 6 Deviatoric stress to resilient modulus values at different stages of deterioration for soil A-6 at 4%CC

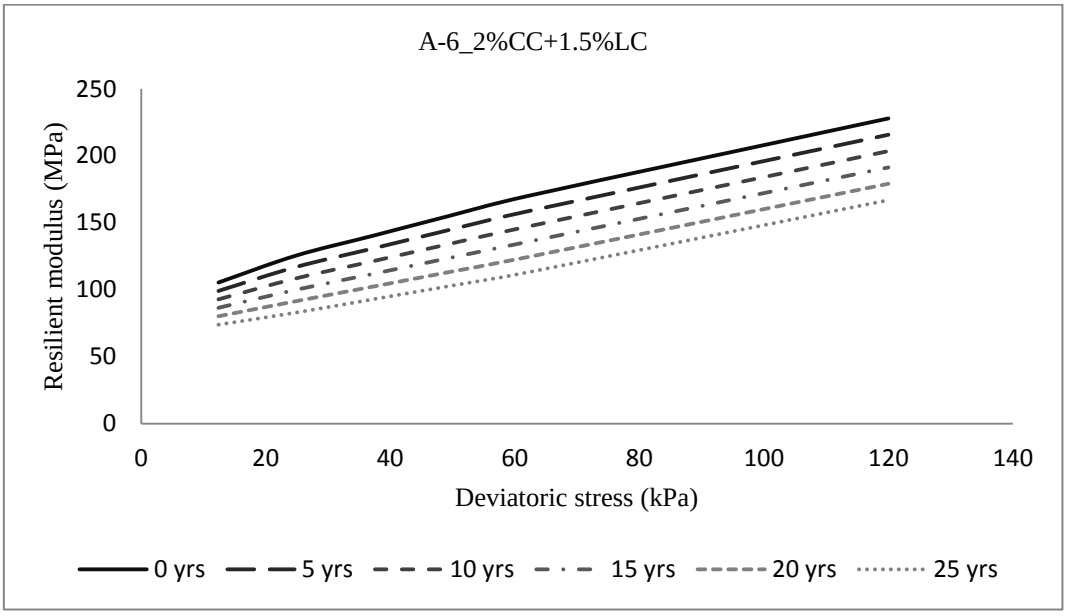

Figure D. 7 Deviatoric stress to resilient modulus values at different stages of deterioration for soil A-6 at 2%CC+1.5%LC

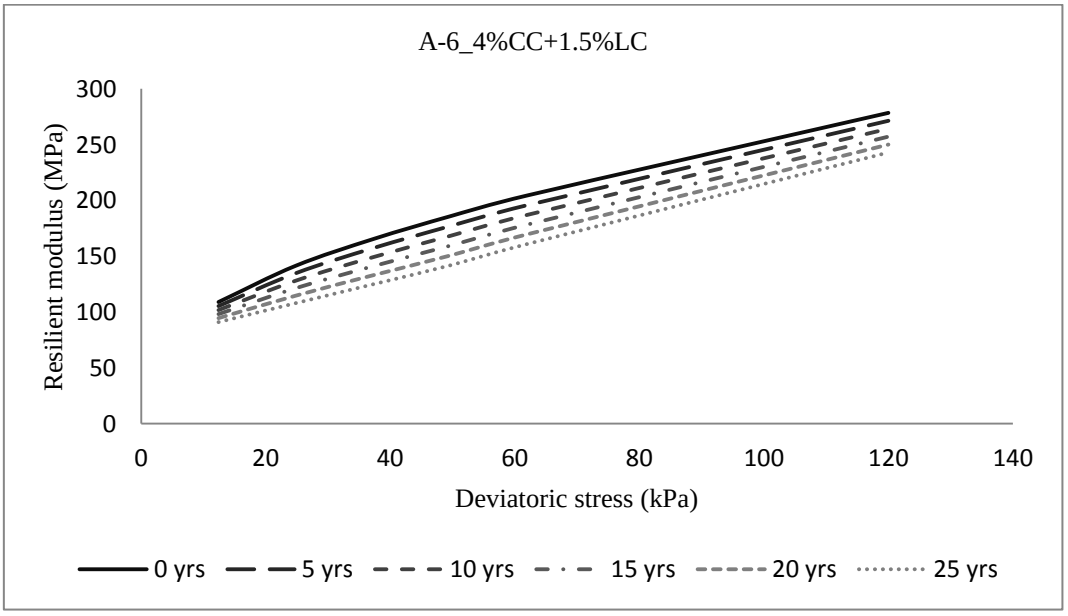

Figure D. 8 Deviatoric stress to resilient modulus values at different stages of deterioration for soil A-6 at 2%CC+1.5%LC

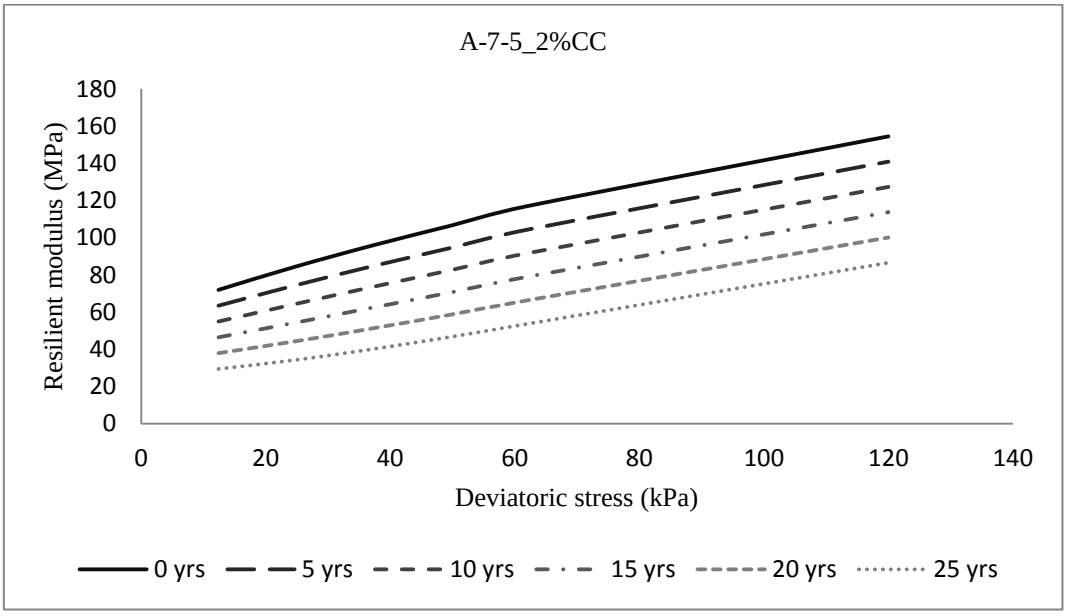

Figure D. 9 Deviatoric stress to resilient modulus values at different stages of deterioration for soil A-7-5 at 2%CC

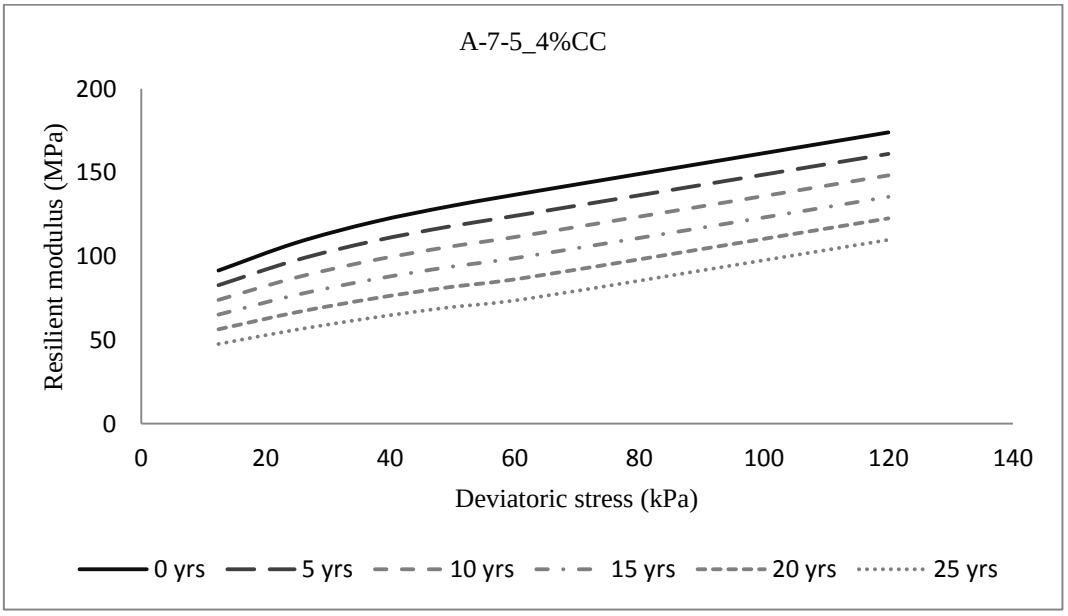

Figure D. 10 Deviatoric stress to resilient modulus values at different stages of deterioration for soil A-7-5 at 4%CC

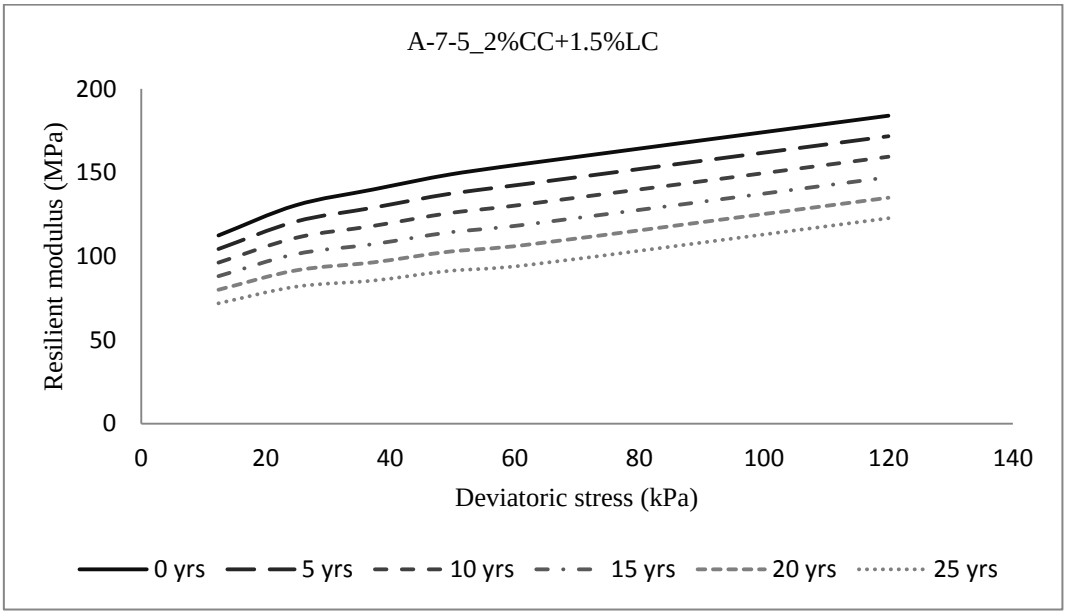

Figure D. 11 Deviatoric stress to resilient modulus values at different stages of deterioration for soil A-7-5 at 2%CC+1.5%LC

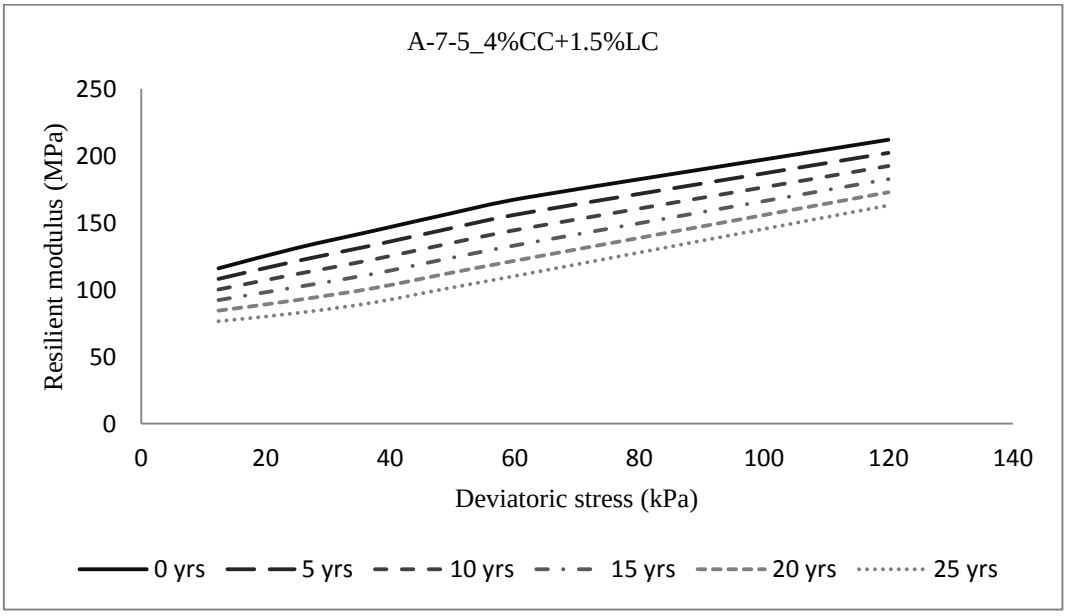

Figure D. 12 Deviatoric stress to resilient modulus values at different stages of deterioration for soil A-7-5 at 4%CC+1.5%LC

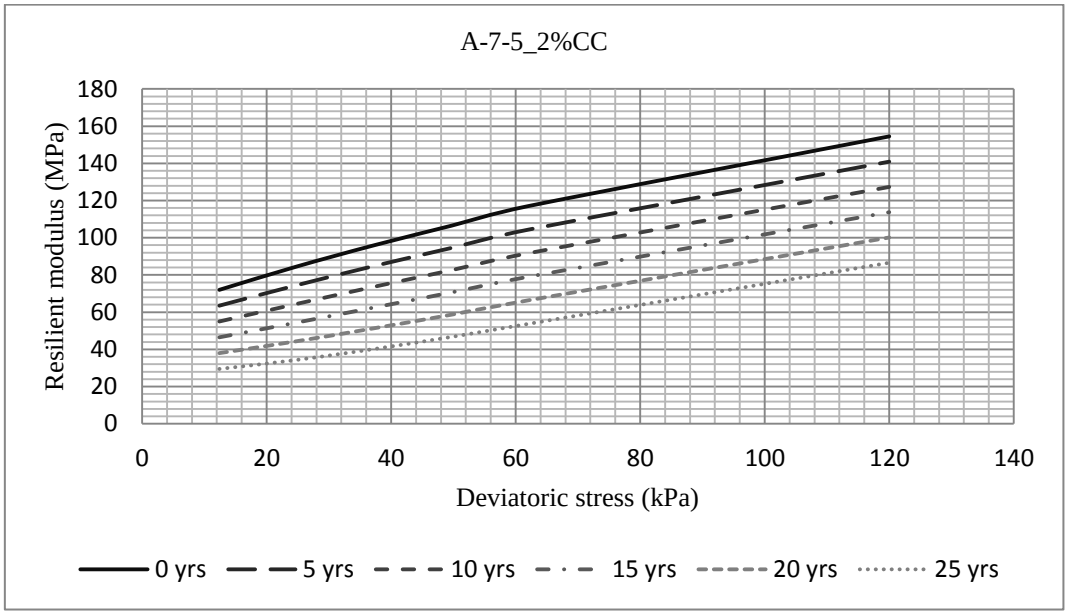

Figure D. 13 Deviatoric stress to resilient modulus values at different stages of deterioration for soil A-7-5 at 2%CC

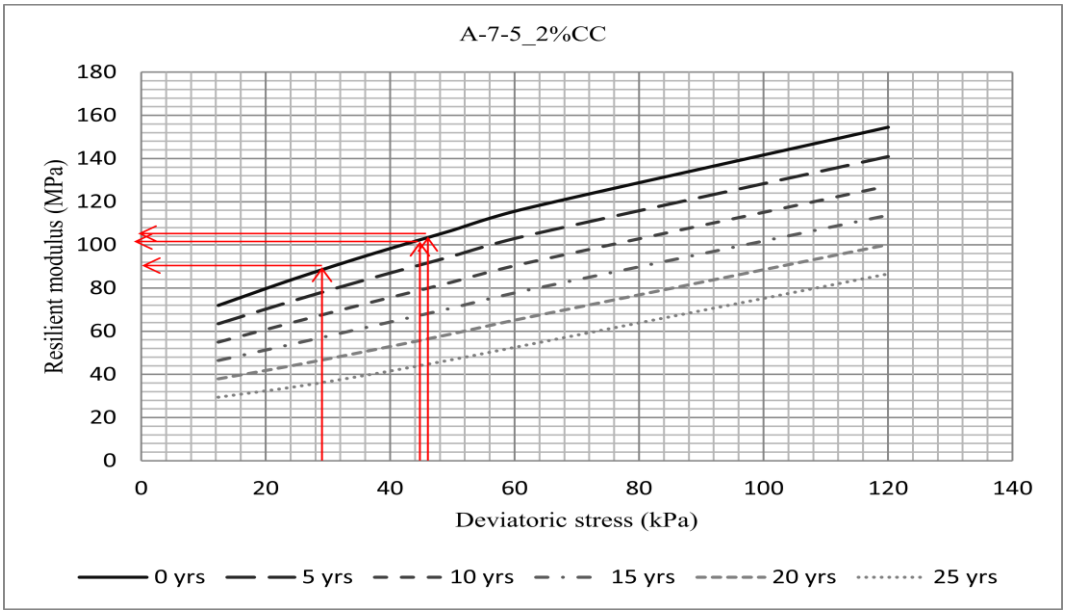

Figure D. 14 Deviatoric stress to resilient modulus values at different stages of deterioration for soil A-7-5 at 2%CC with iterations for resilient modulus and deviatoric stress convergence

Appendix E

E.1 The Relationship between Permanent Deformation and Energy Absorption

The change in material's capability in energy absorption affects the development of permanent deformation; (Wu et al., 2011a) indicated this behaviour in their research on stabilised subgrade soils. From Figure 152 this concept is clearly presented. In addition to the permanent deformation which is directly proportional to the area of the enclosed by the loading and unloading cycle, the resilient modulus behaviour is also can be interpreted that with increase the number of load repetitions the resilient modulus increases as can be seen from the slope of the cycles. Figures 153-156 show the same relationships for unstabilised soils at 62.0 kPa deviatoric stress.

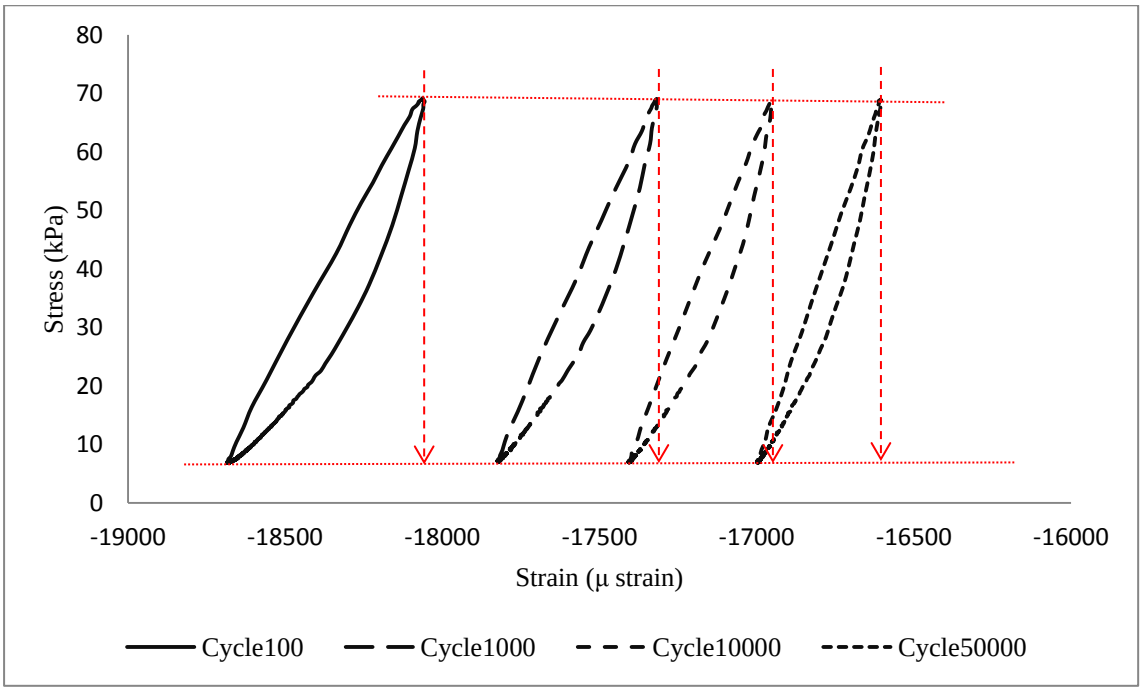

Figure E. 1 Comparison of energy absorption for cycles 100, 1000, 10000, 50000 for soil A-4 at 62.0 kPa deviatoric stress at 100%OMC

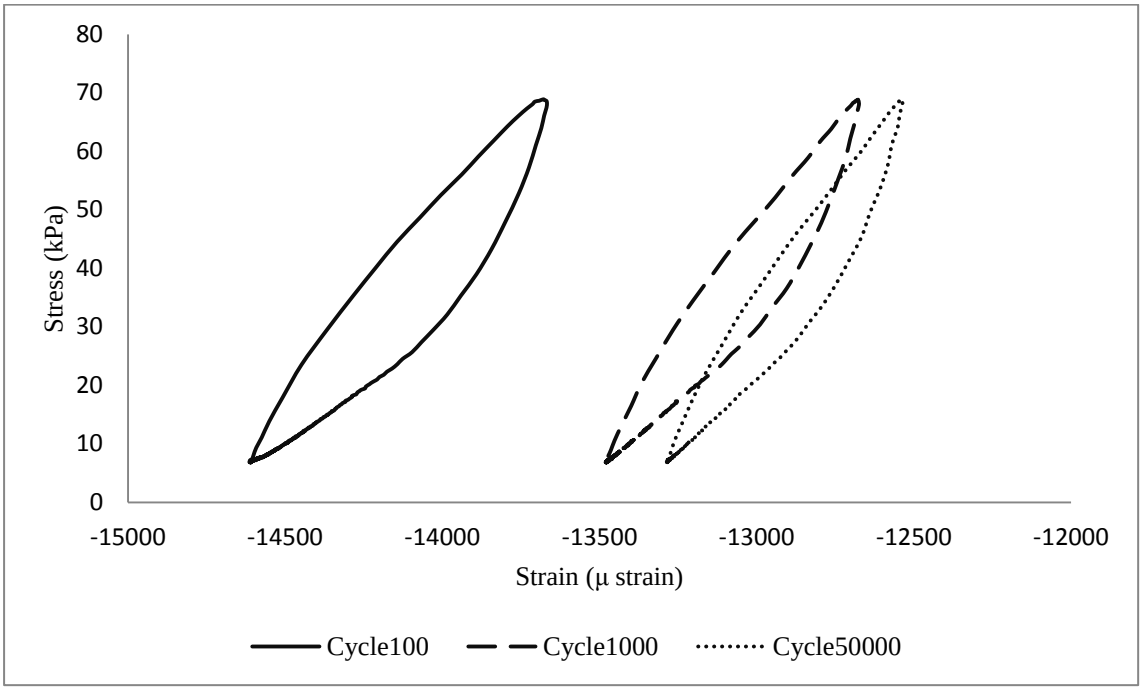

Figure E. 2 Comparison of energy absorption for cycles 100, 1000, 50000 for soil A-6 at 62.0 kPa deviatoric stress at 100%OMC

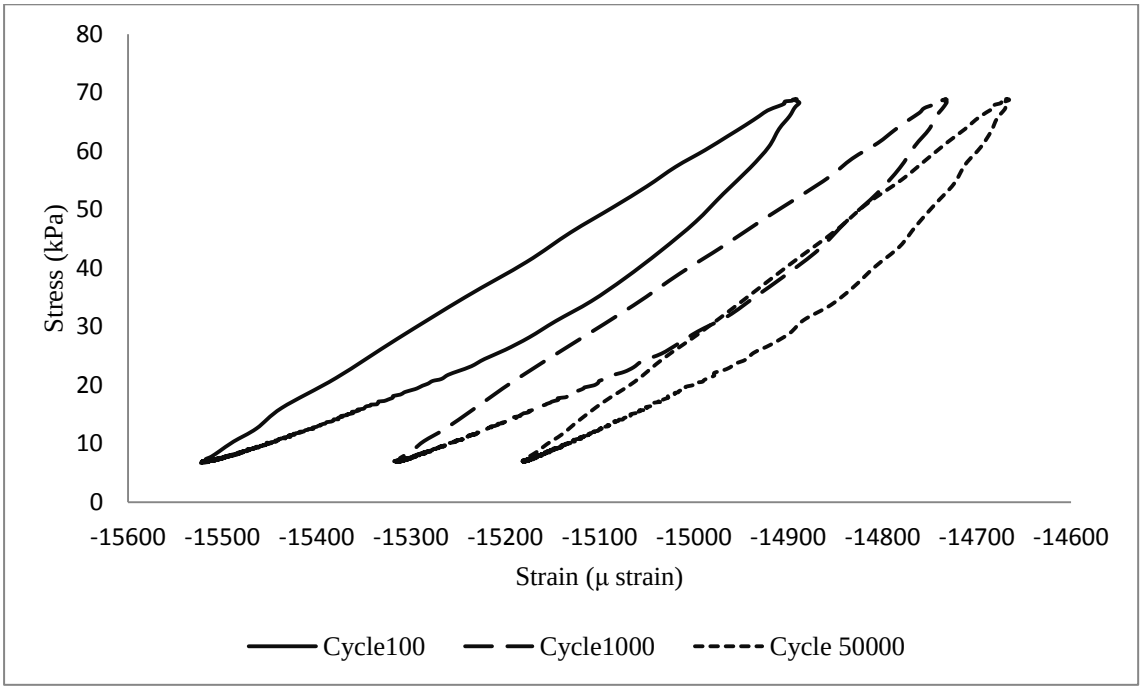

Figure E. 3 Comparison of energy absorption for cycles 100, 1000, 50000 for soil A-6 at 62.0 kPa deviatoric stress at 80%OMC

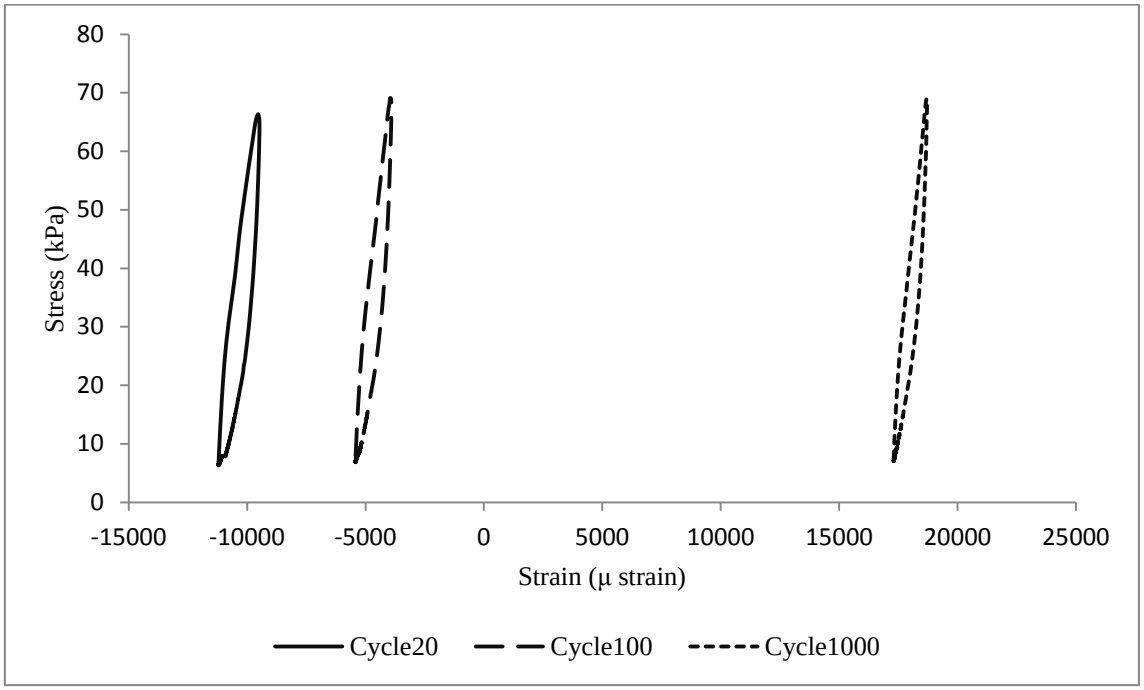

Figure E. 4 Comparison of energy absorption for cycles 100, 1000, 50000 for soil A-6 at 62.0 kPa deviatoric stress at 120%OMC

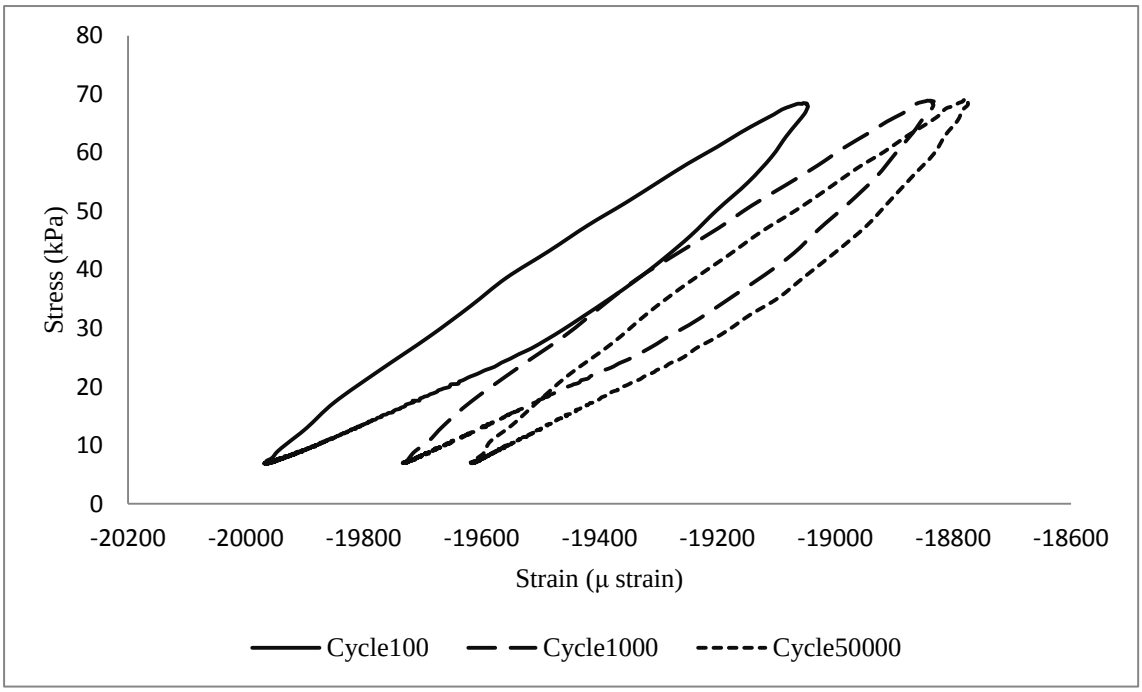

Figure E. 5 Comparison of energy absorption for cycles 100, 1000, 50000 for soil A-7-5 at 62.0 kPa deviatoric stress at 100%OMC

The strain-stress relationships for stabilised at different stabiliser contents are presented in Figures 157 and 158. From these figures it is clear the same concept is can be applied. One important conclusion from these figures is that, the smaller the area of the cycle is the less possibility of further progress of the permanent deformation. This matches well with the interpretations and explanations presented in Chapters 3, 4 and 5 about the resilient modulus and permanent deformation in unstabilised and stabilised subgrade soils.

Figures 159-161 show the hysteric cycles at cycle 100th and 50000th for unstabilised soils A-4, A-6 and A-7-5. From these figures it can be seen that soil A-7-5 is still exposed to further permanent deformation with the current stress state, while soil A-4 show opposite and stabilised with the current stress state and may show further permanent deformation with increase in stress level.

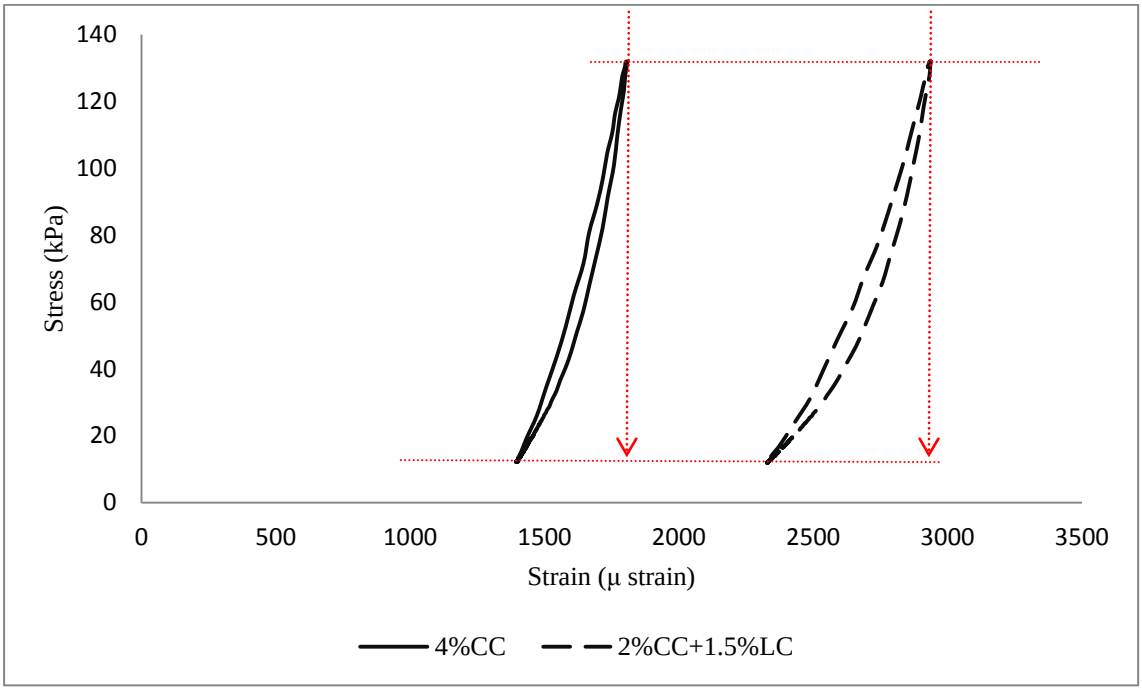

Figure E. 6 Comparison of energy absorption for 50000th cycle of soil A-4 stabilised with 4%CC and 2%+1.5%LC

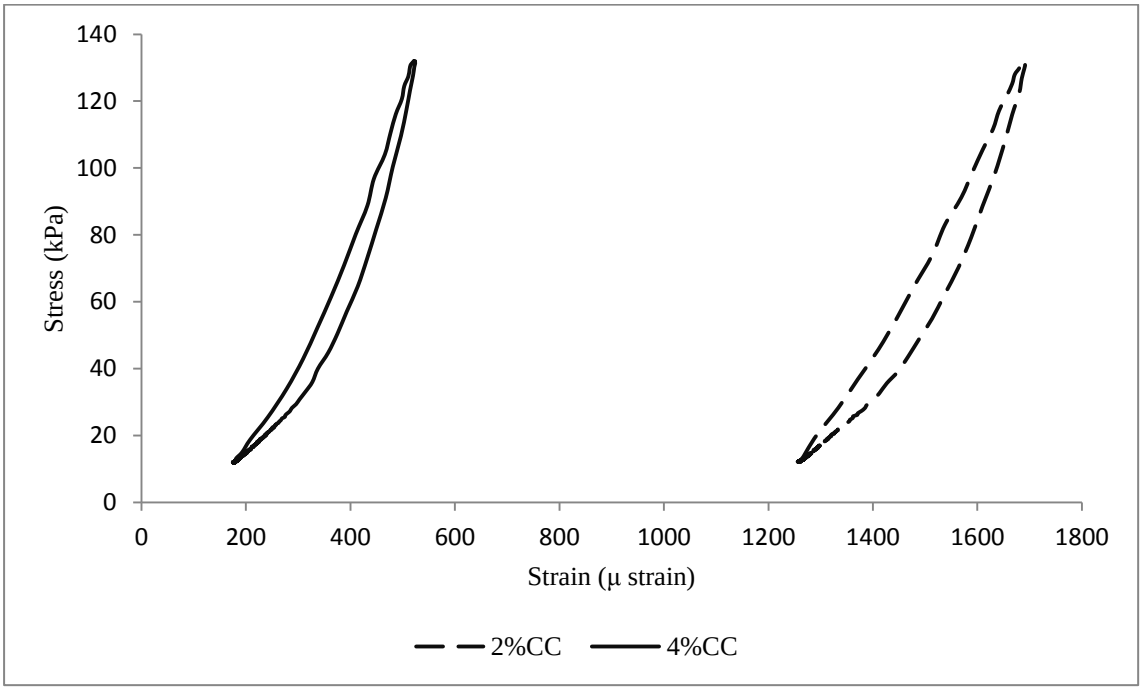

Figure E. 7 Comparison of energy absorption for 50000th cycle of soil A-6 stabilised with 2%CC and 4%CC

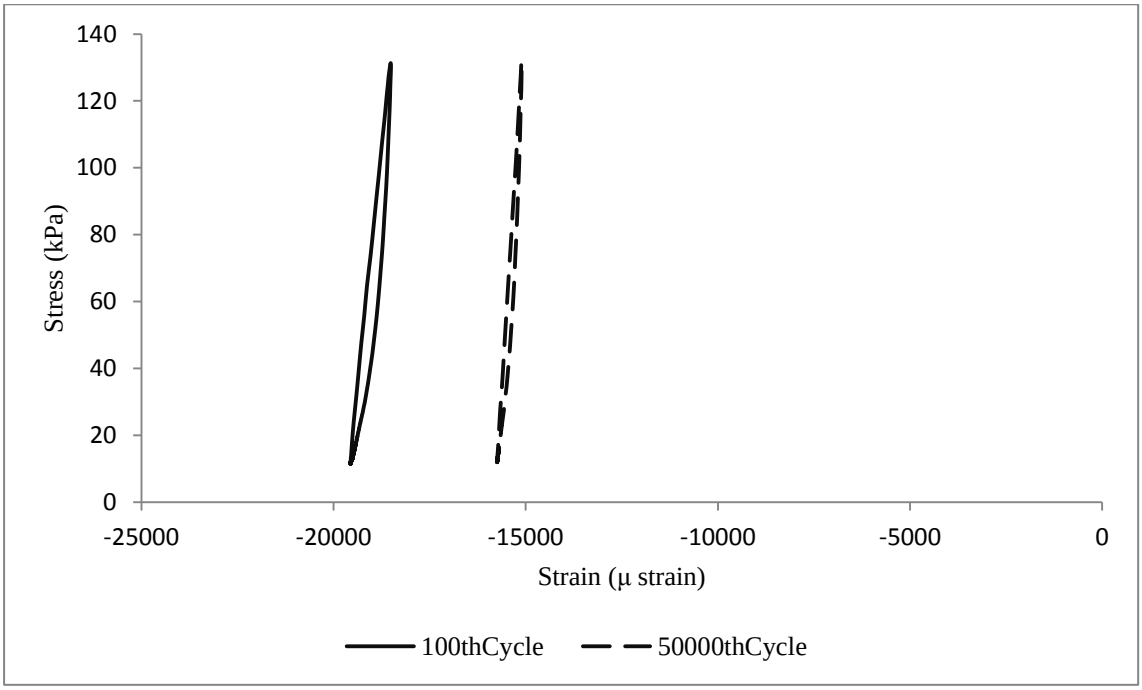

Figure E. 8 Comparison of cycles 100 and 50000 for unstabilised soil A-4 at 120 kPa deviatoric stress

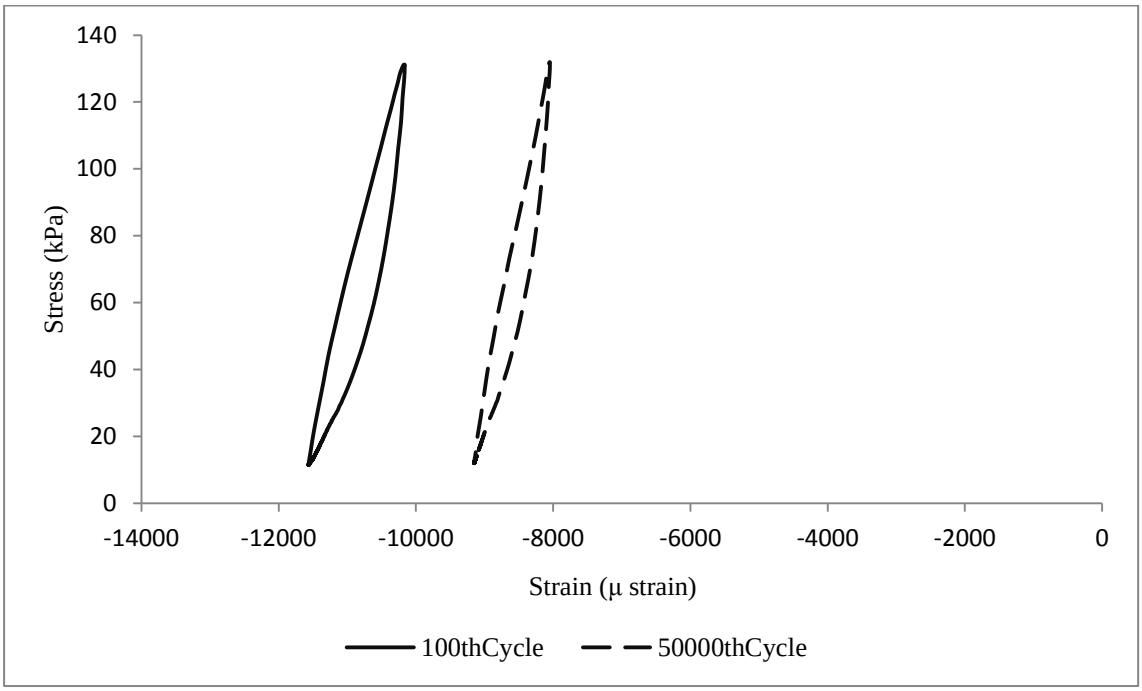

Figure E. 9 Comparison of cycles 100 and 50000 for unstabilised soil A-6 at 120 kPa deviatoric stress

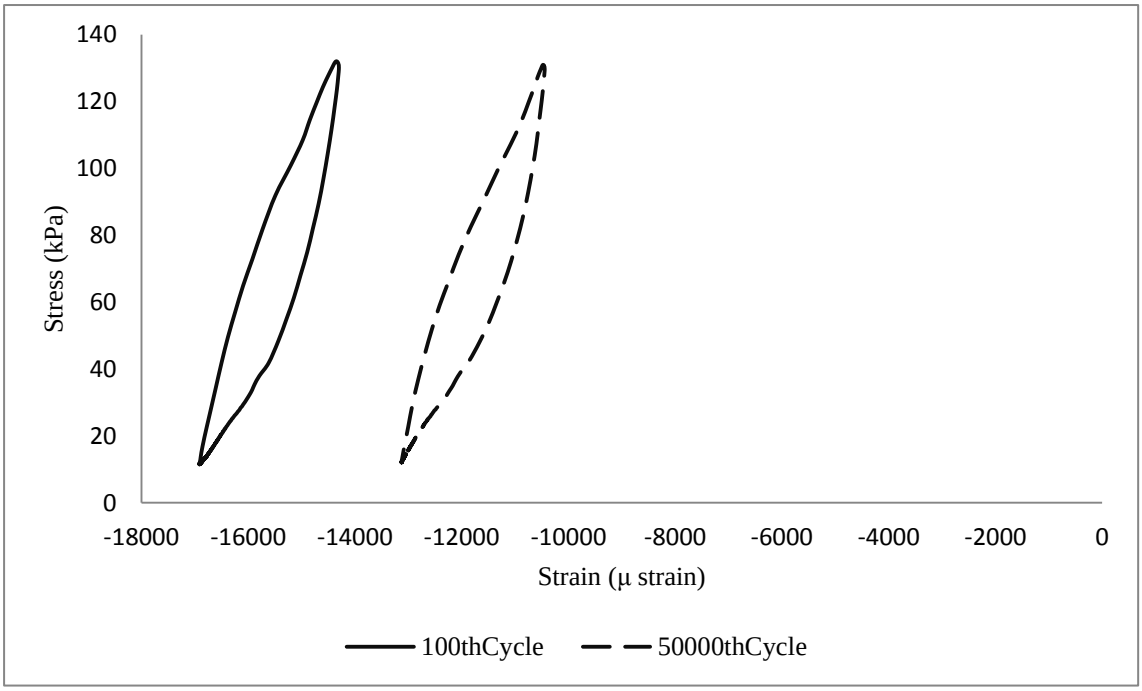

Figure E. 10 Comparison of cycles 100 and 50000 for unstabilised soil A-7-5 at 120 kPa deviatoric stress

Appendix F

F1. Pavement Design Example

For pavement section shown in Figure 7.16 all the design parameters are as example 1. The material properties available are the unconfined compressive strength (UCS) at 7 days curing and the resilient modulus values and Mohr-Coulomb parameters for native soils as following:

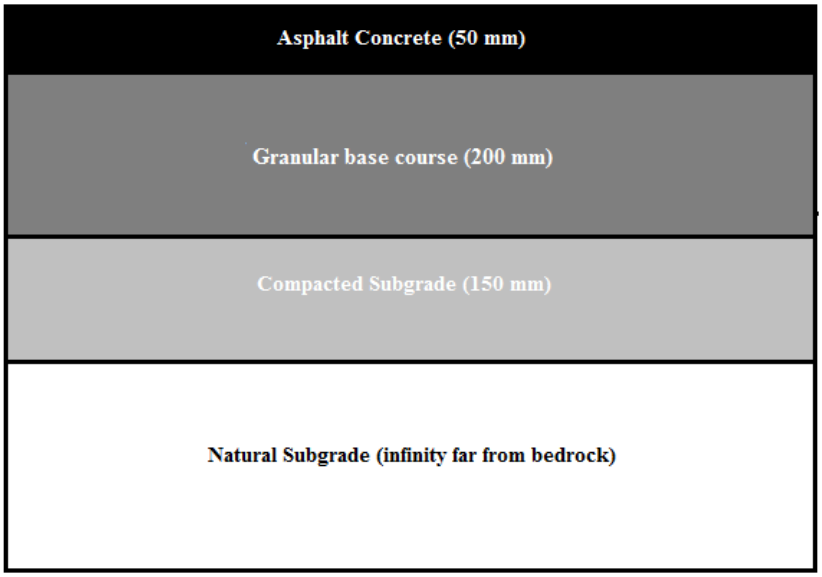

Figure F. 1 Road pavement section for pavement design example

Table F. 1 Mohr-Coulomb parameters for the three soil types at three different moisture contents

UU Triaxial Test		
Soil type and MC%	**Friction angle (ϕ)**	**Cohesion, C (kPa)**
A-480%OMC	31	45
A-4100%OMC	31	32
A-4120%OMC	17	44
A-680%OMC	29	40
A-6100%OMC	31	30
A-6120%OMC	9	50
A-7-580%OMC	24	74
A-7-5100%OMC	23	60
A-7-5120%OMC	20	54

Table F. 2 Resilient modulus values for the three unstabilised subgrade soils

Deviatoric stress (kPa)	Resilient modulus (Mpa)		
	A-4	A-6	A-7-5
12.4	99	101	70
24.8	132	100	72
37.3	146	95	68
49.7	157	89	62
62	165	86	57
120	169	95	47

Table F. 3 unconfined compressive strength for the three soils at four different stabiliser contents

Soil type and stabilizer	UCS(kPa)
A-4_2%CC	580
A-4_4%CC	969
A-4_2%CC+1.5%LC	618
A-4_4%CC+1.5%LC	955
A-6_2%CC	559
A-6_4%CC	845
A-6_2%CC+1.5%LC	574
A-6_4%CC+1.5%LC	774
A-7-5_2%CC	275
A-7-5_4%CC	357
A-7-5_2%CC+1.5%LC	427
A-7-5_4%CC+1.5%LC	501

Design

Material properties

- The pavement section is analysed for three seasons of the first year in which the year is divided into three seasons 4 months each.
- For these seasons the resilient modulus values are adjusted using equation 7.4

$$log\frac{M_R}{M_{Ropt}} = a + \frac{b-a}{1+EXP[ln\frac{-b}{a}+k_m*(S-S_{opt})]}$$

The degrees of saturation for the three soils are as following from Table 4.1:

Soil type & M.C	**Degree of saturation (%)**
A-480%OMC	44.9
A-4100%OMC	57.0
A-4120%OMC	68.3
A-680%OMC	48.4
A-6100%OMC	61.1
A-6120%OMC	75.0
A-7-580%OMC	44.3
A-7-5100%OMC	55.5
A-7-5120%OMC	66.5

From the resilient modulus values in Table 7.9, degree of saturation from Table 4.1 and the equation 7.4 the resilient modulus values for the three soils at wet and dry side of optimum moisture are found and Tabulated in Table 11.

Next the material parameters used in Drucker-Prager model are determined for soils A-4 and A-6 for stress dependency consideration of natural subgrade, Table 6.9 is repeated here. However, due to unavailability of consolidation test parameters for soil A-7-5 for Cam-clay model parameters, the method of iteration is used.

Table F. 4 determination of the resilient modulus values at wet and dry of optimum moisture content for the three soils

Deviatoric stress (kPa)	Resilient modulus (Mpa)			Resilient modulus (Mpa)			Resilient modulus (Mpa)		
	A-4			A-6			A-7-5		
	80% OMC	100% OMC	120% OMC	80% OMC	100% OMC	120% OMC	80% OMC	100% OMC	120% OMC
12.4	129	99	76	134	101	74	99	70	48
24.8	173	132	102	133	100	73	101	72	49
37.3	192	146	113	126	95	69	96	68	46
49.7	206	157	121	119	89	65	87	62	42
62	216	165	127	115	86	63	80	57	39
120	221	169	130	126	95	69	66	47	32

UU Triaxial Test					Drucker-Prager parameters	
Soil type and MC%	**Friction angle (ϕ)**	**Cohesion, C (kPa)**	**σs at 27kPa Confining pressure**	τf	**Friction angle (β)**	**Cohesion, d**
A-480%OMC	31	45	300	225	41.7	66.8
A-4100%OMC	31	32	236	180	41.7	47.5
A-4120%OMC	17	44	181	99	26.9	72.9
A-680%OMC	29	40	257	182	40	60.6
A-6100%OMC	31	30	229	168	41.7	44.5
A-6120%OMC	9	50	129	70	15	85.5

For resilient modulus values of stabilised soils, the UCS test results and equation 4.10 are used. A series of deviatoric stresses can be selected for resilient modulus determination depending on the expected stresses for a specified pavement section. However, in this example the deviatoric stresses used for native soil are used and higher stresses are used according to necessity of iteration procedure. Table 7.12 shows the results from the equation for a series of deviatoric stresses and four different stabilisation ratios. Figures 7.17 through 7.19 show the deviatoric stress to resilient modulus relation for the three soils at four stabiliser ratios.

$$Mr = UCS^{a+b*\sigma_d}$$

$$Mr = UCS^{0.758+0.001*\sigma_d}$$

Table F. 5 Resilient modulus calculation from UCS test results

Soil type and stabilizer	UCS (kPa)	Deviatoric Stress (kPa)	**12.4**	**24.8**	**37.3**	**49.7**	**62.0**	**120.0**	**150**
A-4_2%CC	580	**Resilient modulus (MPa)**	135	146	158	171	185	267	323
A-4_4%CC	969		200	218	237	258	281	419	515
A-4_2%CC+1.5%LC	618		141	153	166	180	194	282	342
A-4_4%CC+1.5%LC	955		198	215	234	255	278	413	508
A-6_2%CC	559		131	141	153	166	179	258	312
A-6_4%CC	845		180	195	213	231	251	371	455
A-6_2%CC+1.5%LC	574		133	144	156	169	183	264	320
A-6_4%CC+1.5%LC	774		168	183	198	215	234	344	420
A-7-5_2%CC	275		76	81	87	93	100	139	164
A-7-5_4%CC	357		93	100	107	115	124	174	208
A-7-5_2%CC+1.5%LC	427		106	115	124	133	144	204	245
A-7-5_4%CC+1.5%LC	501		120	130	140	152	164	235	283

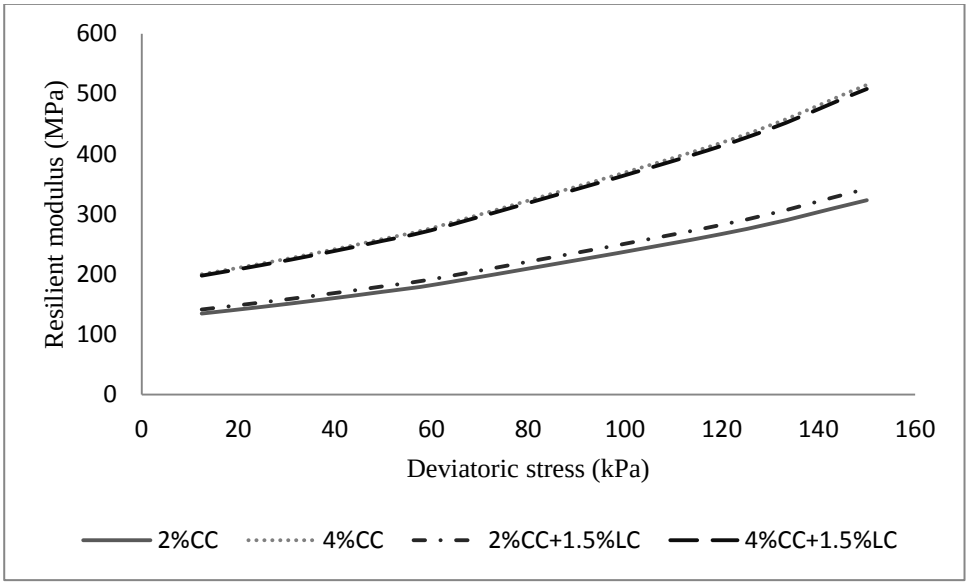

Figure F. 2 Deviatoric to resilient modulus curves for soil A-4

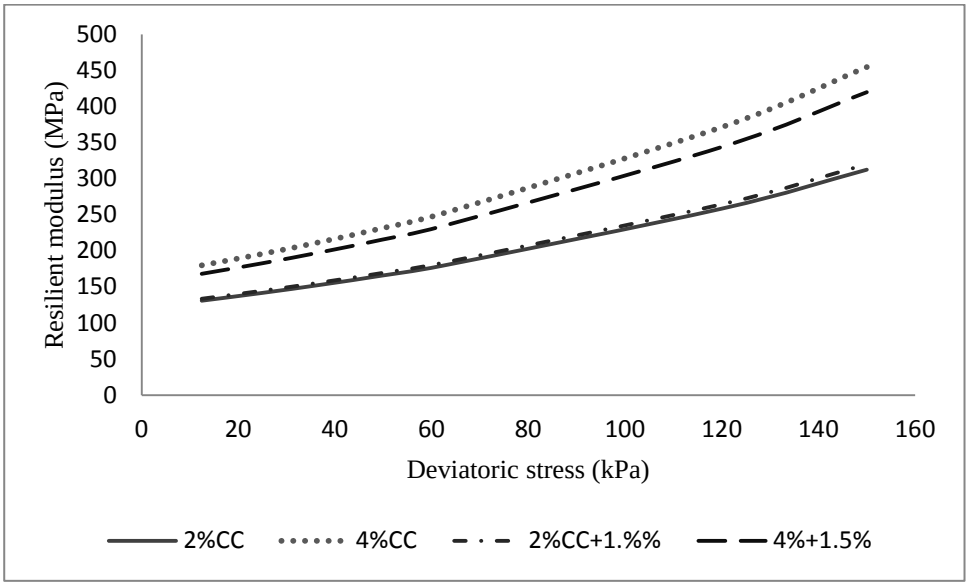

Figure F. 3 Deviatoric to resilient modulus curves for soil A-6

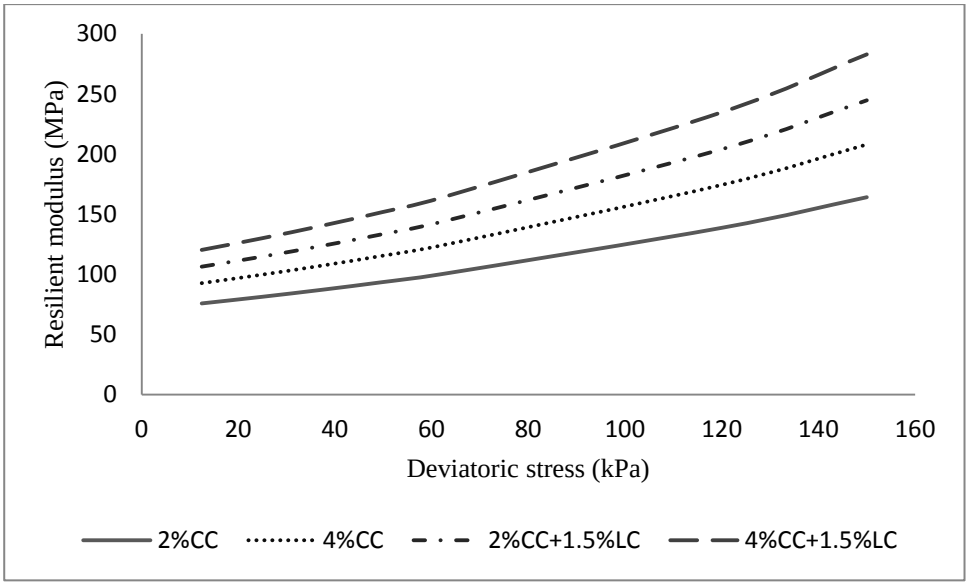

Figure F. 4 Deviatoric to resilient modulus curves for soil A-7-5

Traffic

- Assume the traffic is distributed evenly between the 12 months of the year.
- Average daily number of traffic; assume single axle for the whole year = 300000/365= 822 average daily number of heavy vehicles

  Number of heavy vehicles for dry season = number of heavy vehicles for wet season=number of heavy vehicles for optimum moisture content=122 days *822 vehicles= 10284

Analysis for stresses, strains and permanent deformation

Tables 7.13 to 7.15 show the analyses results of the pavement section.

Table F. 6 analysis results for stress and resilient modulus converge and plastic deformation calculation for soil A-4

	A-4_2%CC+15%LC			A-4_4%CC+15%LC		
	80% OMC	100% OMC	120% OMC	80% OMC	100% OMC	120% OMC
Resilient modulus MDL3 (Mpa)	260	260	245	400	380	360
Vertical stress MDL3 (kPa)	113	104	96	115	106	98
Resilient modulus L4 (Mpa)	220	165	130	220	165	130
Vertical stress L4 (kPa) Top	81	73	66	79	71	64
Resilient strain MDL3 (μ strain)	464	457	473	329	340	353
Resilient strain L4 (μ strain) Top	351	425	495	339	406	469
Resilient modulus 6 cm below TS	218	165	128	218	162	120
Vertical stress 6 cm below TS	65	59	54	64	57	52
Resilient strain 6 cm below TS	286	346	403	277	333	384
Number of heavy trucks	10284	10284	10284	10284	10284	10284
parameter *(a)*	1075.3	1075.3	1075.3	1075.3	1075.3	1075.3
parameter *(b)*	0.042	0.042	0.042	0.042	0.042	0.042
Permanent strain MDL3 (μ strain)	688.91	634.04	621.10	455.72	442.16	431.50
Permanent strain MDL3 (mm)	0.138	0.127	0.124	0.091	0.088	0.086
Total permanent strain MDL3 (mm)	0.389			0.266		
parameter *(a)*	1955.4	1707.8	1239.8	1955.4	1707.8	1239.8
parameter *(b)*	0.086	0.171	0.44	0.086	0.171	0.44
Permanent strain 6 cm below L4 (μ strain)	1290.43	2964.03	30470.51	1270.58	2916.58	31298.10
Permanent strain 6 cm below L4 (mm)	0.155	0.356	3.656	0.152	0.350	3.756
Total permanent strain 6 cm below L4(mm)	4.167			4.258		

Table F. 7 analysis results for stress and resilient modulus converge and plastic deformation calculation for soil A-6

	A-6_2%CC+15%LC			A-6_4%CC+15%LC		
	80% OMC	100% OMC	120% OMC	80% OMC	100% OMC	120% OMC
Resilient modulus MDL3 (Mpa)	220	210	200	290	277	262
Vertical stress MDL3 (kPa)	92	84	76	93	85	77
Resilient modulus L4 (Mpa)	114	87	66	113	88	66
Vertical stress L4 (kPa) Top	63	56	49	62	55	48
Resilient strain MDL3 (μ strain)	509	522	538	415	428	447
Resilient strain L4 (μ strain) Top	541	633	735	525	603	699
Resilient modulus 6 cm below TS	117	90	68	118	91	68
Vertical stress 6 cm below TS	51	46	40	50	45	39
Resilient strain 6 cm below TS	440	516	600	428	493	573
Number of heavy trucks	10284	10284	10284	10284	10284	10284
parameter *(a)*	1227.7	1227.7	1227.7	1227.7	1227.7	1227.7
parameter *(b)*	0.047	0.047	0.047	0.047	0.047	0.047
Permanent strain MDL3 (μ strain)	792.57	758.11	720.20	607.79	581.58	557.01
Permanent strain MDL3 (mm)	0.159	0.152	0.144	0.122	0.116	0.111
Total permanent strain MDL3 (mm)	0.454			0.349		
parameter *(a)*	1055.2	1842.8	2030.6	1055.2	1842.8	2030.6
parameter *(b)*	0.076	0.107	0.341	0.076	0.107	0.341
Permanent strain 6 cm below L4 (μ strain)	928.23	2530.97	27881.92	902.32	2448.75	27184.88
Permanent strain 6 cm below L4 (mm)	0.111	0.304	3.346	0.108	0.294	3.262
Total permanent strain 6 cm below L4(mm)	3.761			3.664		

Table F. 8 analysis results for stress and resilient modulus converge and plastic deformation calculation for soil A-7-5

	A-7-5_2%CC+15%LC			A-7-5_4%CC+15%LC		
	80% OMC	100% OMC	120% OMC	80% OMC	100% OMC	120% OMC
Resilient modulus MDL3 (Mpa)	160	154	148	186	180	165
Vertical stress MDL3 (kPa)	81	73	64	82	74	64
Resilient modulus L4 (Mpa)	82	62	44	84	62	44
Vertical stress L4 (kPa) Top	56	49	41	56	48	41
Resilient strain MDL3 (μ strain)	629	640	655	568	578	612
Resilient strain L4 (μ strain) Top	673	786	935	655	770	919
Resilient modulus 6 cm below TS	90	66	48	91	67	47
Vertical stress 6 cm below TS	46	40	34	45	39	33
Resilient strain 6 cm below TS	547	640	764	533	628	751
Number of heavy trucks	10284	10284	10284	10284	10284	10284
parameter *(a)*	2205.0	2205.0	2205.0	2205.0	2205.0	2205.0
parameter *(b)*	0.059	0.038	0.038	0.038	0.038	0.038
Permanent strain MDL3 (μ strain)	1925.28	1484.83	1354.54	1380.94	1287.75	1214.98
Permanent strain MDL3 (mm)	0.385	0.297	0.271	0.276	0.258	0.243
Total permanent strain MDL3 (mm)	0.953			0.777		
parameter *(a)*	1232.6	1068.3	1581.6	1232.6	1068.3	1581.6
parameter *(b)*	0.035	0.055	0.067	0.035	0.055	0.067
Permanent strain 6 cm below L4 (μ strain)	870.48	1076.13	2080.36	842.20	1033.57	2062.13
Permanent strain 6 cm below L4 (mm)	0.104	0.129	0.250	0.101	0.124	0.247
Total permanent strain 6 cm below L4(mm)	0.483			0.473		

Conclusions from pavement design example:

- The results in this pavement section analysis confirm the discussion and explanation presented in Chapters 4 and 5, specifically Figures 4.12, 5.4 and 5.14 in which the increase in moisture content significantly affected the resilient modulus value and resistance to permanent deformation soils A-4 and A-6. Although soil A-7-5 has a lower resilient modulus value, increase in moisture produced a lower permanent deformation with increase in moisture. From the analysis, the increase in moisture content from dry season to wet season has increased the permanent deformation from 0.15 mm to 3.65 mm for soil A-4 and from 0.11 mm to 3.34 mm for soil A-6. While with the same conditions soil A-7-4 has a deformation of 0.104 mm to 0.250 mm, this clearly presented in above mentioned chapters and figures.
- Having the same conditions for the three soils, stabilisation has improved the resistance to permanent deformation of soil A-4 more than the other two soils. The permanent deformation of soils A-4, A-6 and A-7-5 for stabilisation with 4% cement content plus 1.5% lime content is 0.266 mm, 0.349 mm and 0.777 mm, respectively for the first year of the analysis.
- The criterion of limiting the resilient strain on the top of the subgrade for rutting in pavement design seems to sound appropriate. While the gradual deterioration or cumulative permanent deformation calculation gives absolute values of rutting, the analysis in this example shows the close relation between the accumulation of permanent deformation and resilient strain on the top of the subgrade. With any increase in resilient strain on the top of the subgrade, the permanent deformation increased correspondingly.

- Equation 7.3 for predicting the resilient modulus value at various moisture contents showed to be a reasonable tool for resilient modulus adjustment for different seasons of the year, with only the availability of degree of saturation of the soil at different seasons.
- The correlation equation developed in this research (equation 4.13) gives an excellent opportunity to use analytical procedures for road pavement design considering the stabilised subgrade soils, since by knowing the UCS value a range of resilient modulus values can be obtained and used in the design procedure. See Table 10 and Figures 17-19.
- Practically the stabilisation with 4%CC+1.5%LC is not suitable with pavement section as its resilient modulus value is higher than the resilient modulus of base course layer. The modular ratio of two successive layers at least should be 1 or more. Therefore the resilient modulus of base course layer may improve by lightly stabilisation with a stabiliser, otherwise the repetition of loads causes the base course layer de-compact due to excessive tensile strains exercised at the bottom of this layer.
- This example shows the effect of underlay layer on the resilient modulus value of base or subbase layers that change considerably with type and resilient modulus of natural subgrade layer.
- The pavement section analysed in this example must be replaced by a more durable one with increased the asphalt concrete and stabilised subgrade layer thicknesses, or any other geometric configuration must be tried.